To the Graduate Council:

I am submitting herewith a dissertation written by Steven Lee Horner entitled "An Effective Algorithm for Enhancing a Non-invasive Fetal Electrocardiogram." I have examined the final copy of this dissertation for form and content and recommend that it be accepted in partial fulfillment of the requirements for the degree of Doctor of Philosophy, with a major in Electrical Engineering.

Dr. Paul Benjamin Crilly, Major Professor

We have read this dissertation
and recommend its acceptance:

Accepted for the Council:

Associate Vice Chancellor and
Dean of The Graduate School

AN EFFECTIVE ALGORITHM FOR ENHANCING A NON-INVASIVE FETAL ELECTROCARDIOGRAM

A Dissertation

Presented for the

Doctor of Philosophy

Degree

The University of Tennessee, Knoxville

Steven Lee Horner

May 1996

Copyright ® Steven Lee Horner, 1996

All rights reserved

ACKNOWLEDGMENTS

The following dissertation documents research conducted at the University of Tennessee Medical Center and the University of Tennessee Knoxville from January 1992 to March 1996. A research grant from the University of Tennessee Medical Center made this project possible. Furthermore, the University of Tennessee Medical Center and Dr. Bill Holls supplied equipment necessary for the study.

The following people deserve recognition for their patience and time devoted to this project. These people include Dr. Bill Holls who is a physician at the University of Tennessee Medical Center Department of OB/GYN, Dr. Paul Crilly, Dr. Daniel Koch, and Dr. Don Bouldin who are professors at the University of Tennessee Knoxville. These four people were extremely important in obtaining the necessary equipment, research approvals, and patients to carry out the research. I would also like to give special thanks to Dr. Holls and Dr. Crilly for their devout commitment to this project.

ABSTRACT

Currently, the invasive scalp electrode and Doppler ultrasound (DUS) have proved to be reliable techniques for monitoring fetal status via heart rate (HR). However, these methods have various limitations. The invasive scalp electrode has risk factors and a monitoring window that only occurs around delivery time because of the requirement of ruptured fetal membranes. Both techniques, particularly the DUS, cannot be used to acquire fetal electrophysiological information. A non-invasive fetal electrocardiogram (FECG) has potential to convey fetal HR and electrophysiological information for many gestational ages. From the above information, certain conditions of the fetus such as stress, acidosis, and uterine activity from the abdominal electromyographic signal can be determined along with other clinical information.

Research in the area of non-invasive FECG monitoring was first reported by Cremer in 1906. In the last 90 years, many advances have been made. However, only one commercial monitor (Hewlett Packard 8040) currently exists. The lack of commercial monitors is directly related to the inability to acquire an abdominal electrocardiogram (AECG) for a variety of patients that has a clinically useful FECG. Clinical information cannot be determined because the AECG's FECG has a poor signal-to-noise ratio (SNR). Therefore, much signal processing has to be done before a clinically applicable FECG can be obtained. Signal processing embodies abdominal maternal electrocardiogram (MECG) cancellation and FECG SNR enhancement. This study focuses on developing the CH^2 (Crilly - advisor, Holls - second inventor, and Horner - first inventor) algorithm for suppressing the abdominal MECG and ascertaining its effectiveness. Effectiveness determination will be done with synthesized and clinical data along with comparing the CH^2 method to eight previous publications. Synthesized and clinical data from 14 patients produced promising results. Furthermore, the CH^2 technique for abdominal MECG cancellation had more favorable quantitative effectiveness marks than the eight previous publications studied. The results from synthesized and clinical data and the eight comparisons indicate that the CH^2 technique is a stable and flexible method for abdominal MECG cancellation. Thus, the CH^2 algorithm would be a good method to combine with an FECG SNR enhancement technique to obtain a non-invasive FECG.

TABLE OF CONTENTS

PAGE

CHAPTER 1
INTRODUCTION 1
1.1 Historical Perspective 3
1.2 Dissertation Goals 5

CHAPTER 2
LITERATURE REVIEW OF FECG SYSTEMS 7
2.1 Abdominal MECG Cancellation Techniques 14
2.1.1 Single Lead 14
2.1.2 Dual Lead 16
2.1.3 Multiple Lead 17
2.2 FECG SNR Enhancement Techniques 39
2.2.1 Spatial Filtering 39
2.2.2 Temporal Filtering 45
2.2.3 Digital Impulse Response Filtering 47

CHAPTER 3
METHOD 52
3.1 Analog Signal Processing 54
3.1.1 Preamplifier Design 54
3.1.2 Theoretical and Measured AECG System Specifications 57
3.2 Digital Signal Processing 59
3.2.1 Abdominal MECG Cancellation 59
3.2.2 FECG Averaging 63
3.2.3 FECG Average Filtering 64

CHAPTER 4
PROCEDURE 65

CHAPTER 5
RESULTS 75
5.1 Synthesized Data 77
5.2 Clinical Data 83
5.2.1 Subjective Analysis 98
5.2.2 Objective Analysis 108
5.3 Discussion 109

CHAPTER 6
COMPARISON 113
6.1 Analysis One 115
6.1.1 Explanation of Tables and Respective Figures 117
6.1.2 Single Lead Method Two Versus the CH^2 Technique 128
6.2 Analysis Two 131
6.2.1 Explanation of Tables and Respective Figures 131
6.2.2 Quadratic Programming Versus the CH^2 Technique 146
6.3 Discussion 149

CHAPTER 7
CONCLUSION 153
7.1 Effectiveness with Synthesized and Clinical Data 153
7.2 Effectiveness Compared to Eight Previous Publications 154
7.3 Future Research 156

REFERENCES 158

APPENDICES 168

APPENDIX A
ECG WAVEFORM DESCRIPTION 169

APPENDIX B
PATENT, HUMAN STUDIES COMMITTEE APPROVALS, AND PATIENT SIGNATURE FORM 172

APPENDIX C
ONE BLOCK CLINICAL DATA 177

APPENDIX D
CONTINUOUS CLINICAL DATA 189

APPENDIX E
DISSERTATION GOAL II INFORMATION 198

APPENDIX F
DISSERTATION GOAL II RESULTS 203

APPENDIX G
DISSERTATION GOAL III INFORMATION 207

APPENDIX H
DISSERTATION GOAL III ANALYSIS I DATA 214

APPENDIX I
DISSERTATION GOAL III ANALYSIS II DATA 231

VITA 251

LIST OF TABLES

TABLE		PAGE
5-1.	Inspection results for MECG cancellation effectiveness of Figs. 5-3 to 5-8	99
5-2.	Inspection results for MECG cancellation effectiveness of Figs. 5-9 to 5-14	100
5-3.	Inspection results of Figs. 5-15 to 5-18 and C-1 to C-2	101
5-4.	Inspection results for MECG cancellation effectiveness of Figs. C-3 to C-8	102
5-5.	Inspection results of Figs. C-9 to C-11 and D-1 to D-3	103
5-6.	Inspection results for MECG cancellation effectiveness of Figs. D-4 to D-8	104
5-7.	Percentage successes of the 12 test conditions	110
5-8.	Percentage potentials for the clinical applications	111
6-1.	Single lead method two vs. the CH^2 method for AECG MECG cancellation	118
6-2.	Single lead method three vs. the CH^2 method for AECG MECG cancellation	119
6-3.	Single lead method five vs. the CH^2 method for AECG MECG cancellation	120
6-4.	Adaptive filter vs. the CH^2 method for AECG MECG cancellation	121
6-5.	Orthogonal basis vs. the CH^2 method for AECG MECG cancellation	122
6-6.	Quadratic programming vs. the CH^2 method for AECG MECG cancellation	132
6-7.	SVD method one vs. the CH^2 method for AECG MECG cancellation	133
6-8.	SVD method two vs. the CH^2 method for AECG MECG cancellation	134
6-9.	Summary of the scores for the eight comparisons of analysis I and II	149
6-10.	Effectiveness marks for the eight comparisons of analysis I and II	150
E-1.	Description of test conditions 1-5 for dissertation goal II	199
E-2.	Description of test conditions 6-9 for dissertation goal II	200
E-3.	Description of test conditions 10-12 for dissertation goal II	201
E-4.	Description of clinical applications 1-3 for dissertation goal II	202
F-1.	MECG suppression ratios for patients 1 through 3 of the objective analysis	204
F-2.	MECG suppression ratios for patients 3 through 9 of the objective analysis	205
F-3.	MECG suppression ratios for patients 10 through 16 of the objective analysis	206
G-1.	Description of test conditions 1-5 for dissertation goal III	208
G-2.	Description of test conditions 6-7 and intrinsic characteristics 1-4 for dissertation goal III	209
G-3.	Description of clinical applications 1-3 for dissertation goal III	210

LIST OF FIGURES

FIGURE		PAGE
1-1.	Block diagram of the dissertation's goals	6
2-1.	Clinical AECG signals	10
2-2.	Bandpass filtered time plots of the abdominal MECG	11
2-3.	Bandpass filtered plots of the FECG	12
2-4.	Bandpass filtered plots of an AECG with MECG and FECG	13
2-5.	Single lead methods based on MECG averaging and subtraction	15
2-6.	Adaptive filters for abdominal MECG cancellation	19
2-7.	Conventional LMS adaptive filter converging	21
2-8.	Conventional LMS adaptive filter after converging	22
2-9.	Time-sequenced adaptive filter converging	24
2-10.	Time-sequenced adaptive filter after converging	25
2-11.	Orthogonal basis method	28
2-12.	Quadratic programming technique	31
2-13.	Synthesized ECG signals used to reimplement SVD method one	34
2-14.	Results of reimplementing SVD method one	35
2-15.	AECG signals used with singular value decomposition method two	37
2-16.	Results of singular value decomposition method two	38
2-17.	Eight AECG signals used with singular value decomposition method three	40
2-18.	Results of the first transformation of SVD method three	41
2-19.	Results of the second transformation of SVD method three	42
2-20.	Results of reimplementing the additive spatial filter method	43
2-21.	The resulting signals from SVD method two for FECG SNR enhancement	46
2-22.	FECG averaging technique	48
2-23.	Block diagram of the time-sequenced adaptive filter for FECG SNR enhancement	50
2-24.	Results of the time-sequenced adaptive filter for FECG SNR enhancement	51
3-1.	Block diagram of the CH^2 FECG system	53
3-2.	Flowgraph of the CH^2 FECG system	53
3-3.	Preamplifier circuit diagram	55
3-4.	A graphical explanation of the CH^2 method for MECG cancellation	60
4-1.	A photo of the CH^2 FECG system	67
4-2.	A demonstration of the necessity for oversampling with a signal that is sampled approximately five times faster than the Nyquist frequency	69

4-3. A demonstration of the necessity for oversampling with a signal that is sampled approximately 11.5 times faster than the Nyquist frequency 70
4-4. Clinical data with a 1 kHz sampling rate 71
4-5. Clinical data with a 500 Hz sampling rate 72
4-6. Clinical data with a 250 Hz sampling rate 73
5-1. Block diagram describing the layout of Chapter 5 76
5-2. Synthesized data set one, original signals separated 78
5-3. Synthesized data set one results 79
5-4. Synthesized data set two results 82
5-5. Clinical data from patient 1 at 36 weeks of gestation 84
5-6. Clinical data from patient 2 at 36 weeks of gestation 85
5-7. Clinical data from patient 3 at 34 weeks of gestation 86
5-8. Clinical data from patient 4 at 21 weeks of gestation 87
5-9. Clinical data from patient 5 at 36 weeks of gestation 88
5-10. Clinical data from patient 7 at 39 weeks of gestation 89
5-11. Clinical data from patient 8 at 36 weeks of gestation 90
5-12. Clinical data from patient 9 at 27 weeks of gestation 91
5-13. Clinical data from patient 10 at 37 weeks of gestation 92
5-14. Clinical data from patient 11 at 38 weeks of gestation 93
5-15. Clinical data from patient 12 at 34 weeks of gestation 94
5-16. Clinical data from patient 13 at 39 weeks of gestation 95
5-17. Clinical data from patient 15 at 41 weeks of gestation 96
5-18. Clinical data from patient 16 at 26 weeks of gestation 97
6-1. Block diagram describing the layout of Chapter 6 114
6-2. Synthesized signals used in the eight comparisons 116
6-3. Single lead method two vs. the CH^2 method demonstrating test condition four 123
6-4. Single lead method two vs. the CH^2 method demonstrating test condition five 124
6-5. Single lead method two vs. the CH^2 method demonstrating test condition six 125
6-6. Single lead method two vs. the CH^2 method demonstrating test condition seven 126
6-7. AECG signals used to compare the quadratic programming and CH^2 methods 135
6-8. CH^2 and CH^2 & SVD results demonstrating test condition four 136
6-9. Quadratic programming vs. the CH^2 method demonstrating test condition four 137
6-10. CH^2 and CH^2 & SVD results demonstrating test condition five 138
6-11. Quadratic programming vs. the CH^2 method demonstrating test condition five 139
6-12. CH^2 and CH^2 & SVD results demonstrating test condition six 140

6-13. Quadratic programming vs. the CH^2 method demonstrating test condition six 141
7-1. A photo of the invasive intrauterine catheter FECG monitoring system..... 157
A-1. An example ECG complex for one heart beat 170
A-2. The parts of the heart that are associated with the ECG complex..... 170
A-3. Propagation of action potentials through the right and left atriums that result in the P wave of the ECG complex..... 171
A-4. Propagation of action potentials between the atriums and ventricles that result in the QRS complex of the ECG waveform 171
C-1. Clinical data from patient 3 at 23 weeks of gestation 178
C-2. Clinical data from patient 3 at 24 weeks of gestation 179
C-3. Clinical data from patient 3 at 25 weeks of gestation 180
C-4. Clinical data from patient 3 at 26 weeks of gestation 181
C-5. Clinical data from patient 3 at 31 weeks of gestation 182
C-6. Clinical data from patient 3 at 33 weeks of gestation 183
C-7. Clinical data from patient 3 at 35 weeks of gestation 184
C-8. Clinical data from patient 3 at 36 weeks of gestation 185
C-9. Clinical data from patient 3 at 38 weeks of gestation 186
C-10. Clinical data from patient 3 at 39 weeks of gestation 187
C-11. Clinical data from patient 16 at 36 weeks of gestation 188
D-1. A demonstration of continuous AECG MECG cancellation from 0.0 to 8.0 seconds 190
D-2. A demonstration of continuous AECG MECG cancellation from 8.0 to 16.0 seconds 191
D-3. A demonstration of continuous AECG MECG cancellation from 16.0 to 24.0 seconds 192
D-4. A demonstration of continuous AECG MECG cancellation from 24.0 to 32.0 seconds 193
D-5. A demonstration of continuous AECG MECG cancellation from 32.0 to 40.0 seconds 194
D-6. A demonstration of continuous AECG MECG cancellation from 40.0 to 48.0 seconds 195
D-7. A demonstration of continuous AECG MECG cancellation from 48.0 to 56.0 seconds 196
D-8. A demonstration of continuous AECG MECG cancellation from 56.0 to 64.0 seconds 197
H-1. Single lead method three vs. the CH^2 method demonstrating test condition four..... 215
H-2. Single lead method three vs. the CH^2 method demonstrating test condition five 216
H-3. Single lead method three vs. the CH^2 method demonstrating test condition six..... 217
H-4. Single lead method three vs. the CH^2 method demonstrating test condition seven..... 218
H-5. Single lead method five vs. the CH^2 method demonstrating test condition four..... 219
H-6. Single lead method five vs. the CH^2 method demonstrating test condition five 220
H-7. Single lead method five vs. the CH^2 method demonstrating test condition six..... 221
H-8. Single lead method five vs. the CH^2 method demonstrating test condition seven 222

H-9. Time-sequenced adaptive filter vs. the CH^2 method demonstrating test condition four 223
H-10. Time-sequenced adaptive filter vs. the CH^2 method demonstrating test condition five..... 224
H-11. Time-sequenced adaptive filter vs. the CH^2 method demonstrating test condition six 225
H-12. Time-sequenced adaptive filter vs. the CH^2 method demonstrating test condition seven..... 226
H-13. Orthogonal basis vs. the CH^2 method demonstrating test condition four 227
H-14. Orthogonal basis vs. the CH^2 method demonstrating test condition five..... 228
H-15. Orthogonal basis vs. the CH^2 method demonstrating test condition six 229
H-16. Orthogonal basis vs. the CH^2 method demonstrating test condition seven..... 230
I-1. ECG signals used to compare SVD method one and the CH^2 method 232
I-2. SVD method one, CH^2, and CH^2 & SVD results demonstrating test condition four 233
I-3. SVD method one vs. the CH^2 method demonstrating test condition four..... 234
I-4. SVD method one, CH^2, and CH^2 & SVD results demonstrating test condition five..... 235
I-5. SVD method one vs. the CH^2 method demonstrating test condition five 236
I-6. SVD method one, CH^2, and CH^2 & SVD results demonstrating test condition six 237
I-7. SVD method one vs. the CH^2 method demonstrating test condition six..... 238
I-8. SVD method one, CH^2, and CH^2 & SVD results demonstrating test condition seven..... 239
I-9. SVD method one vs. the CH^2 method demonstrating test condition seven..... 240
I-10. AECG signals $S_{2\text{-}11}(n)$ used to compare SVD method two and the CH^2 method. 241
I-11. SVD method two results demonstrating test condition four 242
I-12. Results of the CH^2 method demonstrating test condition four..... 243
I-13. SVD method two vs. the CH^2 method demonstrating test condition four..... 244
I-14. SVD method two results demonstrating test condition five..... 245
I-15. Results of the CH^2 method demonstrating test condition five 246
I-16. SVD method two vs. the CH^2 method demonstrating test condition five 247
I-17. SVD method two results demonstrating test condition six 248
I-18. Results of the CH^2 method demonstrating test condition six..... 249
I-19. SVD method two vs. the CH^2 method demonstrating test condition six..... 250

LIST OF ABBREVIATIONS

ADC	Analog-to-Digital Conversion
ANS	Autonomic Nervous System
AECG	Abdominal Electrocardiogram
BJT	Bipolar Junction Transistor
CH^2	Crilly, Holls, and Horner
CMRR	Common Mode Rejection Ratio
DSP	Digital Signal Processing
ECG	Electrocardiogram
EMG	Electromyography
ENI	Equivalent Noise Current
ENV	Equivalent Noise Voltage
FECG	Fetal Electrocardiogram
FIR	Finite Impulse Response
GA	Genetic Algorithm
GSVD	Generalized Singular Value Decomposition
HR	Heart Rate
IIR	Infinite Impulse Response
JFET	Junction Field Effect Transistor
LMS	Least-Mean-Squares
MECG	Maternal Electrocardiogram
Orth.	Orthogonal Basis
PCMCIA	Personal Computer Memory Card International Association
PVC	Premature Ventricular Contraction
Quad.	Quadratic Programming
RMS	Root-Mean-Square
SL2	Single Lead Method Two
SL3	Single Lead Method Three
SL5	Single Lead Method Five
SNR	Signal-to-Noise Ratio
SVD	Singular Value Decomposition
SVD1	Singular Value Decomposition Method One
SVD2	Singular Value Decomposition Method Two

TECG	Thoracic Electrocardiogram
TSAF	Time-sequenced Adaptive Filter

CHAPTER 1

INTRODUCTION

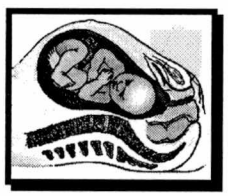

The objective of this chapter is to convey an overview of non-invasive fetal electrocardiogram† (ECG) monitoring. Chapter 1 includes a discussion of the clinical applications of the fetal electrocardiogram (FECG) and engineering considerations to acquire an FECG. Furthermore, a brief discussion of the historical developments of the non-invasive FECG from its initial discovery to the present will be presented as well as identifying research trends. The goals of the dissertation are introduced in Section 1.2.

Currently, the invasive scalp electrode is used to monitor the status of the fetus via heart rate (HR) [1]. The invasive procedure can lead to complications (infections) and requires the rupturing of fetal membranes that limits monitoring time to immediately before delivery. A non-invasive procedure would allow physicians to obtain heart rate and electrophysiological information throughout the pregnancy without rupturing the membranes. From this information, the status of the fetus can be determined similar to the invasive procedure along with the following [2, 3, 4, 5, 6, 7, 8, 9, 10, 11, 12]:

- Acidosis
- Premature ventricular contractions (PVC)
- Cardiac arrhythmia

† A description of the ECG waveform is given in Appendix A.

- Uterine contraction information via abdominal electromyography (EMG)
- The activity of the Autonomic Nervous System (ANS) by spectral HR analysis
- Other clinical conditions that are being correlated with HR variability.

There are difficulties in acquiring a clinically useful non-invasive FECG. These difficulties include several biopotential signals and artifacts that interfere with the FECG of the abdominal electrocardiogram (AECG). The interfering signals include the following [13, 14, 15, 16, 17, 18]:

- An abdominal maternal electrocardiogram‡ (MECG) that can be from two to one thousand or more times larger than the FECG
- EMG noise from abdominal smooth and skeletal muscle activity of the patient
- EMG noise from the fetus
- Artifact noise from patient and fetal movements
- Artifact noise from electrodes
- 50 or 60 Hz noise depending on the base frequency of the power grid
- Instrumentation noise
- Skin resistance thermal noise.

Furthermore, obtaining an FECG with a favorable signal-to-noise ratio (SNR) is dependent on the gestational age of the patient. Researchers have reported that during the first 26 to 34 weeks of gestation the FECG is significantly attenuated [13, 19, 20, 21]. The source of the attenuation is open for debate, but speculation and a study have attributed this phenomena to the vernix that builds up around the fetus and electrically isolates it during the 26 to 36 weeks of gestation [21, 22]. The literature also indicates that during the 20 to 26 week period the FECG seems to be somewhat uniform in amplitude on the abdominal surface area and from 34 weeks to delivery a large variety of amplitudes occur on the abdominal surface area [20]. To better understand the conduction of the FECG to the abdominal surface area, several studies have been

---

‡ The abdominal MECG will never be referred to as noise throughout the dissertation.

done on the conductive medium of the FECG and the potential distribution of the FECG across the abdomen at various gestational ages [20, 22, 23, 24, 25]. Finally, the fetus is not stationary in the uterus which causes the FECG to vary over time because it is measured with a set of spatially fixed electrodes. Thus, the number and positioning of abdominal leads for short and long monitoring have been studied [26].

1.1 Historical Perspective

Historical developments of FECG systems can be divided into two time periods. The first period or pre-signal processing era occurred from the discovery of the FECG in 1906 to 1957 when signal processing was introduced to cancel the interfering signals of the AECG. Period two or the signal processing era goes from 1957 to the present.

Cremer in 1906 was the first to discover and publish the FECG which marked the beginning of the pre-signal processing era [1, 27, 28, 29, 30, 31, 32]. This era occurred three years after Einthoven published the finding of the adult ECG. Cremer detected the FECG with a string galvanometer connected to a vaginal electrode and an abdominal electrode [1, 27, 28, 32]. From 1906 to 1930, only four papers were published concerning the recording of an FECG and all used the string galvanometer [27, 32]. Furthermore, the FECG was not used clinically for 30 years after Cremer's discovery [29]. Maekawa and Toyoshima in 1930 suggested that an amplifier system would be necessary to record an FECG from the abdominal area. They were the first to introduce a vacuum tube amplifier to obtain an FECG [27, 28]. From 1930 to the early 1960's, several improvements were made to the FECG's amplification system and by the mid 1960's transistor based differential amplifiers were used commonly [33]. Different types of electrodes were utilized to acquire an FECG during this time too. The electrodes included non-invasive and invasive abdominal wall, vaginal, rectal, intrauterine, scalp, and cervical electrodes [29, 32, 34, 35]. By the late 1960's, the invasive scalp and non-invasive AECG were the most widely used in the research community [36, 37, 38, 39, 40, 41, 42, 43, 44]. Since the invasive scalp electrode was connected directly to the fetus' head, a clinically useful FECG was obtained with a small MECG and noise component. The non-invasive AECG was corrupted substantially by the MECG and noise which made it difficult to obtain a clinically useful FECG [27]. Thus, many signal processing algorithms have been introduced in the last 40 years to enhance the FECG's SNR of the AECG.

The first signal processing method to cancel the abdominal MECG was reported in 1957. This method was based on subtracting a scaled thoracic electrocardiogram (TECG) with a similarly shaped MECG as the abdominal MECG from the AECG [45]. FECG averaging (temporal filtering) and the linear combination of several AECGs (spatial filtering) were introduced in 1961 and 1963 respectively to enhance the FECG's SNR and suppress the abdominal MECG [46, 47]. Two techniques were reported to attenuate the abdominal MECG in 1966 where the first subtracted an averaged abdominal MECG complex from each abdominal MECG complex and the second blanked out the abdominal MECG's QRS complexes [48, 49]. An adaptive filter was proposed in 1975 that filtered four TECG signals with digital finite impulse response (FIR) filters to cancel the MECG of an AECG [50]. In 1977, the orthogonal basis technique was published. This method suppressed the abdominal MECG by linearly combining three TECG signals and subtracted the resulting signal from an AECG [51]. In 1981, a spatial filtering method was introduced that used quadratic programming that simultaneously removed the abdominal MECG and improved the FECG's SNR by linearly combining several AECG signals [52]. Finally, time-sequenced adaptive filtering was published in 1982 to improve the FECG's SNR [53]. All the abdominal MECG cancellation and FECG SNR enhancement techniques that are discussed above were first reports.

Several systems have been reported to cancel the abdominal MECG and enhance the FECG's SNR, since 1982. However, these systems have been variations and/or refinements of previous publications that are based on abdominal MECG averaging and subtraction, combining several ECG signals (adaptive and spatial filtering methods), or FECG averaging. The majority of the non-invasive systems reported in the last 20 years have achieved abdominal MECG cancellation through combining several ECG signals. Twenty-five publications were found that cancel the abdominal MECG by combining several ECG signals and seven publications were found that were based on MECG averaging and subtraction (See Sections 2.1.1 and 2.1.3 for articles.). The findings appear to indicate the research community presumes that combining several ECG signals is a superior approach for canceling the abdominal MECG as opposed to MECG averaging and subtraction. Finally, two papers have been published using the intrauterine catheter electrode in the last seven years which may be an alternative to the scalp electrode that is being used currently [54, 55]. One of the techniques uses a non-invasive abdominal MECG cancellation method to suppress the invasive intrauterine catheter electrode's MECG signal [55]. The non-invasive method is the adaptive filter technique which again reinforces that the research

community presumes that MECG cancellation is best achieved through combining several ECG signals instead of MECG averaging and subtraction.

1.2 Dissertation Goals

The objective of this dissertation is to develop an effective non-invasive FECG monitoring system designated the CH^2 (Crilly - advisor, Holls - second inventor, and Horner - first inventor) FECG system. Goals that fulfill the objective are as follows:

- Research, design, and develop the CH^2 non-invasive FECG monitoring system
- Ascertain the effectiveness of the CH^2 method for abdominal MECG cancellation with synthesized and clinical data
- Ascertain the effectiveness of the CH^2 method for abdominal MECG cancellation compared to eight previous publications
- Conclude from goals two and three whether the CH^2 FECG system's method for abdominal MECG cancellation has been effective.

Figure 1-1 presents a block diagram of the dissertation's goals.

The effectiveness determination of the CH^2 FECG system specifically targets abdominal MECG cancellation. However, the CH^2 FECG system and most previously reported methods contain an algorithm for abdominal MECG suppression and FECG SNR enhancement. Some systems, including the CH^2, perform these two operations sequentially, but others accomplish them simultaneously. Most of the analyses performed in Chapter 5 are for abdominal MECG cancellation, but there are some for FECG SNR enhancement. Chapter 6 only performs abdominal MECG cancellation analyses, but two of the eight previous reported methods simultaneously achieve abdominal MECG cancellation and FECG SNR enhancement. **In summary, the effectiveness conclusions of dissertation goal four pertain to the CH^2 FECG system's method for abdominal MECG cancellation and not FECG SNR enhancement!**

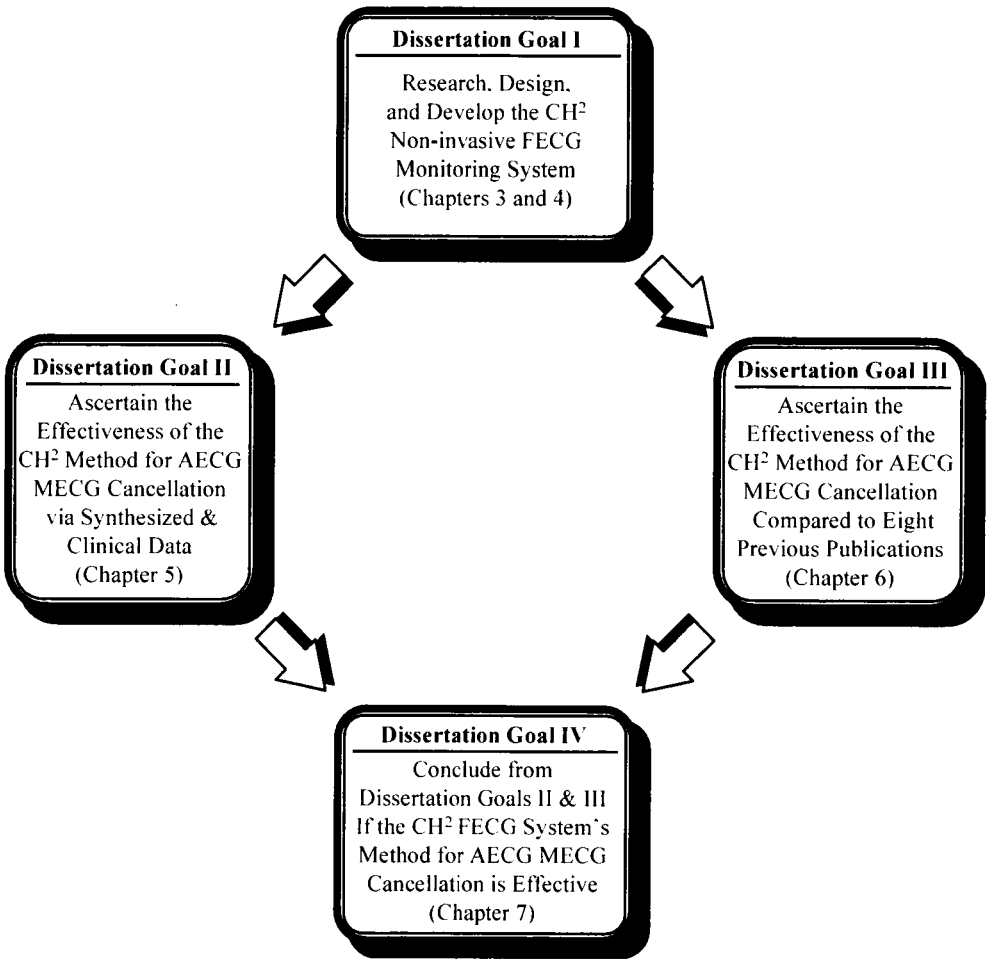

Figure 1-1. Block diagram of the dissertation's goals.



LITERATURE REVIEW OF FECG SYSTEMS

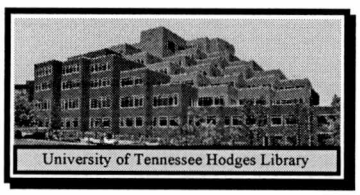

Since Cremer discovered the FECG in 1906, there have been many different non-invasive FECG systems developed. The promising systems contain three subsystems. The first subsystem consists of analog signal processing that includes a skin preparation procedure, electrodes, amplifiers, and filters. The second and third subsystems perform analog or digital signal processing that cancels the abdominal MECG and enhances the FECG's SNR respectively. Many different techniques have been reported to cancel the abdominal MECG and can be divided into the single, dual, and multiple ECG lead methods based on the number of leads attached to the patient. Several techniques have been developed for enhancing the FECG SNR enhancement and are usually based on spatial, temporal, or digital impulse response filters. This chapter describes in detail several of the published techniques for abdominal MECG cancellation and FECG SNR enhancement. Since much emphasis is placed on abdominal MECG cancellation in this study, several of the previously reported MECG cancellation algorithms have been reimplemented. Results from the reimplementations with synthesized or clinical data will be presented to demonstrate and gain more insight into these methods (Synthesized data is from a non-pregnant patient with an FECG average from a previously logged data file from a pregnant patient. The FECG average was added to the AECG with a typical heart rate and rate change to simulate the FECG frequency content. Synthesized data sets should not be interrupted as clinical data obtained under typical clinical conditions. If this were the case, the results of the reimplementations would be much worse in most of the cases.).

Before a detailed presentation of the previously reported FECG systems is performed, a mathematical description of an ECG and other biopotential signals that are present during the measurement of the ECG signal is presented. $S_k(t)$ or (1) describes a measured signal from the periphery of a pregnant woman

$$S_k(t) = Md_k(t)M_k(t) + F_k(t) + N_{k,EMG}(t) + N_{k,60Hz}(t) + N_{k,amp}(t) + N_{k,therm}(t) + N_{k,art}(t) \quad (1)$$

where k is the ECG lead or channel number, $S_k(t)$ bandwidth is usually from 0.05 to 100.0 Hz, $M_k(t)$ is the MECG, $Md_k(t)$ is a modulation function of the MECG and is usually caused from respiration and other movements, $F_k(t)$ is the FECG, $N_{k,EMG}(t)$ is EMG activity that is random and/or high rate semi-periodic impulses (200 to 700 impulses per minute), $N_{k,60Hz}(t)$ is 50 or 60 Hz noise depending on the frequency of the power grid, $N_{k,amp}(t)$ is amplifier electronic noise, $N_{k,therm}(t)$ is thermal noise from the signal source resistance, and $N_{k,art}(t)$ is artifact from patient and fetal movements, electrodes, and unknown sources [13, 14, 15, 16, 17, 18, 56]. If $S_k(t)$ is measured on the thoracic area or any other position on the patient's periphery other than the anterior, lateral, or posterior abdominal wall, $F_k(t)$ or the FECG is very small compared to the MECG and is assumed zero. By sampling the continuous time signal $S_k(t)$ at a sampling rate of f_s with a sample sequence from $n = 0$ to $N - 1$, (2) or the signal vector can be written

$$\boldsymbol{S}_{K,N} = [S_1(n) \cdots S_K(n)]^T \quad (2)$$

where

$$S_k(n) = Md_k(n)M_k(n) + F_k(n) + N_k(n) \quad (3)$$

and

$$N_k(n) = N_{k,EMG}(n) + N_{k,60Hz}(n) + N_{k,amp}(n) + N_{k,therm}(n) + N_{k,art}(n). \quad (4)$$

Furthermore, the nth sample of any of the sampled signals of duration N discussed throughout this dissertation will be notated in lower case (e.g. $S_k(n)$ at the nth sample is $s_k(n)$). Finally,

$M_k(n)$ and $F_k(n)$ overlap in frequency content, but the significant frequency content of $M_k(n)$ is from 0.05 to 40.0 Hz versus $F_k(n)$ which has its significant energy from 0.05 to 70.0 Hz [21].

Figure 2-1 contains three sampled clinical AECG signals (f_s = 1000.0 Hz and bandwidth is 0.05 to 100.0 Hz) that all contain an MECG (large ECG signal). Figure 2-1(a) contains an FECG (small ECG signal) with a relatively high SNR. Figure 2-1(b) is corrupted with 60 Hz and other noise sources such that the FECG is almost indistinguishable. Figure 2-1(c) contains no noticeable FECG, but has significant EMG noise in the form of semi-periodic impulses which have been falsely identified as an FECG or parasitic oscillations arising in the electrode-amplifier part of the system [57, 58, 59]. Figure 2-2, Figure 2-3, and Figure 2-4 presents bandpass filtered MECG, FECG, and MECG and FECG to demonstrate time domain signal content in different frequency bands. Figure 2-2(a) is a clinical AECG with an MECG, but no FECG. The seven signals of Figure 2-2(b) are the bandpass filtered MECG where the passbands are 0.05 to 1.0 Hz, 1.0 to 10.0 Hz, 10.0 to 20.0 Hz, 20.0 to 30.0 Hz, 30.0 to 40.0 Hz, 40.0 to 50.0 Hz, and 50.0 to 100.0 Hz respectively. Figures 2-3 and 2-4 are the same layout as Figure 2-2, but Figure 2-3(a) contains a synthesized FECG and Figure 2-4(a) contains a clinical AECG that has an MECG and FECG. Finally, Figures 2-3(b) and 2-4(b) are the bandpasss filtered plots of the FECG of Figure 2-3(a) and the composite AECG of Figure 2-4(b) respectively.

The MECG and FECG signals of (3) originate from a time-dependent current dipole or source signal vector $\boldsymbol{SS}_{r,N} = [SS_1(n) \cdots SS_r(n)]^T$ provided $S_k(n)$ was measured at a considerable distance from the maternal and fetal hearts and in an 0.5 to 100.0 Hz bandwidth [13, 14, 60, 61]. The source signal vector contains r orthogonal source signals. Furthermore, $S_k(n)$ can be written as a linear combination of the signal vector and a noise term by a lead vector $\boldsymbol{L}_k = [L_{k,1} \cdots L_{k,r}]$ or

$$S_k(n) = L_{k,1}SS_1(n) + L_{k,2}SS_2(n) + \cdots + L_{k,r}SS_r(n) + N_k(n) \tag{5}$$

where

$$M_k(n) = L_{k,1}SS_1(n) + L_{k,2}SS_2(n) + \cdots + L_{k,r_m}SS_{r_m}(n), \tag{6}$$

$$F_k(n) = L_{k,r_m+1}SS_{r_m+1}(n) + L_{k,r_m+2}SS_{r_m+2}(n) + \cdots + L_{k,r}SS_{r_m+r_f}(n), \tag{7}$$

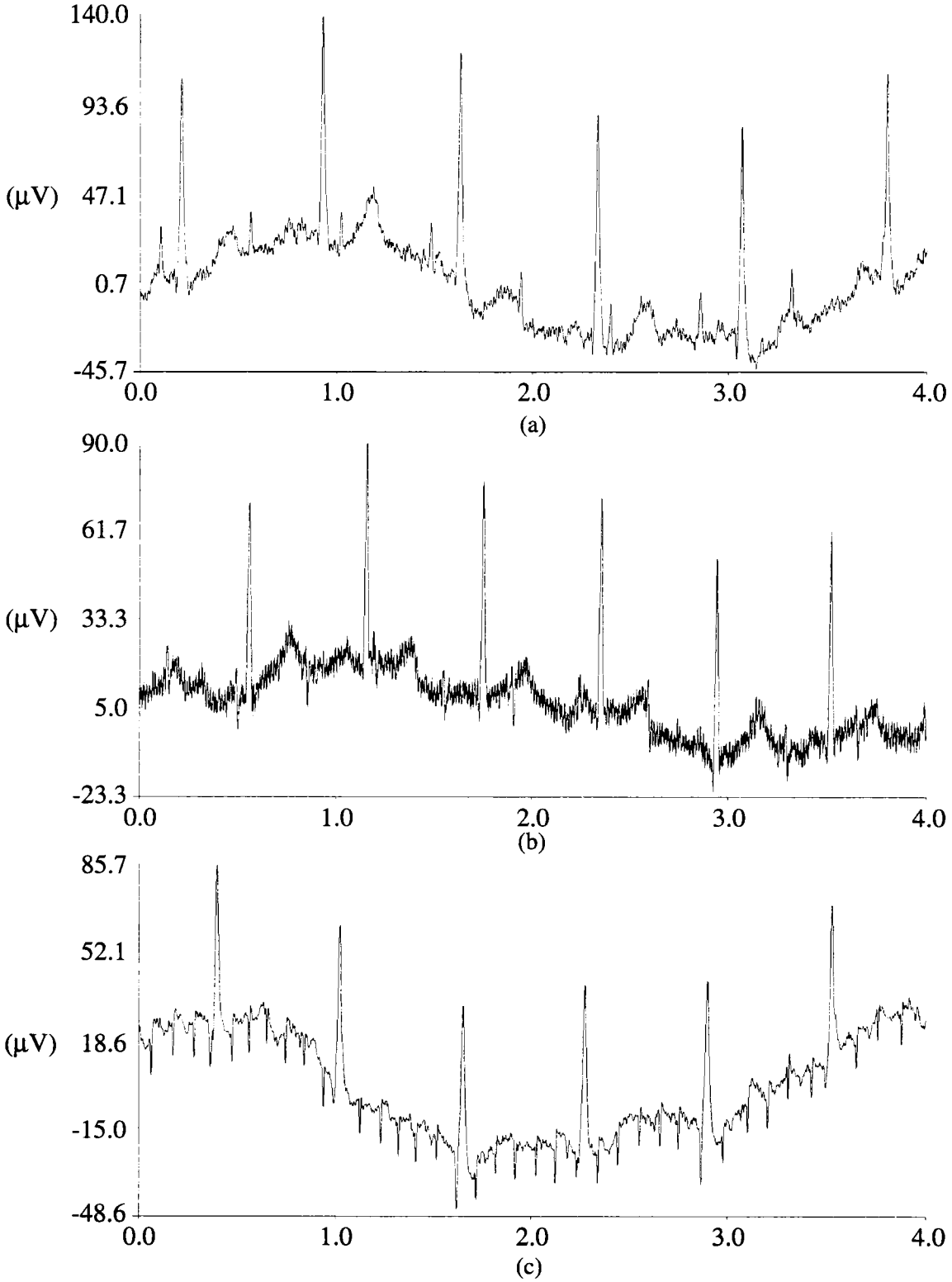

Figure 2-1. Clinical AECG signals (all x-axes in seconds). (a) An AECG where the FECG SNR ratio is relatively large. (b) An AECG signal with 60 Hz noise. (c) An AECG signal with EMG impulses and no noticeable FECG.

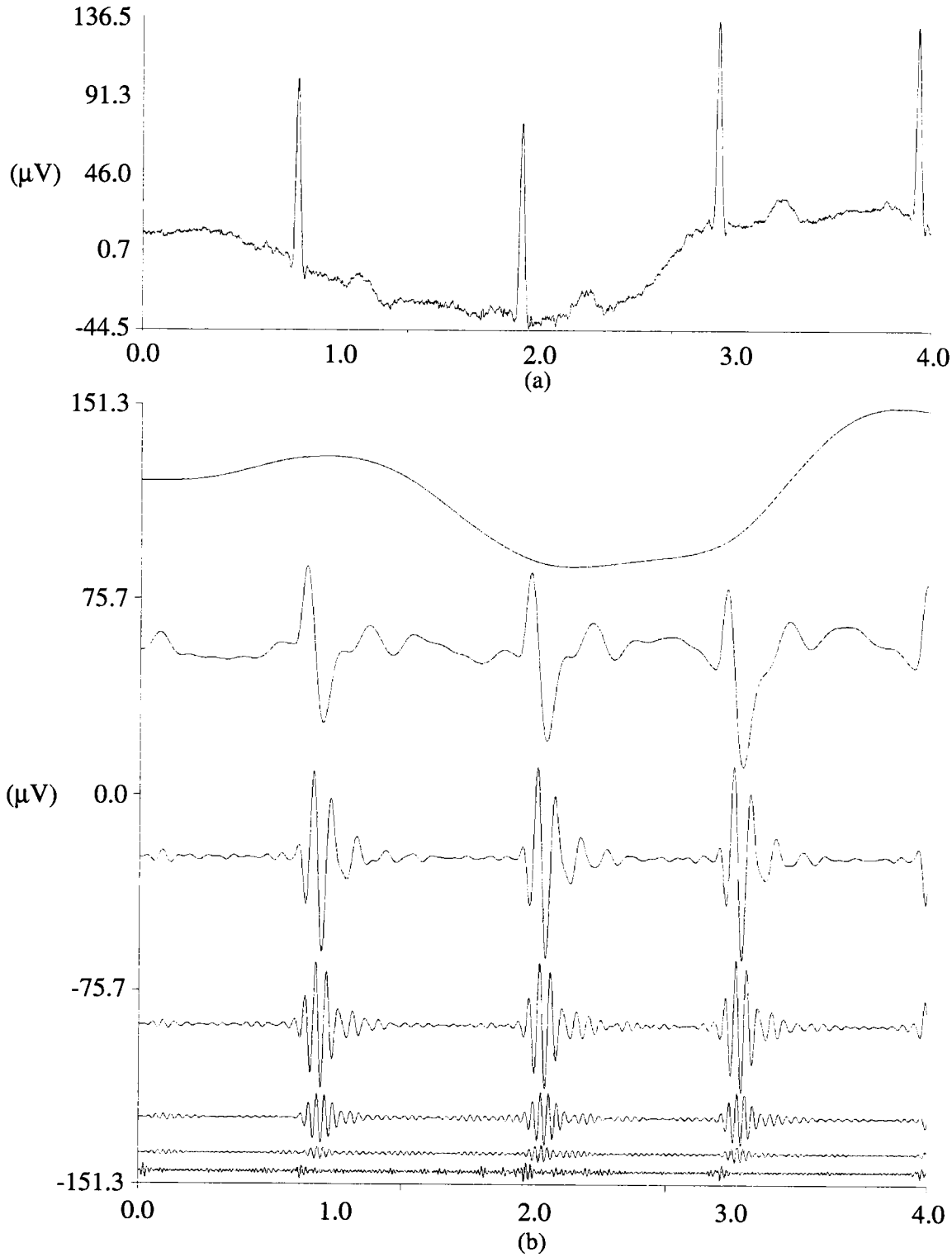

Figure 2-2. Bandpass filtered time plots of the abdominal MECG (all x-axes in seconds). a) Abdominal MECG with no FECG. (b) Bandpass filtered MECG in 0.05 to 1.0 Hz, 1.0 to 10.0 Hz, 10.0 to 20.0 Hz, 20.0 to 30.0 Hz, 30.0 to 40.0 Hz, 40.0 to 50.0 Hz, and 50.0 to 100.0 Hz bandwidths.

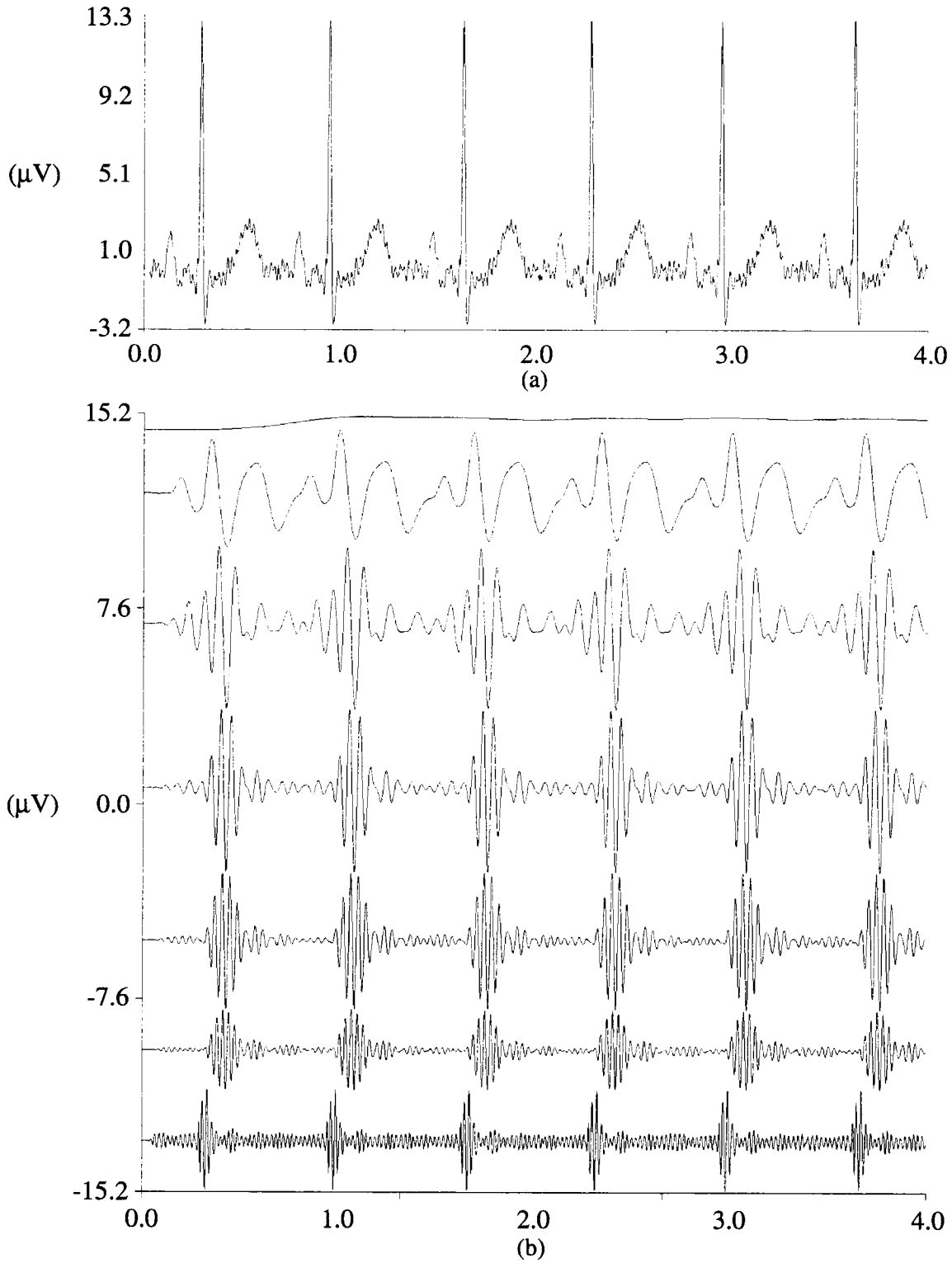

Figure 2-3. Bandpass filtered plots of the FECG (all x-axes in seconds). a) FECG. (b) Filtered FECG in 0.05 to 1.0 Hz, 1.0 to 10.0 Hz, 10.0 to 20.0 Hz, 20.0 to 30.0 Hz, 30.0 to 40.0 Hz, 40.0 to 50.0 Hz, and 50.0 to 100.0 Hz bandwidths.

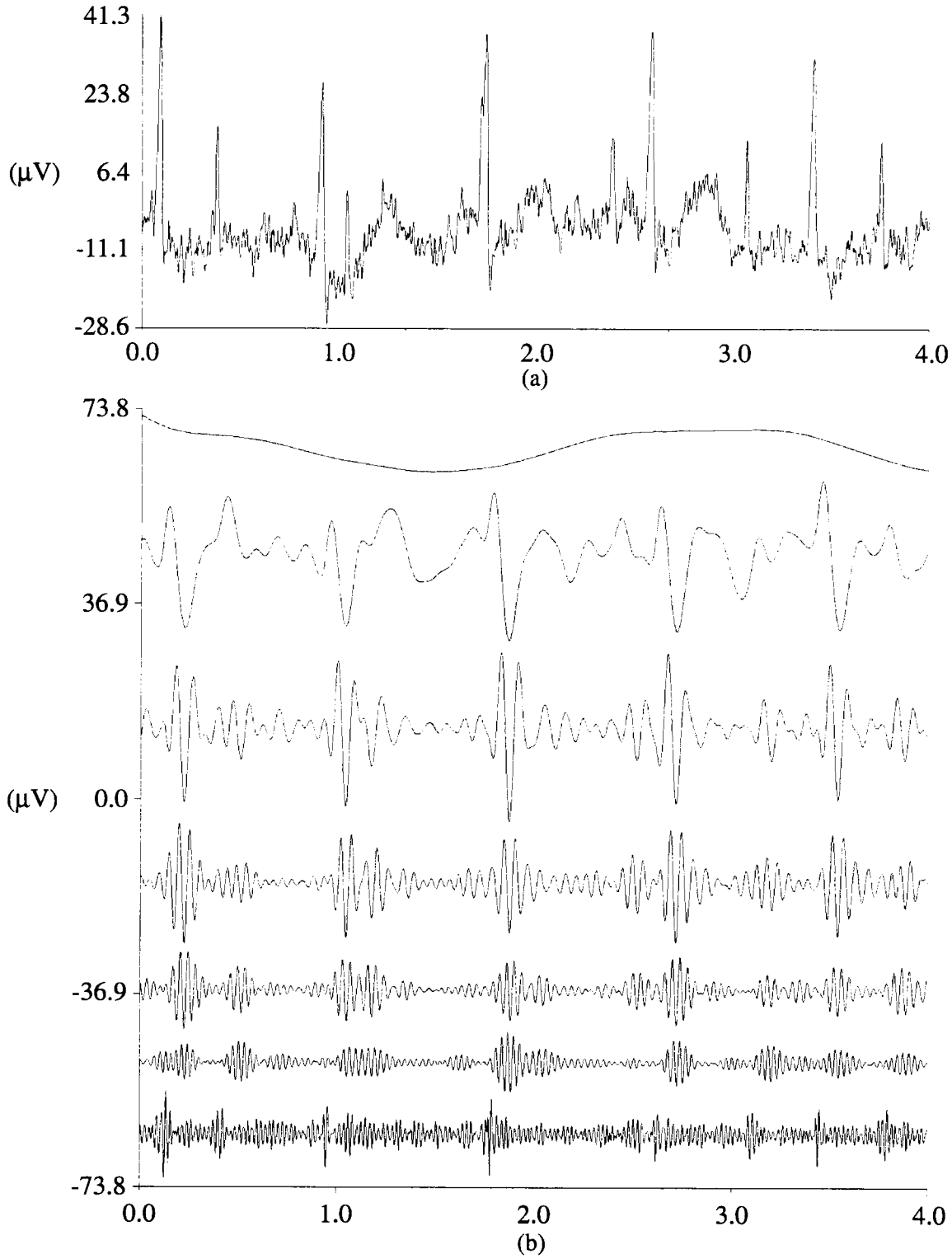

Figure 2-4. Bandpass filtered plots of an AECG with MECG and FECG (all x-axes in seconds). a) AECG. (b) Filtered AECG in 0.05 to 1.0 Hz, 1.0 to 10.0 Hz, 10.0 to 20.0 Hz, 20.0 to 30.0 Hz, 30.0 to 40.0 Hz, 40.0 to 50.0 Hz, and 50.0 to 100.0 Hz bandwidths.

and

$$r = r_m + r_f. \tag{8}$$

$Md_k(n)$ of (5) is assumed to be unity. The lead vector $\boldsymbol{L}_k$ is dependent on the electrode position with respect to the source position, conductivity of the body tissue, and the geometry of the body; r_m and r_f are usually three [14, 52]. Finally, $S_k(n)$ will be referred to as an TECG, AECG, or ECG depending on the location the measurement was made and the context of the discussion.

The aforementioned mathematical model, symbols, and terminology will be used to explain the previously reported methods and will be used throughout the dissertation for consistency. The description is generally different from the documentation in the journal articles, but both have a final common result. The change was made so that a consistent mathematical model, nomenclature, and terminology could be used throughout the dissertation to obtain better insight into the relationship between the various reported methods and the CH^2 method.

2.1 Abdominal MECG Cancellation Techniques

2.1.1 Single Lead

The single lead algorithms for abdominal MECG cancellation consist of five techniques that use characteristics of a single AECG (that contains the desired FECG) to cancel its MECG. The first single lead technique detects the MECG, FECG, and simultaneous MECG and FECG complexes along with determining the fetal heart rate. This information is used to synchronize a previously detected relatively pure MECG complex with no FECG with the presently detected MECG complex to subtract them to produce an AECG free of the MECG [62]. The second, third, and fifth single lead techniques for abdominal MECG cancellation are based on determining an abdominal MECG average or template and subtracting it from each abdominal MECG complex. The three methods differ based on the algorithm used to align each abdominal MECG complex for averaging and subtraction. The following explains single lead method two, three, and five that will be reimplemented with clinical data of Figure 2-5 where Figure 2-5(a) contains an AECG.

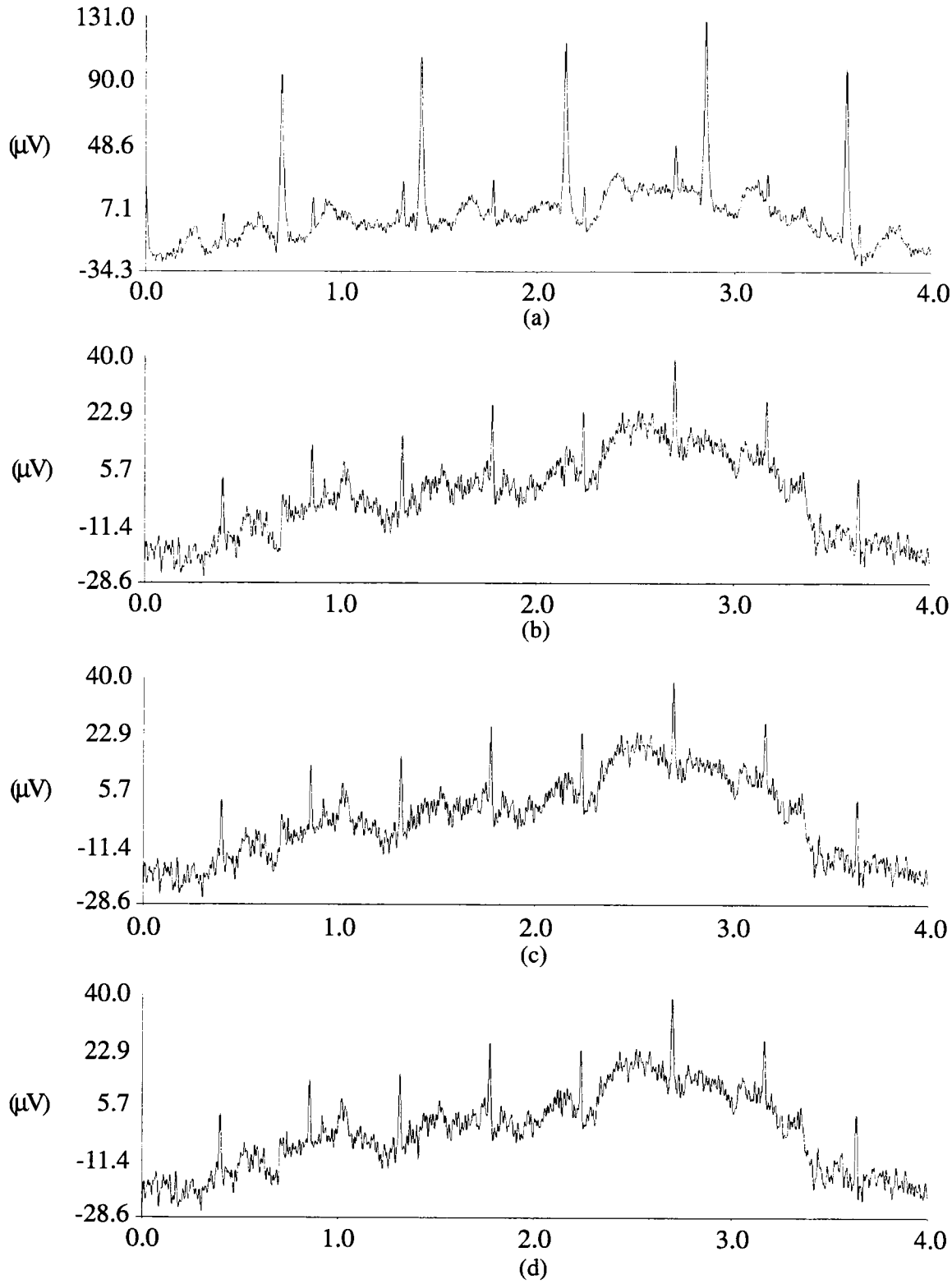

Figure 2-5. Single lead methods based on MECG averaging and subtraction (all x-axes in seconds). (a) AECG. (b) Results of method two. (c) Results of method three that scales the MECG average. (d) Results of method five.

The second single lead method uses a peak detection algorithm to determine the time locations of the peaks of the abdominal MECG's R waves [48, 63, 64]. The time locations are used as alignment points for each abdominal MECG complex for the calculation of the MECG average. Finally, the time locations are used to synchronize the subtraction of the average from the AECG. Figure 2-5(b) demonstrates method two. Method three obtains abdominal MECG cancellation in the same fashion as two, but scales the average during the subtraction process [65]. Figure 2-5(c) is the result of introducing a scale factor during the subtraction of the MECG to increase the MECG suppression. Method four computes the MECG averages of the first and second derivatives of the AECG (still using the abdominal MECG's R wave peaks as references) and subtracts them from their respective signals. The resulting first and second derivatives are used for fetal HR determination and FECG averaging [66, 67, 68].

The fifth method of the single lead systems determines the abdominal MECG's R wave peak time locations similarly to the second method, but performs a correlation step to obtain better alignment of the abdominal MECG complexes during averaging and subtraction [2, 69, 70, 71]. The first step of the algorithm allows the operator to select a relatively ideal abdominal MECG complex as a basis to build an average complex (This complex usually contains no FECG complexes and has a high SNR). The first detected abdominal MECG's R wave peak time location is determined and locally correlated with the preselected complex. Then the two signals are averaged together at the maximum correlation point. To obtain an averaged abdominal MECG complex with a high SNR, the previously calculated average is correlated with several more abdominal MECG periods that are also averaged into the template. When a sufficient number of complexes have been averaged (usually 10 or more), the template is subtracted from the AECG. Subtraction is performed by using the R wave peak time locations as a reference point for locally correlating the template and each abdominal MECG complex until maximum correlation is obtained. The maximum correlation time location is then used as an alignment point for the abdominal MECG complexes and average for subtraction. Figure 2-5(d) demonstrates the reimplementation of this method.

2.1.2 Dual Lead

The dual lead techniques for abdominal MECG suppression can be divided into three subsets that include blanking, scaled subtraction, and scaled and time-shifted subtraction. These

methods use a reference ECG that is dominated by the MECG and contains no FECG to assist in the removal of the abdominal MECG.

The blanking methods for abdominal MECG removal use the reference ECG to blank out the abdominal MECG's QRS complexes [49, 72, 73]. Blanking is done by determining the time location and period of each MECG QRS complex of the reference ECG and setting to zero (clipping) the AECG during these time periods. A major disadvantage of these methods is that the FECG complexes, if coincident, and EMG are also blanked out with the abdominal MECG's QRS complexes. The absence of FECG complexes and EMG make accurate determination of instantaneous fetal HR information and uterine contraction information difficult.

Several techniques have reported to obtain abdominal MECG cancellation by scaling and subtracting from the AECG a reference ECG with a similar shape MECG as the abdominal MECG [45, 74, 75]. Some of these systems were implemented with an analog computer with three amplifiers [45, 75]. Two of the amplifiers were used as preamplifiers for the AECG and reference ECG and the third amplifier was used to subtract the preamplified ECG signals. The gain or scale factor of one of the preamplifiers is adjusted by the user to obtain near optimal cancellation of the abdominal MECG. Another method uses a potentiometer to adjust the scale factor before the ECG signals are amplified to obtain cancellation between the two signals. Then the signals are amplified and subtracted [74]. The above mentioned techniques can produce abdominal MECG cancellation even during simultaneous MECG and FECG complexes. However, the operator must adjust the scale factor and the reference ECG lead position so that its MECG will have a similar amplitude and shape as the abdominal MECG.

Another method used a scale factor, time-shift, and the genetic algorithm (GA) to obtain better matching possibilities for the MECG of the two ECG signals [76, 77]. Since the GA finds the scale and time-shift, less operator intervention was needed. This method, from the scale and time-shift degrees of freedom, allows for more flexibility in the placement of the ECG leads compared to the scale factor method. However, the operator still has to somewhat match the shape of the MECG complexes through lead adjustment to obtain adequate cancellation.

2.1.3 Multiple Lead

The multiple lead techniques for abdominal MECG cancellation include adaptive filter, orthogonal basis, quadratic programming, and single value decomposition (SVD). These

techniques obtain attenuation by combining several adaptively filtered or scaled TECG and/or AECG signals.

2.1.3.1 Adaptive Filter Techniques

There have been two reported adaptive filter techniques for canceling the abdominal MECG. These techniques combine multiple filtered TECG signals and subtract the resulting signal from a single AECG. The first adaptive filter technique uses a conventional multiple channel least-mean-square (LMS) adaptive filter or noise canceler [50, 68, 78, 79, 80] and the second uses a multiple channel time-sequenced adaptive filter [17, 53, 81, 82]. Figure 2-6 presents the LMS and time-sequenced adaptive filters block diagrams for abdominal MECG cancellation.

The conventional LMS adaptive filter method obtains abdominal MECG cancellation by summing four adaptively filtered TECG signals and subtracts the result from the AECG [50, 78, 79]. Figure 2-6(a) shows the multichannel LMS adaptive noise canceler where the filter coefficients for each TECG transversal filter are found via the LMS algorithm. The following describes the multichannel adaptive noise canceler in more detail. From Figure 2-6(a)

$$r(n) = s_5(n) - y(n) \tag{9}$$

and

$$yn)=(\boldsymbol{S}')^{T}\mathbf{W} \tag{10}$$

where $r(n)$ is the output of the adaptive filter, $s_5(n)$ is the nth sample of the AECG, $y(n)$ is the filtered TECG signals summed, $\boldsymbol{S}' = [S'_1(n)\ S'_2(n)\ S'_3(n)\ S'_4(n)]^T$, $\mathbf{W}^T = [\boldsymbol{W}_1\ \boldsymbol{W}_2\ \boldsymbol{W}_3\ \boldsymbol{W}_4]$ which contains the weight or filter vectors for each TECG channel, $S'_k(n) = [1\ s_k(n)\ s_k(n\text{-}1)\ s_k(n\text{-}2)\ \cdots\ s_k(n\text{-}l\text{-}1)]$ which is the portion of the four TECG signals used by the LMS algorithm to update the weight vectors and $r(n)$, $\boldsymbol{W}_k = [w_{k,0}\ w_{k,1}\ w_{k,2}\ \cdots\ w_{k,l}]$ which contains the weights or filter coefficients for the TECG channels k = 1 to 4, and l is the number of coefficients of each TECG transversal filter [50, 78, 79]. (As previously discussed, lower case signal descriptions are the

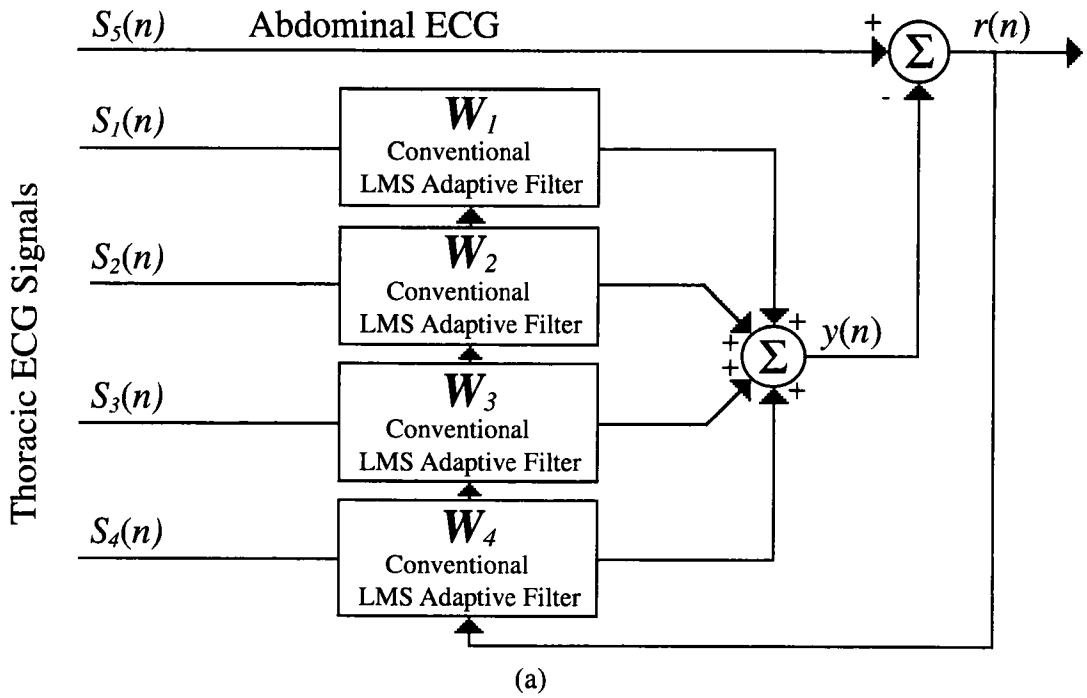

(a)

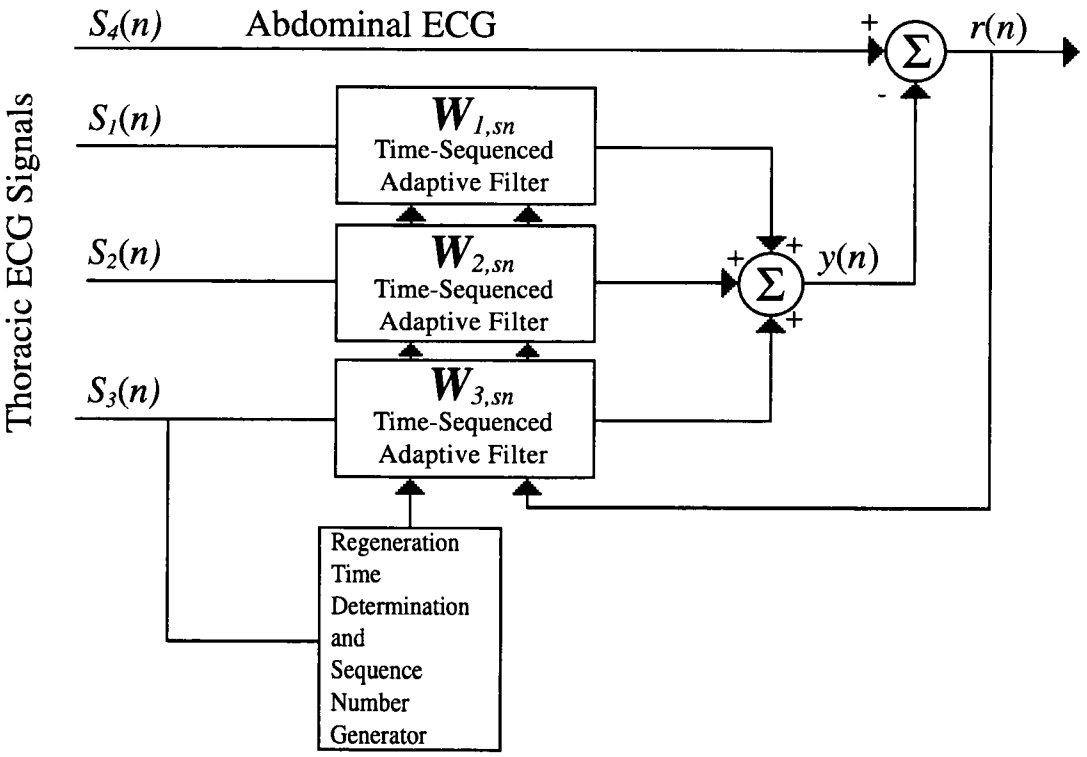

(b)

Figure 2-6. Adaptive filters for abdominal MECG cancellation. (a) Conventional LMS adaptive filter. (b) Time-sequenced adaptive filter.

nth sample of the upper case corresponding signal. e.g. $r(n)$ is the nth sample instance of $R(n)$). Finally, using the LMS algorithm, $\mathbf{W}$ is updated by

$$\mathbf{W}_{n+1} = \mathbf{W}_n + 2\mu r(n)(\mathbf{S}')^T \tag{11}$$

where μ is the convergence coefficient.

Figure 2-7 and Figure 2-8 show a typical result with synthesized data of the multichannel conventional LMS adaptive filter canceling the abdominal MECG. Figure 2-7(a) contains four TECG signals and Figure 2-7(b) contains the AECG. Figure 2-7(c) demonstrates the adaptive filter converging to cancel the MECG of Figure 2-7(b). Finally, Figure 2-8(a) and Figure 2-8(b) are TECG signals and the AECG respectively, but occurs several seconds after the data of Figure 2-7. Figure 2-8(c) demonstrates the cancellation of the MECG after the multichannel conventional LMS adaptive filter has converged.

The time-sequenced adaptive filter has been designed to filter signals that are cyclostationary, such as the ECG, as compared to the conventional LMS adaptive filter which has been designed for use with stationary signals. Furthermore, the time-sequenced adaptive filter is a time-varying filter whereas the LMS adaptive filter is time-invariant [82, 83]. Because of the aforementioned, this filter has proven to be more effective for canceling the MECG as compared to the traditional LMS adaptive filter [84]. The time-sequenced adaptive filter method for abdominal MECG suppression combine the filtered TECG signals similar to the LMS adaptive filter method, but differs from the fact that the time-sequenced adaptive filter uses multiple time-sequenced weight vectors instead of one weight vector to filter each TECG signal and that three TECG channels are used instead of four [17, 81].

The time-sequenced adaptive filter method first detects the TECG $S_3(n)$ QRS complexes [85]. The TECG QRS complexes are used to determine the regeneration times which occur 150 ms before the R wave of the detected QRS complexes [17]. Next, the sequence number is set to zero at each regeneration time and a specific weight vector is assigned to each sequence number to filter a designated section of each TECG. The time-sequenced weight vectors are used to filter 300 ms after each regeneration time. Finally, the sections of the AECG that do not fall into the time-sequenced sections are filtered using the traditional LMS adaptive filter.

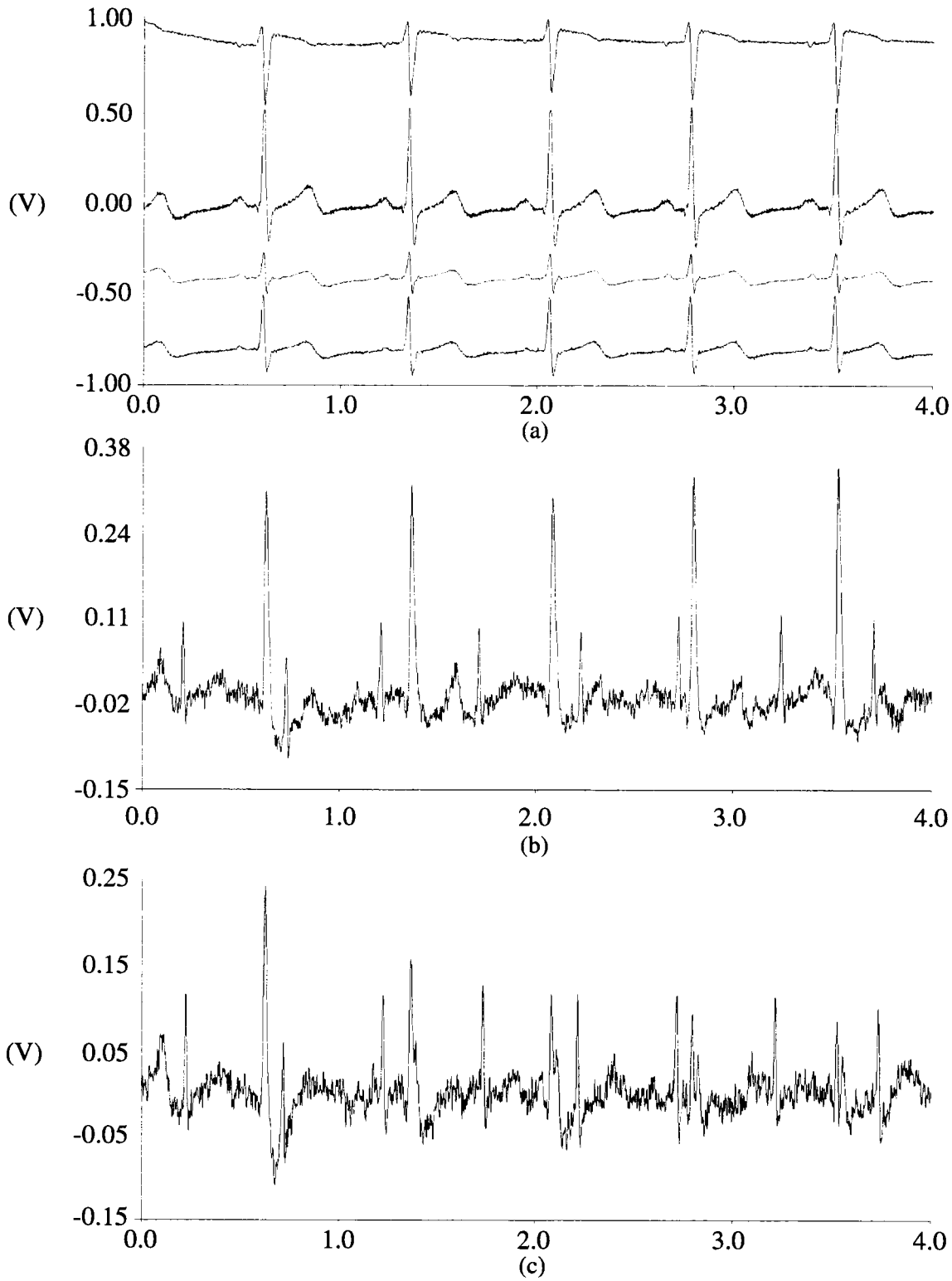

Figure 2-7. Conventional LMS adaptive filter converging (all x-axes in seconds). (a) Four reference TECG signals. (b) AECG. (c) The LMS adaptive filter converging to cancel the abdominal MECG.

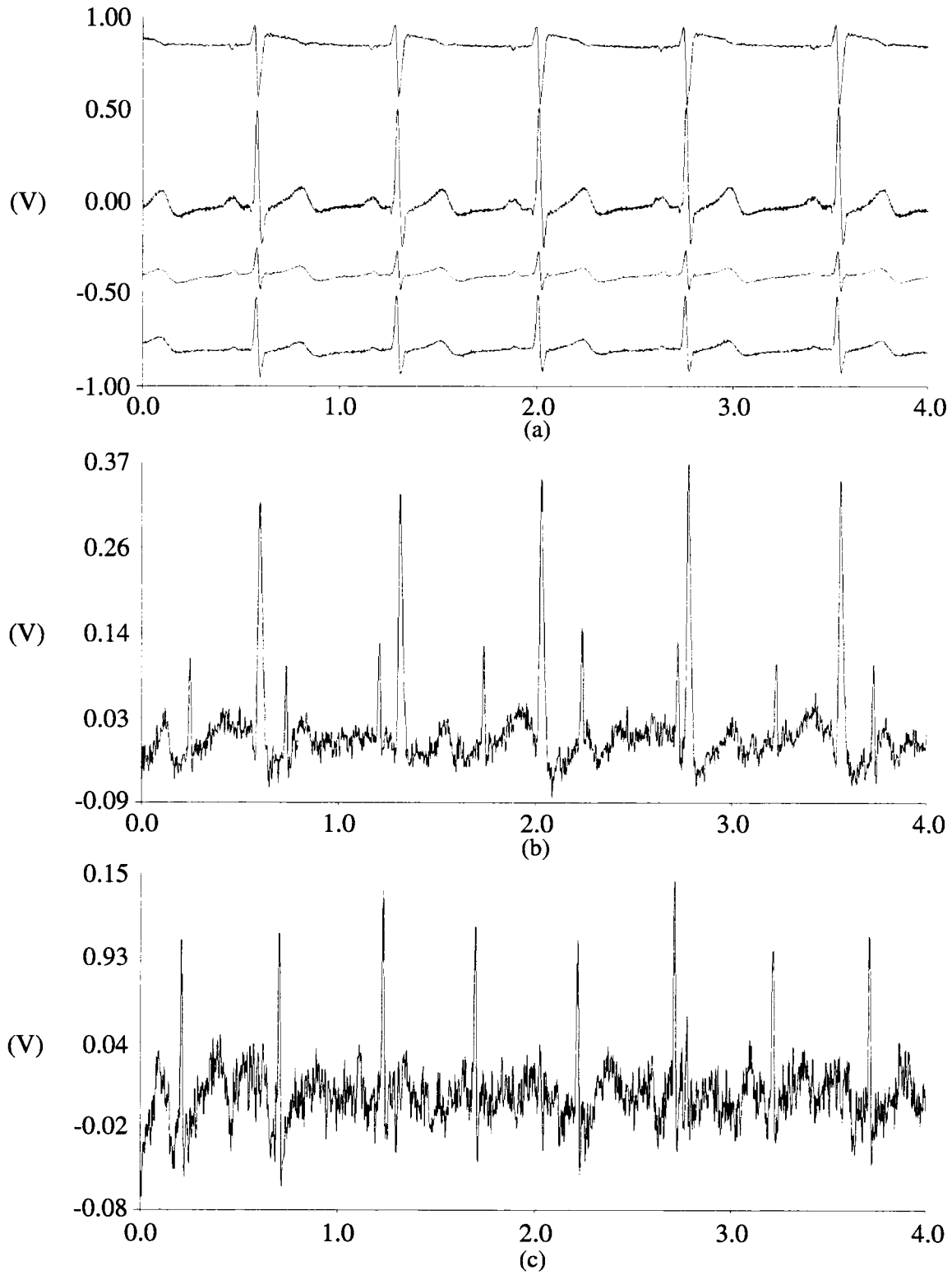

Figure 2-8. Conventional LMS adaptive filter after converging (all x-axes in seconds). (a) Four reference TECG signals. (b) AECG. (c) LMS adaptive filter output that has converged.

Figure 2-6(b) contains a block diagram of the time-sequenced adaptive filter for abdominal MECG cancellation and the following describes the filter in more detail [17, 81, 82, 83, 86]. From Figure 2-6(b)

$$r(n) = s_A(n) - y(n), \tag{12}$$

$$y(n) = (\boldsymbol{S}')^T \boldsymbol{W}_{sn}, \quad \text{Time-sequenced adaptive filter section} \tag{13}$$

and

$$y(n) = (\boldsymbol{S}')^T \boldsymbol{W} \quad \text{LMS adaptive filter section} \tag{14}$$

where $r(n)$ is the output of the filter, $s_A(n)$ is the nth sample of the AECG, $y(n)$ is the filtered TECG signals summed, $\boldsymbol{S}' = [S'_1(n)\ S'_2(n)\ S'_3(n)]^T$ that contains the three TECG signals, $\boldsymbol{W}_{sn}^T = [W_{1,sn}\ W_{2,sn}\ W_{3,sn}]$ and $\boldsymbol{W}^T = [W_1\ W_2\ W_3]$ which contain the weight vectors for each TECG channel, $S'_k(n) = [1\ s_k(n)\ s_k(n-1)\ s_k(n-2)\ \cdots\ s_k(n-l-1)]$ and is the portion of the signal used by the adaptive filter to update the weight vectors and $r(n)$, $\boldsymbol{W}_{k,sn} = [w_{k,sn,0}\ w_{k,sn,1}\ w_{k,sn,2}\ \cdots\ w_{k,sn,l}]$ and $\boldsymbol{W}_k = [w_{k,0}\ w_{k,1}\ w_{k,2}\ \cdots\ w_{k,l}]$ which contain the weights for channels k = 1 to 4, sn is the sequence number, and l is the number of coefficients of each TECG transversal filter. Finally, using time-sequencing and the LMS algorithm, $\boldsymbol{W}_{rgt,sn}$ and $\boldsymbol{W}_n$ are updated by

$$\boldsymbol{W}_{next\ rgt,sn} = \boldsymbol{W}_{rgt,sn} + 2\mu_{sn} r(n)(\boldsymbol{S}')^T \quad \text{Time-sequenced adaptive filter section} \tag{15}$$

and

$$\boldsymbol{W}_{n+1} = \boldsymbol{W}_n + 2\mu r(n)(\boldsymbol{S}')^T \quad \text{LMS adaptive filter section} \tag{16}$$

where rgt is the regeneration time, μ_{sn} is the convergence coefficient for the time-sequenced part of the adaptive filter and has different values that are referenced by the sequence number, and μ is the convergence coefficient of the LMS adaptive filter section.

Figure 2-9 and Figure 2-10 show typical results with synthesized data of the multichannel time-sequenced adaptive filter canceling the abdominal MECG. Figure 2-9(a) contains three

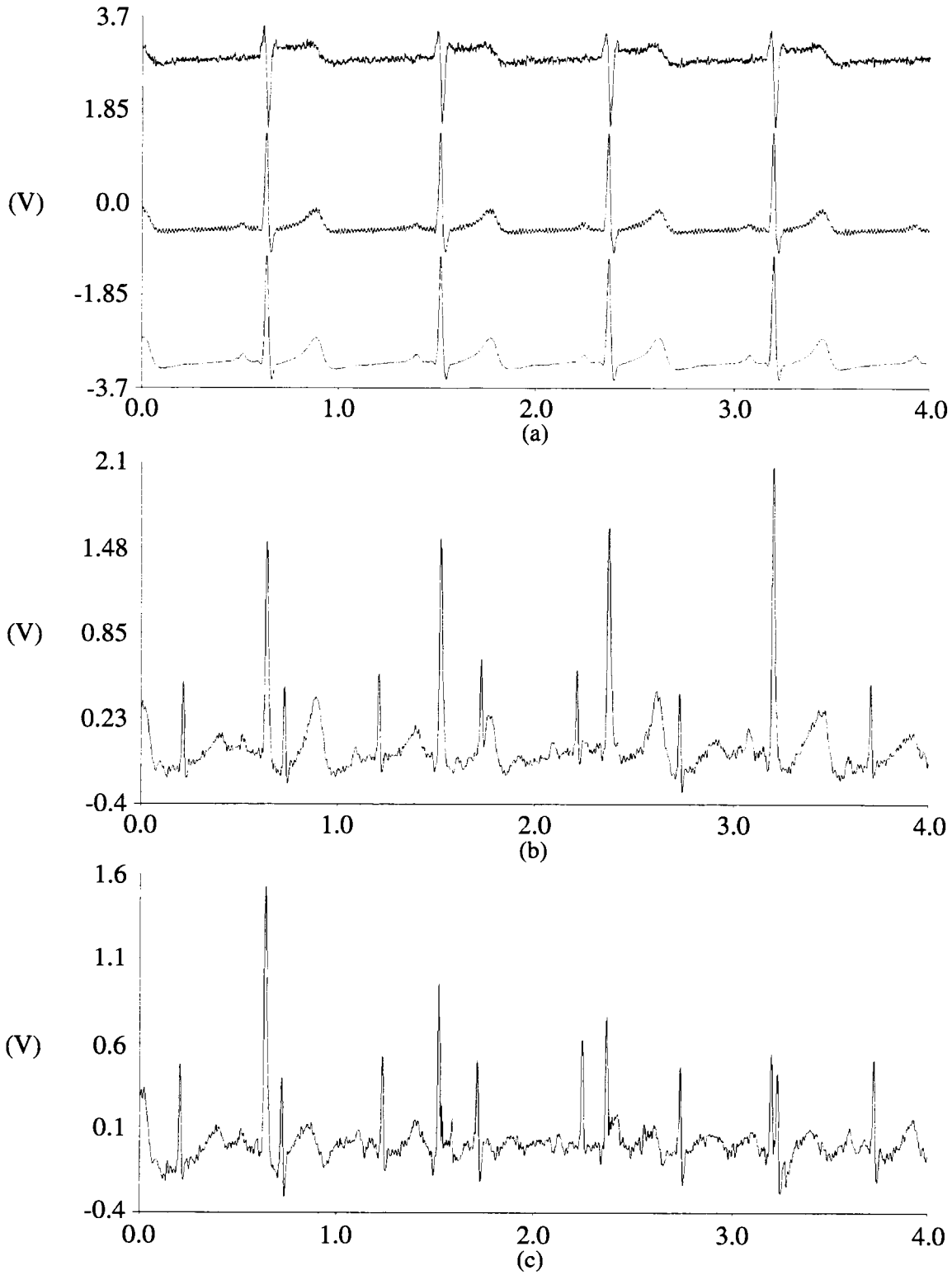

Figure 2-9. Time-sequenced adaptive filter converging (all x-axes in seconds). (a) Three reference TECG signals. (b) AECG. (c) Time-sequenced adaptive filter converging to cancel the abdominal MECG.

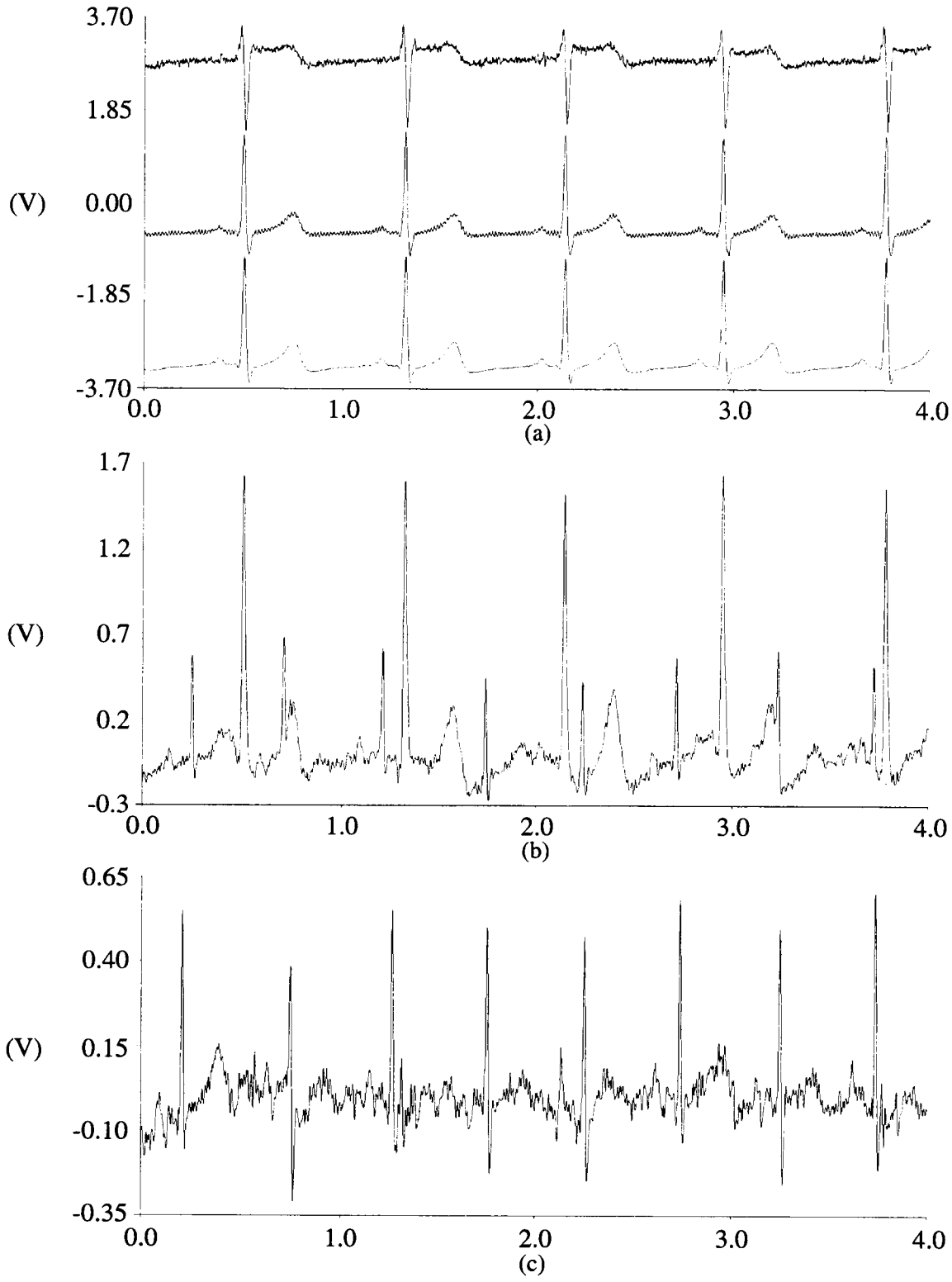

Figure 2-10. Time-sequenced adaptive filter after converging (all x-axes in seconds). (a) Three reference TECG signals. (b) AECG. (c) Time-sequenced adaptive filter output after converging.

TECG signals and Figure 2-9(b) contains the AECG. Figure 2-9(c) demonstrates the adaptive filter converging to cancel the AECG of Figure 2-9(b). Finally, Figure 2-10(a) and Figure 2-10(b) are TECG signals and the AECG respectively, but occurs several seconds after the data of Figure 2-9. Figure 2-10(c) demonstrates the cancellation of the MECG after the time-sequenced adaptive filter has converged.

2.1.3.2 Orthogonal Basis Technique

The orthogonal basis method uses three TECGs $S_{1\text{-}3}(n)$ to cancel the abdominal MECG [51, 87]. Cancellation is accomplished by transforming $S_{1\text{-}3}(n)$ into orthogonal signals $S`_{1\text{-}3}(n)$ via the Gram-Schmidt procedure. Next, the resulting signals are scaled and added to the AECG to cancel the MECG.

The following describes the orthogonal basis method in more detail. The first orthogonal signal $S`_1(n)$ is found by

$$S`_1(n) = S_1(n). \tag{17}$$

The other two orthogonal signals $S`_{2\text{-}3}(n)$ are then found from

$$S`_k(n) = S_k(n) - \sum_{j=1}^{k-1} \alpha_{kj} S`_j(n) \qquad k = 2, 3 \tag{18}$$

where

$$\alpha_{kj} = 1/\beta_j \sum_{n=0}^{N-1} S_k(n) S`_j(n), \tag{19}$$

and

$$\beta_j = \sum_{n=0}^{N-1} [S`_j(n)]^2. \tag{20}$$

From the orthogonal signals and weighting coefficients, (21) can be written

$$R(n) = w_1 S`_1(n) + w_2 S`_2(n) + w_3 S`_3(n) + S_A(n) \tag{21}$$

where $S_A(n)$ is the AECG, $R(n)$ is $S_A(n)$ with the MECG canceled, and w_k`s are scale factors given by

$$w_k = -1.0/\beta_k \sum_{n=0}^{N-1} S_A(n) S`_k(n). \tag{22}$$

Figure 2-11 contains synthesized data where Figure 2-11(a) presents the three TECG signals, Figure 2-11(b) contains the AECG, and Figure 2-11(c) is the result of orthogonal basis technique for abdominal MECG cancellation.

The accuracy of the orthogonalization of $S_{1\text{-}3}(n)$, the calculation of $w_{1\text{-}3}$, and ultimately the cancellation of the abdominal MECG of (21) is dependent on the time period N of the summation in (19), (20), and (22). If N includes one period of the abdominal MECG, cancellation of the FECG may occur from correlation between the FECG and the abdominal MECG [51]. To avoid this problem, two or more periods of the MECG are recommended to avoid correlation to accurately obtain abdominal MECG cancellation. Since the TECG and AECG signals have to be broken into blocks of samples of length N to implement the aforementioned procedure, a variation on the orthogonal basis technique that uses a near-orthogonal procedure has been developed by relaxing the strict orthogonality requirement to allow for a continuous mode of operation [51]. Finally, a second variation on the orthogonal basis technique has been reported [88, 89].

2.1.3.3 Quadratic Programming Technique

The quadratic programming technique for abdominal MECG cancellation linearly combines K AECG signals such that the MECG is canceled and the SNR of the FECG is not decreased and possibly increased [13, 52, 90]. An iterative quadratic programming procedure by Hildreth and d'Esopo is used to determine the coefficients that linearly combine the AECG signals [91]. The following describes the method in more detail [13].

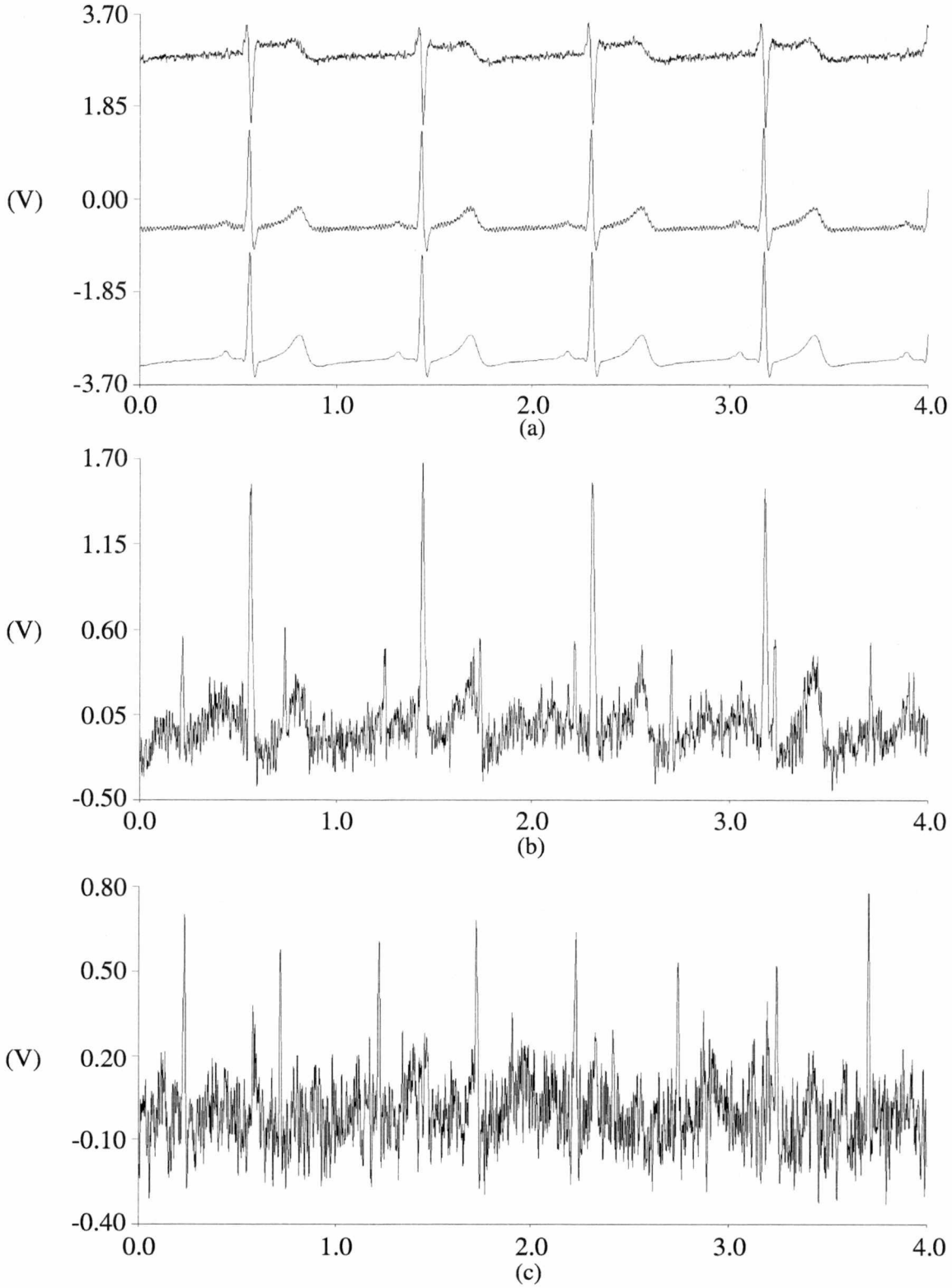

Figure 2-11. Orthogonal basis method (all x-axes in seconds). (a) Three reference TECG signals. (b) AECG. (c) The output of the orthogonal basis technique.

An AECG can be linearly combined with other AECG signals through weighting coefficients to produce a resulting signal

$$R(n) = \sum_{k=1}^{K} w_k S_k(n). \tag{23}$$

By replacing each AECG of (23) with (3) where $Md_k(n)$ is unity, then

$$R(n) = \sum_{k=1}^{K} w_k M_k(n) + \sum_{k=1}^{K} w_k F_k(n) + \sum_{k=1}^{K} w_k N_k(n). \tag{24}$$

To cancel the MECG of (24) without decreasing the resulting FECG's SNR compared to the individual AECG signals,

$$\sum_{k=1}^{K} w_k M_k(n) = \mathbf{0} \tag{25}$$

and

$$\sum_{k=1}^{K} w_k F_k(n) \neq \mathbf{0} \tag{26}$$

have to be true. The weighting coefficients that satisfy (25) and (26) are found by creating a quadratic programming problem and solving it with a procedure developed by Hildreth and d'Esopo.

The quadratic programming problem is formed from (25) and (26) by developing a quadratic function and boundary conditions. The quadratic function is formed from (25) where $M_k(n)$ is substituted with $M'_k(n)$ which is an MECG complex average with zero mean from the kth AECG or

$$q(n) = \sum_{k=1}^{K} w_k M'_k(n). \tag{27}$$

The variance of $q(n)$ or the quadratic function is written as

$$\sigma^2_q = E[q(n)q^{\mathrm{T}}(n)]. \tag{28}$$

If the MECG of each AECG contains positive and negative contributions from the MECG source signals $SS_{1\text{-}3}(n)$ through the placement of electrodes, then (28) can be minimized such that (25) will be true [92]. The boundary conditions of the quadratic programming problem are determined from (26) and are

$$\sum_{k=1}^{K} w_k \neq 0 \tag{29}$$

and

$$w_k \geq 0 \tag{30}$$

where (29) excludes the zero solution and (30) requires all weighting coefficients to be positive so that the resulting FECG's SNR of (24) is not decreased compared to the kth AECG. For (30) to be effective, the AECG leads have to be positioned such that the FECG is positively correlated in all the AECG leads. Furthermore, if the noise of each AECG is partly uncorrelated or completely uncorrelated, (29) and (30) will cause the resulting FECG's SNR to increase compared to the kth AECG. Finally, the quadratic programming procedure of Hildreth and d'Esopo is then used to minimize (28) subject to the boundary conditions of (29) and (30) to find the desired weighting coefficients. Once the coefficients are determined, the AECG signals are linearly combined to produce a resulting signal of (23) that contains no MECG and the FECG's SNR is possibly increased provided the AECG leads were positioned correctly.

Figure 2-12 presents a reimplementation of the quadratic programming technique with synthesized data. Figure 2-12(a) contains six AECG signals and Figure 2-12(b) is the resulting

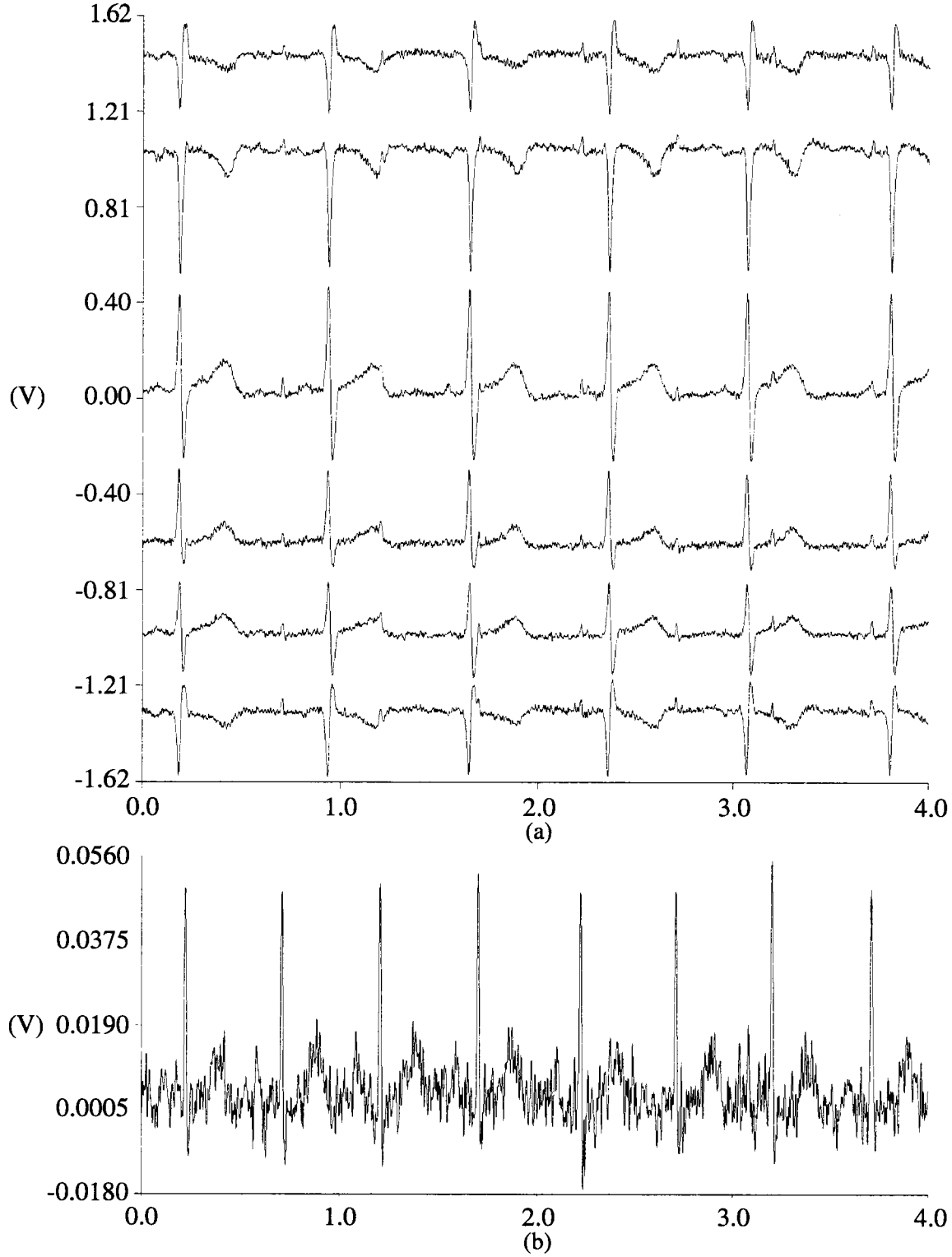

Figure 2-12. Quadratic programming technique (all x-axes in seconds). (a) AECG signals. (b) Output of the quadratic programming technique with the MECG canceled and the FECG's SNR increased compared to the *k*th AECG.

signal of the quadratic programming technique such that the linear combination of the six signals of Figure 2-12(a) suppresses the MECG and increases the FECG's SNR.

A real-time implementation of the quadratic programming technique has been developed. First, a digital computer computes the weighting coefficients. Second, the analog AECG signals are multiplied by their respective coefficients and the resulting analog signals are summed with an analog summing amplifier [13]. Finally, since the coefficients are relatively time-invariant, they only have to be calculated as an initialization procedure and are updated somewhat regularly to compensate for any time-variant characteristics [13].

2.1.3.4 Singular Value Decomposition Techniques

Basically, three different techniques that use the singular value decomposition algorithm with multiple TECG and/or AECG to cancel the abdominal MECG have been reported [14, 15, 61, 93, 94, 95, 96, 97, 98, 99]. The first SVD method for abdominal MECG attenuation is based on decomposing three TECG and three AECG signals [14]. (31) defines the singular value decomposition of $\boldsymbol{S}^{\mathrm{T}}_{K,N}$

$$\boldsymbol{S}^{\mathrm{T}}_{K,N} = \boldsymbol{U}_{N,K}\boldsymbol{\Sigma}_{K,K}\boldsymbol{V}^{\mathrm{T}}_{K,K} \tag{31}$$

where the first three rows of $\boldsymbol{S}_{K,N}$ are the TECG signals and the last three are the AECG signals or $\boldsymbol{S}_{K,N} = [\boldsymbol{S}_1(n)\ \boldsymbol{S}_2(n)\ \boldsymbol{S}_3(n)\ \boldsymbol{S}_4(n)\ \boldsymbol{S}_5(n)\ \boldsymbol{S}_6(n)]^{\mathrm{T}}$, the columns of $\boldsymbol{U}$ contain the orthonormal source signals of the rows of $\boldsymbol{S}$, the diagonal elements of $\boldsymbol{\Sigma}$ are the non-negative singular values in decreasing order of the orthonormal source signals of the columns of $\boldsymbol{U}$, and $\boldsymbol{V}$ is the orthogonal transformation matrix. The first three singular values of $\boldsymbol{\Sigma}$ are associated with the MECG if the three TECG signals contain three dominant source signals due to TECG lead placement compared to the FECG and noise. The fourth and fifth singular values are associated with the FECG if two source signals of the FECG are present and the sixth singular value is attributed to noise. Method one finds the orthogonal source signals of the MECG and FECG by computing $\boldsymbol{\Sigma}$ and $\boldsymbol{V}$. Then $\boldsymbol{S}$ is transformed with $\boldsymbol{V}$ or

$$\boldsymbol{S}\boldsymbol{S}^{\mathrm{T}}_{K,N} = \boldsymbol{S}^{\mathrm{T}}_{K,N}\boldsymbol{V}_{K,K}. \tag{32}$$

The first three rows of $\boldsymbol{SS}_{K,N}$ are the MECG orthogonal source signals $SS_{1\text{-}3}(n)$ and the fourth and fifth are the FECG orthogonal source signals $SS_{4\text{-}5}(n)$ with no MECG. The last row is noise. ($\boldsymbol{U}$ is not found because it requires much computation time with the Golub and Reinsch SVD procedure and from (32) is not needed [100, 101].) Finally, SVD method one can be modified into an on-line adaptive algorithm that computes the $\boldsymbol{V}$ matrix of (32) [15, 95].

The data of Figure 2-13 is synthesized data where Figure 2-13(a) contains the three TECG and Figure 2-13(b) presents the two AECG used to reimplement the SVD method one. Figure 2-14(a) presents the resulting MECG source signal $SS_{1\text{-}3}(n)$. Figure 2-14(b) contains the source signals of the FECG $SS_4(n)$ and noise. Only one source signal of the FECG is present because the synthesized data contained only one component of the FECG.

The second SVD method for abdominal MECG suppression is similar to the first because it decomposes several ECG signals, but the rows of $\boldsymbol{S}_{K,N}$ contain K AECG signals where K has to be greater than four or $\boldsymbol{S}_{K,N} = [\boldsymbol{S}_1(n)\ \boldsymbol{S}_2(n)\ \boldsymbol{S}_3(n)\ \boldsymbol{S}_4(n)\ \cdots\ \boldsymbol{S}_K(n)]^{\mathrm{T}}$ [14, 61]. Via visual inspection of $\boldsymbol{S}_{K,N}$, $\boldsymbol{S}^{M}{}_{K,N'}$ is created by manually selecting portions of the AECG signals that contain no FECG and only the MECG components such as the P, QRS, and T waves to accurately describe the MECG. Once the desired signal components of the MECG have been determined, all the non-desired parts of each AECG signal are discarded from $\boldsymbol{S}_{K,N}$, to form $\boldsymbol{S}^{M}{}_{K,N'}$. All signals of the rows of $\boldsymbol{S}^{M}{}_{K,N'}$ contain N' samples. Next, the SVD of $\boldsymbol{S}^{M}{}_{K,N'}$ is computed, but only $\boldsymbol{\Sigma}$ and $\boldsymbol{V}$ are determined. Then $\boldsymbol{V}$ is used to transform $\boldsymbol{S}^{\mathrm{T}}{}_{K,N}$ or (33) to produce several ECG signals

$$\boldsymbol{R}^{\mathrm{T}}{}_{K,N} = \boldsymbol{S}^{\mathrm{T}}{}_{K,N}\,\boldsymbol{V}^{T}{}_{K,K} \tag{33}$$

that do not contain the MECG or the null space of the MECG. The singular values of $\boldsymbol{\Sigma}$ that are zero or near zero indicate the null space of the MECG. The columns of $\boldsymbol{V}$ that correspond to these singular values will cancel the MECG of $\boldsymbol{S}_{K,N}$ or

$$(\boldsymbol{R}'_{K\text{-}r_m,N})^{\mathrm{T}} = \boldsymbol{S}^{\mathrm{T}}{}_{K,N}\boldsymbol{V}^{0}{}_{K,K\text{-}r_m} \tag{34}$$

where $\boldsymbol{V}^{0}$ contains the columns of $\boldsymbol{V}$ that correspond to the singular values of $\boldsymbol{\Sigma}$ that are zero or near zero, $\boldsymbol{R}'$ is the null space of the MECG, and r_m is the rank of $\boldsymbol{S}^{M}{}_{K,N'}$. Furthermore, $\boldsymbol{V}^{0}$ can also be determined from $\boldsymbol{V}$ from the rank of $\boldsymbol{S}^{M}{}_{K,N'}$. For example, if $K = 10$ and the rank of $\boldsymbol{S}^{M}{}_{K,N'}$

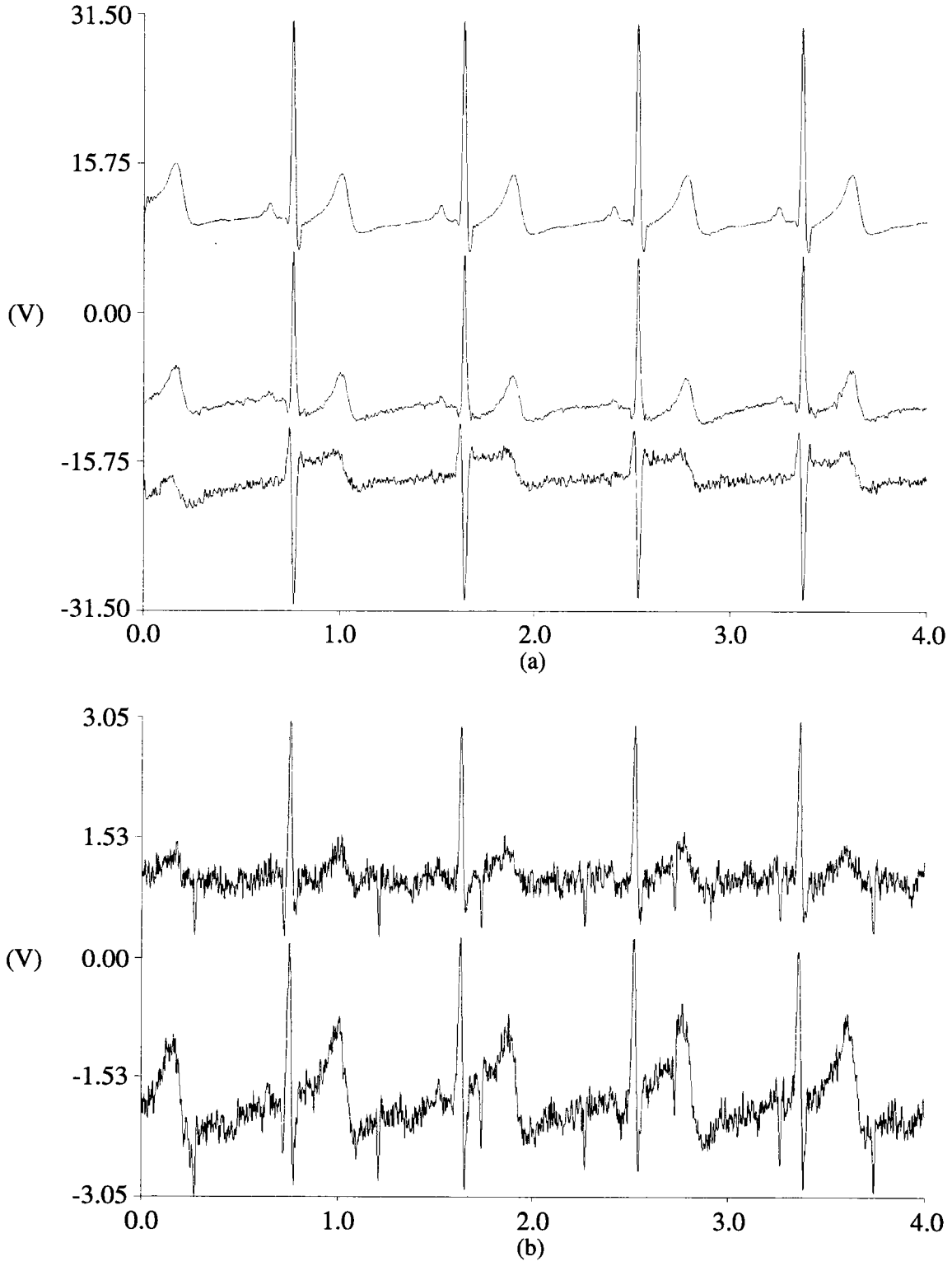

Figure 2-13. Synthesized ECG signals used to reimplement SVD method one (all x-axes in seconds). (a) Three reference TECG signals. (b) Two AECG signals.

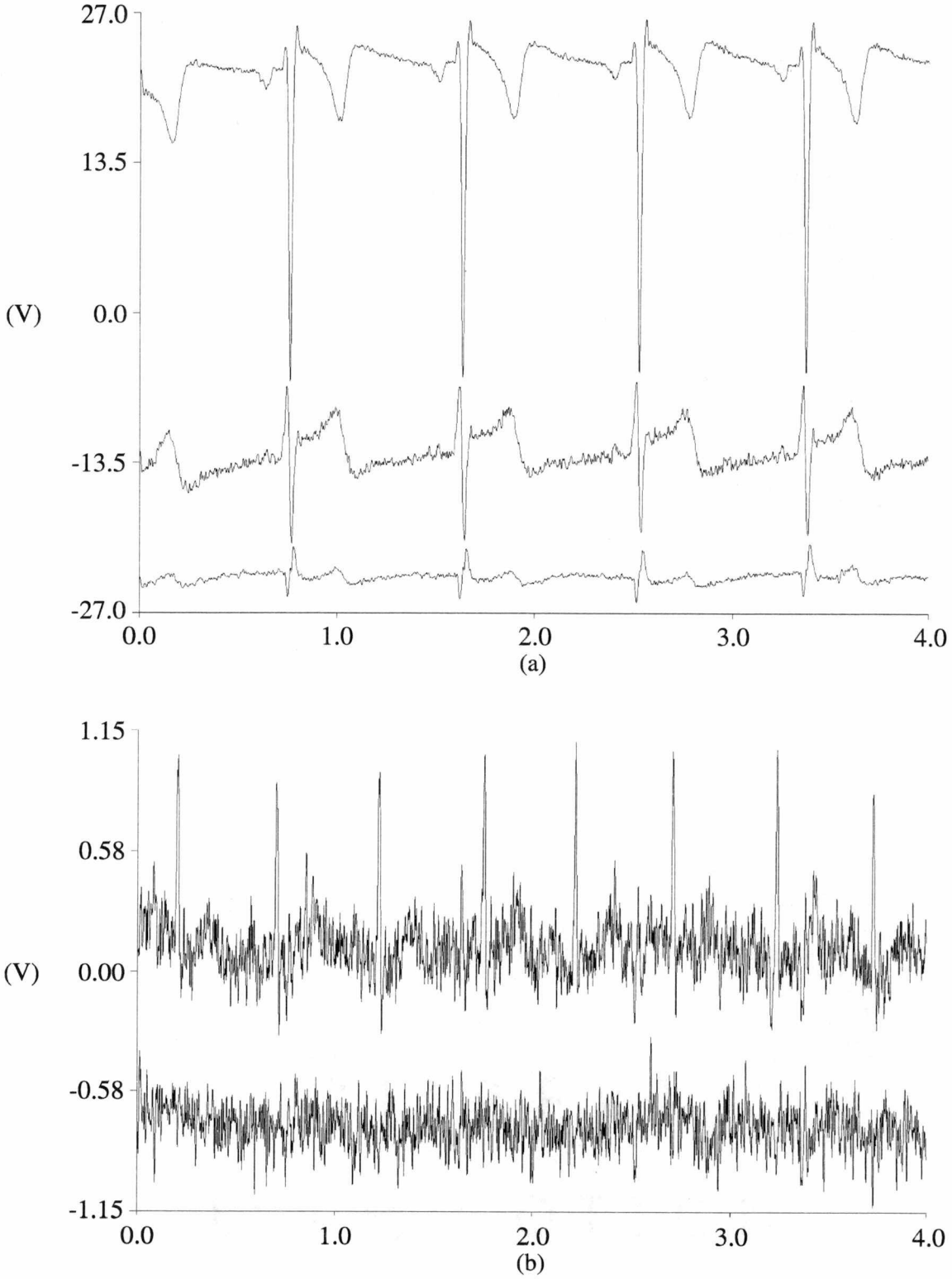

Figure 2-14. Results of reimplementing SVD method one (all x-axes in seconds). (a) Source signals $SS_{1\text{-}3}(n)$ of the MECG. (b) Source signal $SS_4(n)$ of the FECG and noise.

was five, then V^0 would contain the last five columns of V. SVD method two can be modified to operate in an on-line fashion that adaptively modifies the coefficients of V^0 to compensate for the time-variant characteristics of the FECG from fetal movements [15, 95].

Figure 2-15 presents ten synthesized AECG signals used to reimplement the SVD method two. Figure 2-16(a) presents the first five rows or resulting signals of $\boldsymbol{R}_{K,N}$. Figure 2-16(b) present the rows of $\boldsymbol{R}'_{K,N}$ or resulting signals that contain no MECG and make up the null space of the MECG. Finally, Figure 2-16(a) and Figure 2-16(b) are the ten rows of $\boldsymbol{R}_{K,N}$.

The third SVD method is based on the generalized singular value decomposition (GSVD) algorithm [14]. GSVD decomposes the matrix pair $(\boldsymbol{S}^{\mathrm{T}}{}_{K,N}, (\boldsymbol{S}^{M}{}_{K,N'})^{\mathrm{T}})$ as described in method two, but $\boldsymbol{S}^{M}{}_{K,N'}$ only contains MECG QRS complexes and no P and T waves. To compute the GSVD of $(\boldsymbol{S}^{\mathrm{T}}{}_{K,N}, (\boldsymbol{S}^{M}{}_{K,N'})^{\mathrm{T}})$, the SVD of $\boldsymbol{S}^{M}{}_{K,N'}$ or

$$(\boldsymbol{S}^{M}{}_{K,N'})^{\mathrm{T}} = (\boldsymbol{U}_M)(\boldsymbol{\Sigma}_M)(\boldsymbol{V}_M)^{\mathrm{T}} \tag{35}$$

is computed. Using $\boldsymbol{\Sigma}_M$ and $\boldsymbol{V}_M$, a transformation of $\boldsymbol{S}_{K,N}$ is made or

$$(\boldsymbol{S}^{*}{}_{K,N})^{\mathrm{T}} = (\boldsymbol{S}^{\mathrm{T}}{}_{K,N})(\boldsymbol{V}_M)(\boldsymbol{\Sigma}_M)^{-1} \tag{36}$$

and the SVD of $\boldsymbol{S}^{*}{}_{K,N}$ is computed or

$$(\boldsymbol{S}^{*}{}_{K,N})^{\mathrm{T}} = (\boldsymbol{U}^{*})(\boldsymbol{\Sigma}^{*})(\boldsymbol{V}^{*})^{\mathrm{T}}. \tag{37}$$

Finally, $(\boldsymbol{S}^{*}{}_{K,N})^{\mathrm{T}}$ is transformed with $\boldsymbol{V}^{*}$ or

$$(\boldsymbol{R}_{K,N})^{\mathrm{T}} = (\boldsymbol{S}^{*}{}_{K,N})^{\mathrm{T}}\boldsymbol{V}^{*}{}_{K,K}. \tag{38}$$

$\boldsymbol{S}^{\mathrm{T}}{}_{K,N}$ is transformed with $(\boldsymbol{V}_M)(\boldsymbol{\Sigma}_M)^{-1}$ and then with $\boldsymbol{V}^{*}$ to form $\boldsymbol{R}_{K,N}$ where the first two or three rows only contain non-orthogonal FECG components and the rest of the rows contain non-orthogonal MECG components and noise. SVD method three can be modified to an on-line adaptive algorithm that modifies $\boldsymbol{V}^{*}$ to compensate for fetal movements [15, 95].



Figure 2-15. AECG signals used with singular value decomposition method two.

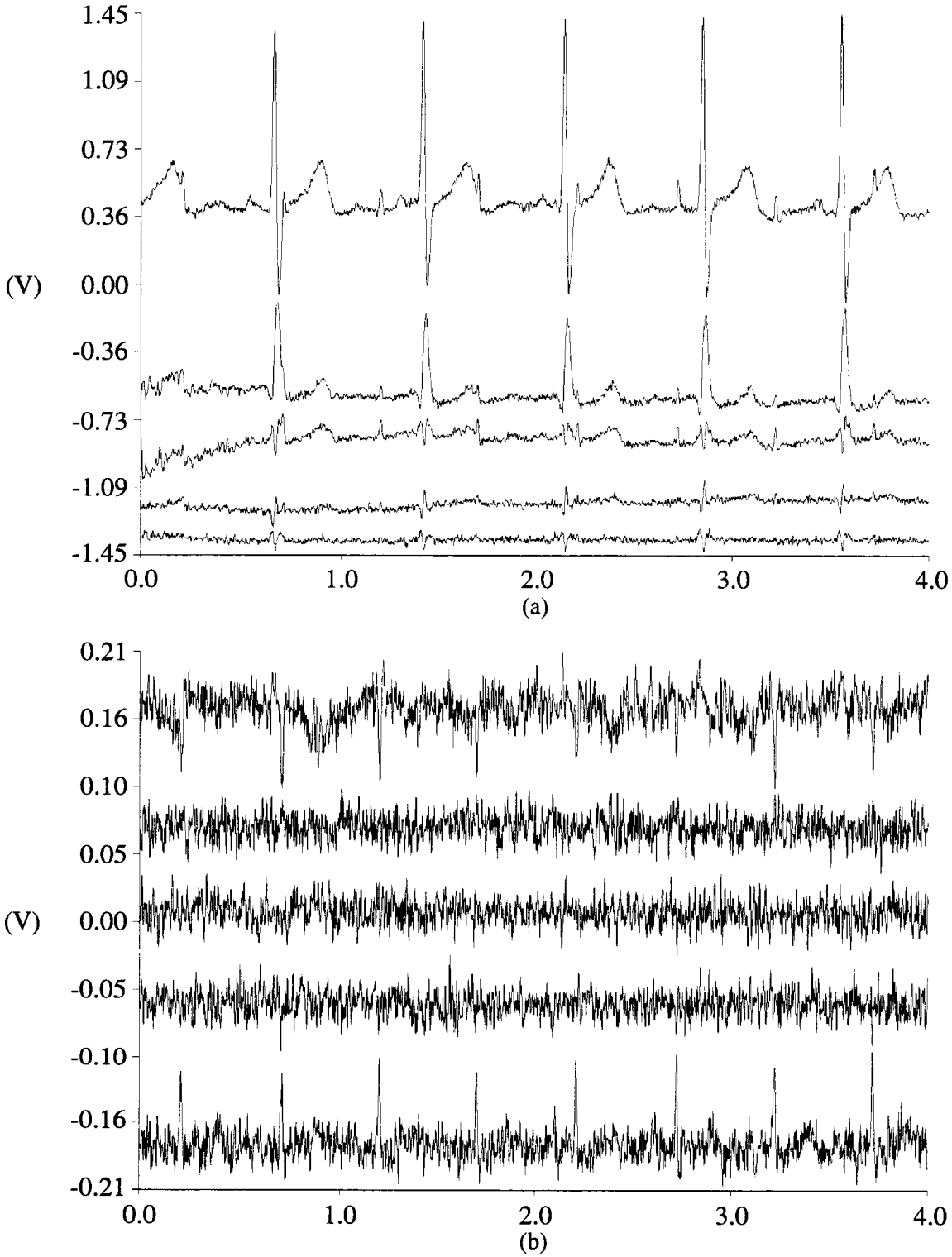

Figure 2-16. Results of singular value decomposition method two (all x-axes in seconds). (a) The first five signals of $\boldsymbol{R}$. (b) The rows of $\boldsymbol{R}'$ or the last five signals of $\boldsymbol{R}$.

Figure 2-17 presents eight synthesized AECG signals that will be used to demonstrate SVD method three. Figure 2-18 contains the rows of $\boldsymbol{S}^*_{K,N}$ of (36) found from the transformation of $\boldsymbol{S}^{\mathrm{T}}_{K,N}$ by $\boldsymbol{V}_M$ and $(\boldsymbol{\Sigma}_M)^{-1}$. Figure 2-19 presents the rows of $\boldsymbol{R}_{K,N}$ of (38) found by the transformation of $(\boldsymbol{S}^*_{K,N})^{\mathrm{T}}$ by $\boldsymbol{V}^*$. The first signal of 2-19 is the FECG and the last seven signals are non-orthogonal MECG components and noise. Only one FECG component is present in the rows of $\boldsymbol{R}_{K,N}$ because the original synthesized AECG signals in the rows of $\boldsymbol{S}_{K,N}$ only contain one FECG component.

2.2 FECG SNR Enhancement Techniques

Several different techniques have been developed for FECG SNR enhancement and can be divided into three filter types. The first is based on spatial filtering that linearly combines several spatially measured AECG signals simultaneous in time. The second is based on temporal filtering or developing an FECG average complex from several complexes that occur sequentially in time. Finally, the third type uses a digital impulse response filter to improve the FECG's SNR.

2.2.1 Spatial Filtering

Three different groups of spatial filtering techniques have been reported in the literature that include additive, quadratic programming, and singular value decomposition. The additive methods are the simplest of the three spatial filtering techniques and are based on summing several spatially measured AECG signals [46, 49, 102]. If the noise of each AECG is uncorrelated and if the FECG of each AECG is positively correlated with its respective lead, the variance of the white gaussian noise $\sigma_{ave,spatial}$ of the resulting signal will be reduced by a factor of the square root of K, where K is the number of AECG leads of the summation, compared to the original variance of each AECG $\sigma_{orig,spatial}$ [49] or

$$\sigma_{ave,spatial} = (\sigma_{orig,spatial})/(K^{1/2}). \tag{39}$$

Two of the reported additive methods attempt to obtain partial abdominal MECG suppression during the summation [46, 102]. The third technique cancels the MECG after the summation by blanking it out as described in Section 2.1.2 [49]. Finally, Figure 2-20 is a reimplementation of

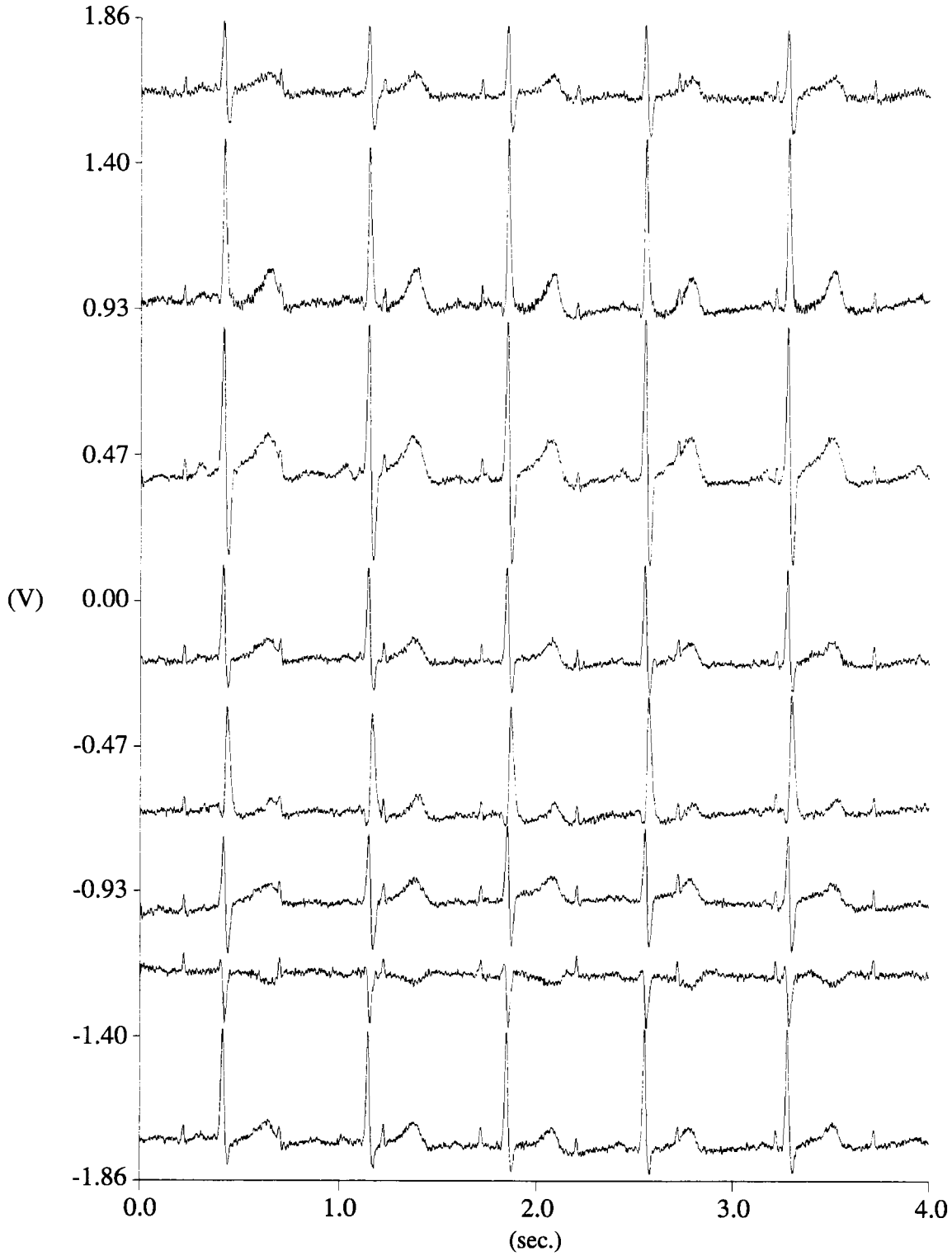

Figure 2-17. Eight AECG signals used with singular value decomposition method three.

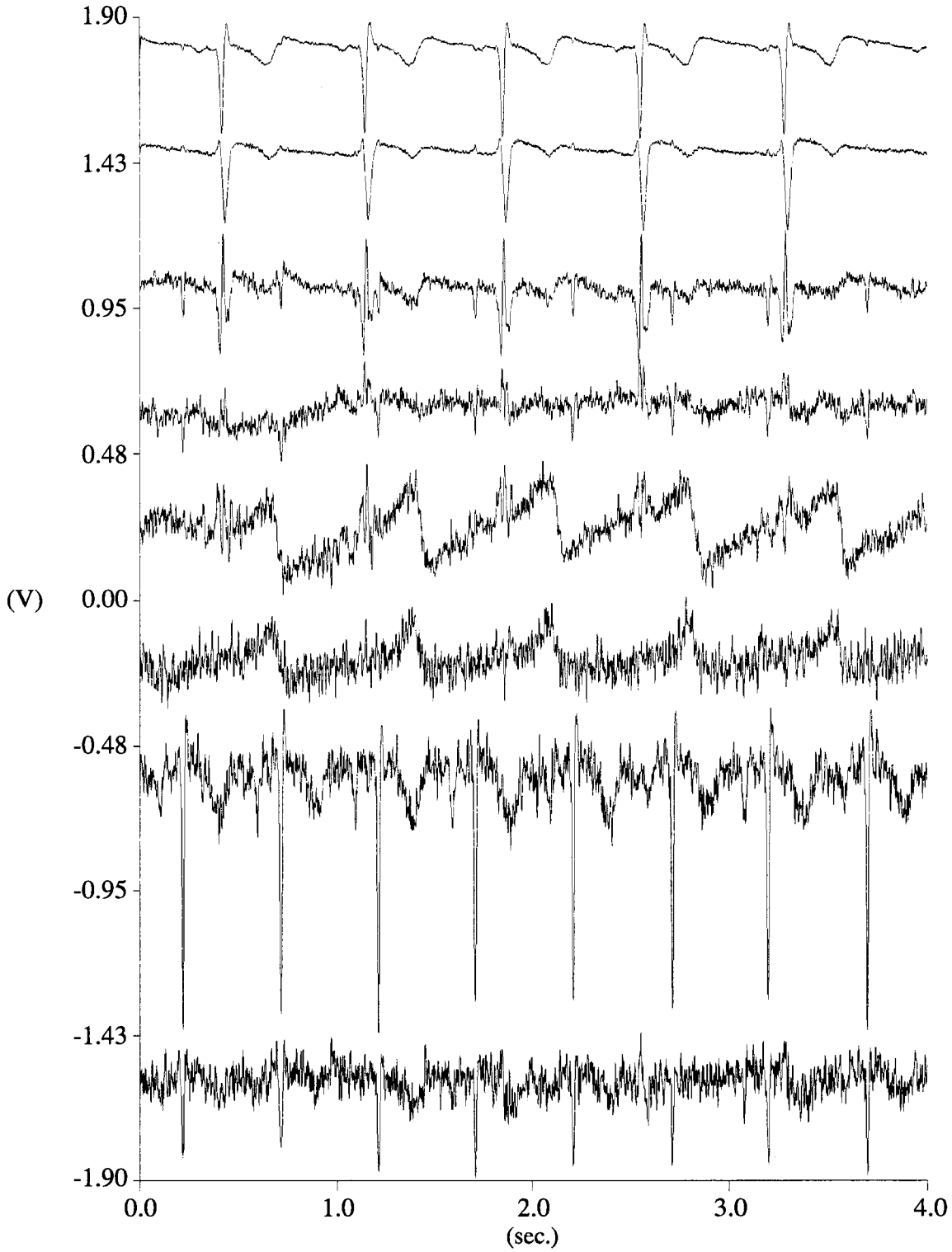

Figure 2-18. Results of the first transformation of SVD method three. Each above signal is a row of $S^*_{K,N}$ found from the transformation of $S^T_{K,N}$ by V_M and $(\Sigma_M)^{-1}$.

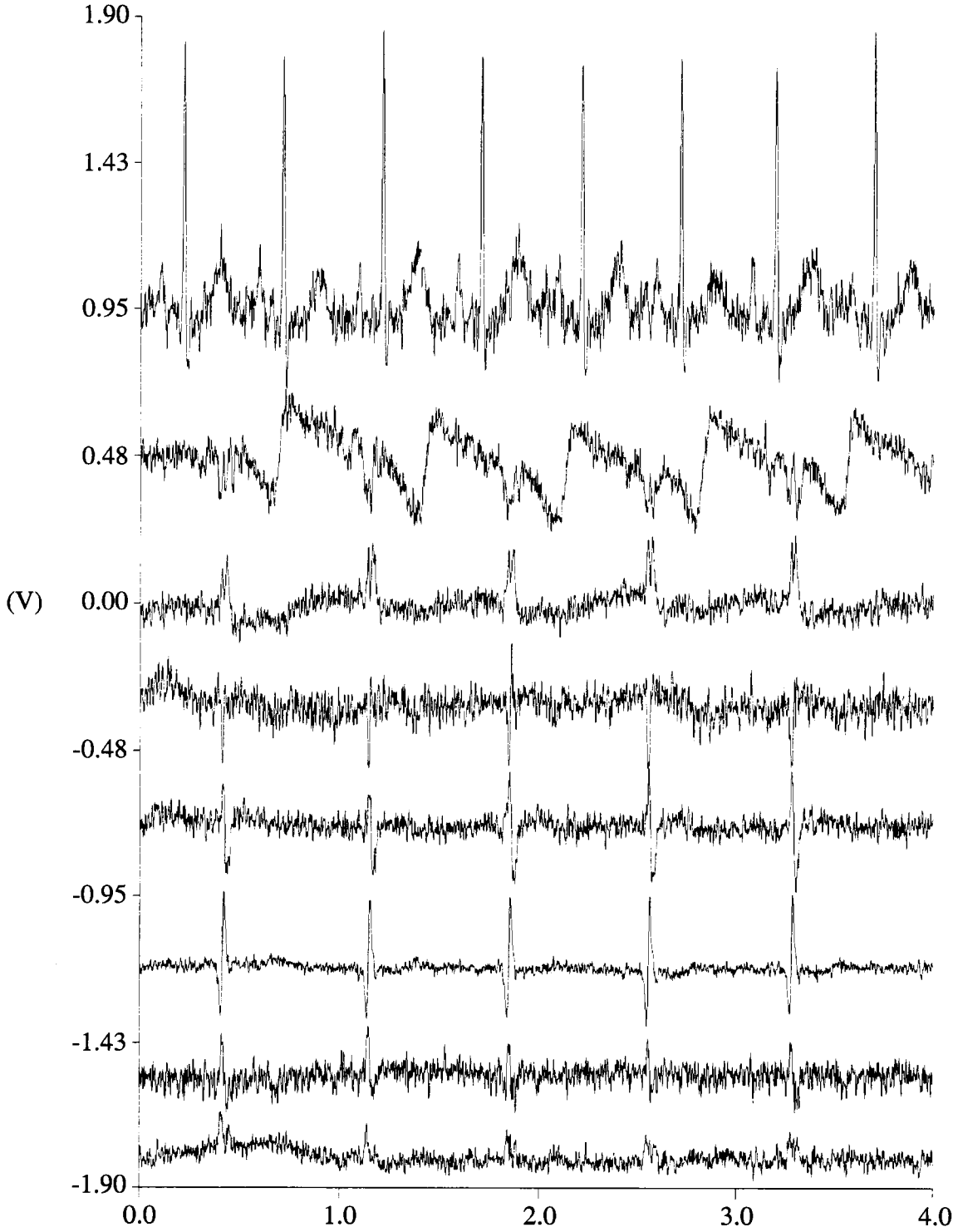

Figure 2-19. Results of the second transformation of SVD method three. Each above signal is a row of $\boldsymbol{R}_{K,N}$ found from the transformation of $(\boldsymbol{S}^{*}_{K,N})^{T}$ by $\boldsymbol{V}^{*}$. The first signal is the FECG and the last seven signals are non-orthogonal MECG components and noise (x-axis in seconds).

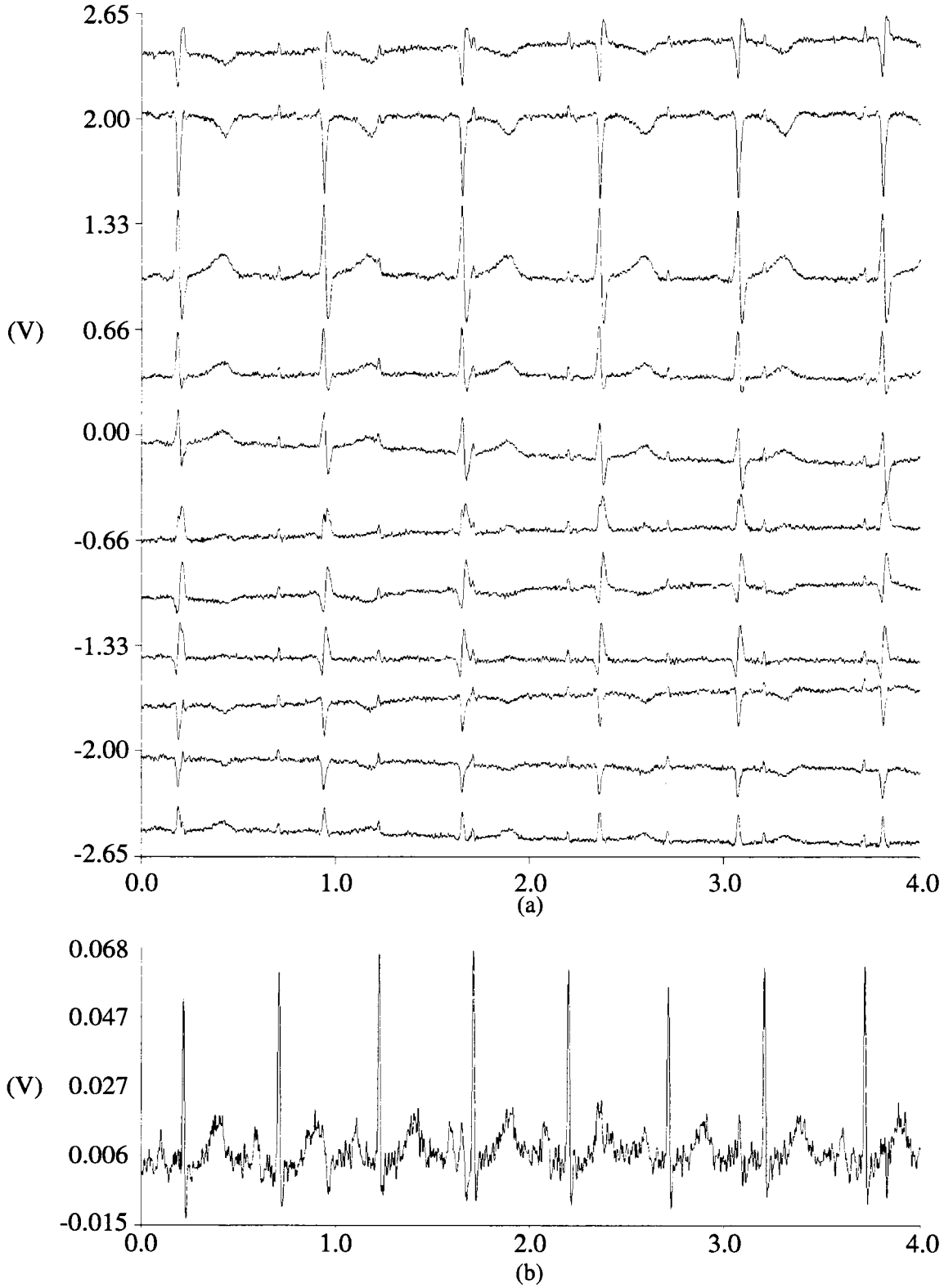

Figure 2-20. Results of reimplementing the additive spatial filter method (all x-axes in seconds). (a) 11 synthesized AECG signals. (b) The resulting FECG.

the additive technique that sums 11 AECG signals to increase the FECG's SNR and partially suppress the MECG [102]. Figure 2-20(a) contains the 11 synthesized AECG signals and Figure 2-20(b) is the resulting signal from the summation of the 11 AECGs.

The quadratic programming procedure enhances the FECG's SNR by linearly combining several AECG signals with weighting coefficients such that the FECG's SNR is increased [13, 52, 90]. The FECG enhancement occurs simultaneously with the cancellation of the abdominal MECG as described in Section 2.1.3.3. The quadratic programming technique for MECG cancellation devises a quadratic programming problem by deriving a quadratic function and boundary conditions. The quadratic function is determined from conditions necessary to cancel the MECG, but the boundary conditions are derived to improve the SNR of the FECG. Equations (29) and (30) are the boundary conditions that exclude the zero solution and guarantee that the weighting coefficients are positive. Provided the AECGs were spatially measured so that the FECG is positively correlated with each lead and that the noise is mostly uncorrelated between AECGs, then the linear combination of the AECG signals through non-zero positive weighting coefficients will result in an enhanced FECG's SNR compared to the original AECG signals. Finally, Figure 2-12 is an example of the quadratic programming technique for FECG SNR enhancement reimplemented and applied to synthesized data. Figure 2-12(a) presents six AECG signals and Figure 2-12(b) is the resulting FECG after the linear combination of the AECG signals.

The final spatial filtering techniques for enhancing the FECG's SNR are based on the SVD procedure. As with the quadratic programming technique, the SVD methods improve the FECG's SNR simultaneously with the cancellation of the MECG. Because of the simultaneous filtering, the three SVD methods for canceling the MECG that are described in Section 2.1.3.4 will be referred to in the following description as SVD methods one, two, and three for FECG SNR enhancement.

A full description of SVD method one is given in Section 2.1.3.4 and will usually enhance the FECG's SNR because the resulting FECG signals of (32) are optimal with respect to extremal oriented energy [14]. Figures 2-13 and 2-14 demonstrate SVD method one. Figure 2-13(b) are the two original AECG signals used to reimplement method one and the first signal of Figure 2-14(b) is the enhanced FECG or the fourth row of $\boldsymbol{SS}_{K,N}$ of (32). SVD method two improves the FECG's SNR by computing the SVD of $(\boldsymbol{R}')^{\mathrm{T}}$ of (34) or

$$(\boldsymbol{R}'_{K\text{-}r_m,N})^{\mathrm{T}} = \boldsymbol{U}_{N,K\text{-}r_m} \sum_{K\text{-}r_m,K\text{-}r_m} \boldsymbol{V}_{K\text{-}r_m,K\text{-}r_m}. \tag{40}$$

Then $\boldsymbol{V}$ is used to transform $(\boldsymbol{R}')^{\mathrm{T}}$ or

$$(\boldsymbol{R}`_{K\text{-}r_m,N})^{\mathrm{T}} = (\boldsymbol{R}'_{K\text{-}r_m,N})^{\mathrm{T}} \boldsymbol{V}_{K\text{-}r_m,K\text{-}r_m} \tag{41}$$

where the first row of $\boldsymbol{R}`$ has the greatest FECG component and improved FECG's SNR compared to the original AECG signals of the rows of $\boldsymbol{S}_{K,N}$ [14, 61]. Figure 2-21 contains results from reimplementing SVD method two. Figure 2-16(b) contains the rows of $\boldsymbol{R}'$ of (34). Figure 2-21 contains the rows of $\boldsymbol{R}`$ after the SVD of $\boldsymbol{R}'$ and the transformation of $\boldsymbol{R}'$ by $\boldsymbol{V}$ was computed. The first signal of Figure 2-21 is the FECG with an improved SNR compared to the AECGs' FECG's SNR of Figure 2-15. Finally, a full description of SVD method three is given in Section 2.1.3.4. The FECG's SNR is enhanced because the resulting FECG signals of (38) are optimal with respect to extremal oriented signal-to-signal ratio [14]. Figure 2-19 demonstrates SVD method three for improving the FECG's SNR with synthesized data. The first signal of Figure 2-19 or the first row of $\boldsymbol{R}_{K,N}$ of (38) is the enhanced FECG where the SNR is improved compared to the original AECG signals of Figure 2-17.

2.2.2 Temporal Filtering

A significant number of the reported FECG systems perform temporal filtering or FECG averaging to enhance the FECG's SNR [14, 23, 25, 63, 65, 68, 69, 70, 71, 72, 73, 103, 104, 105, 106, 107, 108, 109]. These methods differ by the method used for detecting and aligning the FECG complexes for averaging. Furthermore, some of these FECG averaging techniques perform abdominal MECG suppression after the FECG average has been computed as opposed to canceling it before averaging [25, 104]. Finally, by averaging M FECG complexes, the resulting FECG average will have a white gaussian noise variance $\sigma_{ave,temporal}$ that is reduced by a factor of the square root of M compared to the variance $\sigma_{orig,temporal}$ of each detected FECG complex [110] or

$$\sigma_{ave,temporal} = (\sigma_{orig,temporal})/(M^{1/2}). \tag{42}$$

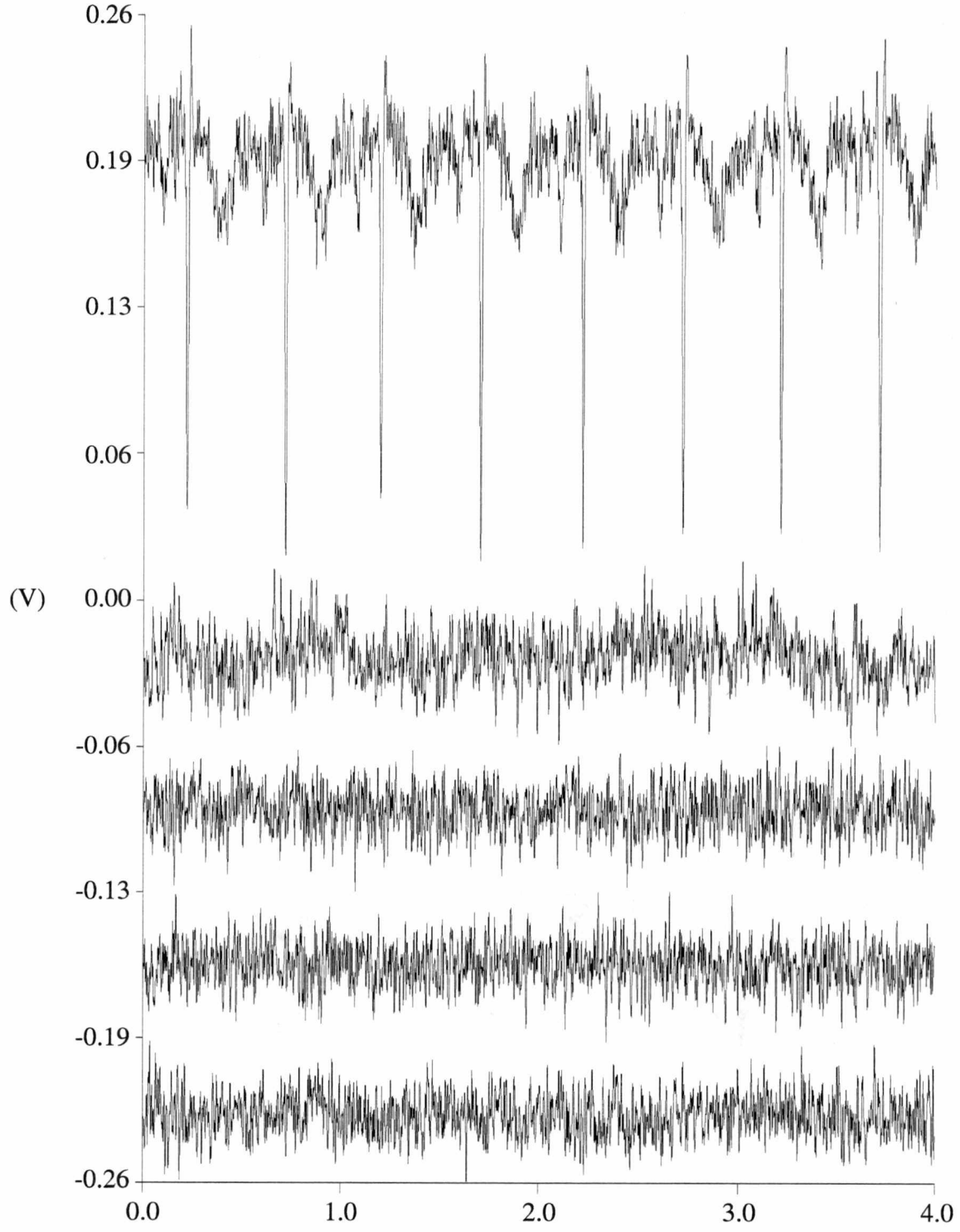

Figure 2-21. The resulting signals from SVD method two for FECG SNR enhancement (x-axis in seconds).

A typical FECG averaging procedure is similar to the third abdominal MECG attenuation method of Section 2.1.1 [69]. The first step of a common FECG averaging algorithm allows the operator to select an FECG complex to build an average complex from. Next, the first detected FECG's R wave peak time location is determined and correlated with the preselected complex. Then the two signals are averaged together at the maximum correlation point. Finally, to obtain an averaged FECG complex with a high SNR, the previously calculated average is correlated with several more FECG periods that are also averaged into the template. Figure 2-22 demonstrates the FECG averaging method described above where Figure 2-22(a) is the original AECG and Figure 2-22(b) is the AECG with the MECG canceled by method three of Section 2.1.1. Figure 2-22(c) presents the FECG average computed from Figure 2-22(b).

2.2.3 Digital Impulse Response Filtering

Simple non-adaptive digital FIR filters and more sophisticated adaptive FIR filters have been used to enhance the FECG's SNR. The simple FIR filter methods are bandpass in nature and have passbands in the frequency region that the FECG has the most signal energy [111]. The adaptive filter methods find a near-optimal FIR filter to suppress the noise of the MECG free AECG [17, 53, 81]. As with abdominal MECG cancellation, the time-sequenced adaptive filter has proven to be more effective for filtering the cyclostationary FECG as compared to the conventional LMS adaptive filter that was designed for use with stationary signals [53, 84]. Since this has been previously studied, only the time-sequenced adaptive filter will be discussed and reimplemented.

Time-sequenced adaptive filtering for FECG SNR enhancement uses an MECG free AECG with a relatively good FECG's SNR as a reference to adaptively develop several FIR filters that are time-sequenced to filter a second MECG free AECG with a poor FECG's SNR. The time-sequenced adaptive filter method first determines the regeneration times that will be used to sequence the FIR filters. Two different techniques have been used to determine these times. The first detects the FECG's QRS complexes of the AECGs with the MECG suppressed and the second uses a Doppler echo-ultrasound signal [17, 53, 81]. The regeneration times are then set to be 100 ms before the FECG's R waves based on the FECG's QRS complexes or the Doppler echo-ultrasound signal [17]. Next, the sequence number is set to zero at each regeneration time and a specific weight vector is assigned to each sequence number to filter a designated section of

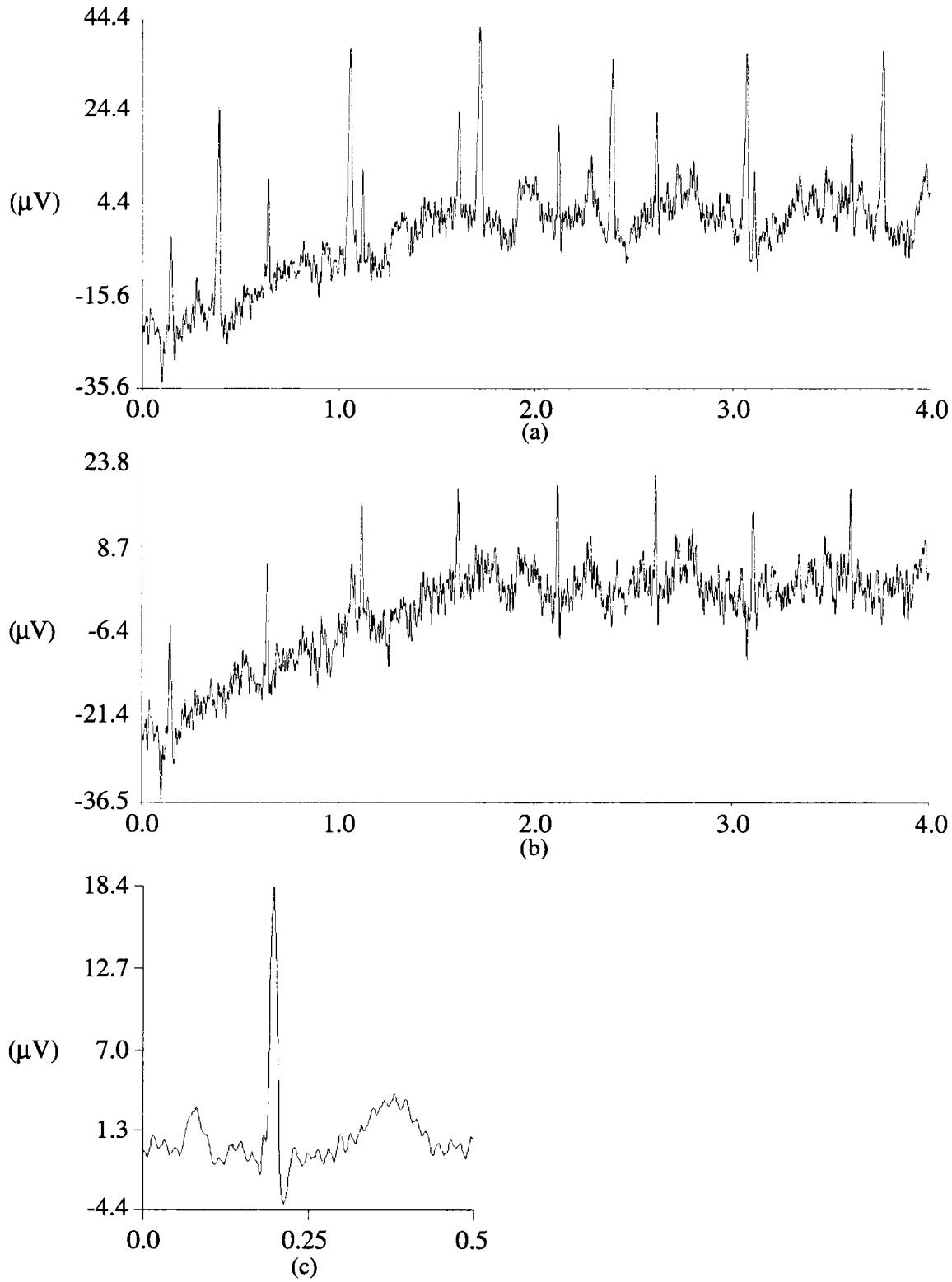

Figure 2-22. FECG averaging technique (all x-axes in seconds). (a) AECG. (b) AECG with the MECG canceled and the resulting FECG complexes are averaged. (c) Resulting FECG averaging from the AECG of (b).

the second AECG. The time-sequenced weight vectors are used to filter 200 ms after each regeneration time. Finally, the sections of the AECG that do not fall into the time-sequenced sections are filtered using the traditional LMS adaptive filter.

Figure 2-23 contains a block diagram of the time-sequenced adaptive filter for enhancing the FECG's SNR and the following describes the filter in more detail [17, 81, 82, 83, 86]. From Figure 2-23

$$e(n) = r_1(n) - r`_2(n), \tag{43}$$

$$r`_2(n) = R'_2(n)\boldsymbol{W}_{sn}, \quad \text{Time-sequenced adaptive filter section} \tag{44}$$

and

$$r`_2(n) = R'_2(n)\boldsymbol{W} \quad \text{LMS adaptive filter section} \tag{45}$$

where $r_1(n)$ and $r_2(n)$ are the MECG free AECGs, $e(n)$ is the error signal between $r_1(n)$ and $r_2`(n)$ that is being minimized by the filter, $r`_2(n)$ is the output of the filter or the filtered AECG $R_2(n)$, $R'_2(n) = [1\ r_2(n)\ r_2(n\text{-}1)\ r_2(n\text{-}2)\ \cdots\ r_2(n\text{-}l\text{-}1)]$ and is the portion of the AECG signal $R_2(n)$ used by the adaptive filter to update the filter weights and $e(n)$, $\boldsymbol{W}_{sn} = [w_{sn,0}\ w_{sn,1}\ w_{sn,2}\ \cdots\ w_{sn,l}]$ and $\boldsymbol{W} = [w_0\ w_1\ w_2\ \cdots\ w_l]$ which contain the filter weights, sn is the sequence number, and l is the number of coefficients of the AECG $R_2(n)$ transversal filter. $US(n)$ is the Doppler echo-ultrasound signal used to determine the regeneration times. Finally, using time-sequencing and the LMS algorithm, $\boldsymbol{W}_{rgt,sn}$ and $\boldsymbol{W}_n$ are updated by

$$\boldsymbol{W}_{next\ rgt,sn} = \boldsymbol{W}_{rgt,sn} + 2\mu_{sn}e(n)(R'_2(n))^{\mathrm{T}} \quad \text{Time-sequenced adaptive filter section} \tag{46}$$

and

$$\boldsymbol{W}_{n-1} = \boldsymbol{W}_n + 2\mu e(n)(R'_2(n))^{\mathrm{T}} \quad \text{LMS adaptive filter section} \tag{47}$$

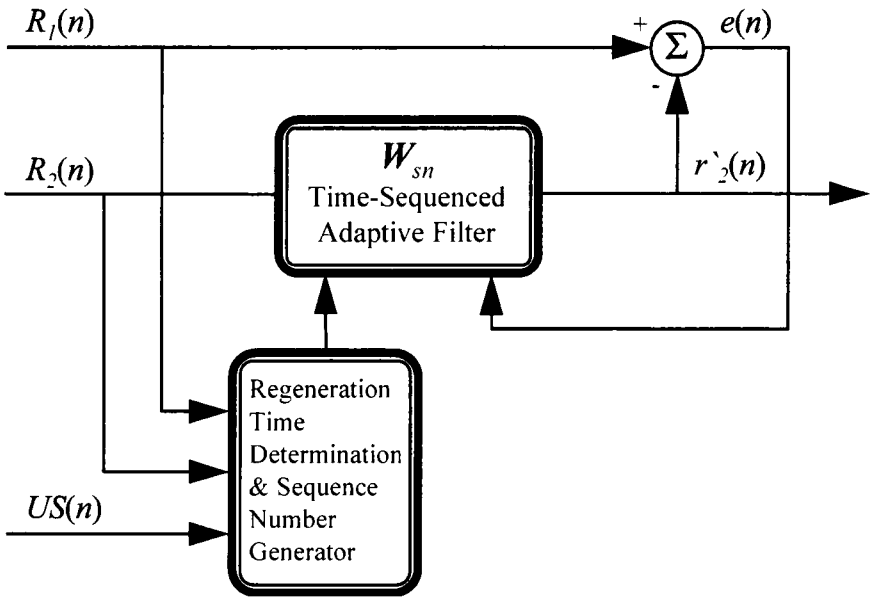

Figure 2-23. Block diagram of the time-sequenced adaptive filter for FECG SNR enhancement. $R_1(n)$ and R_2(n) are AECG signals where the MECG has been canceled. $US(n)$ is the Doppler ultrasound signal used to determine the regeneration times and sequence numbers. $R`_2(n)$ is the enhanced FECG of $R_2(n)$.

where *rgt* is the regeneration time, μ_{sn} is the convergence coefficient for the time-sequenced part of the adaptive filter and has different values that are referenced by the sequence number, and μ is the convergence coefficient of the LMS adaptive filter section.

Figure 2-24 shows a typical result with synthesized data of the time-sequenced adaptive filter for enhancing the FECG's SNR. Figure 2-24(a) contains the two original AECG signals and Figure 2-24(b) contains the AECG of Figure 2-24(a) with the MECG canceled using method three of Section 2.1.1 or $R_1(n)$ and $R_2(n)$. Figure 2-24(c) is the output of the time-sequenced adaptive filter or $R`_2(n)$ after converging to enhance the SNR of the second AECG of Figure 2-24(b).

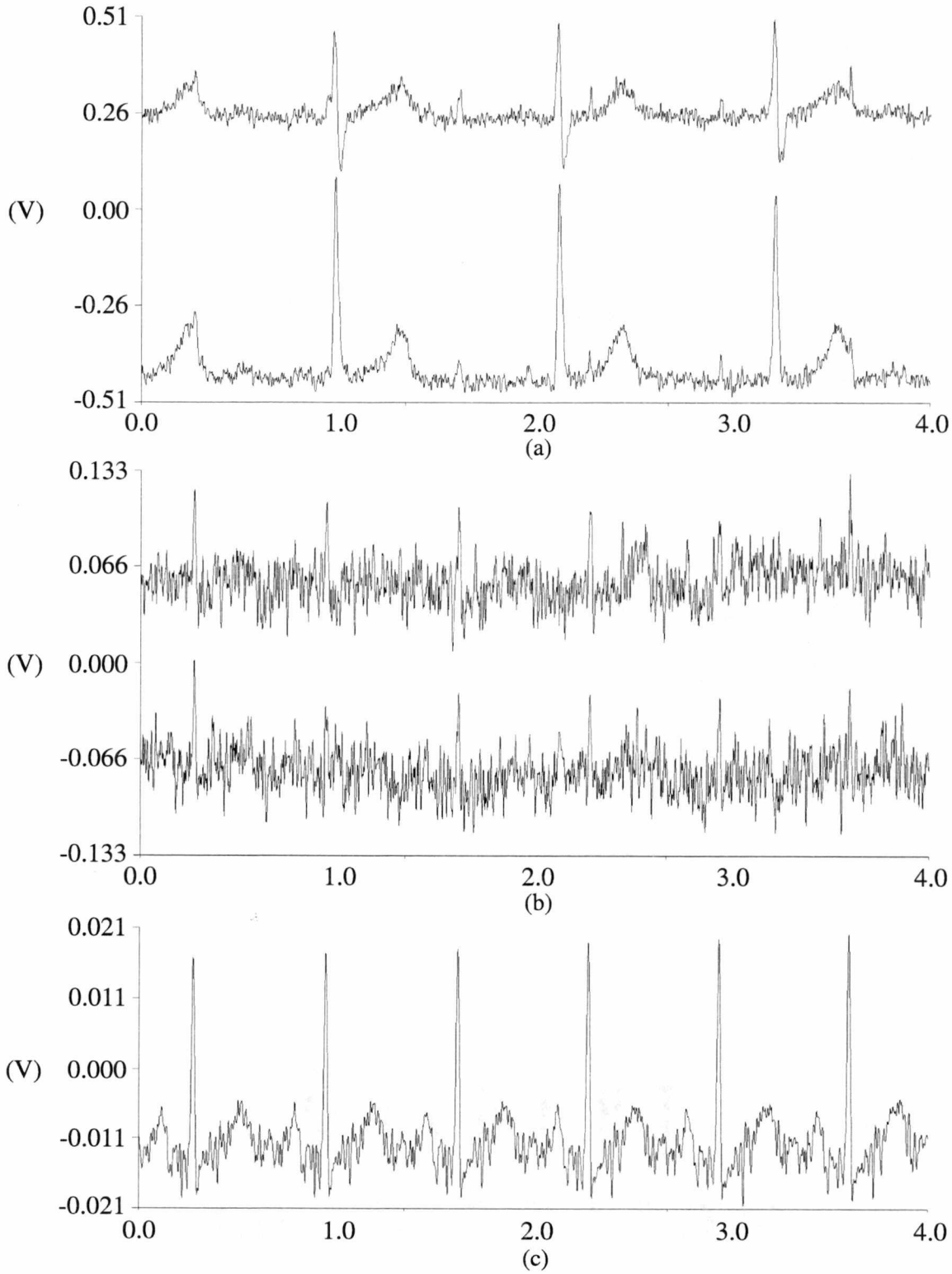

Figure 2-24. Results of the time-sequenced adaptive filter for FECG SNR enhancement (all x-axes in seconds). (a) AECG signals. (b) AECG's signals of (a) with the MECG canceled. (c) The output of the time-sequenced adaptive filter that enhances the FECG's SNR.

CHAPTER 3

METHOD

Dissertation Goal I

Research, Design, and Develop the CH^2 Non-invasive FECG Monitoring System

This chapter describes the details of the published and patented† CH^2 non-invasive FECG system [112, 113, 114]. It consists of an analog and digital signal processing subsystems. The analog subsystem contains a preamplifier for the AECG and two adult ECG amplifiers to amplify the output of the preamplifier and an TECG. The digital subsystem performs abdominal MECG cancellation and enhances the SNR of the FECG via FECG averaging and filtering. Furthermore, the abdominal MECG cancellation algorithm is based on MECG averaging and subtraction, but is novel concerning the procedure used to align the abdominal MECG complexes for averaging and subtraction. Figure 3-1 presents a block diagram and Figure 3-2 a flowgraph of the CH^2 FECG system. Finally, Chapter 3 presents the finalized details of dissertation goal one as described by Figure 1-1 of researching, designing, and developing a non-invasive FECG monitoring system.

† Appendix B contains a copy of the first page of the patent.

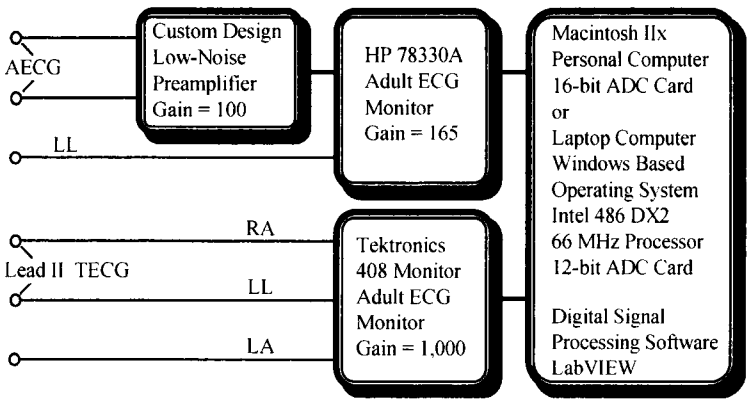

Figure 3-1. Block diagram of the CH^2 FECG system.

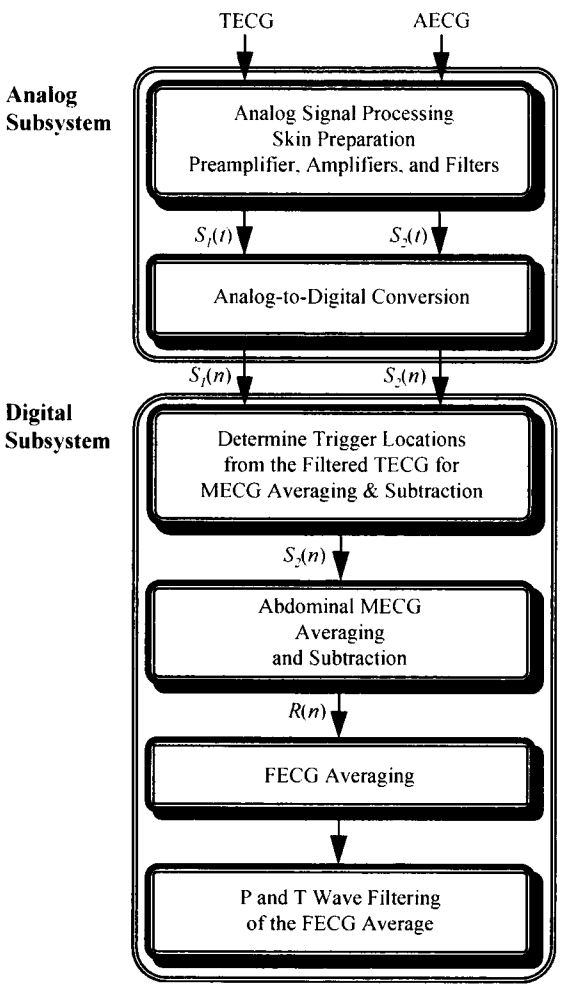

Figure 3-2. Flowgraph of the CH^2 FECG system.

3.1 Analog Signal Processing

The FECG can be from 40.0 μV_{pp} (max.) to unmeasurable (min.) and the combined abdominal EMG and artifact will typically range from 12.0 μV_{pp} to 25.0 μV_{pp} [25, 61, 65, 94, 95, 103]. Skin preparation and high quality electronics are required to accurately obtain a non-invasive FECG and abdominal EMG, due to the low signal amplitudes. Skin preparation is done to reduce the patient skin resistance which can cause a significant amount of motion artifact and thermal noise [115, 116, 117, 118, 119]. Without skin preparation, the skin resistance of the patient can typically be 50 kΩ which produces 2.29 μV_{pp} of thermal noise for a bandwidth of 0.5 to 100.0 Hz, temperature of 298.0 K, and V_{rms} to V_{pp} transformation factor of 8.0 which comes from a crest factor of 4.0. (These parameters will be used throughout the rest of the dissertation for noise calculations and noise measurements) [18, 116, 117, 118, 120, 121]. With skin preparation, the skin resistance will usually be 1 to 10 kΩ which produces 0.324 μV_{pp} to 1.024 μV_{pp} of thermal noise [18, 116, 117, 118, 120, 121]. Furthermore, the electrode-electrolyte interface resistance is typically 200 Ω [118]. Finally, the combined skin and electrode-electrolyte resistance ranges from 1.4 to 10.4 kΩ which produces 0.383 μV_{pp} to 1.044 μV_{pp} of thermal noise [18, 120].

The AECG system noise ($V_{noise\ system}$) which is produced from skin resistance thermal noise, electrode-electrolyte resistance thermal noise, and instrumentation noise should be approximately six times less than the typical minimal value of 12.0 μV_{pp} of the AECG EMG and artifact. The aforementioned will insure that the FECG, AECG EMG, and artifact will have negligible corruption. Since a 2.0 μV_{pp} ($V_{noise\ system}$) noise specification is desired and the available adult ECG monitor (Hewlett Packard HP78330A) has a measured noise specification of 1.38 μV_{rms} or 11.0 μV_{pp}, a custom designed low-noise preamplifier was added to the front end of the adult ECG monitor to improve the total noise specification of the AECG system.

3.1.1 Preamplifier Design

This section gives a description of the preamplifier shown in Figure 3-3. The preamplifier consists of four stages. Stage one consists of a safety circuit that protects the patient from the supply voltages (two 9 V batteries create ±9 V supplies) from being applied to the patient if several devices fail simultaneously. During device failure(s), the possibility exists for a dc

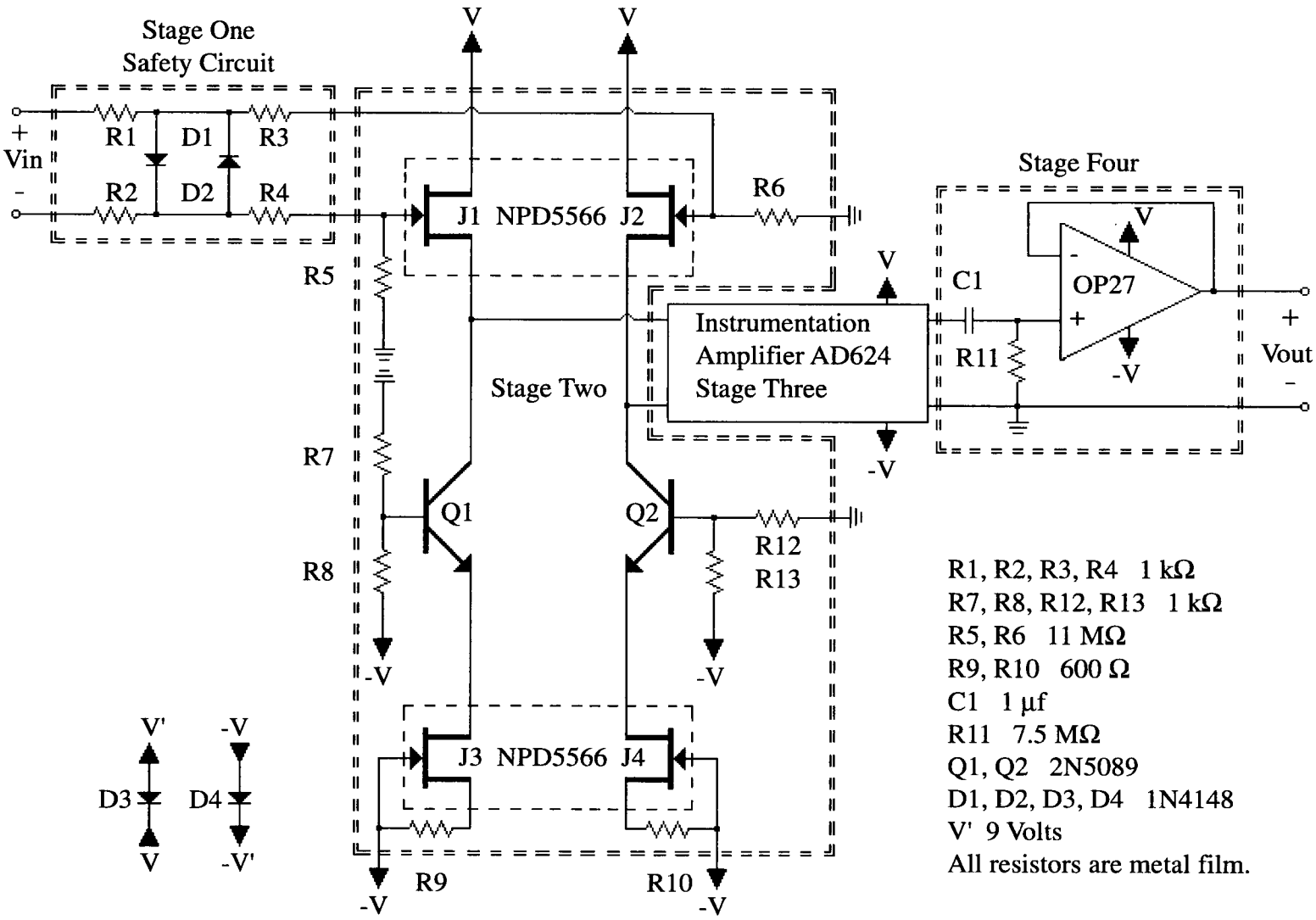

R1, R2, R3, R4 1 kΩ
R7, R8, R12, R13 1 kΩ
R5, R6 11 MΩ
R9, R10 600 Ω
C1 1 μf
R11 7.5 MΩ
Q1, Q2 2N5089
D1, D2, D3, D4 1N4148
V' 9 Volts
All resistors are metal film.

Figure 3-3. Preamplifier circuit diagram.

voltage to appear across the patient terminals. If a supply voltage appears at the gates of J_1 and/or J_2 (NPD5566), the voltage will be dropped across R_3 and R_4 (all resistors used in the preamplifier are metal film) because diodes D_1 or D_2 (1N4148) will turn on and clamp the patient terminals at approximately ±0.6 V. If the supply voltage from device failures was not dropped to ±0.6 V and a voltage of 3.0 V or greater occurs between the patient terminals, skin burns can result [122]. Finally, D_3 and D_4 prevent supply currents from going in the opposite direction of original design during device failure(s).

The second stage is a differential unity gain buffer stage and consists of two junction field effect transistors (JFET) in a source follower configuration (J_1, J_2 National Semiconductor NPD5566 Process 96) [123]. Each source follower is biased with a current sink with I_D = 1.5 mA (current sink1 Q_1-2N5089 by National Semiconductor, J_3-NPD5566, R_9 and current sink2 Q_2-2N5089, J_4-NPD5566, R_{10}). The JFETs are used because they have low current noise and a high input resistance as compared to bipolar junction transistors (BJT) [121]. JFETs (J_3 and J_4) are used to bias J_1 and J_2 because they are self biasing and will be affected only a small amount by a drop in the supply voltages which occurs much from battery discharge [123]. Since stage two is the first stage that active devices are in the signal path, this stage contributes significantly to the total noise of the AECG amplification system [121].

Stage three is the first non-unity gain stage and consists of an instrumentation amplifier (Analog Devices AD624) that has a gain of 100 V/V. Since stage two is unity gain, this stage also contributes significantly to the total noise of the AECG amplification system.

The final stage of the proposed preamplifier consists of a resistive capacitive (R_{11} and C_1) first order highpass filter (Cutoff frequency = 0.021 Hz) followed by a unity gain buffer amplifier (OP-27). This stage filters the dc and low frequency components of the AECG so that the input to the HP78330A adult ECG monitor does not become saturated. Finally, the HP78330A amplifier further filters the AECG with a bandpass filter with a passband of 0.05 to 100.0 Hz, which prevents aliasing during analog-to-digital conversion, and amplifies the AECG by a factor of 165 V/V to produce a total gain of 16,500 V/V for the AECG system.

The preamplifier output dc offset are adjusted to zero (< 10 mV) by paralleling large resistors with R_9 and R_{10} to slightly adjust I_D in each current sink until the differential dc offset at the current sink outputs are close to zero. After dc offset adjustments, the common mode rejection ratio (CMRR) is fine-tuned by following the procedure for adjusting the CMRR of the instrumentation amplifier (AD624).

3.1.2 Theoretical and Measured AECG System Specifications

As discussed previously, the preamplifier input equivalent noise is dominated by the equivalent source resistance noise, the active noise of stage two, and the equivalent input noise of stage three. Before the theoretical noise analysis for the AECG system is performed, the source resistance noise (combined skin resistance of 1 to 10 kΩ, electrode-electrolyte resistance of 400 Ω, and safety circuit resistance of 4 kΩ) and the single ended source follower output resistance of stage two will be theoretically determined for the preamplifier. The worst case value for the source resistance R_s is 14.4 kΩ which produces 0.154 μV_{rms} or 1.23 μV_{pp} of thermal noise (V_s) [18, 120].

Each single ended source follower output resistance R_{out} is

$$R_{out} = [R_o \parallel 1/g_m \parallel r_{o1}] \tag{48}$$

where r_{o1} is approximately the output resistance of J_1 or J_2, g_m is the transconductance of J_1 or J_2, and R_o is the output resistance of the single ended current sink [123]. Since R_o and r_{o1} are much greater than $1/g_m$, R_{out} can be approximated by $1/g_m$ [123]. From the data sheet for the NPD5566, g_m is 9.0 mmhos at I_D equal to 1.5 mA, and R_{out} is calculated to be 111.1 Ω.

The following theoretical analysis of the total noise in the AECG system ($V_{noise\ system}$) which includes thermal noise from the source resistance R_s and noise from the active devices of the AECG amplification system will be derived by expressing the total noise of the AECG system interms of equivalent noise voltage (ENV) and equivalent noise current (ENI) [18, 120]. By dividing the circuit into subcircuits that can be represented by a noise equivalent circuit or a linear two-port that assume that the ENV's and ENI's are uncorrelated or to small for correlation to be significant, (49) can be written for the total noise of the AECG amplification system [18, 120, 121, 124].

$$V_{noise\ amp.} \cong [2V^2_{source\ follower} + 2((I_{JFET}R_s)/2)^2 + V^2_{IA} + 2(R_{out}I_{IA})^2 + V^2_{stage4} + V^2_{HP78330A}]^{1/2} \tag{49}$$

By using a noise equivalent circuit for each transistor of the differential unity gain source follower or stage two, $V_{source\ follower}$ is found to be

$$V_{source\ follower} \cong [(1/g_m)^2(I^2_{td} + I^2_{fd} + V^2_{tR9,10}/(1/g_m + R_{9,10})^2)]^{1/2} \quad (50)$$

where $I_{td} = [4kT(2g_m/3)\Delta f]^{1/2}$, $I_{fd} = [K_f I_D \Delta f/f]^{1/2}$, $V_{tR9,10} = [4kTR_{9,10}\Delta f]^{1/2}$, g_m is the transconductance of J_1, J_2, J_3, or J_4, and $K_f = 16/3kTf_f(K/I_D)^{1/2}$ [124]. I_{JFET} is the ENI for J_1 or J_2 and V_{IA} and I_{IA} are the ENV and ENI for the instrumentation amplifier (AD624). V_{stage4} is the ENV from the unity gain buffer output stage and $V_{HP78330A}$ is the noise from the HP78330A adult ECG monitor. All ENV and ENI values are referred to the input.

By disregarding the insignificant terms I_{JFET} and V_{stage4}, (49) can be simplified. I_{JFET} produces negligible noise for a R_s of 14.4 kΩ compared to the ENV [121, 124]. With I_{JFET} and V_{stage4} assumed zero, (49) simplifies to (51).

$$V'_{noise\ amp.} \cong [2V^2_{source\ follower} + V^2_{IA} + (2R_{out}I_{IA})^2 + V^2_{HP78330A}]^{1/2} \quad (51)$$

Finally, the total noise of the AECG system which includes the amplifier and thermal noise from the source resistance (R_s) is

$$V_{noise\ system} \cong [V^2_s + V'^2_{noise\ amp.}]^{1/2} \quad (52)$$

The specifications for the variables in (50) and (51) used to calculate $V'_{noise\ amp.}$ and $V_{noise\ system}$ are $f_f = 1.0$ Hz which is the flicker-noise corner frequency of the JFETs, $I_D = 1.5$ mA, $f = 0.5$ Hz, $V_{IA} = 119.0\ nV_{rms}$, and $I_{IA} = 0.03898\ nA_{rms}$. Finally, $V'_{noise\ amp.}$ and $V_{noise\ system}$ are theoretically calculated to be 0.123 μV_{rms} or 0.980 μV_{pp} and 0.197 μV_{rms} or 1.573 μV_{pp} respectively.

The measured values for the total noise in the AECG amplification system and HP78330A adult ECG monitor were made by short circuiting the input of the amplifiers and providing adequate gain (gain = 600,000 V/V for the AECG amplifier system and gain = 6,000 V/V for the HP78330A adult ECG) so that the signal output of the amplifiers could be digitized with negligible quantization error. Next, the root-mean-square (RMS) value of the digitized signal was calculated for 10 different time intervals each 120 seconds in duration. These 10 values were then averaged together to produce the final measured noise specifications. The AECG amplifier system produced a $V_{noise\ amp.}$ of 141.3 nV_{rms} or 1.13 μV_{pp} and the HP78330A monitor noise specification was 1.375 μV_{rms} or 11.0 μV_{pp}. By combining the theoretical source resistance

noise with $V_{noise\ amp.}$ measured, produces $V_{noise\ system}$ of 1.67 μV_{pp}. Finally, $V_{noise\ system}$ theoretical and $V_{noise\ system}$ measured are less than the 2.0 μV_{pp} required specification.

The CMRR was measured for the AECG amplifier system by short circuiting the two input or patient connection terminals of the preamplifier and applying a 0.2 V_{pp} sinusoidal signal at 10.0 Hz between ground and the short circuited terminals. A gain of 600,000 V/V was applied to the short circuited input which was digitized (100 V/V preamplifier and 6,000 V/V HP78330A). The peak-to-peak value of 1.15 μV_{pp} (referred to input) was measured which was basically similar to the noise developed in the AECG amplification system. The CMRR was determined to be 105 dB by dividing 0.2 V_{pp} by the peak-to-peak value of 1.15 μV_{pp} which is the same specification for the HP78330A adult ECG monitor.

3.2 Digital Signal Processing

3.2.1 Abdominal MECG Cancellation

The CH^2 technique for abdominal MECG cancellation of the digital subsystem consists of using an TECG (lead II) as a trigger to align the abdominal MECG complexes to determine its average. Then the abdominal MECG average is used to cancel each MECG complex of the non-invasive AECG. The following describes the method in detail. Figure 3-4 is used to facilitate the explanation.

The non-invasive TECG and AECG are digitized into blocks 8.0 seconds in length (Figure 3-4 only contains two seconds because fine resolution was needed to demonstrate the description of the method.). Step one of the method bandpass filters the TECG from 2.0 to 35.0 Hz with a second order Bessel filter (A Bessel filter from the LabVIEW analysis library was employed.). Figure 3-4(a) demonstrates the filtering. Figure 3-4(a)(i) is the original TECG and Figure 3-4(a)(ii) is the filtered TECG (The y-axis scale of Figure 3-4(a) is only for display purposes.). The second step of this method determines the absolute maximum of the filtered TECG block of data. This maximum is indicated by a square in Figure 3-4(a)(ii) at the peak of the first MECG's R wave.

Step three divides the maximum by two. Furthermore, step three uses the resulting value as a threshold to determine the time locations of the ascending MECG's R waves that exceed the threshold via a peak detection algorithm. (A peak detection algorithm from the analysis library

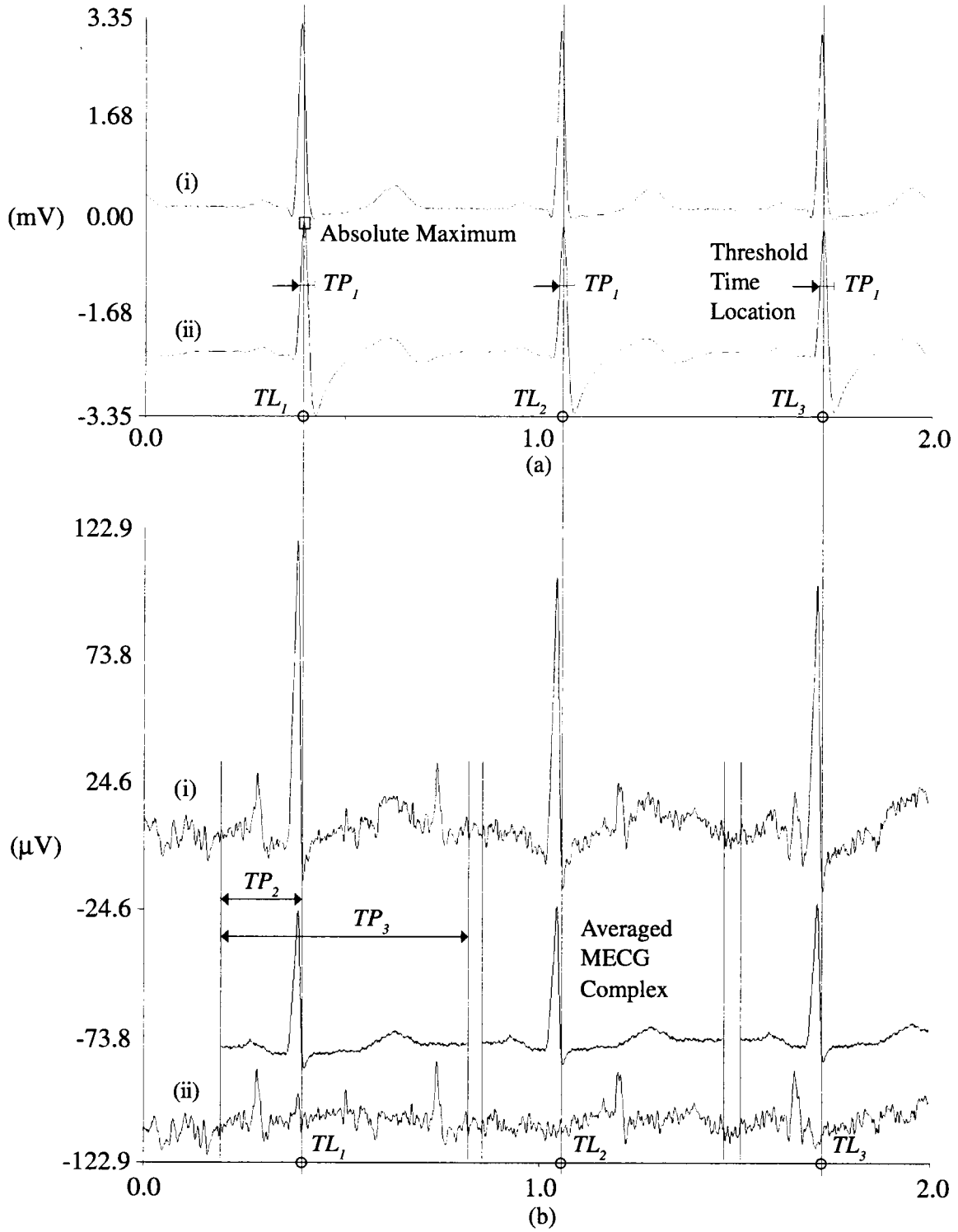

Figure 3-4. A graphical explanation of the CH² method for MECG cancellation (all x-axes in seconds). (a)(i) TECG. (a)(ii) Filtered TECG. (b)(i) AECG (above) and AECG MECG average (below) that is subtracted from each MECG complex at the appropriate trigger location. (b)(ii) AECG with the MECG canceled.

of LabVIEW was used.). Figure 3-4(a)(ii) indicates the locations of each ascending MECG's R wave that exceeds the threshold with a single ended horizontal arrow. With these threshold time locations, step four determines the time locations of each MECG's R wave peak of the filtered TECG. The peaks are found by utilizing a local maximum algorithm to determine the maximum value of time period one (TP_1) that is 0.04 the sampling rate seconds forward in time of each threshold time location. The maximum values correspond to the MECG's R wave peaks of the filtered TECG or the trigger locations (TL_1 through TL_x where x is the number of MECG complexes minus two of the 8.0 seconds of AECG) used for abdominal MECG averaging and subtraction. Figure 3-4(a)(ii) identifies TP_1 for the three MECG complexes by the horizontal lines that are forward in time of the horizontal arrows and TL_1 through TL_3 by the circles on the x-axes. The bandpass filtering of step one is done to flatten the baseline, center the baseline at the zero crossing, and suppress upper frequency noise of the TECG. Therefore, the filtered TECG can be used to ascertain more accurately the desired trigger locations used for abdominal MECG averaging and subtraction.

As discussed, the trigger locations determined by step four are used to align each abdominal MECG complex to find the abdominal MECG average. The alignment procedure is possible because the trigger locations will coincide to the same part of each abdominal MECG complex since the ECG seems to propagate through the body uniformly. The following is an example. When the heart rate decreases or increases, the MECG's R wave peak of the filtered TECG will still correspond to the same part of the abdominal MECG complex. This corresponding part of the abdominal MECG complex will probably not be the abdominal MECG's R wave peak, but either the ascending or descending portion of the R wave. As noted, this depends on how the ECG propagates through the body and position of the ECG electrodes.

Step five determines the abdominal MECG average. The average is found using step four trigger locations to section out each MECG complex from the AECG block as a smaller sub-block. First, time period two (TP_2) that is 0.2 seconds in duration is subtracted from the trigger locations (TL_1 through TL_x minus TP_2). Next, the MECG complexes are removed by extracting the portions of the AECG starting at TL_1 through TL_x minus TP_2 time locations with a time duration of TP_3 (time period three). The values of 0.2 for TP_2 and 0.6 for TP_3 seconds vary a small amount for a large variation of the maternal heart rate. Figure 3-4(b)(i) indicates graphically the meaning of the values TP_2 and TP_3 in relation to the trigger locations TL_1 through TL_3. Furthermore, to keep the baseline of the MECG average close to the zero crossing, each

MECG complex is filtered. This filtering averages the first and last 0.005 the sampling rate seconds of each sub-block and then subtracts the average value from each sample of the corresponding sub-block. These filtered sub-blocks are summed until all the MECG complexes of the AECG block have been added together (The first and last abdominal MECG complexes of the block of data are thrown out because they may not contain a full MECG complex from the data acquisition). Then the summed MECG complexes are divided by the total number of abdominal MECG complexes averaged to produce the abdominal MECG average. The ECG complex below Figure 3-4(b)(i) and above Figure 3-4(b)(ii) is the abdominal MECG average.

During averaging, the noise corrupting the abdominal MECG will be reduced approximately by the square root of M, where M is the number of MECG complexes averaged [110]. The FECG will be attenuated by a factor of approximately M because the FECG and MECG have different heart rates and act independent of each other. The SNR of the MECG average will be larger than the SNR of each MECG complex. With these facts, step six or the subtraction of the abdominal MECG average from each abdominal MECG complex using the trigger locations produces an AECG with the MECG greatly suppressed. Figure 3-4(b)(ii) is the AECG with the MECG canceled.

The CH^2 method for abdominal MECG cancellation can be implemented in block mode real-time or the analog AECG can be digitally processed and displayed uninterrupted while connected to a patient. However, a double-buffer data acquisition procedure must be used; therefore, the continuous analog ECG signals must be digitized and broken into blocks of data (The blocks are usually 8.0 seconds in duration, but can be varied.). The CH^2 method was implemented in two fashions for block mode real-time operation. The first approach computed the abdominal MECG average for each block of data as they were acquired and subtracted the average from its corresponding AECG block to obtain abdominal MECG cancellation (The synthesized and clinical data of Chapter 5 and Appendix C were processed similarly, but only one block 16.0 seconds in duration was usually used.). The second approach placed into memory the abdominal MECG complexes of previous AECG blocks and block currently being processed. Then the abdominal MECG average is calculated from the complexes in memory. Next, the resulting abdominal MECG average is subtracted from each MECG complex of the AECG block currently being operated on (The clinical data of Appendix D was processed in this fashion.).

3.2.2 FECG Averaging

With the abdominal MECG attenuated, an improvement in the FECG's SNR is necessary. FECG SNR enhancement can be done by averaging several FECG periods. Averaging produces an attenuation of the noise by the square root of M [110]. The following described the FECG averaging procedure in details where the processing is done off-line.

Steps one through four are the same as steps one through four of Section 3.2.1, but the AECG with the MECG suppressed is used instead of the TECG. Furthermore, the filtered AECG (obtained in step one) FECG's R wave peak time locations are determined as trigger locations (TL_1 through TL_x where x is the number of detected FECG complexes minus two of the 8.0 seconds of AECG) instead of the filtered TECG MECG's R wave peak time locations. Step five verifies the time durations between the FECG's R wave peaks to be consistent with a somewhat typical fetal heart rate (120 to 150 beats-per-minute). This step assures that a noise spike is not mistaken for an FECG complex. Step six extracts the FECG complexes from the unfiltered AECG with the MECG suppressed (The filtered AECG with the MECG suppressed was used to find the FECG's R wave peak time locations of steps one through four.) using the trigger locations or FECG's R wave peak time locations found in steps one through four. This step is similar to step five of Section 3.2.1 that extracts the abdominal MECG complexes. However, TP_2 is usually 0.18 to 0.2 and TP_3 is usually 0.45 to 0.6 seconds.

Step seven uses correlation to near-optimally align the FECG complexes so an accurate FECG average can be obtained. Step seven is accomplished by correlating the first two detected FECG complexes QRS complexes plus and minus 1/200 second around their trigger locations. The correlation shift that produces the most correlation is used as the trigger location for the summation of the two FECG complexes. Before the FECG complexes are summed, each FECG complex is filtered similar to the MECG complexes of Section 3.2.1 step five. Then the two periods are summed using the modified trigger location. This process is repeated for the next or third period of the FECG, but the FECG template developed from previous averaging is used in the correlation. This localized correlation is performed until each FECG complex of the unfiltered AECG with the MECG suppressed has been summed into an estimate of the FECG complex. Finally, step eight divides the summed FECG complexes by the total number of complexes summed to obtain the FECG average.

3.2.3 FECG Average Filtering

The SNR of the FECG average can be further improved through P and T wave filtering. This filtering was done off-line. P and T wave filtering is based on the fact that these waves have an 0.05 to 20.0 Hz bandwidth (see Figures 2-2 through 2-4) [21]. Since noise and bandwidth are directly related, reducing the bandwidth of the P and T waves to 0.05 to 20.0 Hz improves their SNR without filtering information. However, since the QRS complex has a bandwidth of 0.05 to 100.0 Hz, filtering cannot be done to the complex. The first step of the filtering procedure determines the beginning and end times of the FECG average QRS complex via a visual inspection. Step two filters the FECG average with a Bessel filter to the beginning time of the QRS complex. The filtered section corresponds to the P wave. Step three filters the QRS complex in an 0.05 to 200.0 Hz bandwidth with a second order Bessel filter to somewhat compensate for the phase shift of P wave filtering of step two. This filtering keeps the time period between the P and R wave peaks the same or comparable to before P and T filtering. Then, step four filters the remaining segment of the FECG average starting at the end of the QRS complex. Step four is equivalent to filtering the T wave.

The two Bessel filters utilized to process the P and T waves were first order with a passband of 0.05 to the upper cutoff frequency (Bessel filters from the LabVIEW analysis library were employed.). The upper cutoff frequency of the filters are determined by the FECG average's SNR. For a high SNR (The P and T waves are visually noticeable in the FECG average.), a low upper cutoff frequency was used for the filters (usually 20.0 Hz). A low frequency can be used because the FECG average will have obvious visual distortion if the cutoff is too low. If distortion occurs, a higher cutoff frequency is used. For a low SNR (The P and T waves are not visually noticeable.), a cutoff frequency of greater then 20.0 Hz was used for the filters (usually 35.0 Hz). A value greater than 20.0 Hz was used so filtering cannot be attributed to distorting the signal.



PROCEDURE

Chapter 4 describes the procedural aspects of the CH^2 FECG system. The procedures include the protocol required for patient connection, data acquisition specifications, digital signal processing (DSP) characteristics, and history regarding the computers employed. The importance of oversampling will also be examined.

ECG signals were taken from the thoracic (lead II) and abdominal areas of the patients† using 3M red dot Ag/AgCl electrodes. Omni Prep (Weaver + Co.) was applied to the abdominal surface area to reduce the stratum corneum or skin resistance. Skin preparation can decrease skin resistance to about 1 kΩ. A conductive paste called Redux Paste (Hewlett Packard) was applied to the electrodes. Then the electrodes were attached to the prepped skin. Experimentation was required for electrode placement. Several locations on the abdominal area were examined until a location was found that produced a noticeable FECG. If no observable FECG was detected, the two abdominal electrodes were placed mid way down on each side of the abdominal surface of the patient. Data was obtained so abdominal MECG cancellation could still be evaluated.

As discussed in Chapter 3, Figure 3-1 shows a block diagram of the non-invasive FECG system. AECG electrodes were connected to a custom designed battery powered preamplifier with a low-noise specification (described in Sections 3.1.1 and 3.1.2). The output of the

---

† Consent for this study had been obtained from the patients under protocol approved by the University of Tennessee Medical Center and University of Tennessee, Knoxville Humans Studies Committees. Appendix B contains copies of the letters of approval and an example patient signature form.

preamplifier was connected to the input of an adult ECG monitor (HP78330A Monitor). TECG electrodes were also connected to an adult ECG monitor (Tektronix 408 Monitor). Both of the signals were amplified by either the preamplifier and/or monitor to minimize quantization error of the analog-to-digital converter (ADC). The AECG has a passband of 0.05 to 100.0 Hz (set by the adult ECG monitor) and the TECG has a passband of 0.5 to 100.0 Hz (also set by the adult ECG monitor). The signals were then sampled at 1 kHz and quantized with 16-bits via a data acquisition board (NB-MIO-16X by National Instruments) inside a Macintosh IIx computer (Apple). An explanation of the high sampling rate (1 kHz as opposed to the Nyquist frequency of 200 Hz) will be presented later in this chapter. The ADC was done using double buffer acquisition to achieve block mode real-time with help from a direct memory access card (NB-DMA2800 by National Instruments). This card increased throughput by reducing the central processing unit's load by moving data from the ADC card to random access memory. Finally, the digitized signals were processed using custom developed software in the LabVIEW (National Instruments) programming environment.

The Macintosh computer in conjunction with LabVIEW logged the clinical data to hard disk, filtered 60 Hz noise if required, suppressed the abdominal MECG, displayed the AECG, displayed the AECG with the MECG suppressed, and displayed the abdominal MECG average in block mode real-time. As discussed, FECG averaging and filtering were done off-line. All clinical data in Chapter 5 was obtained with the Macintosh computer and the 16-bit ADC in block mode real-time. The 60 Hz filter consisted of several first order Bessel filters with stopbands of 55 to 65 Hz, 115 to 125 Hz, 175 to 185, and 235 to 245 for filtering the first, second, third, and fourth harmonics respectively (Bessel filters from the LabVIEW analysis library were employed.). Mid way through this research project, a laptop computer with Microsoft Windows was procured. The laptop and the compatible ADC (12-bit ADC card called the DAQCard-700 by National Instruments) were programmed with the CH^2 method in LabVIEW for Windows. The updated computer and hardware could be used to acquire clinical data with the preamplifier and two adult ECG monitors in block mode real-time similar to the Macintosh based system. Logging and processing of the ECG signals were initially done on the Macintosh computer, but all data in the dissertation were processed by the laptop via retrieving the previously stored signals.

Figure 4-1 is a portrait of the CH^2 FECG system. The Tektronics 408 adult ECG monitor that obtains the TECG trigger signal used to cancel the abdominal MECG is indicated with the

arrow in Figure 4-1 along with the Macintosh computer. To the immediate right of the Tektronics monitor is the laptop computer where the 12-bit ADC card (DAQCard-700) is the white rectangular shape object (about the size of a credit card) below the laptop's display screen. The DAQCard-700 interfaces the laptop computer through the Personal Computer Memory Card International Association (PCMCIA) slot. Finally, the HP78330A adult ECG monitor and preamplifier are on the left side of the Macintosh IIx computer where the preamplifier is the small white box on top of the monitor. As noted, the Macintosh was initially used to log and process data. Then the Macintosh was replaced with the laptop approximately half way through the research project. Improvements were obtained with the laptop in processing speed, but the Macintosh was still fast enough to perform block mode real-time acquisition and processing as discussed.

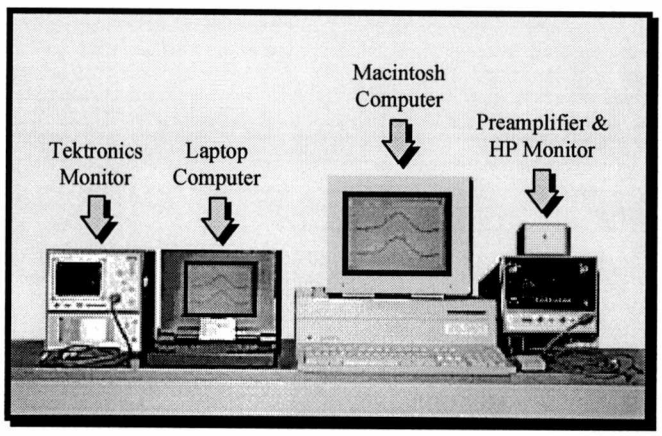

Figure 4-1. A photo of the CH^2 FECG system.

The sampling rate utilized to digitize the two ECG signals cannot be blindly ascertained via the Nyquist frequency which is 200 Hz (The Nyquist frequency is twice the highest frequency (100.0 Hz) of the signal being sampled.). Determination of the sampling rate is complicated by the non-periodic nature of the ECG signals (MECG and FECG) and the type of filtering algorithm used to cancel the abdominal MECG. Since the MECG complexes are non-periodic, each complex is sampled slightly different. This difference is not an issue for FIR and infinite impulse response (IIR) filters provided the Nyquist frequency is employed, but is disastrous for a time domain subtractive filter if significant oversampling is not performed. The following

describes the importance of oversampling of the TECG and AECG for abdominal MECG attenuation.

Figures 4-2 and 4-3 demonstrate the necessity of oversampling of the ECG signals. To simplify the explanation, two sinusoid periods with the same amplitude and frequency will be used to illustrate the point. Since the ECG signals can be described as the sum of several sinusoids of different amplitudes and frequencies (from Fourier transform theory), the results from the two sinusoid periods will be analogous to what could be expected with ECG signals. Figures 4-2(a) and 4-3(a) contain two sinusoid periods separated with a zero amplitude interval starting at the tenth and twenty third samples respectively that are less than the period of each figure's respective sinusoid periods. This duration makes the sinusoid periods non-periodic. Thus, during sampling, the first sinusoid period samples are different values compared to the second. The different values are particularly noticeable for samples one and seventeen and for samples five and twenty one of the two sinusoid periods respectively of Figure 4-2(a). The slightly different sample instantaneous of each period is not critical if the two sinusoid periods are averaged, but becomes a problem when the average is subtracted from the original signal to cancel the sinusoid periods. Figures 4-2(b) and 4-3(b) are the averages of the two sinusoid periods of Figures 4-2(a) and 4-3(a) respectively. Figures 4-2(c) and 4-3(c) are the resulting signals when the averages of Figures 4-2(b) and 4-3(b) are subtracted from the two sinusoid periods of Figures 4-2(a) and 4-3(a) respectively. Notice the residuals of Figures 4-2(c) and 4-3(c) caused from the slightly dissimilar sampling of the sinusoid periods. Furthermore, Figure 4-3(c) residual peak-to-peak value is less than the residual peak-to-peak value of Figure 4-2(c). Since the signals of Figures 4-2 and 4-3 are the same and only differ by the sampling rate which is 2.4 times faster for the signal of Figure 4-3, indicates the need for oversampling for a time domain subtractive filter.

To further reinforce the necessity for oversampling, Figures 4-4 through 4-6 present clinical data that are exactly the same, but with different sampling rates. The TECG and AECG of Figures 4-4(a) and 4-4(b)(i) respectively were sampled at 1 kHz with the same upper cutoff filter frequency for both signals of 100.0 Hz (Analog filters of the adult ECG monitors set the 100.0 Hz cutoff frequency.). Furthermore, the TECG and AECG of Figure 4-4 were filtered digitally with a fourth order Butterworth lowpass filter with a cutoff frequency of 100.0 Hz before abdominal MECG cancellation was performed. Figures 4-5 and 4-6 ECG signals were obtained by downsampling the ECG signals of Figure 4-4 by a factor of two and four respectively.

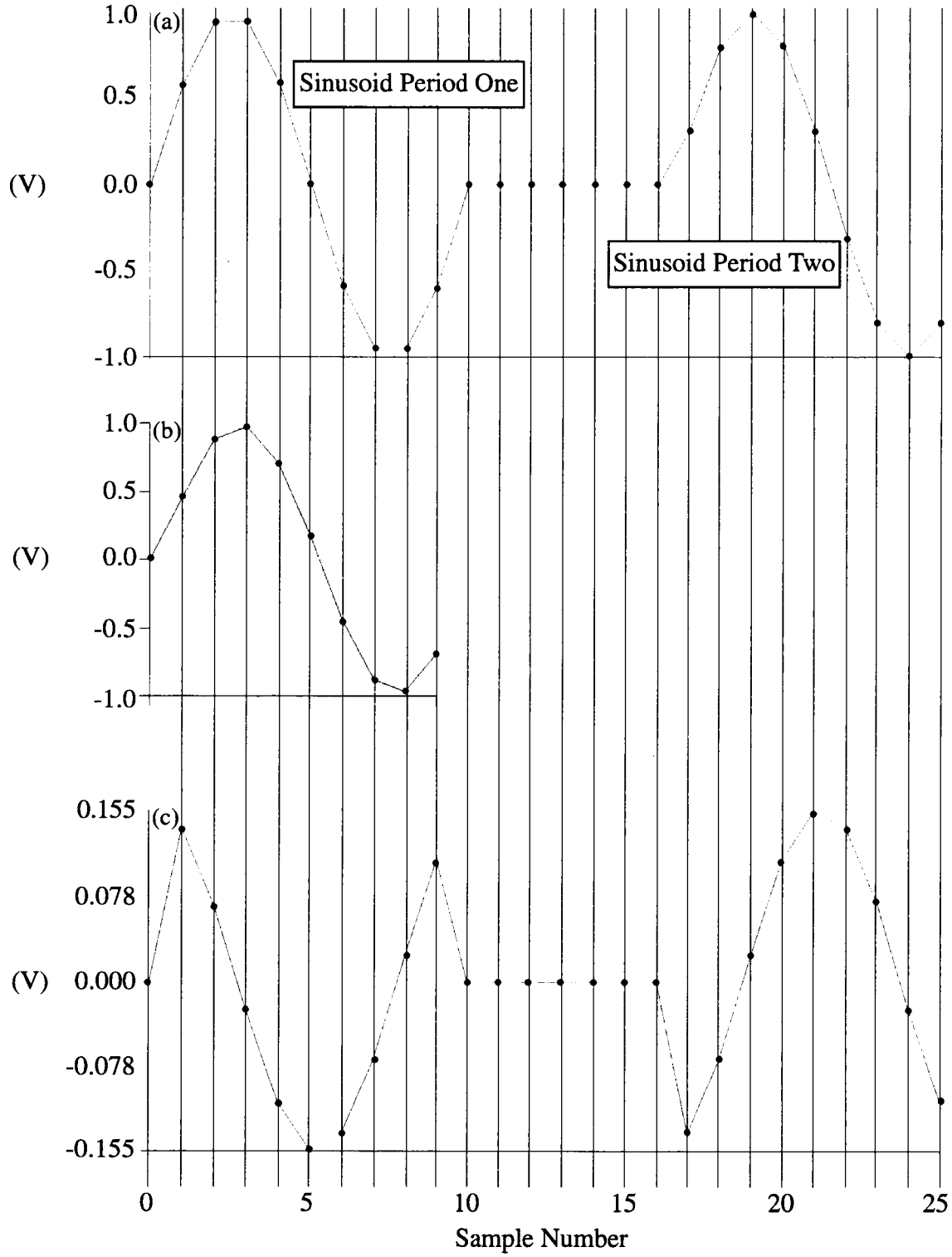

Figure 4-2. A demonstration of the necessity for oversampling with a signal that is sampled approximately five times faster than the Nyquist frequency. (a) A non-periodic signal. (b) The average of the two sinusoid periods of (a). (c) The resulting signal from subtracting the sinusoid period in (b) from each sinusoid period in (a).

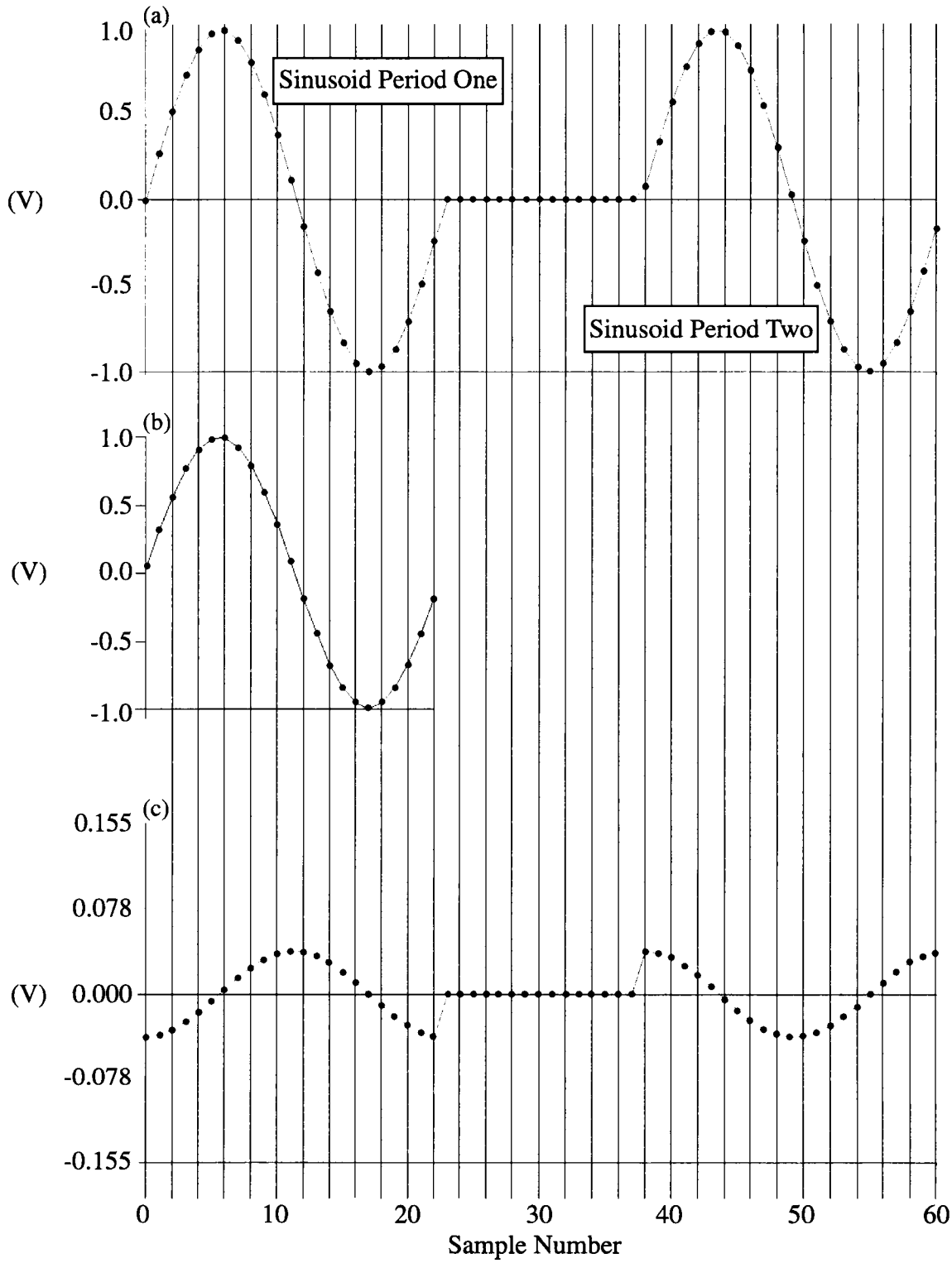

Figure 4-3. A demonstration of the necessity for oversampling with a signal that is sampled approximately 11.5 times faster than the Nyquist frequency. (a) A non-periodic signal. (b) The average of the two sinusoid periods of (a). (c) The resulting signal from subtracting the sinusoid period in (b) from each sinusoid period in (a).

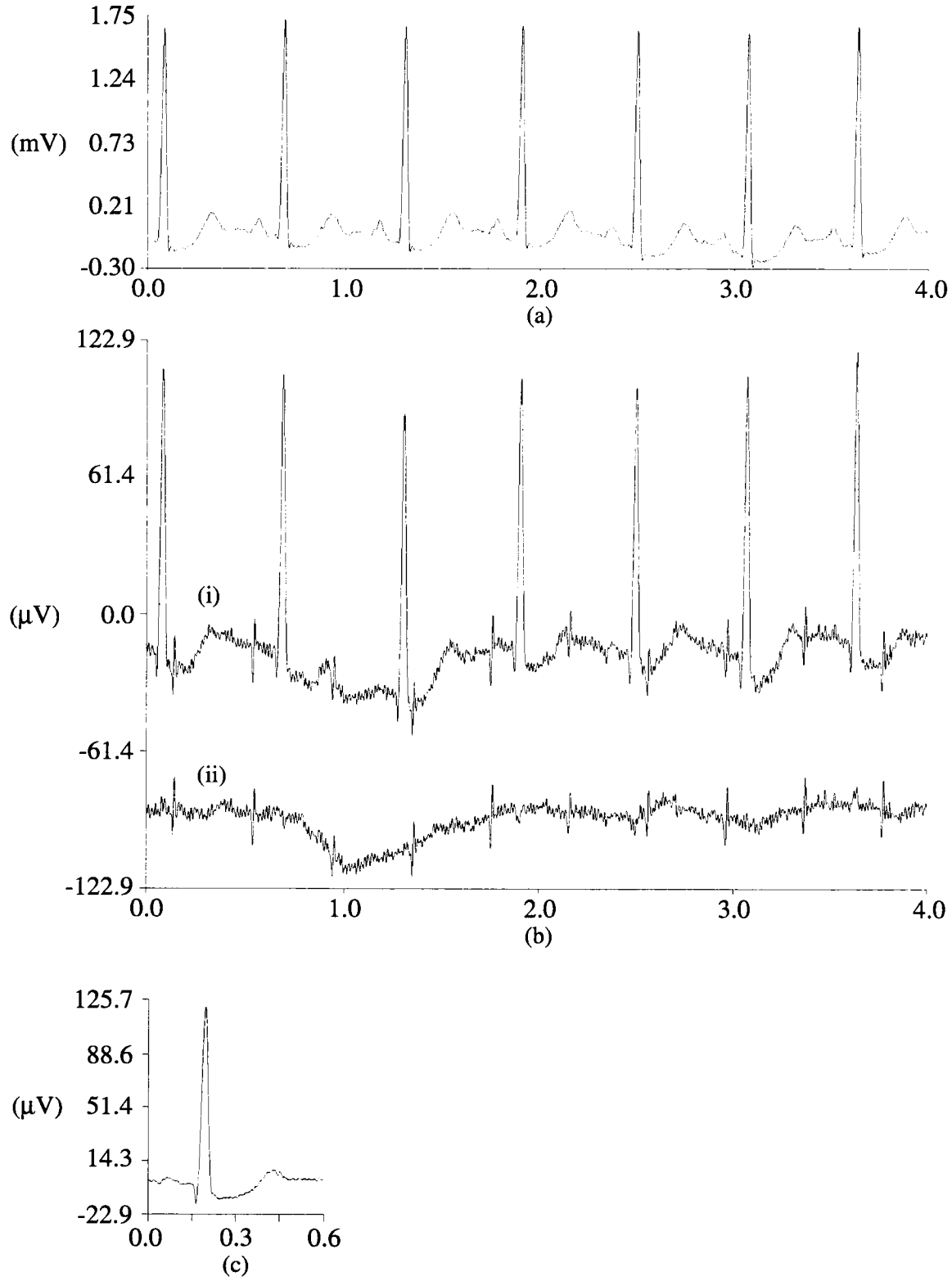

Figure 4-4. Clinical data with a 1 kHz sampling rate (all x-axes in seconds). (a) TECG. (b)(i) AECG. (b)(ii) AECG with the MECG canceled. (c) AECG MECG average (26 complexes averaged).

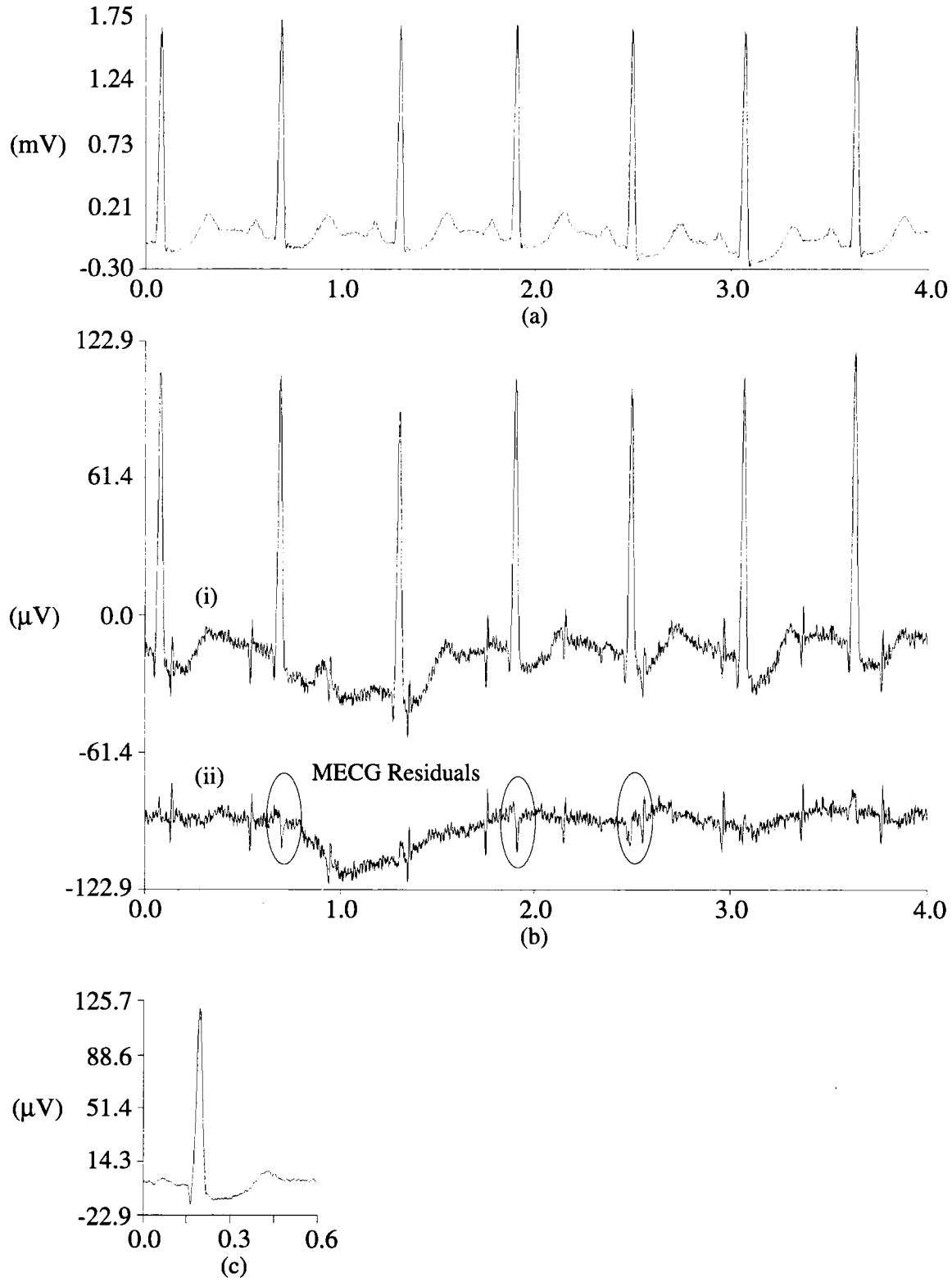

Figure 4-5. Clinical data with a 500 Hz sampling rate (all x-axes in seconds). (a) TECG. (b)(i) AECG. (b)(ii) AECG with the MECG canceled. (c) AECG MECG average (26 complexes averaged).

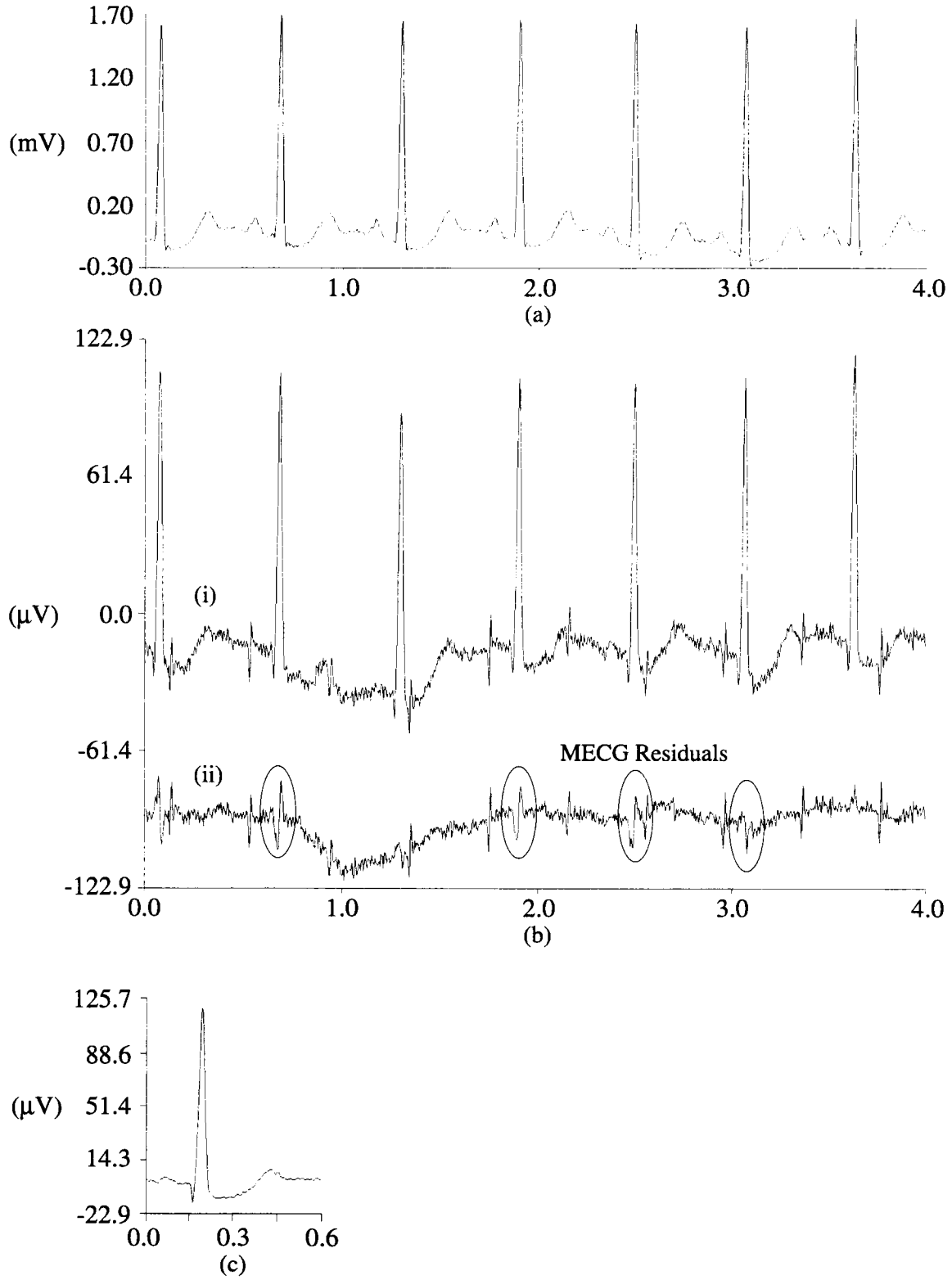

Figure 4-6. Clinical data with a 250 Hz sampling rate (all x-axes in seconds). (a) TECG. (b)(i) AECG. (b)(ii) AECG with the MECG canceled. (c) AECG MECG average (26 complexes averaged).

Therefore, the resulting TECG and AECG signals of Figures 4-5 and 4-6 have effective sampling rates of 500 and 250 Hz respectively. Finally, the fourth order Butterworth lowpass filter was used to avoid any chance of aliasing from downsampling being attributed to residuals that might result during abdominal MECG cancellation. Figures 4-4(c), 4-5(c), and 4-6(c) present the abdominal MECG averages used to suppress the MECG for the three figures.

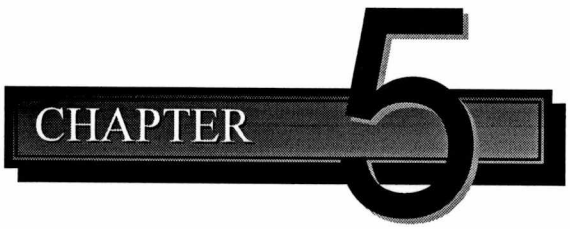

RESULTS

Dissertation Goal II
Ascertain the Effectiveness of the CH^2 Method for AECG MECG Cancellation via Synthesized & Clinical Data

The goal of this chapter is to ascertain the effectiveness of the CH^2 FECG system with synthesized and clinical data. The focus will be on subjective and objective analyses of abdominal MECG cancellation. In addition, the analyses presented will be rigorous and designed to thoroughly probe the strengths and weaknesses of the CH^2 FECG system. In summary, Figure 5-1 presents the layout of this chapter. Finally, this study will accomplish dissertation goal two as outlined by Figure 1-1.

The clinical data sets test the CH^2 FECG system and are intended to be representative data. A non-invasively obtained AECG will somewhat typically have much noise, non-ideal signal components from a variety of sources, and an extremely weak or indistinguishable FECG compared to other signals of the AECG. Therefore, not all the data sets are the most ideal, but samples that contain ideal, typical, and non-ideal data. The clinical AECGs of Figure 2-1(a), Figure 2-1(b), and Figure 2-1(c) would be considered somewhat ideal, somewhat ideal to typical, and very non-ideal respectively. Representative data was deliberately used because some of the previous literature had a tendency to report the most prized data. The use of only prized data misleads the reader to believe an AECG with a visible FECG was obtained from all patients studied which is unlikely. Furthermore, some of the formerly reported techniques' data sets give the reader little insight into how the methods work with typical clinical data or with non-ideal signals. Finally, by using representative data to test the CH^2 FECG system, the reader should gain much insight into the effectiveness of the CH^2 technique.

Chapter 5 is divided into two sections that present and analyze synthesized data and clinical data from 14 patients, as noted. Other clinical data can be found in Appendix C that contains

results from additional gestational ages of two of the 14 patients studied in this chapter. Finally, Appendix D contains clinical data that demonstrates 64 seconds of continuous abdominal MECG cancellation from one of the 14 patients studied. This data was included to give an intuitive feel for the effectiveness of the CH^2 technique for abdominal MECG suppression during real-time operation.

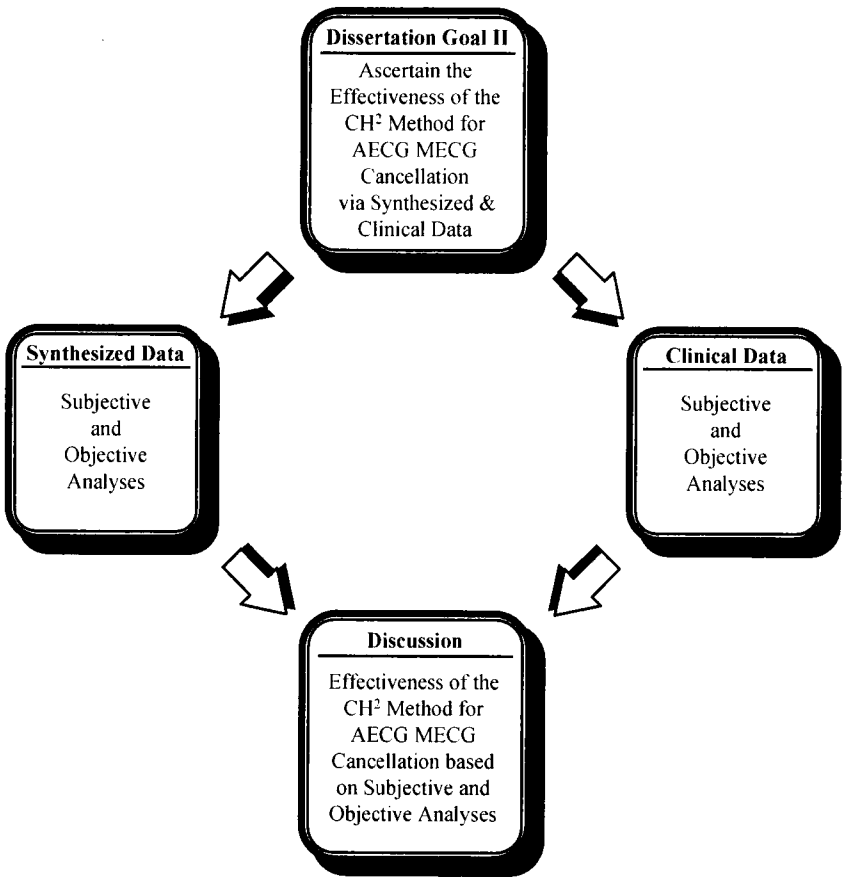

Figure 5-1. Block diagram describing the layout of Chapter 5.

5.1 Synthesized Data



Synthesized data was used to verify the effectiveness and accuracy of the DSP of the CH^2 FECG system. The test for effectiveness consists of a subjective visual inspection of the data and six objective numerical measures. Furthermore, synthesized data was employed to simulate a signal characteristic that evoked DSP failure. Finally, synthesized data as opposed to clinical data was initially applied to test the system's DSP. The testing was done because the individual signals of clinical data (MECG, FECG, and EMG) cannot be separated. Therefore, an objective comparison of the final results of the DSP to ascertain the residual and introduced noise is impossible.

Figure 5-2 presents synthesized data used to determine the amount of remaining and introduced noise from the DSP steps of abdominal MECG cancellation and FECG SNR enhancement. Figure 5-2(a) is an TECG from a non-pregnant patient. Figure 5-2(b) is an FECG strip synthesized from an averaged FECG complex from a pregnant patient (patient 3 at 38 weeks of gestation). The synthesis was done by linking together several of the averaged FECG complexes at a typical fetal heart rate and rate change to preserve the FECG frequency content. Figure 5-2(c)(i) is an AECG measured simultaneously with the TECG of Figure 5-2(a) and Figure 5-2(c)(ii) is artificially generated gaussian noise (bandwidth 0.05 to 100.0 Hz). Finally, the FECG strip of Figure 5-2(b) is added to the noise of Figure 5-2(c)(ii) to produce the signal of Figure 5-2(c)(iii).

Figure 5-3† demonstrates the two DSP steps of canceling the abdominal MECG and improving the FECG's SNR. Figure 5-3(a) is identical to the signal that appears in Figure 5-2(a). The AECG of Figure 5-3(b)(i) is synthesized by summing the signals of Figure 5-2(c)(i) and 5-2(c)(iii). Figure 5-3(b)(ii) presents the resulting AECG $R(n)$ from applying the CH^2 FECG system's abdominal MECG cancellation algorithm. Figure 5-3(c) is the abdominal MECG average calculated to cancel the MECG. A subjective analysis or visual inspection can easily see that the MECG of Figure 5-3(b)(i) is absent from Figure 5-3(b)(ii). Furthermore, from a subjective perspective, the noise and FECG have been slightly altered. This alteration can be

† The check marks and superscript numbers on this figure will be explained in Section 5.2.1.

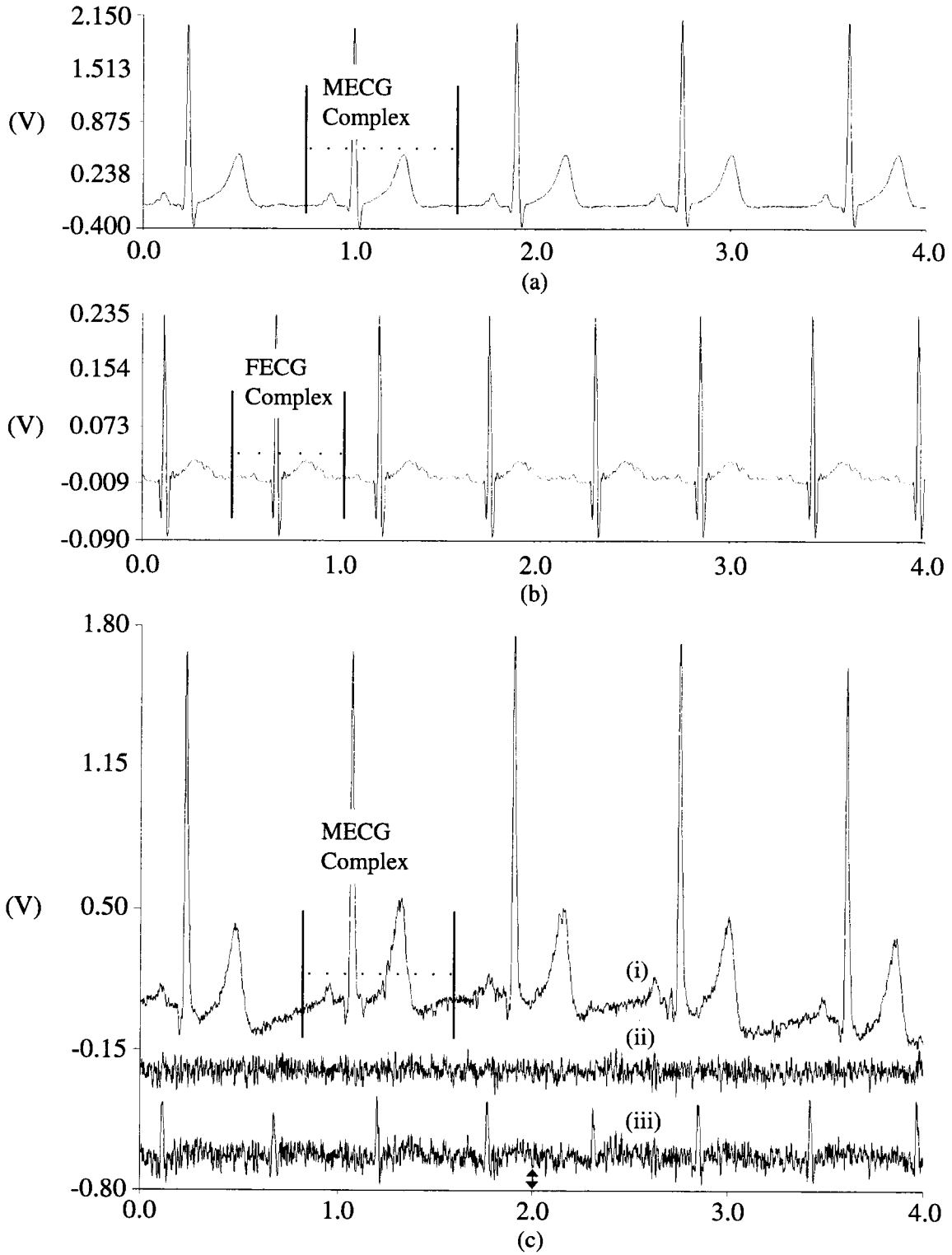

Figure 5-2. Synthesized data set one, original signals separated (all x-axes in seconds). (a) TECG. (b) The pure FECG. (c)(i) The AECG without noise added. (c)(ii) Gaussian noise, bandwidth 0.05 to 100.0 Hz. (c)(iii) The pure FECG of (b) with the noise of (c)(ii) added.

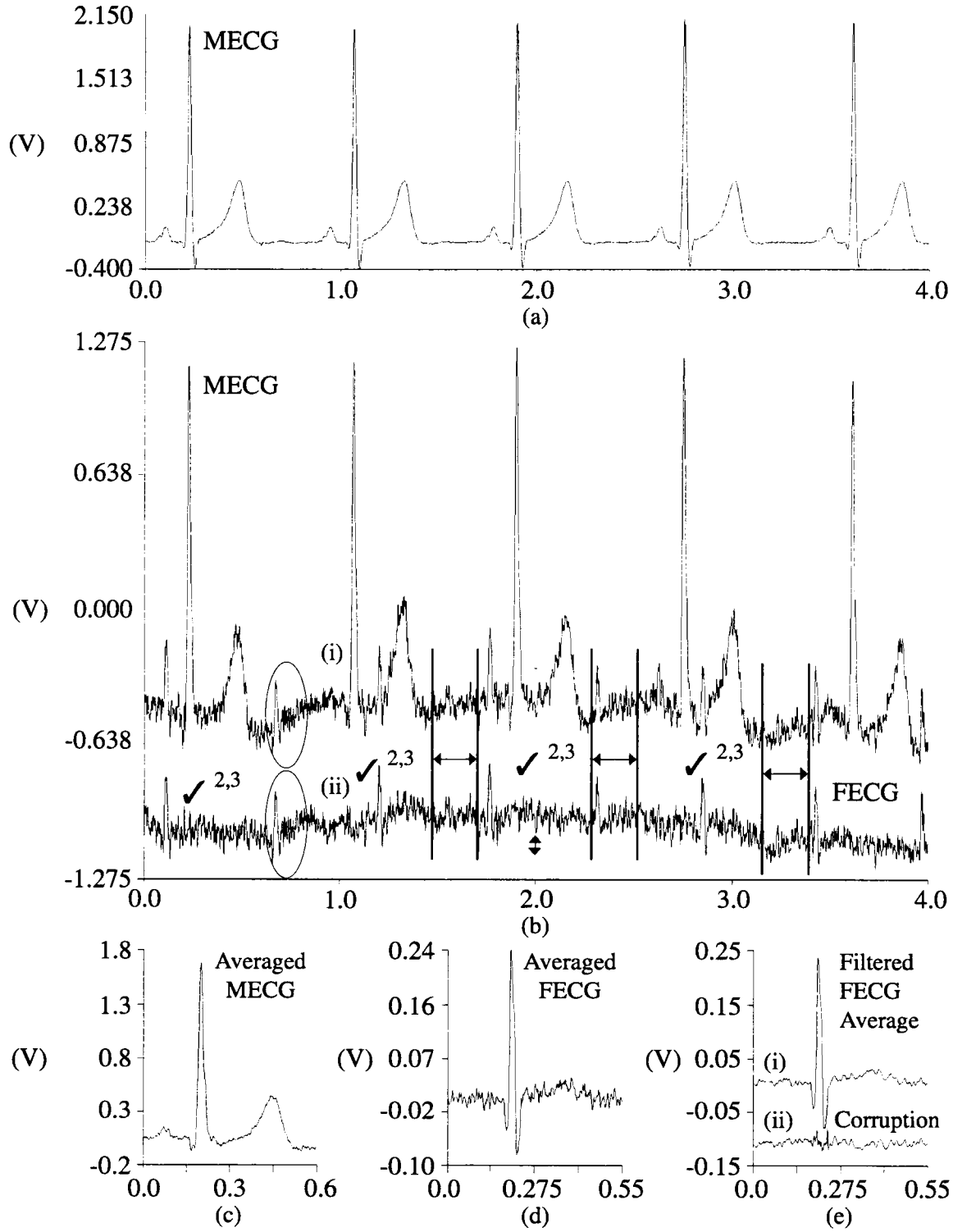

Figure 5-3. Synthesized data set one results (all x-axes in seconds). (a) TECG. (b)(i) AECG. (b)(ii) AECG with the MECG canceled. (c) Abdominal MECG average (20 complexes averaged). (d) FECG average (33 complexes averaged). (e)(i) Filtered FECG average (P wave - f_{cutoff} = 35.0 Hz and T wave - f_{cutoff} = 35.0 Hz). (e)(ii) Noise corrupting (e)(i).

seen by comparing visually the FECG and surrounding noise of the encircled areas of Figures 5-3(b)(i) and 5-3(b)(ii) along with other portions of the two signals (A visual inspection comparing the signals of Figures 5-2(c)(iii) and 5-3(b)(ii) cannot be done because the signal noise of Figure 5-2(c)(i) has not been accounted for in Figure 5-2(c)(iii) signal. This unaccountability will be elaborated further in a future discussion of this section.). Other subjective analyses of Figure 5-3 will be performed in Section 5.2.1. To qualify the subjective analysis or visual inspection, an objective analysis is necessary of the signals of Figure 5-3(b).

A typical analysis of signal corruption will usually include signal to signal plus noise ratio, correlation coefficient, SNR, and other measures. The objective analysis of signal corruption from MECG cancellation and FECG SNR enhancement includes signal to signal plus noise ratio, correlation coefficient, and SNR measures. The first corruption measure is defined by

$$CM_1 = \sigma^2_{S_{ideal}(n)} / (\sigma^2_{S_{ideal}(n)} + \sigma^2_{N(n)}) \qquad \text{(signal to signal plus noise ratio)} \qquad (53)$$

where $\sigma^2_{S_{ideal}(n)}$ is the variance of $S_{ideal}(n)$ which is the desired untainted signal and $\sigma^2_{N(n)}$ is the variance of $N(n)$ which is the noise that contaminates $S_{ideal}(n)$. The second corruption measure is defined by

$$CM_2 = \mathrm{E}[S_{ideal}(n)R(\mathrm{n})]/(\sigma_{S_{ideal}(n)}\sigma_{R(n)}) \qquad \text{(correlation coefficient)} \qquad (54)$$

where $R(n)$ is the resulting AECG from the signal enhancement and $\sigma^2_{R(n)}$ is the variance of $R(n)$. The third corruption measure is defined by

$$CM_3 = \sigma^2_{S_{ideal}(n)} / \sigma^2_{N(n)}. \qquad \text{(SNR)} \qquad (55)$$

A complete objective measure of abdominal MECG cancellation cannot be performed because determining $S_{ideal}(n)$ precisely is impractical. The impracticality comes from the fact that noise variance of the AECG of Figure 5-2(c)(i) will never be zero because of EMG noise. This non-zero noise variance can be intuitively perceived from a visual inspection of Figure 5-2(c)(iii) compared to Figure 5-3(b)(ii) particularly where the vertical arrows indicate the absence and presence of low frequency noise respectively. Artificial data could be used and this problem

would be avoided, but the authenticity of the data would be greatly compromised particularly the relationship between the TECG and AECG. A partial quantitative analysis of the signals of Figure 5-3(b) is performed by analyzing the signal sections that do not have MECG complexes that are marked with horizontal arrows in Figure 5-3(b). Since the CH^2 FECG system's abdominal MECG cancellation method by definition does not process these parts of the AECG, CM_1 is 1.0, CM_2 is 1.0, and CM_3 is infinite. Corruption measures CM_1 and CM_3 indicate the signal of these defined sections of the resulting AECG have unmeasurable signal corruption. Corruption measure CM_2 denotes that the AECG and resulting AECG of these defined sections are completely correlated. Finally, a similar partial analysis will be performed in Chapter 6 for comparing the CH^2 method for abdominal MECG cancellation with previously reported techniques.

Figure 5-3(d) is the FECG average from averaging 33 complexes of the data of Figure 5-3(b)(ii) and Figure 5-3(e)(i) is the filtered FECG average. Figure 5-3(e)(ii) is the noise corrupting the FECG of Figure 5-3(e)(i). Figure 5-3(e)(ii) was obtained by subtracting one of the original FECG complex of Figure 5-2(b) from the filtered FECG average of Figure 5-3(e)(i). From a subjective point of view, the filtered FECG of Figure 5-3(e)(i) is similar to the original complexes of Figure 5-2(b), but with a small amount of noise that the DSP did not remove and introduced. The DSP introduced some noise to the FECG from small alignment errors during FECG averaging. The affects of alignment errors can be seen in Figure 5-3(e)(ii) as small spikes around the corresponding time location of the QRS complex of the signal of Figure 5-3(e)(i).

An objective or quantitative analysis of FECG SNR enhancement is possible by using (53), (54), and (55) with $S_{ideal}(n)$ containing one of the FECG complexes of Figure 5-2(b), $N(n)$ containing the signal of Figure 5-3(e)(ii), and $R(n)$ containing the signal of Figure 5-3(e)(i). CM_1 is 0.974, CM_2 is 0.989, and CM_3 is 38.5 or 0.026 of the signal energy of the FECG of Figure 5-3(e)(i) is noise and the FECG of Figure 5-3(e)(i) is only 0.011 uncorrelated with the FECG complexes of Figure 5-2(b).

Figure 5-4† demonstrates a condition where the CH^2 FECG system's method for abdominal MECG cancellation fails. The ellipses of Figure 5-4(b)(ii) encircle the undesired MECG residuals. The ineffectiveness of the system arises from excessive noise in the trigger TECG. The data of Figure 5-4 is equivalent to the data of Figures 5-2 and 5-3, but with added TECG

† The ✗ s and superscript numbers on this figure will be explained in Section 5.2.1.

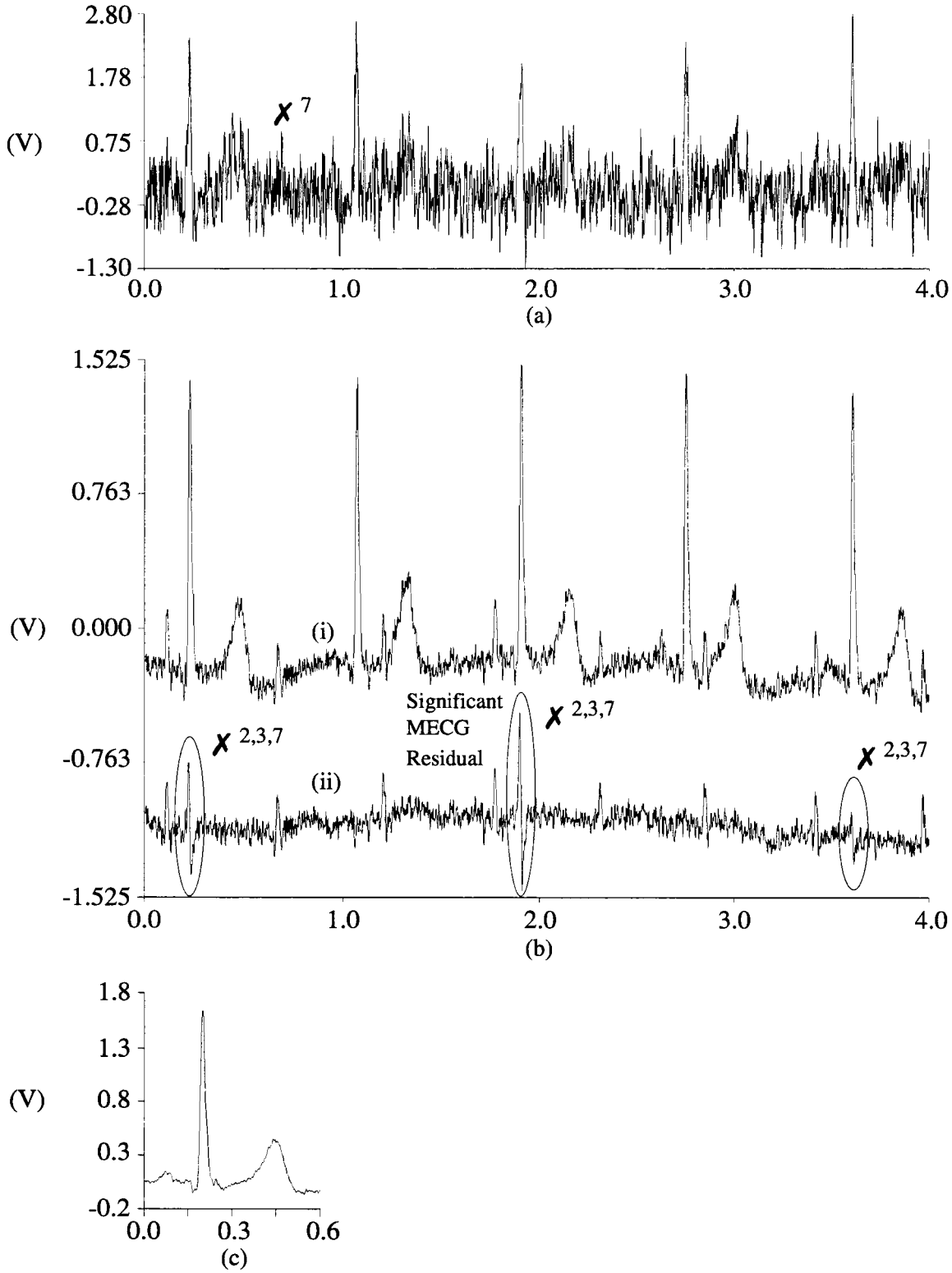

Figure 5-4. Synthesized data set two results (all x-axes in seconds). (a) TECG. (b)(i) AECG. (b)(ii) AECG resulting from attemped MECG cancellation. (c) Abdominal MECG average (20 complexes averaged).

noise. Figure 5-4(a) contains an TECG with added synthetic gaussian noise. The added gaussian noise bandwidth is 0.05 to 100.0 Hz and the resulting TECG SNR is 0.77. The noise hinders an accurate determination of the thoracic MECG's R wave time locations that causes abdominal MECG averaging and subtraction to be erroneous. Excessive noise, as demonstrated in this example, is unlikely to occur to the TECG as long as the patient is still. If the TECG contained significant noise, the AECG would most likely contain much noise that would produce a situation where the FECG would not be visible in the AECG regardless of perfect MECG cancellation. Another reason the CH^2 method for abdominal MECG cancellation may become ineffective will be discussed in Sections 5.2 and 5.3.

5.2 Clinical Data



Clinical data was used to determine the effectiveness of the DSP of the CH^2 FECG system. Several subjective visual inspections and one objective numerical measure that targets abdominal MECG suppression were used to test the system's effectiveness. The intent of the subjective analysis is to develop a rating system that will qualify the effectiveness of the CH^2 method for abdominal MECG cancellation. In addition, the purpose of the objective measure is to determine the average amount of MECG suppression that can be expected from a variety of patients from the CH^2 technique.

As previously discussed, clinical data was obtained from 14 patients of a variety of gestational ages (21-41) and conditions. Figures 5-5 through 5-18 present this data. Appendix C contains several figures that also present clinical data from patient 3 and 16[‡] at additional gestational ages other than the ones presented in this chapter. Appendix D contains clinical data that demonstrates 64 seconds of continuous abdominal MECG cancellation with data from patient 15[‡]. Finally, the subjective analysis was performed on the synthesized data previously presented, clinical data of this chapter, clinical data of Appendix C, and clinical data of Appendix D (Though this section is entitled clinical data, synthesized data is included to facilitate the explanation of the analysis.). The objective analysis of the abdominal MECG

[‡] The labels of patients 6 and 14 were omitted because in data logging the numbers were passed by.

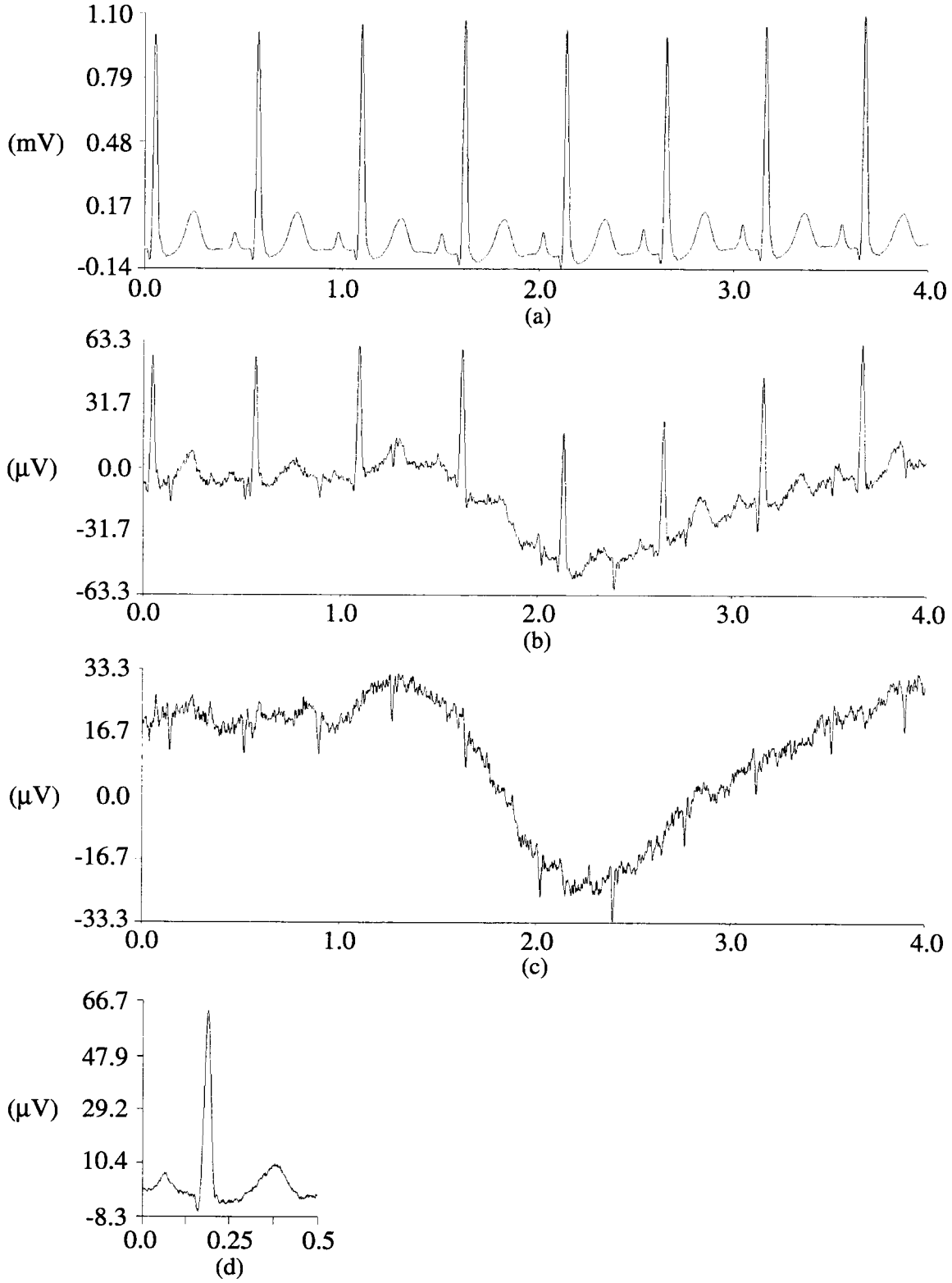

Figure 5-5. Clinical data from patient 1 at 36 weeks of gestation (all x-axes in seconds). (a) TECG. (b) AECG. (c) AECG with the MECG canceled. (d) Abdominal MECG average (27 complexes averaged).

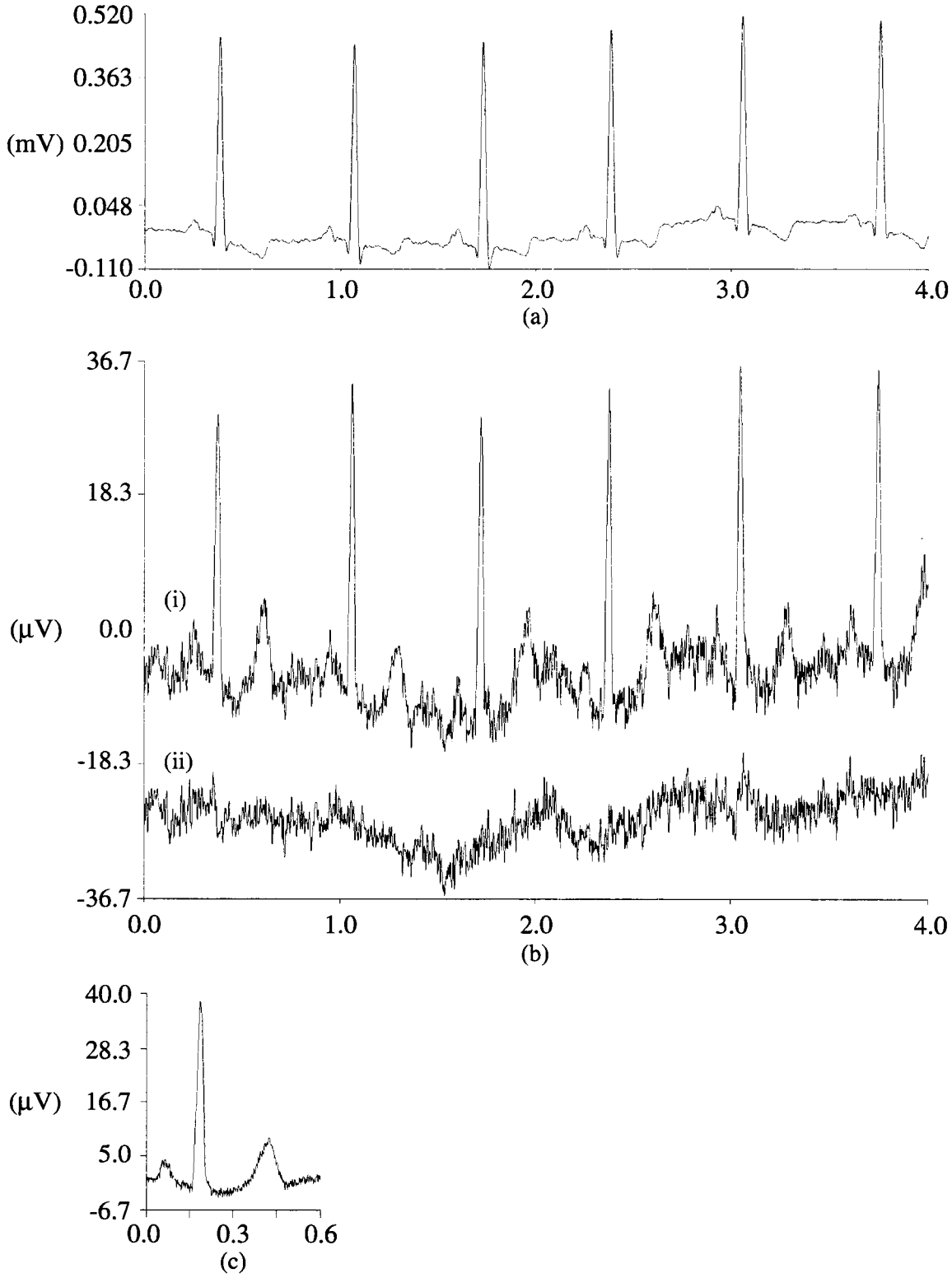

Figure 5-6. Clinical data from patient 2 at 36 weeks of gestation (all x-axes in seconds). (a) TECG. (b)(i) AECG. (b)(ii) AECG with the MECG canceled. (c) Abdominal MECG average (21 complexes averaged).

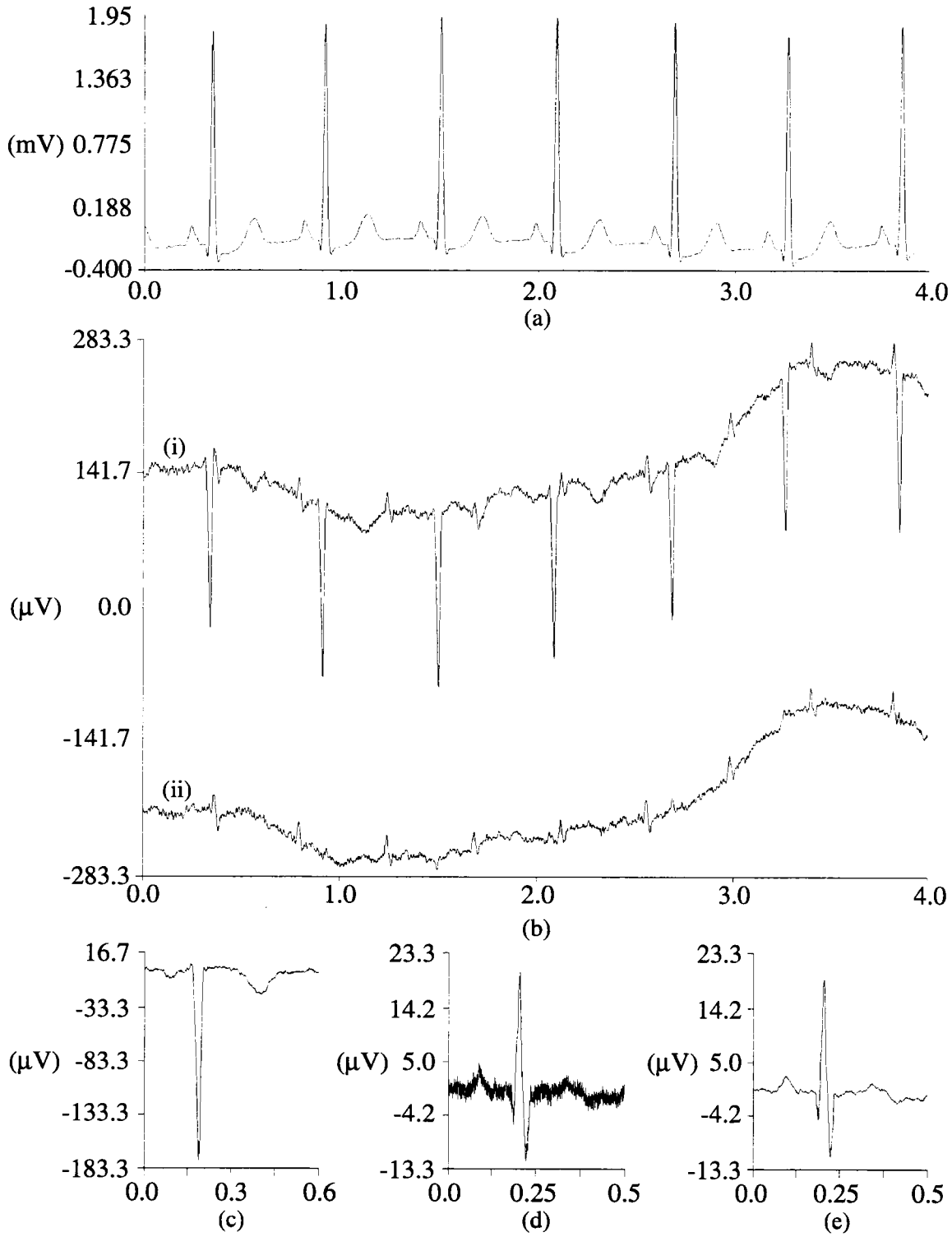

Figure 5-7. Clinical data from patient 3 at 34 weeks of gestation (all x-axes in seconds). (a) TECG. (b)(i) AECG. (b)(ii) AECG with the MECG canceled. (c) Abdominal MECG average (27 complexes averaged). (d) FECG average (34 complexes averaged). (e) Filtered FECG average (P wave - f_{cutoff} = 25.0 Hz and T wave - f_{cutoff} = 25.0 Hz).

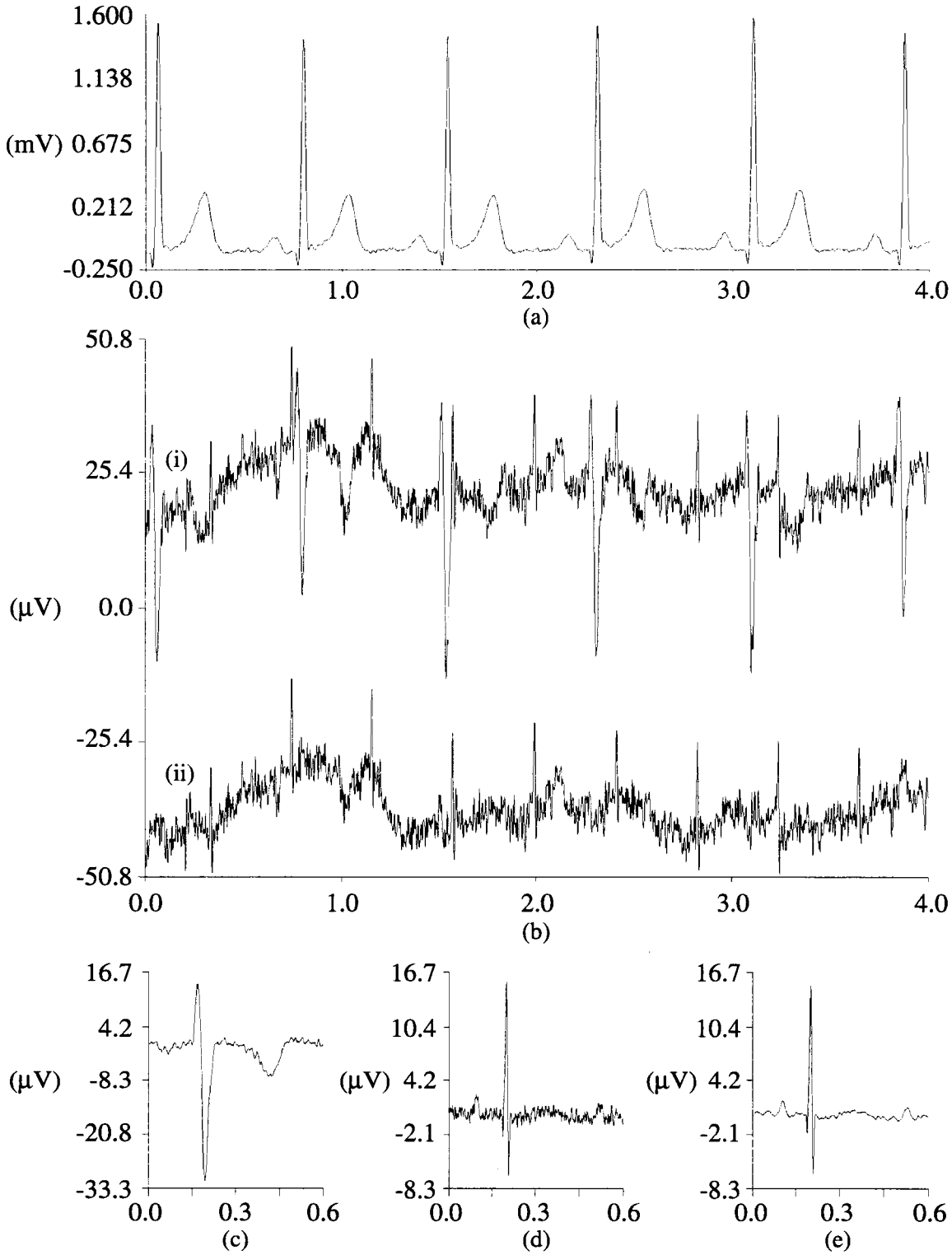

Figure 5-8. Clinical data from patient 4 at 21 weeks of gestation (all x-axes in seconds). (a) TECG. (b)(i) AECG. (b)(ii) AECG with the MECG canceled. (c) Abdominal MECG average (25 complexes averaged). (d) FECG average (33 complexes averaged). (e) Filtered FECG average (P wave - f_{cutoff} = 30.0 Hz and f_{cutoff} = 30.0 Hz).

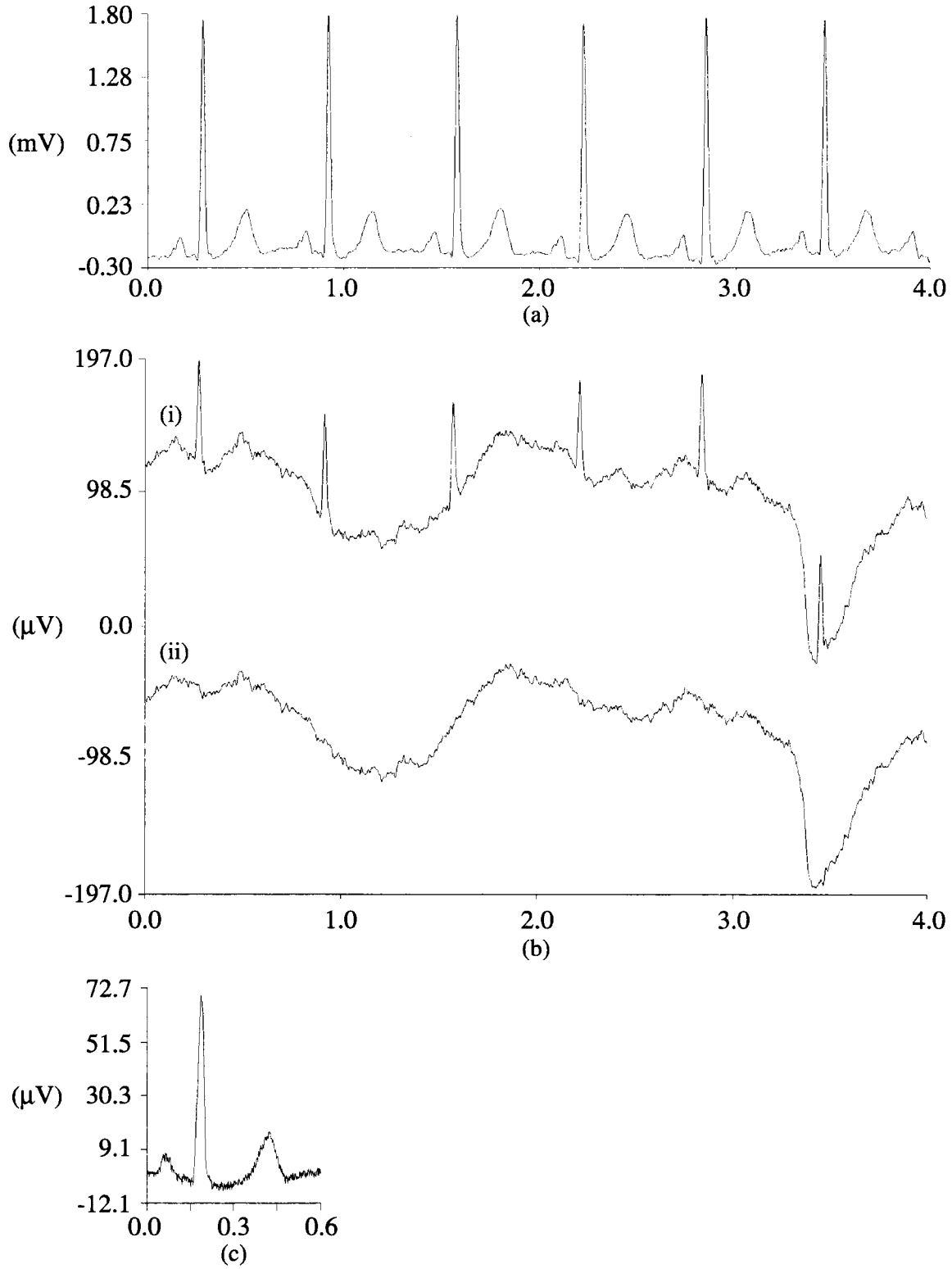

Figure 5-9. Clinical data from patient 5 at 36 weeks of gestation (all x-axes in seconds). (a) TECG. (b)(i) AECG. (b)(ii) AECG with the MECG canceled. (c) Abdominal MECG average (22 complexes averged).

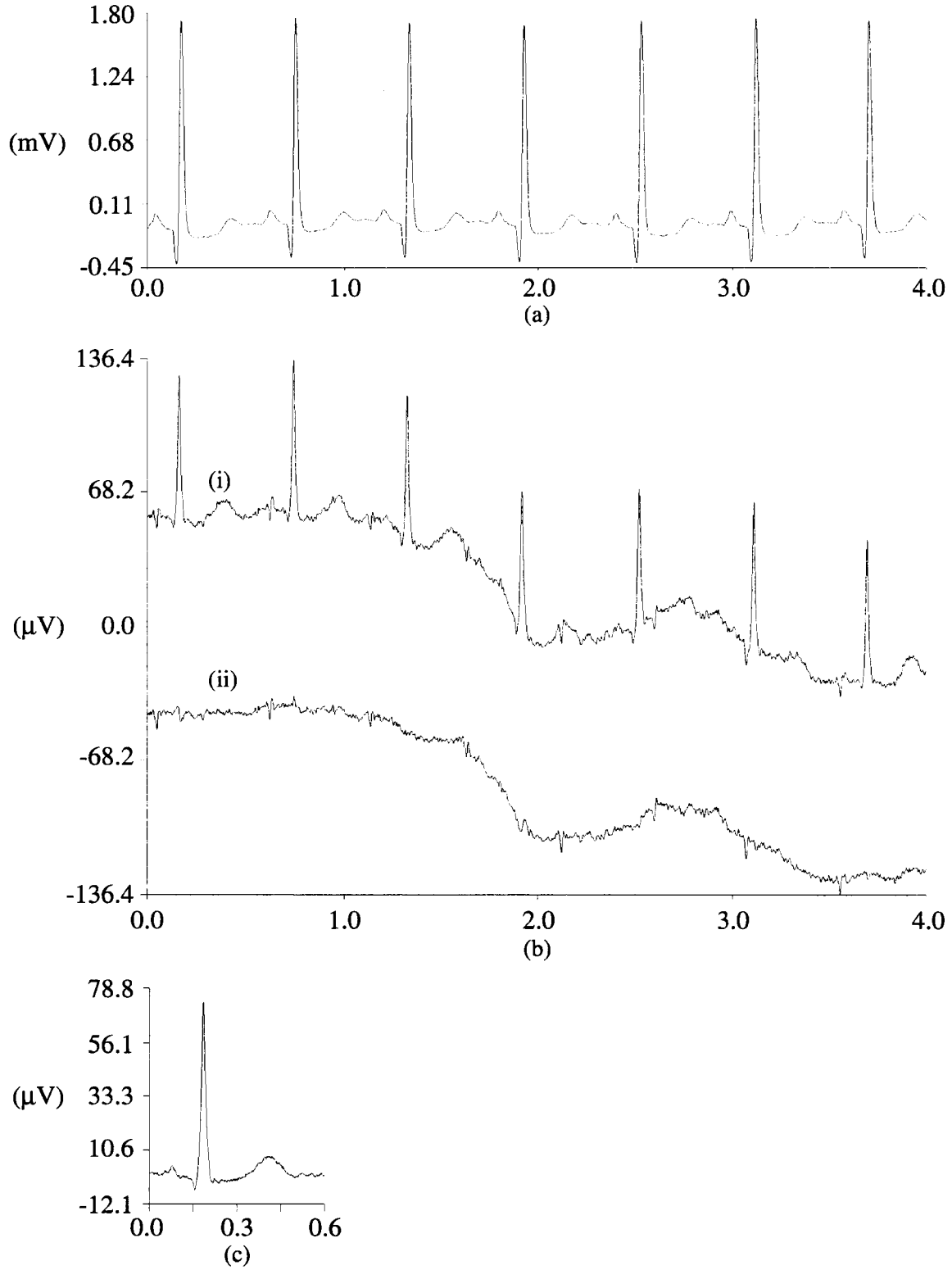

Figure 5-10. Clinical data from patient 7 at 39 weeks of gestation (all x-axes in seconds). (a) TECG. (b)(i) AECG. (b)(ii) AECG with the MECG canceled. (c) Abdominal MECG average (16 complexes averaged).

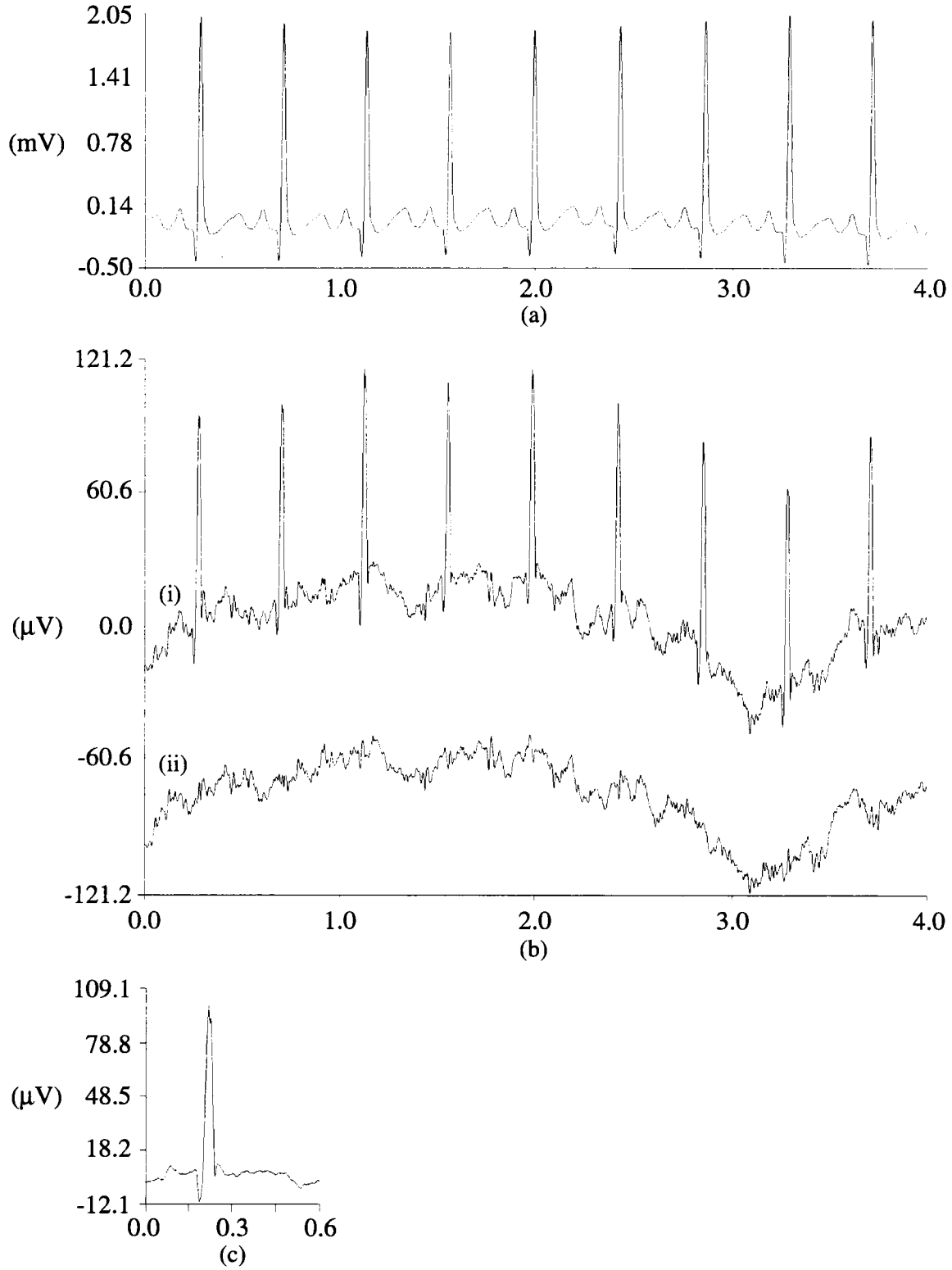

Figure 5-11. Clinical data from patient 8 at 36 weeks of gestation (all x-axes in seconds). (a) TECG. (b)(i) AECG. (b)(ii) AECG with the MECG canceled. (c) Abdominal MECG average (22 complexes averaged).

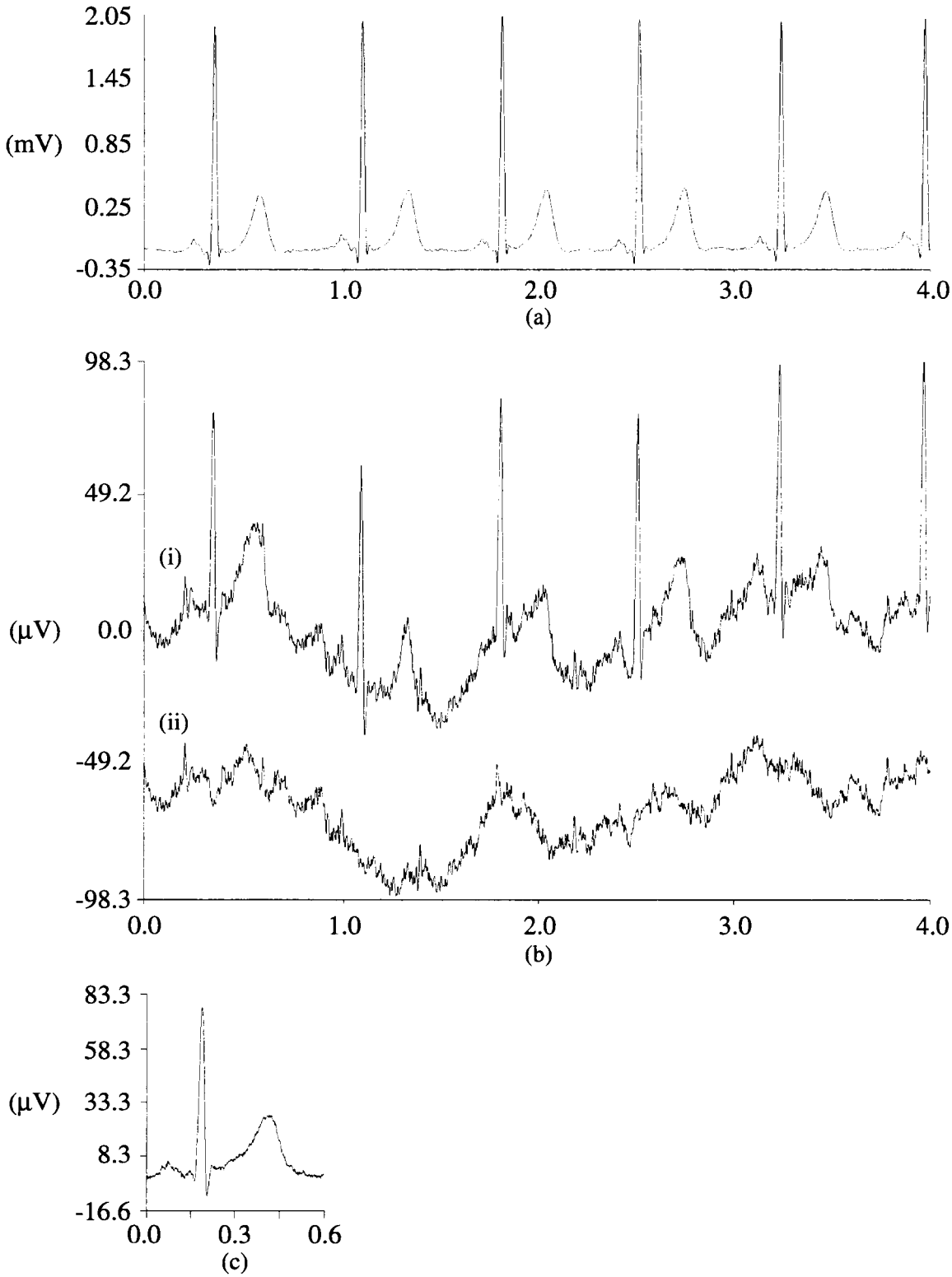

Figure 5-12. Clinical data from patient 9 at 27 weeks of gestation (all x-axes in seconds). (a) TECG. (b)(i) AECG. (b)(ii) AECG with the MECG canceled. (c) Abdominal MECG average (19 complexes averaged).

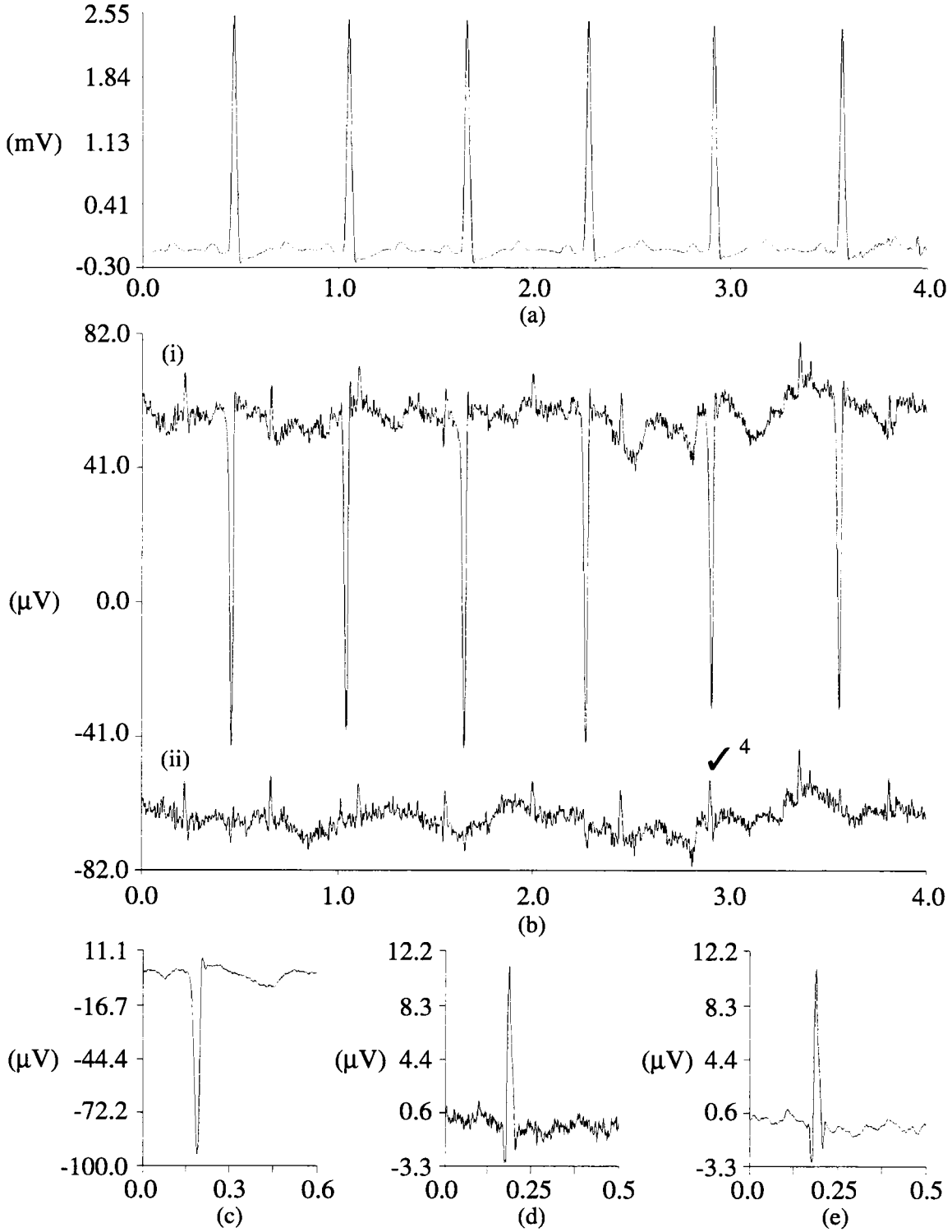

Figure 5-13. Clinical data from patient 10 at 37 weeks of gestation (all x-axes in seconds). (a) TECG. (b)(i) AECG. (b)(ii) AECG with the MECG canceled. (c) Abdominal MECG average (24 complexes averaged). (d) FECG average (28 complexes averaged). (e) Filtered FECG average (P wave - f_{cutoff} = 35.0 Hz and T wave - f_{cutoff} = 35.0 Hz).

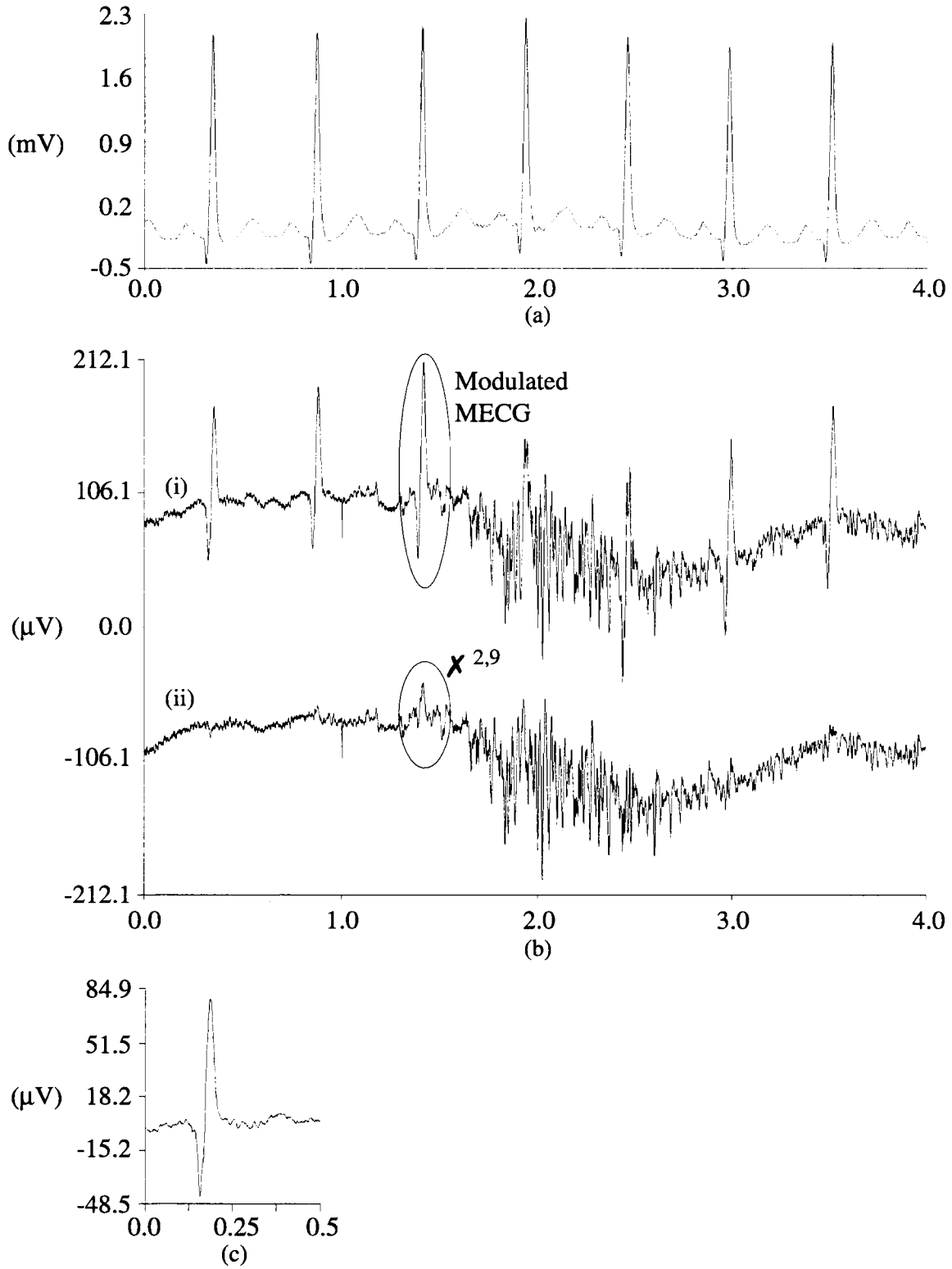

Figure 5-14. Clinical data from patient 11 at 38 weeks of gestation (all x-axes in seconds). (a) TECG. (b)(i) AECG. (b)(ii) AECG with the MECG canceled. (c) Abdominal MECG average (32 complexes averaged).

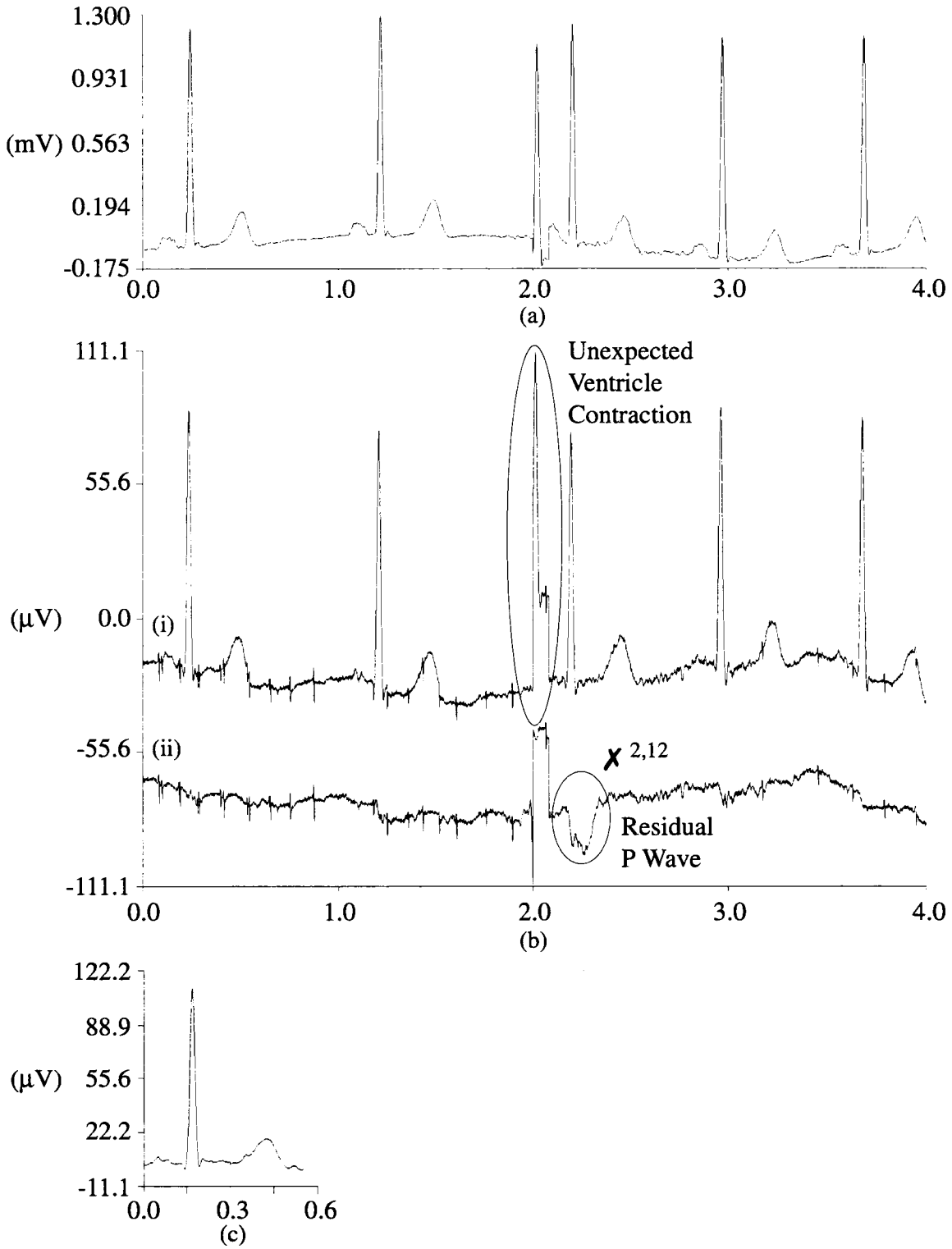

Figure 5-15. Clinical data from patient 12 at 34 weeks of gestation (all x-axes in seconds). (a) TECG. (b)(i) AECG. (b)(ii) AECG with the MECG canceled. The somewhat periodic spikes are EMG impulses and not the FECG. (c) Abdominal MECG average (42 complexes averaged).

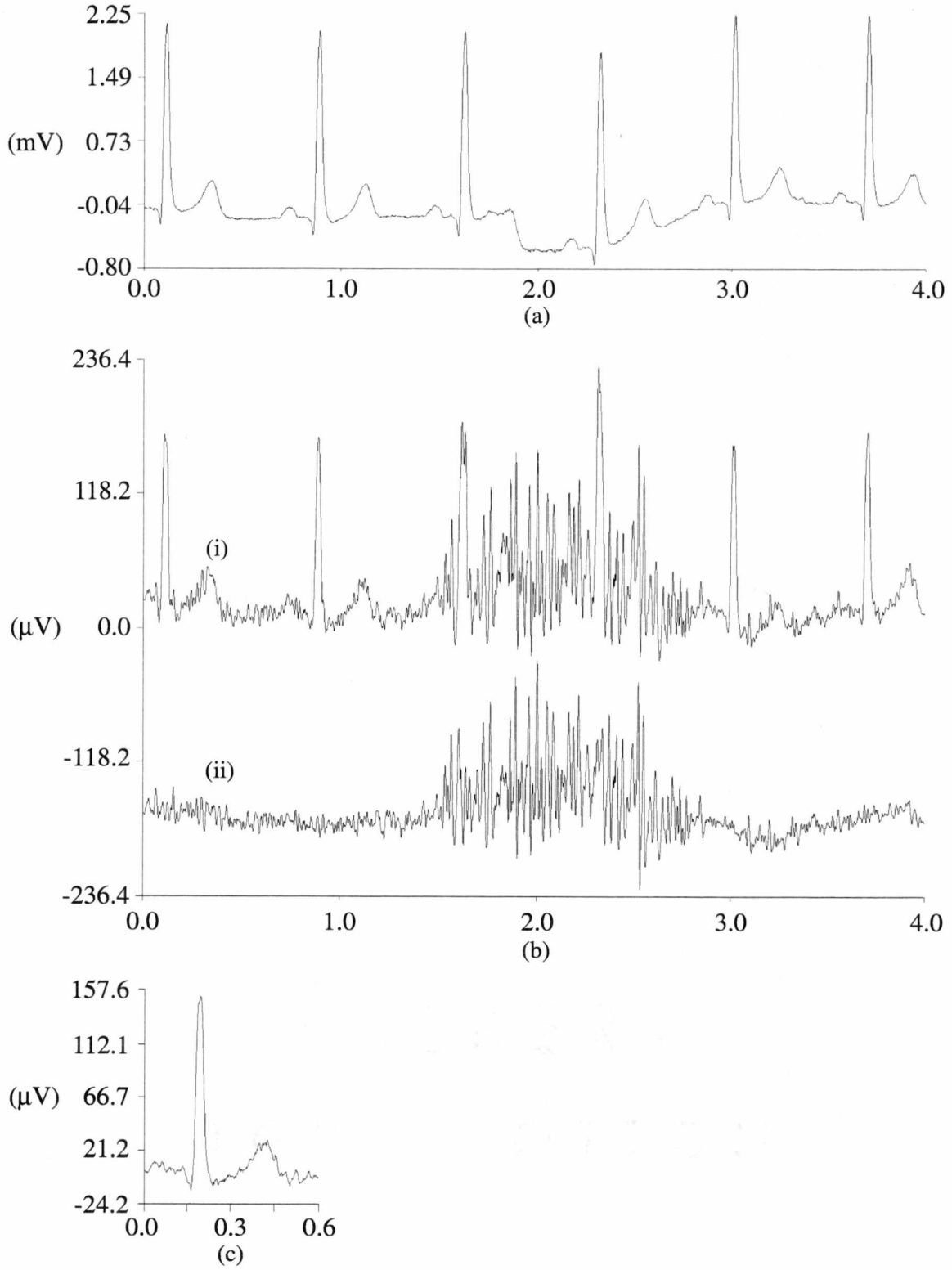

Figure 5-16. Clinical data from patient 13 at 39 weeks of gestation (all x-axes in seconds). (a) TECG. (b)(i) AECG. (b)(ii) AECG with the MECG canceled. (c) Abdominal MECG average (23 complexes averaged).

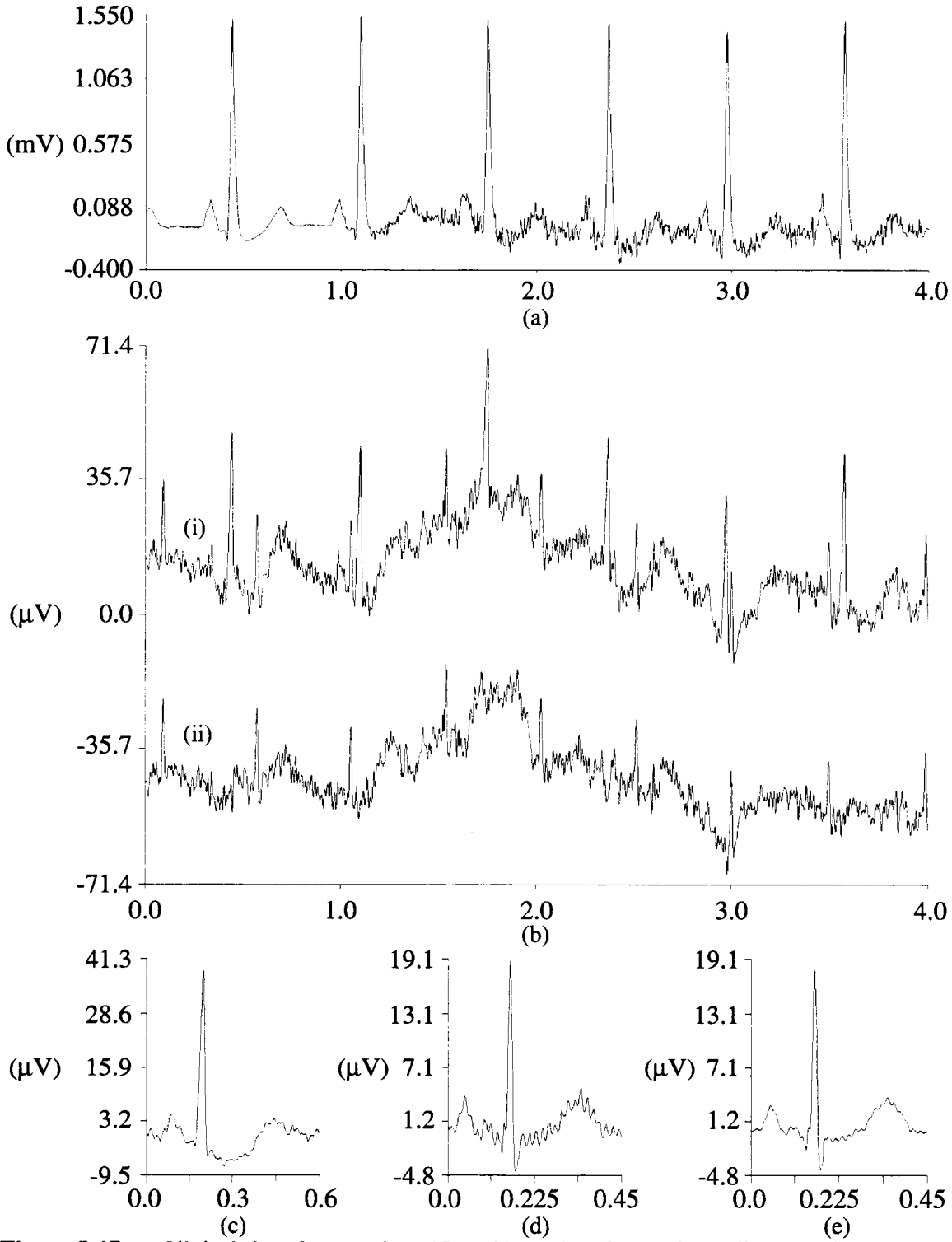

Figure 5-17. Clinical data from patient 15 at 41 weeks of gestation (all x-axes in seconds). (a) TECG. (b)(i) AECG. (b)(ii) AECG with the MECG canceled. (c) Abdominal MECG average (22 complexes averaged). (d) FECG average (32 complexes averaged). (e) Filtered FECG average (P wave - f_{cutoff} = 20.0 Hz and T wave f_{cutoff} = 20.0 Hz).

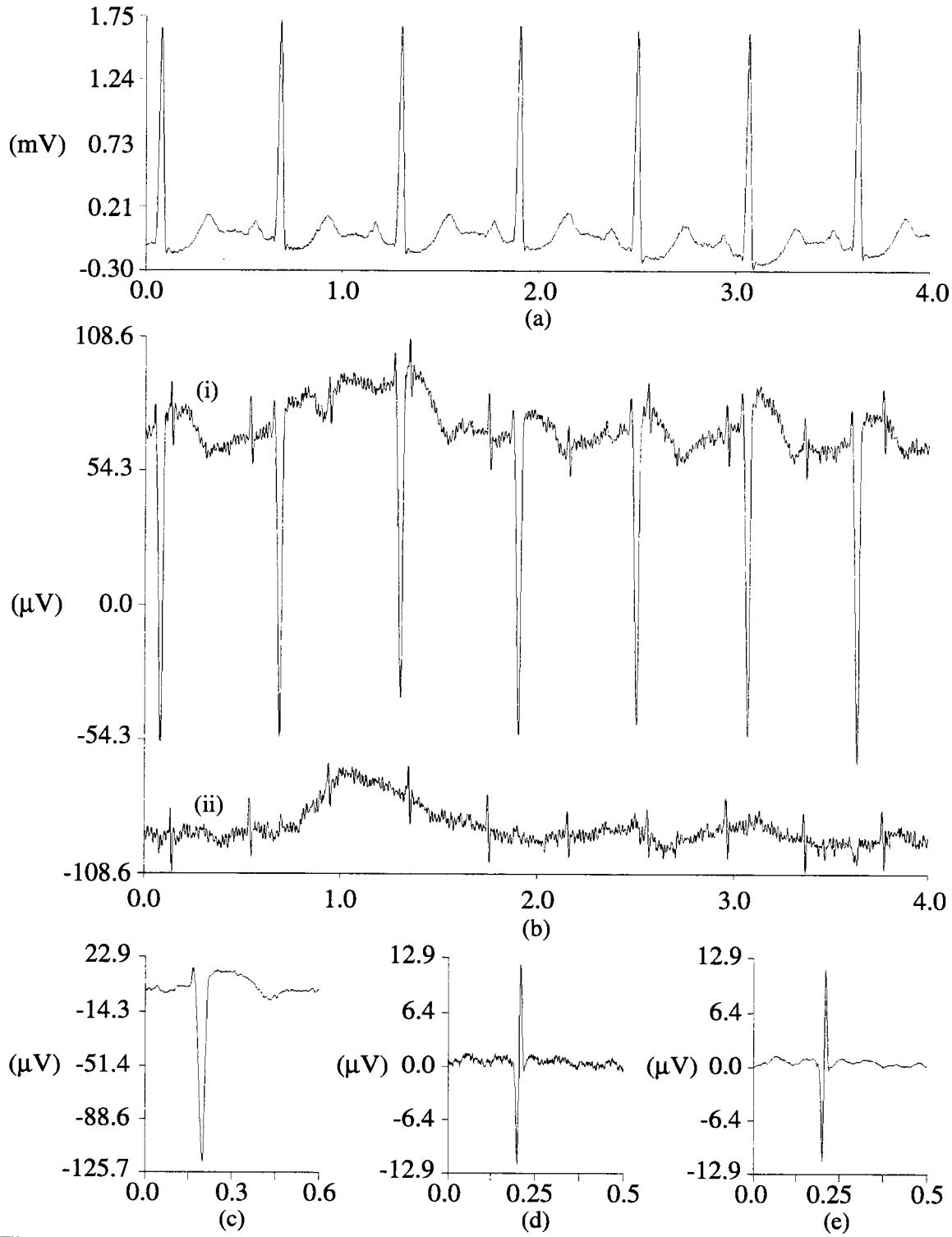

Figure 5-18. Clinical data from patient 16 at 26 weeks of gestation (all x-axes in seconds). (a) TECG. (b)(i) AECG. (b)(ii) AECG with the MECG canceled. (c) Abdominal MECG average (26 complexes averaged). (d) FECG average (39 complexes averaged). (e) Filtered FECG average (P wave - f_{cutoff} = 30.0 Hz and T wave - f_{cutoff} = 20.0 Hz).

cancellation was performed on the clinical data from the 14 patients studied.

Since there are a large number of figures referenced in this chapter, a template description (except for Figure 5-5) of the figures is preferred to efficiently convey their layout format. Figure 5-5 contains the results of clinical data from patient one. The TECG or trigger signal is contained in Figure 5-5(a) and the AECG is presented in Figure 5-5(b). Furthermore, the AECG with the MECG canceled is presented in Figure 5-5(c) where the MECG average of Figure 5-5(d) was used to cancel the MECG. Figures 5-6(a) through 5-18(a) present an TECG and Figures 5-6(b)(i) through 5-18(b)(i) present an AECG. Figures 5-6(b)(ii) through 5-18(b)(ii) present an AECG with the MECG canceled and Figures 5-6(c) through 5-18(c) present an MECG average used to cancel the respective abdominal MECG of Figures 5-6(b)(i) through 5-18(b)(ii). Some of Figures 5-6 through 5-18 have a (d) and (e) part. The (d) figure is the FECG average and the (e) figure is the filtered FECG average. These two formats also apply to the figures of Appendix C.

A discussion of each figure of data will not be performed, but a subjective analysis of the synthesized and clinical data of this chapter, clinical data of Appendix C, and clinical data of Appendix D will be presented in a tabular format. The tabular format was used to efficiently illustrate the subjective results of the CH^2 method for MECG cancellation. Also, the objective measure of the average amount of abdominal MECG suppression that can be expected with the CH^2 FECG system will be presented.

5.2.1 Subjective Analysis

There are five parts to the subjective analysis where the first four study one block of data four seconds in duration from several patients. The first analysis examines the data, mostly by visual inspection, to determine if the CH^2 method for abdominal MECG cancellation passes or fails 12 test conditions that are based on signal characteristics. Subjective analysis two determines the clinical applicability of the resulting AECG. The third and fourth analysis determine the ratings of the 12 test conditions and three clinical applications. Subjective analysis five ascertains the ratings of the 12 test conditions and three clinical applications for 64 seconds of continuous abdominal MECG cancellation. The 64 seconds of data is divided into sixteen four seconds blocks of data where each block is analyzed. Tables 5-1 through 5-6 present the results of abdominal MECG attenuation for the five subjective analyses. To facilitate the organization of the data of the six tables, synthesized and clinical data that were one block four seconds in duration from several patients are not shaded and referred to as **one block** data.

Table 5-1. Inspection results for MECG cancellation effectiveness of Figs. 5-3 to 5-8.

ENGINEERING ASPECTS (See Appendix E for a detailed description)								
Test Conditions		Data Designation & Grading Information						
Possible Outcomes ✓ Passed ✗ Failed - Did Not Occur PA Preamp. NPA No Preamp.		Fig. 5-3 Synth. Data FECG NPA	Fig. 5-4 Synth. Data FECG NPA	Fig. 5-5 Patient 1 36 Weeks FECG NPA	Fig. 5-6 Patient 2 36 Weeks No FECG NPA	Fig. 5-7 Patient 3 34 Weeks FECG NPA	Fig. 5-8 Patient 4 21 Weeks FECG NPA
1	Bandwidth of Resulting AECG is 0.05 to 100 Hz	✓	✓	✓	✓	✓	✓
2	Signal Corruption to FECG & EMG	✓	✗[7*]	✓	✓	✓	✓
3	Overall MECG Cancellation	✓	✗	✓	✓	✓	✓
4	FECG & MECG Overlap	-	-	✓	-	✓	-
5	Significant AECG Low Frequency Noise	-	-	✓	-	✓	-
6	Significant AECG Noise Spike	-	-	-	-	-	-
7	Significant TECG Noise	-	✗	-	-	-	-
8	AECG Noise	✓	✓	✓	✓	✓	✓
9	Modulated MECG of the AECG	-	-	-	-	-	-
10	Modulated MECG of the TECG	-	-	✓	-	-	-
11	Periodic EMG Impulses	-	-	-	-	-	-
12	Unexpected Ventricle Contraction	-	-	-	-	-	-
CLINICAL APPLICABILITY (See Appendix E for a detailed description)								
Clinical Applications		Grading Information						
P Potential NP No Potential		Fig. 5-3	Fig. 5-4	Fig. 5-5	Fig. 5-6	Fig. 5-7	Fig. 5-8	
1	Fetal HR Information via HR Determination Algorithm	P	NP	P	NP	P	P	
2	FECG Electrophysiological Information via FECG Averaging	P	NP	NP	NP	P	P	
3	Uterine Contraction Information via EMG	P	NP	P	P	P	P	
*The failure of test condition 7 caused test conditions 2 to fail.								

Table 5-2. Inspection results for MECG cancellation effectiveness of Figs. 5-9 to 5-14.

ENGINEERING ASPECTS (See Appendix E for a detailed description)							
Test Conditions		Data Designation & Grading Information					
Possible Outcomes ✓ Passed × Failed - Did Not Occur PA Preamp. NPA No Preamp.		Fig. 5-9 Patient 5 36 Weeks No FECG PA	Fig. 5-10 Patient 7 39 Weeks FECG PA	Fig. 5-11 Patient 8 36 Weeks No FECG PA	Fig. 5-12 Patient 9 27 Weeks FECG NPA	Fig. 5-13 Pat. 10 37 Weeks FECG PA	Fig. 5-14 Pat. 11 38 Weeks No FECG PA
1	Bandwidth of Resulting AECG is 0.05 to 100 Hz	✓	✓	✓	✓	✓	✓
2	Signal Corruption to FECG & EMG	✓	✓	✓	✓	✓	×[9*]
3	Overall MECG Cancellation	✓	✓	✓	✓	✓	✓
4	FECG & MECG Overlap	-	✓	-	✓	✓	-
5	Significant AECG Low Frequency Noise	✓	✓	-	-	-	✓
6	Significant AECG Noise Spike	-	-	-	-	-	-
7	Significant TECG Noise	-	-	-	-	-	-
8	AECG Noise	✓	✓	✓	✓	✓	✓
9	Modulated MECG of the AECG	-	-	-	-	✓	×
10	Modulated MECG of the TECG	-	-	✓	-	-	✓
11	Periodic EMG Impulses	-	-	-	-	-	-
12	Unexpected Ventricle Contraction	-	-	-	-	-	-
CLINICAL APPLICABILITY (See Appendix E for a detailed description)							
Clinical Applications		Grading Information					
P Potential NP No Potential		Fig. 5-9	Fig. 5-10	Fig. 5-11	Fig. 5-12	Fig. 5-13	Fig. 5-14
1	Fetal HR Information via HR Determination Algorithm	NP	P	NP	P	P	NP
2	FECG Electrophysiological Information via FECG Averaging	NP	NP	NP	NP	P	NP
3	Uterine Contraction Information via EMG	P	P	P	P	P	NP
*The failure of test condition 9 caused test condition 2 to fail.							

Table 5-3. Inspection results of Figs. 5-15 to 5-18 and C-1 to C-2.

ENGINEERING ASPECTS (See Appendix E for a detailed description)							
Test Conditions		Data Designation & Grading Information					
Possible Outcomes ✓ Passed × Failed - Did Not Occur PA Preamp. NPA No Preamp.		Fig. 5-15 Pat. 12 34 Weeks No FECG PA	Fig. 5-16 Pat. 13 39 Weeks No FECG PA	Fig. 5-17 Pat. 15 41 Weeks FECG PA	Fig. 5-18 Pat. 16 26 Weeks FECG PA	Fig. C-1 Patient 3 23 Weeks FECG NPA	Fig. C-2 Patient 3 24 Weeks FECG NPA
1	Bandwidth of Resulting AECG is 0.05 to 100 Hz	✓	✓	✓	✓	✓	✓
2	Signal Corruption to FECG & EMG	×12*	✓	✓	✓	✓	✓
3	Overall MECG Cancellation	✓	✓	✓	✓	✓	✓
4	FECG & MECG Overlap	-	-	-	-	✓	✓
5	Significant AECG Low Frequency Noise	-	-	-	-	-	✓
6	Significant AECG Noise Spike	✓	-	-	-	-	-
7	Significant TECG Noise	-	✓	✓	-	✓	-
8	AECG Noise	✓	✓	✓	✓	✓	✓
9	Modulated MECG of the AECG	-	-	-	-	-	-
10	Modulated MECG of the TECG	-	-	-	-	-	-
11	Periodic EMG Impulses	✓	-	-	-	-	-
12	Unexpected Ventricle Contraction	×	-	-	-	-	-
CLINICAL APPLICABILITY (See Appendix E for a detailed description)							
Clinical Applications		Grading Information					
P Potential NP No Potential		Fig. 5-15	Fig. 5-16	Fig. 5-17	Fig. 5-18	Fig. C-1	Fig. C-2
1	Fetal HR Information via HR Determination Algorithm	NP	NP	P	P	P	P
2	FECG Electrophysiological Information via FECG Averaging	NP	NP	P	P	P	P
3	Uterine Contraction Information via EMG	NP	P	P	P	P	P
*The failure of test condition 12 caused test condition 2 to fail.							

Table 5-4. Inspection results for MECG cancellation effectiveness of Figs. C-3 to C-8.

ENGINEERING ASPECTS (See Appendix E for a detailed description)								
Test Conditions		Data Designation & Grading Information						
Possible Outcomes ✓ Passed × Failed - Did Not Occur PA Preamp. NPA No Preamp.		Fig. C-3 Patient 3 25 Weeks FECG NPA	Fig. C-4 Patient 3 26 Weeks FECG NPA	Fig. C-5 Patient 3 31 Weeks FECG NPA	Fig. C-6 Patient 3 33 Weeks No FECG NPA	Fig. C-7 Patient 3 35 Weeks FECG NPA	Fig. C-8 Patient 3 36 Weeks FECG NPA
1	Bandwidth of Resulting AECG is 0.05 to 100 Hz	✓	✓	✓	✓	✓	✓
2	Signal Corruption to FECG & EMG	✓	×9*	✓	✓	✓	✓
3	Overall MECG Cancellation	✓	✓	✓	✓	✓	✓
4	FECG & MECG Overlap	✓	-	-	-	✓	✓
5	Significant AECG Low Frequency Noise	-	-	✓	✓	-	-
6	Significant AECG Noise Spike	-	-	-	-	-	-
7	Significant TECG Noise	-	-	-	-	-	-
8	AECG Noise	✓	✓	✓	✓	✓	✓
9	Modulated MECG of the AECG	-	×	-	-	-	-
10	Modulated MECG of the TECG	-	-	-	✓	-	-
11	Periodic EMG Impulses	-	-	-	-	-	-
12	Unexpected Ventricle Contraction	-	-	-	-	-	-
CLINICAL APPLICABILITY (See Appendix E for a detailed description)								
Clinical Applications		Grading Information						
P Potential NP No Potential		Fig. C-3	Fig. C-4	Fig. C-5	Fig. C-6	Fig. C-7	Fig. C-8	
1	Fetal HR Information via HR Determination Algorithm	P	P	P	NP	P	P	
2	FECG Electrophysiological Information via FECG Averaging	P	NP	NP	NP	P	P	
3	Uterine Contraction Information via EMG	P	P	P	P	P	P	
*The failure of test condition 9 caused test condition 2 to fail.								

Table 5-5. Inspection results of Figs. C-9 to C-11 and D-1 to D-3.

ENGINEERING ASPECTS (See Appendix E for a detailed description)								
Test Conditions		Data Designation & Grading Information						
Possible Outcomes ✓ Passed × Failed - Did Not Occur PA Preamp. NPA No Preamp.		Fig. C-9 Patient 3 38 Weeks FECG NPA	Fig. C-10 Patient 3 39 Weeks FECG NPA	Fig. C-11 Pat. 16 36 Weeks No FECG PA	Fig. D-1 Pat. 15 41 Weeks FECG PA	Fig. D-2 Pat. 15 41 Weeks FECG PA	Fig. D-3 Pat. 15 41 Weeks FECG PA
1	Bandwidth of Resulting AECG is 0.05 to 100 Hz	✓	✓	✓	✓ ✓	✓ ✓	✓ ✓
2	Signal Corruption to FECG & EMG	✓	×9*	✓	✓ ✓	✓ ✓	✓ ×9*
3	Overall MECG Cancellation	✓	×	✓	✓ ✓	✓ ✓	✓ ✓
4	FECG & MECG Overlap	✓	×	-	✓ -	- -	- -
5	Significant AECG Low Frequency Noise	-	-	✓	✓ ✓	- -	✓ -
6	Significant AECG Noise Spike	-	-	-	- -	- ✓	- -
7	Significant TECG Noise	-	-	✓	- -	- -	- ✓
8	AECG Noise	✓	✓	✓	✓ ✓	✓ ✓	✓ ✓
9	Modulated MECG of the AECG	-	×	-	- -	- -	- ×
10	Modulated MECG of the TECG	✓	-	-	- -	- -	- -
11	Periodic EMG Impulses	-	-	✓	- -	- -	- -
12	Unexpected Ventricle Contraction	-	-	-	- -	- -	- -
CLINICAL APPLICABILITY (See Appendix E for a detailed description)							
Clinical Applications		Grading Information					
P Potential NP No Potential		Fig. C-9	Fig. C-10	Fig. C-11	Fig. D-1	Fig. D-2	Fig. D-3
1	Fetal HR Information via HR Determination Algorithm	P	NP	NP	P P	P P	P P
2	FECG Electrophysiological Information via FECG Averaging	P	P	NP	P P	P P	P P
3	Uterine Contraction Information via EMG	P	NP	P	P P	P P	P NP
*The failure of test condition 9 caused test condition 2 to fail.							

Table 5-6. Inspection results for MECG cancellation effectiveness of Figs. D-4 to D-8.

ENGINEERING ASPECTS (See Appendix E for a detailed description)								
Test Conditions		Data Designation & Grading Information						
Possible Outcomes ✓ Passed × Failed - Did Not Occur PA Preamp. NPA No Preamp.		Fig. D-4 Pat. 15 41 Weeks FECG PA	Fig. D-5 Pat. 15 41 Weeks FECG PA	Fig. D-6 Pat. 15 41 Weeks FECG PA	Fig. D-7 Pat. 15 41 Weeks FECG PA	Fig. D-8 Pat. 15 41 Weeks FECG PA	Ratio of Success One Block Continuous
1	Bandwidth of Resulting AECG is 0.05 to 100 Hz	✓ ✓	✓ ✓	✓ ✓	✓ ✓	✓ ✓	25/25 16/16
2	Signal Corruption to FECG & EMG	✓ ✓	✓ ✓	✓ ✓	✓ ✓	✓ ✓	21/25 15/16
3	Overall MECG Cancellation	✓ ✓	✓ ✓	✓ ✓	✓ ✓	✓ ✓	24/25 16/16
4	FECG & MECG Overlap	✓ ✓	✓ -	✓ ✓	- ✓	✓ ✓	11/12 9/9
5	Significant AECG Low Frequency Noise	✓ ✓	- -	- -	✓ ✓	✓ ✓	9/9 9/9
6	Significant AECG Noise Spike	- ✓	✓ ✓	✓ -	- -	- -	1/1 5/5
7	Significant TECG Noise	- -	- -	- -	- -	- -	4/4 1/1
8	AECG Noise	✓ ✓	✓ ✓	✓ ✓	✓ ✓	✓ ✓	25/25 16/16
9	Modulated MECG of the AECG	- -	- -	- -	- -	- -	1/4 0/1
10	Modulated MECG of the TECG	- -	- -	- -	- -	- -	5/5 -
11	Periodic EMG Impulses	- -	- -	- -	- -	- -	2/2 -
12	Unexpected Ventricle Contraction	- -	- -	- -	- -	- -	0/1 -
CLINICAL APPLICABILITY (See Appendix E for a detailed description)								
Clinical Applications		Grading Information						
P Potential NP No Potential		Fig. D-4	Fig. D-5	Fig. D-6	Fig. D-7	Fig. D-8	Potentials	
1	Fetal HR Information via HR Determination Algorithm	P P	P P	P P	P P	P P	16/25 16/16	
2	FECG Electrophysiological Information via FECG Averaging	P P	P P	P P	P P	P P	12/25 16/16	
3	Uterine Contraction Information via EMG	P P	P P	P P	P P	P P	22/25 15/16	

Clinical data that was 64 seconds in duration from one patient was broken into sixteen four seconds blocks and is shaded and referred to as **continuous** data. The appropriate grade is awarded for each test condition or clinical application based on the four seconds of data that appears in Figures 5-2 through 5-18 and Figures C-1 through C-11. The data of Figures D-1 through D-8 contain eighth seconds of data. Therefore, two grades were awarded for each test condition and clinical application. The top grade is for the first four seconds of each figure and the bottom for the last four seconds (See Table 5-5 columns four through six and Table 5-6 columns one through five). Finally, Appendix E contains four tables that give a detailed description of the grading for the test conditions and clinical applications.

To further clarify the grading of the test conditions and clinical applications, an example explanation will be presented with the synthesized data of Figures 5-3 and 5-4 of this chapter. Furthermore, synthesized data also demonstrates more conclusively the grading of some of the test conditions. Figures 5-3 and 5-4 are identical, but Figure 5-4(a)'s TECG contains added gaussian noise. Since the applicable tests of Figure 5-3 data were all reported pass, any failures in Figure 5-4 test conditions can be attributed to the TECG noise.

For Figures 5-3 and 5-4, test condition 1 was reported a pass because the resulting AECGs from MECG cancellation by definition are 0.05 to 100.0 Hz (See Chapter 3 for method description.). Test condition 2 was graded pass and fail for Figures 5-3 and 5-4 respectively which was determined from a visual inspection of the two resulting AECGs. The resulting AECGs compared to the AECGs' FECG or EMG had negligible and noticeable MECG residuals for Figures 5-3 and 5-4 respectively. The ✗ superscript seven of Table 5-1 (row: test condition 2, column: Figure 5-4) indicates that test condition 2 was reported a failure because test condition 7 failed. Test condition 7 will be discussed later. Furthermore, the ✓ and ✗ superscript two of Figures 5-3(b)(ii) and 5-4(b)(ii) indicate the time locations of negligible and noticeable MECG residuals that caused test condition 2 to be reported pass and fail respectively. Test condition 3 was reported a pass for Figure 5-3 and a failure for Figure 5-4 because zero and three out of five MECG complexes respectively of the AECGs resulted in noticeable MECG residuals compared to the AECGs' FECG and EMG. Furthermore, the ✓ and ✗ superscript three of Figures 5-3(b)(ii) and 5-4(b)(ii) indicate the time locations of negligible and noticeable MECG residuals that caused test condition 3 to be reported pass and fail respectively.

Test conditions 4 through 6 were awarded a did not occur grade because the FECG and MECG never overlapped, no significant AECG low frequency noise occurred, and no significant

AECG noise spike occurred in the two data sets (A detailed description of significant AECG low frequency noise and a significant AECG noise spike can be found in Table E-1 and E-2 respectively of Appendix E). Test condition 7 for the data of Figure 5-3 was graded a did not occur because significant TECG noise was not present in the TECG of Figure 5-3(a). Test condition 7 for Figure 5-4 was considered a failure because noticeable MECG residuals occurred when the TECG's SNR was much lower than Figure 5-3(a). The MECG residuals during the occurrence of significant TECG noise will not cause test condition 7 to be reported a failure. However, when test conditions 5, 9, 10, and 12 did not occur, test condition 7 is left as the most probably cause of the MECG residuals. The conclusion is further reinforced from the fact that adequate abdominal MECG cancellation was obtained with data of Figure 5-3 that differs from Figure 5-4 only in the TECG's SNR (These deductions are the reason test conditions 2 and 3 failures are attributed to test condition 7.). The ✓ and ✗ superscript two of Figures 5-3(b)(ii) and 5-4(b)(ii) indicate the time locations of negligible and noticeable MECG residuals that caused test condition 7 to be reported pass and fail respectively. Test condition 8 was reported a pass for both data sets because a visual examination of the resulting AECGs of Figures 5-3(b)(ii) and 5-4(b)(ii) compared to the AECGs' of Figures 5-3(b)(i) and 5-4(b)(i) FECG or EMG had similar shaped FECG and EMG. Therefore, no added noise was introduced from MECG averaging and subtraction. Test condition 9 through 12 did not occur which was determined from a visual inspection for modulated AECGs, modulated TECGs, periodic EMG impulses, and unexpected ventricle contractions of the data sets. Figures 5-14, 5-5, 5-15, and 5-15 are examples of occurrences of test conditions 9 through 12 respectively.

Synthesized data of Figures 5-3 and 5-4 are good data sets to explain the grading scheme of the second subjective analysis or clinical applicability. These data sets have grades of potential and no potential respectively for all three clinical applications. The first clinical application pertains to fetal HR information via an HR determination algorithm. Potential and no potential grades were awarded to Figures 5-3 and 5-4 respectively. A potential grade was awarded for Figure 5-3 because the resulting AECG had an observable FECG as well as test condition 3 was graded pass. A no potential grade was awarded to Figure 5-4 data because test condition 3 failed. The second clinical application pertains to the determination of the FECG electrophysiological information via FECG averaging. Potential and no potential grades were awarded to Figures 5-3 and 5-4 respectively. A potential grade was awarded for Figure 5-3 because test conditions 1 and 3 passed. Furthermore, FECG averaging has potential to produce

an FECG average with a favorable SNR because a visual inspection of the AECG of Figure 5-3(b)(i) can discern all FECG's R waves to be averaged without question. A no potential grade was awarded for Figure 5-4 because test condition 3 failed. The final clinical application is uterine contraction information via EMG. This test determines if the EMG signal of the resulting AECG has been corrupted from abdominal MECG cancellation. If the EMG is not tainted, then uterine contraction information can be accurately derived from the EMG and a potential status is awarded. If the EMG is tainted, then uterine contraction information cannot be accurately derived from the EMG and a no potential grade is awarded†. The data of Figure 5-3 has potential to determine uterine contraction information because test conditions 1 and 2 passed. The data of Figure 5-4 has no potential because test condition 2 failed.

Subjective analysis three determines the percentage success of each of the 12 test conditions. The top ratios (none shaded) of the last column of Table 5-6 are the ratios of success for the test conditions. The ratios are determined by computing the number of passes for each test condition and dividing it by the number of occurrences of each test condition. Then the percentage successes are obtained by multiplying the ratios by 100. The data of Figure 5-3 and 5-4 were not included in the calculation since they were synthesized data. Furthermore, the data of Figures D-1 through D-8 were also disregarded because a separate evaluation will be performed for these data sets (Patient 15 at 41 weeks of gestation has been included in this analysis via Figure 5-17).

Subjective analysis four determines the percentage potential for each of the three clinical applications. The top ratios (none shaded) of the last column of Table 5-6 are the ratios of potential for each clinical application. The ratios are determined by computing the number of times each clinical application had potential and divided it by the total clinical cases studied. Then the percentage potentials of the data sets are found by multiplying the ratios by 100. (As discussed, Figures 5-3, 5-4, and D-1 through D-8 are not included in this analysis.).

Subjective analysis five of 64 seconds of continuous abdominal MECG cancellation (Figures D-1 through D-8) consist of percentage successes and potentials of the 12 test

---

† **The grading of potential and no potential is an indicator that the EMG is undistorted or distorted and should not be interpreted as indicators for uterine contraction information being present or not present!**

conditions and three clinical applications respectively. The bottom ratios (shaded) of the last column of Table 5-6 are the ratios of success. These ratios were obtained by determining the total number of passes of each data set of Figures D-1 through D-8 and dividing it by the number of occurrences of each test condition. (As discussed, two grades are awarded for the data of Figures D-1 through D-8. The top grade is for the first four seconds and the bottom for the last four. See Table 5-5 columns four through six and Table 5-6 columns one through five). Then the percentage successes are found by multiplying the ratios by 100. Finally, the percentage potentials for the clinical applications are determined similarly, but potential instead of pass grades are counted and divided by the total number of patients.

5.2.2 Objective Analysis

The objective analysis of the clinical data consists of a statistical computation that determines the expected (mean) value of abdominal MECG suppression with the CH^2 FECG system. This analysis gives the reader an expected numerical value for abdominal MECG attenuation if he/she was to reimplement the cancellation algorithm. An analysis of 14 patients with a variety of gestational ages and signal characteristics was performed to obtain a representative expected value.

The analysis starts with the measurement of abdominal MECG suppression for 60 continuous MECG complexes. For each of the 14 patients, only one period of 60 continuous MECG complexes was examined except for patient three. Since this patient has clinical data from several gestational ages, one period of 60 continuous MECG complexes for each gestational age was studied. The abdominal MECG suppression was determined by measuring the peak-to-peak values of each AECG's QRS complex and resulting AECG at the time location corresponding to the AECG's QRS complex. Then the peak-to-peak value of the AECG's QRS complex is divided by the peak-to-peak value of the corresponding resulting AECG's residual to obtain the abdominal MECG suppression ratio for that particular MECG complex. Tables F-1 through F-3 of Appendix F contain all the computed suppression ratios for each patient and gestational age analyzed. Furthermore, the mean and standard deviation values for each patient and gestational age studied are also given in the tables below the patient/gestational age identification (see the first column of Tables F-1 through F-3). The expected or mean value of abdominal MECG suppression was then found by summing all the suppression ratios of Tables F-1 through F-3. Then the sum was dividing by 1,440 which is the total number of abdominal

MECG complexes analyzed. The expected value was computed to be 12 V/V. The standard deviation of the suppression ratios was also calculated and found to be 6 V/V.

5.3 Discussion

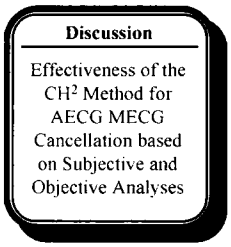

This section qualifies the effectiveness of the CH^2 FECG system based on the results of the subjective and objective analyses of synthesized and clinical data. The results from synthesized data contain measures for the accuracy of MECG suppression and the filtered FECG average. Clinical data results comprise measures for abdominal MECG suppression and recommendations for the clinical usefulness of the resulting AECG.

The main reason for employing synthesized data was to determine the accuracy of the DSP of the CH^2 FECG system (MECG cancellation and FECG SNR enhancement). Three objective measures (signal over signal plus noise or CM_1, correlation coefficient or CM_2, and SNR or CM_3) were used to obtain the accuracy of abdominal MECG suppression and FECG SNR enhancement. These measures produced favorable values (CM_1 is 1.0, CM_2 is 1.0, and CM_3 is infinite for abdominal MECG suppression and CM_1 is 0.974, CM_2 is 0.989, and CM_3 is 38.5 for FECG SNR enhancement). The objectively derived values and favorable subjective visual inspections are indicators that the CH^2 FECG system's DSP is performing satisfactorily or effectively. Therefore, the synthesized data analysis verifies that the CH^2 FECG system's DSP has significant potential to enhance clinical data accurately. Finally, the synthesized data analysis was basically a simulation to substantiate the functional accuracy of the DSP so that the application of clinical data can be done with confidence.

Since an objective analysis similar to the one done with synthesized data cannot be achieved with clinical data, a subjective analysis was performed. This analysis qualifies the effectiveness of the CH^2 MECG cancellation algorithm via summarizing the results of the 12 test conditions in a percentage success specification. Table 5-7 contains the percentage successes. The percentage success row is divided into two sub-rows. The top (none shaded) and bottom (shaded) sub-rows contain the percentage successes for the one block (Figures 5-5 through 5-18 and C-1 through C-11) and continuous (Figures D-1 through D-8) clinical data respectively.

Table 5-7. Percentage successes of the 12 test conditions.

- Didn't Occur		Test Conditions											
		1	2	3	4	5	6	7	8	9	10	11	12
Percentage	One block	100	84	96	92	100	100	100	100	25	100	100	0
Successes	Continuous	100	94	100	100	100	100	100	100	0	-	-	-

Nine of the twelve test conditions for the one block data scored greater than 90% and seven of the twelve scored 100%. Considering that the data sets contain ideal, typical, and non-ideal data, the scores of greater than 90% for nine of the twelve tests definitely suggests that the abdominal MECG cancellation algorithm is performing effectively. Furthermore, these nine test conditions also indicate the strengths of the CH^2 method's abdominal MECG cancellation algorithm. The scores of 84% and 25% of test conditions 2 and 9 respectively suggest that improvements can still be made to the abdominal MECG cancellation algorithm (Test condition 2 is the most difficult test condition of the twelve because it is dependent on a passing grade from tests conditions 5 through 12. See Table E-1 of Appendix E). Three of the four failures of test condition 2 were directly related to test condition 9 which indicates a weakness in the abdominal MECG cancellation algorithm during abdominal MECG modulation. Even though this modulation does not occur regularly (as demonstrated by the fact that only four occurrences were reported in the one block data sets), future research is advisable to increase the percentage success of test condition 9. Since only one case of an unexpected ventricle contraction occurred in all the data sets, the 0% success of test condition 12 carries little meaning. Finally, the synthesized data section suggests that significant TECG noise interferes with abdominal MECG suppression. There was not a problem with the clinical data studied since excessive TECG noise did not occur. Therefore, test condition 7 was reported 100% success for one block and continuous data.

The percentage successes of the continuous data were computed to give a feel for the abdominal MECG cancellation algorithm during a continuous mode of operation. Nine test conditions occurred during 64 seconds of the AECG and favorable results were obtained. Eight of the nine test conditions scored 94% or greater. The 0% success of test condition 9 would be meaningless similar to test condition 12 of the one block data, but the 25% success of test condition 9 of the one block data should be considered. In light of the 25% and 0% successes of the one block and continuous data respectively, indicate again that future research is needed to resolve the abdominal MECG modulation scenario. Since eight of the nine applicable tests

scored 94 % or greater, the abdominal MECG suppression algorithm definitely proved to be effective in a real-time mode of operation.

Table 5-8 contains the percentage potentials of the three clinical applications of the data sets. Potentials of 64% and 48% for fetal HR and FECG electrophysiological information respectively of the one block data indicate a limitation of non-invasive FECG monitoring. This restriction is directly related to the FECG's signal strength because the potential grading is highly dependent on a positive visual identification of the FECG in the AECG. The 88% potential for uterine contraction information suggest that the EMG of the AECG can be obtained undistorted the majority of the time, but again improvements are needed concerning the abdominal MECG modulation affect on abdominal MECG cancellation. Finally, the percentage potentials of the one block data are much more representative than the potentials for the continuous data. Since the one block data is calculated from a variety of patients at different gestational ages, the results are more credible.

Table 5-8. Percentage potentials for the clinical applications.

Clinical Applications		**Percentage Potentials**	
		One Block Data	Continuous Data
1	Fetal HR Information via HR Determination Algorithm	64%	100%
2	FECG Electrophysiological Information via FECG Averaging	48%	100%
3	Uterine Contraction Information via EMG	88%	94%

The final test for abdominal MECG cancellation with clinical data consists of an objective measure for the expected value of abdominal MECG suppression. Obtaining an accurate ratio of suppression is difficult. The difficulty comes from the inability to accurately determine the peak-to-peak value of the residual in the resulting AECG from noise and no pure reference signal (There is no signal to reference that has had the MECG canceled perfectly). A large number of abdominal MECG complexes were examined. From analyzing the suppression of 1,440 abdominal MECG complexes from a variety of patients and gestational ages, the expected value was found to be a favorable 12 V/V. The AECGs studied included the following signals characteristics:

- High energy EMG (>15.0 μV_{pp})
- Low frequency noise (<1.0 Hz and as high as 1.1 mV in amplitude)
- Noise spikes
- High and variable heart rates of both the mother and fetus (70-150 beats-per-minute for the mother and 120-150 beats-per-minute for the fetus)
- Various rates and amplitudes ratios between the abdominal MECG and FECG (MECG/FECG rate ratios from 1.0 to 2.14 and amplitude ratios from 2.2 to unmeasurable).

Considering that the 12 V/V expected value was obtained under a variety of signal characteristics, suggests once again the abdominal MECG attenuation algorithm performed effectively.

CHAPTER 6

COMPARISON

Dissertation Goal III
Ascertain the Effectiveness of the CH^2 Method for AECG MECG Cancellation Compared to Eight Previous Publications

The goal of this chapter is to ascertain the effectiveness of the CH^2 technique for abdominal MECG cancellation compared to eight previous publications. The methods will be paired with the CH^2 technique for a total of eight comparisons. Two analyses have been created to facilitate the goal of this chapter. Analysis I embodies five of the eight comparisons in which the previously reported methods achieve abdominal MECG cancellation via processing one AECG. Analysis II contains the remaining three comparisons in which the formerly reported methods obtain cancellation via processing several AECGs.

Each of the eight comparisons analyzes engineering aspects and clinical applicability of a previous publication and the CH^2 method. Engineering aspects encompass seven test conditions and four intrinsic characteristics in which their combined ratings indicate the overall engineering quality of the technique for abdominal MECG attenuation. Ratings for the test conditions are intended to summarize the success of the algorithm studied concerning signal characteristics. Test conditions 1 through 7 for this chapter are similar to test condition 1 through 7 used to analyze the synthesized and clinical data of Chapter 5, but test condition 2 is altered slightly. The ratings for the intrinsic characteristics indicate the ease for which a technique can be operated in a clinical setting and implemented. Clinical applicability encompasses four clinical applications. The combined ratings of the applications indicate the amount of potential clinical information that can be obtained via the previous publications and the CH^2 method for abdominal MECG cancellation.

To qualify effectiveness of the CH^2 method versus the eight previous publications, scores will be derived for the engineering aspects and clinical applicability of each algorithm from the

noted ratings. Furthermore, each method's scores will be combined to form an effectiveness mark. If the CH^2 technique has the highest mark for each of the eight comparisons, then the CH^2 method for abdominal MECG attenuation has been effective compared to the eight former publications. In summary, Figure 6-1 presents the layout of this chapter. Finally, this study will accomplish dissertation goal III as described by Figure 1-1.

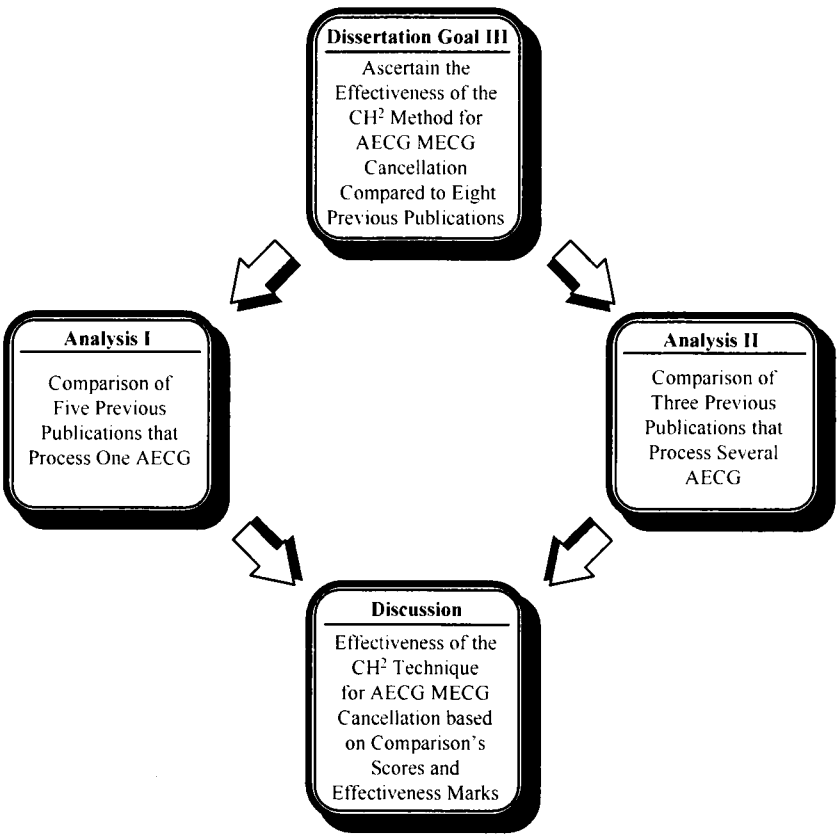

Figure 6-1. Block diagram describing the layout of Chapter 6.

A tabular format will be used to present the analysis information (grades, ratings, and scores) of the eight comparisons. The comparison tables will each be one page with a standard format to efficiently convey all the analysis information of each formerly published method versus the CH^2 algorithm. Finally, the description of the grading, rating, and scoring for all the comparison tables in this chapter is shown in Appendix G.

This chapter contains two analysis sections. Since there are many figures used in these analyses (46 figures), most of them will be placed in Appendix H or I. Appendix H and I will

contain the figures from analysis I and II respectively. The ECG signals of these figures are synthesized data and used for the analysis as opposed to clinical data because more control could be exercised over their signal characteristics. Furthermore, the synthesized data was created similarly to the synthesized data of Chapter 5 (See Section 5.1.) where Figure 6-2 presents the signals used in the data creation. Figures 6-2(a), 6-2(b), and 6-2(b) contain an ideal FECG, low frequency noise, and noise spike respectively. The ideal FECG is an FECG strip synthesized from an averaged FECG complex from a pregnant patient (patient 15 at 41 weeks of gestation). For prior publications that required more than one TECG and/or AECG, the ECG signals were taken from the same patient as the synthesized data of Chapters 2 and 5. Since quadratic programming and SVD method two required several AECGs and only five were available, the other AECGs (one for quadratic programming and five for SVD method two) were synthesized from the existing five by linearly combining them. Then gaussian noise with an 0.05 to 100.0 Hz bandwidth was added to the original five and newly created AECGs. Finally, in every analysis that a previously reported method was reimplemented and graded with synthesized data, the CH^2 technique was also implemented and graded with the exact same data.

6.1 Analysis One

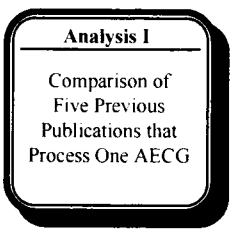

Analysis I compares five previously reported methods for abdominal MECG cancellation with the CH^2 technique. As discussed, the formerly published techniques of analysis I process one AECG to cancel its MECG. The five methods include single lead method two (SL2), single lead method three (SL3), single lead method five (SL5), time-sequenced adaptive filtering (TSAF), and orthogonal basis (Orth.). In addition, each of these methods has been described in Chapter 2. Finally, some confusion may exist concerning TSAF and Orth. being labeled as multiple lead methods in Chapter 2 and techniques that processes only one AECG in Chapter 6. They are multiple lead techniques because three TECGs are used to suppress the abdominal MECG, but the TECGs are used to cancel the MECG from one AECG. Therefore, only one AECG is processed which meets the criteria for analysis I.

Analysis I contains five tables that are used to present the analysis information (grades, ratings, and scores) for the five previously reported methods and the CH^2 technique for abdominal MECG cancellation. Appendix G contains a detailed description of the engineering aspects and clinical applicability grading, rating, and scoring schemes for these tables.

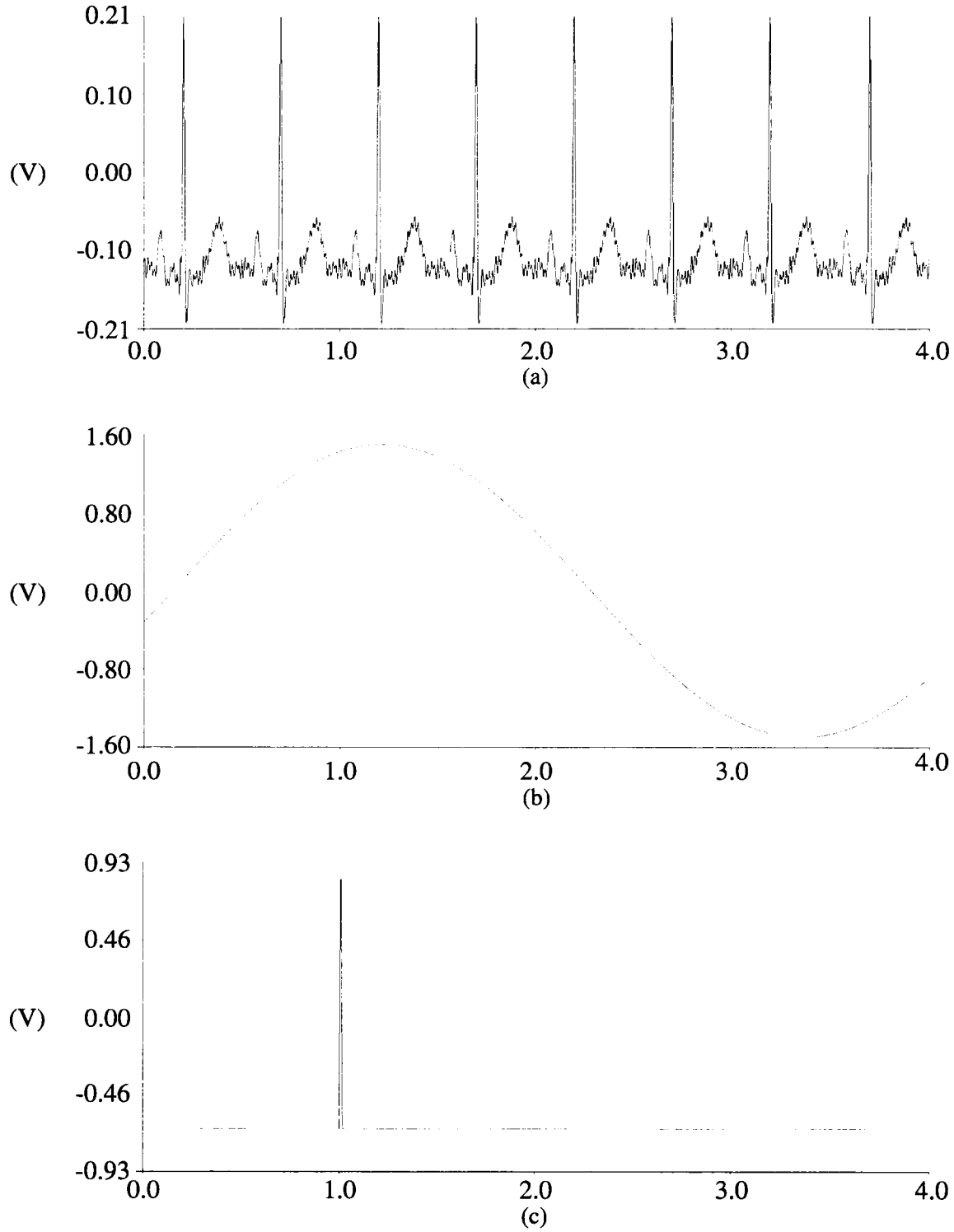

Figure 6-2. Synthesized signals used in the eight comparisons. (a) Ideal FECG. (b) Ideal low frequency noise or a sinusoid with a frequency of approximately 0.25 Hz. (c) Ideal noise spike.

Furthermore, Section 6.1.1 gives a general explanation for these tables and a description of the figures referenced by them. Finally, Section 6.1.2 contains an example explanation of the grading, rating, and scoring for single lead method two versus the CH^2 method of Table 6-1.

6.1.1 Explanation of Tables and Respective Figures

Tables 6-1, 6-2, 6-3, 6-4, and 6-5 contain the analysis information for SL2, SL3, SL5, TSAF, and Orth. versus the CH^2 method respectively. The seven test conditions and four clinical applications of Tables 6-1 through 6-5 grade data sets contained in Figures 6-3 through 6-6 and Figures H-1 through H-16. The following describes the layout of Figures 6-3 through 6-6 and Figures H-1 through H-16 along with a description of the signals inspected for the grading of Tables 6-1 through 6-5.

Figures 6-3(a) through 6-6(a) and Figures H-1(a) through H-8(a) contain an TECG or $S_1(n)$ used by the CH^2 method to cancel the abdominal MECG. Methods SL2, SL3, and SL5 do not use this signal. However, TSAF and Orth. do use this TECG and two others to obtain abdominal MECG suppression. The three TECGs are presented in Figures H-9(a) through H-16(a) where the third TECG $S_3(n)$ is used by the CH^2 method. Figures 6-3(b) through 6-6(b) and Figures H-1(b) through H-16(b) present the AECG and resulting AECGs used to compare the previous methods with the CH^2. Since all the these figures have the same format, a general description will be given. The first ECG signal of these figures is the AECG $S_k(n)$ where k is the lead number and 2 for SL2, SL3, and SL5. For TSAF and Orth., k is 4. Signal two is the AECG blanked out during the MECG complexes or $Sb_k(n)$. The third signal is the resulting AECG from the previously reported method or $R(n)_X$ where X is SL2, SL3, SL5, TSAF, or Orth. Signal four or $Rb(n)_X$ is $R(n)_X$ blanked out during the MECG complex at the same time locations as $Sb_k(n)$. The fifth signal is

$$C(n)_X = Rb(n)_X - Sb_k(n) \tag{56}$$

or the signal corruption caused by the method being analyzed to the AECG via cancellation during the times the MECG does not occur. Signals six through eight have the same description as signals three through five, but the signals are processed by the CH^2 method. Therefore, X is CH^2. Finally, the reason for blanking the AECG and resulting AECGs is explained in Section 5.1 paragraph five.

Table 6-1. Single lead method two vs. the CH^2 method for AECG MECG cancellation.

ENGINEERING ASPECTS (See Appendix G for a detailed description)			**Scores** = 475^{SL2}, 481^{CH^2}				
Test Conditions			Data Designation, Grading, & Rating Information				
✓ Passed × Failed - Did Not Occur			Fig. 6-3	Fig. 6-4	Fig. 6-5	Fig. 6-6	Rating
1^{100}	Bandwidth of Resulting	SL2	✓	✓	✓	✓	4/4
	AECG is 0.05 to 100 Hz	CH^2	✓	✓	✓	✓	4/4
2^{100}	Signal Corruption to	SL2	✓	✓	×[6*]	✓	3/4
	FECG & EMG	CH^2	✓	✓	✓	✓	4/4
3^{100}	Overall MECG	SL2	✓	✓	✓	✓	4/4
	Cancellation	CH^2	✓	✓	✓	✓	4/4
4^{100}	FECG & MECG	SL2	✓	✓	✓	✓	4/4
	Overlap	CH^2	✓	✓	✓	✓	4/4
5	Significant AECG Low	SL2	-	✓	-	-	
	Frequency Noise	CH^2	-	✓	-	-	
6	Significant AECG	SL2	-	-	×	-	
	Noise Spike	CH^2	-	-	✓	-	
7	Significant TECG	SL2	-	-	-	✓	
	Noise	CH^2	-	-	-	✓	
Intrinsic Characteristics			Grading & Rating Information				
1^{25}	Flexibility of Lead	SL2	No requirement(s) for lead placement				1
	Positioning	CH^2	Flexible (TECG lead needs to be in a lead II position)				0.5
2^{25}	Number of Extra Leads	SL2	None				1
	Required	CH^2	One TECG				0.75
3^{25}	User Interaction	SL2	No				1
	Required	CH^2	No				1
4^{25}	Computational	SL2	Low (about a second for 8 seconds of data)				1
	Complexity	CH^2	Low (about a second for 8 seconds of data)				1
CLINICAL APPLICABILITY (See Appendix G for a detailed description)			**Scores** = 3.75^{SL2}, 4^{CH^2}				
Clinical Applications			Data Designation, Grading, & Rating Information				
P Potential NP No Potential			Fig. 6-3	Fig. 6-4	Fig. 6-5	Fig. 6-6	Rating
1	Fetal HR Information via HR	SL2	P	P	P	P	4/4
	Determination Algorithm	CH^2	P	P	P	P	4/4
2	FECG Electrophysiological	SL2	P	P	P	P	4/4
	Info. via FECG Averaging	CH^2	P	P	P	P	4/4
3	Uterine Contraction	SL2	P	P	NP	P	3/4
	Information via EMG	CH^2	P	P	P	P	4/4
4	Principal Fetal Signal(s) or	SL2	P	P	P	P	4/4
	Source Signal(s) Obtainable	CH^2	P	P	P	P	4/4
*The failure of test condition 6 caused test condition 2 to fail.							

Table 6-2. Single lead method three vs. the CH^2 method for AECG MECG cancellation.

ENGINEERING ASPECTS (See Appendix G for a detailed description)			**Scores** = 375^{SL3}, 481^{CH^2}				
Test Conditions			Data Designation, Grading, & Rating Information				
✓ Passed × Failed - Did Not Occur			Fig. H-1	Fig. H-2	Fig. H-3	Fig. H-4	Rating
1^{100}	Bandwidth of Resulting	SL3	✓	✓	✓	✓	4/4
	AECG is 0.05 to 100 Hz	CH^2	✓	✓	✓	✓	4/4
2^{100}	Signal Corruption to	SL3	✓	✓	×[6*]	✓	3/4
	FECG & EMG	CH^2	✓	✓	✓	✓	4/4
3^{100}	Overall MECG	SL3	✓	✓	✓	✓	4/4
	Cancellation	CH^2	✓	✓	✓	✓	4/4
4^{100}	FECG & MECG	SL3	×	×	×	×	0/4
	Overlap	CH^2	✓	✓	✓	✓	4/4
5	Significant AECG Low	SL3	-	✓	-	-	
	Frequency Noise	CH^2	-	✓	-	-	
6	Significant AECG	SL3	-	-	×	-	
	Noise Spike	CH^2	-	-	✓	-	
7	Significant TECG	SL3	-	-	-	✓	
	Noise	CH^2	-	-	-	✓	
Intrinsic Characteristics			Grading & Rating Information				
1^{25}	Flexibility of Lead	SL3	No requirement(s) for lead placement				1
	Positioning	CH^2	Flexible (TECG lead needs to be in a lead II position)				0.5
2^{25}	Number of Extra Leads	SL3	None				1
	Required	CH^2	One TECG				0.75
3^{25}	User Interaction	SL3	No				1
	Required	CH^2	No				1
4^{25}	Computational	SL3	Low (about a second for 8 seconds of data)				1
	Complexity	CH^2	Low (about a second for 8 seconds of data)				1
CLINICAL APPLICABILITY (See Appendix G for a detailed description)			**Scores** = 2.75^{SL3}, 4^{CH^2}				
Clinical Applications			Data Designation, Grading, & Rating Information				
P Potential NP No Potential			Fig. H-1	Fig. H-2	Fig. H-3	Fig. H-4	Rating
1	Fetal HR Information via HR	SL3	NP	NP	NP	NP	0/4
	Determination Algorithm	CH^2	P	P	P	P	4/4
2	FECG Electrophysiological	SL3	P	P	P	P	4/4
	Info. via FECG Averaging	CH^2	P	P	P	P	4/4
3	Uterine Contraction	SL3	P	P	NP	P	3/4
	Information via EMG	CH^2	P	P	P	P	4/4
4	Principal Fetal Signal(s) or	SL3	P	P	P	P	4/4
	Source Signal(s) Obtainable	CH^2	P	P	P	P	4/4
*The failure of test condition 6 caused test condition 2 to fail.							

Table 6-3. Single lead method five vs. the CH^2 method for AECG MECG cancellation.

ENGINEERING ASPECTS (See Appendix G for a detailed description)			**Scores** = 467^{SL5}, 481^{CH^2}				
Test Conditions			Data Designation, Grading, & Rating Information				
✓ Passed ✗ Failed - Did Not Occur			Fig. H-5	Fig. H-6	Fig. H-7	Fig. H-8	Rating
1^{100}	Bandwidth of Resulting AECG is 0.05 to 100 Hz	SL5	✓	✓	✓	✓	4/4
		CH^2	✓	✓	✓	✓	4/4
2^{100}	Signal Corruption to FECG & EMG	SL5	✓	✓	✓	✓	4/4
		CH^2	✓	✓	✓	✓	4/4
3^{100}	Overall MECG Cancellation	SL5	✓	✓	✓	✓	4/4
		CH^2	✓	✓	✓	✓	4/4
4^{100}	FECG & MECG Overlap	SL5	✓	✓	✓	✓	4/4
		CH^2	✓	✓	✓	✓	4/4
5	Significant AECG Low Frequency Noise	SL5	-	✓	-	-	
		CH^2	-	✓	-	-	
6	Significant AECG Noise Spike	SL5	-	-	✓	-	
		CH^2	-	-	✓	-	
7	Significant TECG Noise	SL5	-	-	-	✓	
		CH^2	-	-	-	✓	
Intrinsic Characteristics			Grading & Rating Information				
1^{25}	Flexibility of Lead Positioning	SL5	No requirement(s) for lead placement				1
		CH^2	Flexible (TECG lead needs to be in a lead II position)				0.5
2^{25}	Number of Extra Leads Required	SL5	None				1
		CH^2	One TECG				0.75
3^{25}	User Interaction Required	SL5	Yes (To initialize the algorithm, the user selects an FECG-free near pure AECG MECG complex.)				0
		CH^2	No				1
4^{25}	Computational Complexity	SL5	Medium (about 30 seconds for 8 seconds of data)				0.66
		CH^2	Low (about a second for 8 seconds of data)				1
CLINICAL APPLICABILITY (See Appendix G for a detailed description)			**Scores** = 4^{SL5}, 4^{CH^2}				
Clinical Applications			Data Designation, Grading, & Rating Information				
P Potential NP No Potential			Fig. H-5	Fig. H-6	Fig. H-7	Fig. H-8	Rating
1	Fetal HR Information via HR Determination Algorithm	SL5	P	P	P	P	4/4
		CH^2	P	P	P	P	4/4
2	FECG Electrophysiological Info. via FECG Averaging	SL5	P	P	P	P	4/4
		CH^2	P	P	P	P	4/4
3	Uterine Contraction Information via EMG	SL5	P	P	P	P	4/4
		CH^2	P	P	P	P	4/4
4	Principal Fetal Signal(s) or Source Signal(s) Obtainable	SL5	P	P	P	P	4/4
		CH^2	P	P	P	P	4/4

Table 6-4. Adaptive filter vs. the CH^2 method for AECG MECG cancellation.

ENGINEERING ASPECTS (See Appendix G for a detailed description)			**Scores** = 256^{TSAF}, 481^{CH^2}				
Test Conditions			Data Designation, Grading, & Rating Information				
✓ Passed × Failed - Did Not Occur			Fig. H-9	Fig. H-10	Fig. H-11	Fig. H-12	Rating
1^{100}	Bandwidth of Resulting AECG is 0.05 to 100 Hz	TSAF	✓	✓	✓	✓	4/4
		CH^2	✓	✓	✓	✓	4/4
2^{100}	Signal Corruption to FECG & EMG	TSAF	×	$\times^{5*}$	$\times^{6*}$	$\times^{7*}$	0/4
		CH^2	✓	✓	✓	✓	4/4
3^{100}	Overall MECG Cancellation	TSAF	✓	×	✓	×	2/4
		CH^2	✓	✓	✓	✓	4/4
4^{100}	FECG & MECG Overlap	TSAF	✓	×	✓	✓	3/4
		CH^2	✓	✓	✓	✓	4/4
5	Significant AECG Low Frequency Noise	TSAF	-	×	-	-	
		CH^2	-	✓	-	-	
6	Significant AECG Noise Spike	TSAF	-	-	×	-	
		CH^2	-	-	✓	-	
7	Significant TECG Noise	TSAF	-	-	-	×	
		CH^2	-	-	-	✓	
Intrinsic Characteristics			Grading & Rating Information				
1^{25}	Flexibility of Lead Positioning	TSAF	Little Flexibility (for the three TECGs)				0
		CH^2	Flexible (TECG lead needs to be in a lead II position)				0.5
2^{25}	Number of Extra Leads Required	TSAF	Three TECGs				0.25
		CH^2	One TECG				0.75
3^{25}	User Interaction Required	TSAF	No (however many parameters have to be set)				1
		CH^2	No				1
4^{25}	Computational Complexity	TSAF	Very High (about 168 seconds for 8 seconds of data)				0
		CH^2	Low (about a second for 8 seconds of data)				1
CLINICAL APPLICABILITY (See Appendix G for a detailed description)			**Scores** = 1.5^{TSAF}, 4^{CH^2}				
Clinical Applications			Data Designation, Grading, and Rating Information				
P Potential NP No Potential			Fig. H-9	Fig. H-10	Fig. H-11	Fig. H-12	Rating
1	Fetal HR Information via HR Determination Algorithm	TSAF	P	NP	P	NP	2/4
		CH^2	P	P	P	P	4/4
2	FECG Electrophysiological Info. via FECG Averaging	TSAF	P	NP	P	NP	2/4
		CH^2	P	P	P	P	4/4
3	Uterine Contraction Information via EMG	TSAF	NP	NP	NP	NP	0/4
		CH^2	P	P	P	P	4/4
4	Principal Fetal Signal(s) or Source Signal(s) Obtainable	TSAF	P	NP	P	NP	2/4
		CH^2	P	P	P	P	4/4

*The failure of the superscript test conditions caused test condition 2 to fail.

Table 6-5. Orthogonal basis vs. the CH^2 method for AECG MECG cancellation.

ENGINEERING ASPECTS (See Appendix G for a detailed description)			**Scores** = $231^{Orth.}$, 481^{CH^2}				
Test Conditions			Data Designation, Grading, & Rating Information				
✓ Passed ✗ Failed - Did Not Occur			Fig. H-13	Fig. H-14	Fig. H-15	Fig. H-16	Rating
1^{100}	Bandwidth of Resulting AECG is 0.05 to 100 Hz	Orth.	✓	✓	✓	✓	4/4
		CH^2	✓	✓	✓	✓	4/4
2^{100}	Signal Corruption to FECG & EMG	Orth.	✗	✗	✗	✗[7*]	0/4
		CH^2	✓	✓	✓	✓	4/4
3^{100}	Overall MECG Cancellation	Orth.	✗	✗	✗	✗	0/4
		CH^2	✓	✓	✓	✓	4/4
4^{100}	FECG & MECG Overlap	Orth.	✓	✓	✓	✗	3/4
		CH^2	✓	✓	✓	✓	4/4
5	Significant AECG Low Frequency Noise	Orth.	-	✓	-	-	
		CH^2	-	✓	-	-	
6	Significant AECG Noise Spike	Orth.	-	-	✓	-	
		CH^2	-	-	✓	-	
7	Significant TECG Noise	Orth.	-	-	-	✗	
		CH^2	-	-	-	✓	
Intrinsic Characteristics			Grading & Rating Information				
1^{25}	Flexibility of Lead Positioning	Orth.	Little Flexibility (for the three TECGs)				0
		CH^2	Flexible (TECG lead needs to be in a lead II position)				0.5
2^{25}	Number of Extra Leads Required	Orth.	Three TECGs				0.25
		CH^2	One TECG				0.75
3^{25}	User Interaction Required	Orth.	None				1
		CH^2	None				1
4^{25}	Computational Complexity	Orth.	Low (about a second for 8 seconds of data)				1
		CH^2	Low (about a second for 8 seconds of data)				1
CLINICAL APPLICABILITY (See Appendix G for a detailed description)			**Scores** = $0^{Orth.}$, 4^{CH^2}				
Clinical Applications			Data Designation, Grading, & Rating Information				
P Potential NP No Potential			Fig. H-13	Fig. H-14	Fig. H-15	Fig. H-16	Rating
1	Fetal HR Information via HR Determination Algorithm	Orth.	NP	NP	NP	NP	0/4
		CH^2	P	P	P	P	4/4
2	FECG Electrophysiological Info. via FECG Averaging	Orth.	NP	NP	NP	NP	0/4
		CH^2	P	P	P	P	4/4
3	Uterine Contraction Information via EMG	Orth.	NP	NP	NP	NP	0/4
		CH^2	P	P	P	P	4/4
4	Principal Fetal Signal(s) or Source Signal(s) Obtainable	Orth.	NP	NP	NP	NP	0/4
		CH^2	P	P	P	P	4/4
*The failure of test condition 7 caused test condition 2 to fail.							

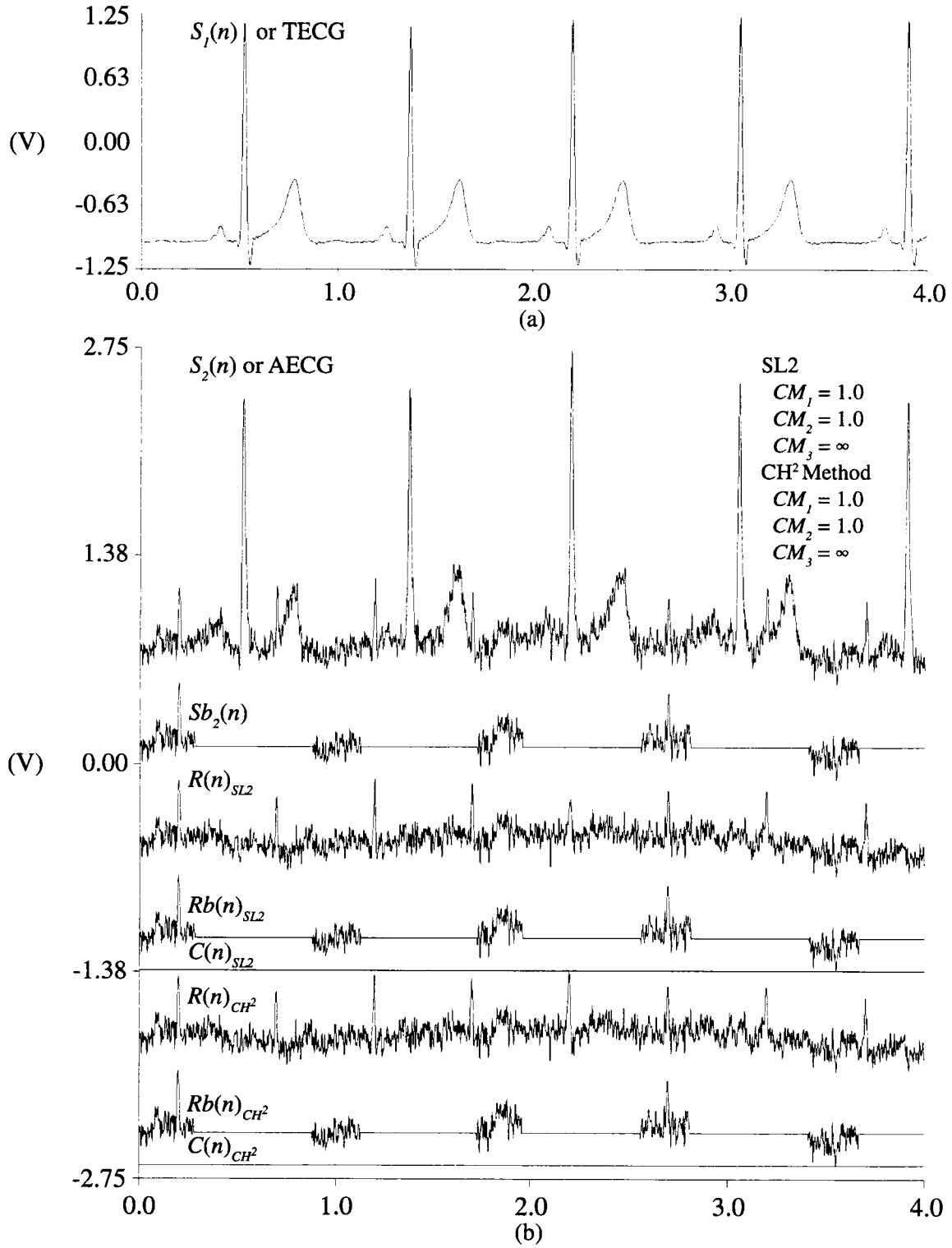

Figure 6-3. Single lead method two vs. the CH² method demonstrating test condition four (all x-axes in seconds). (a) TECG or $S_1(n)$ used only with the CH² method. (b) AECG or $S_2(n)$, AECG blanked out during the MECG complexes or $Sb_2(n)$, and resulting AECGs comparing the two methods.

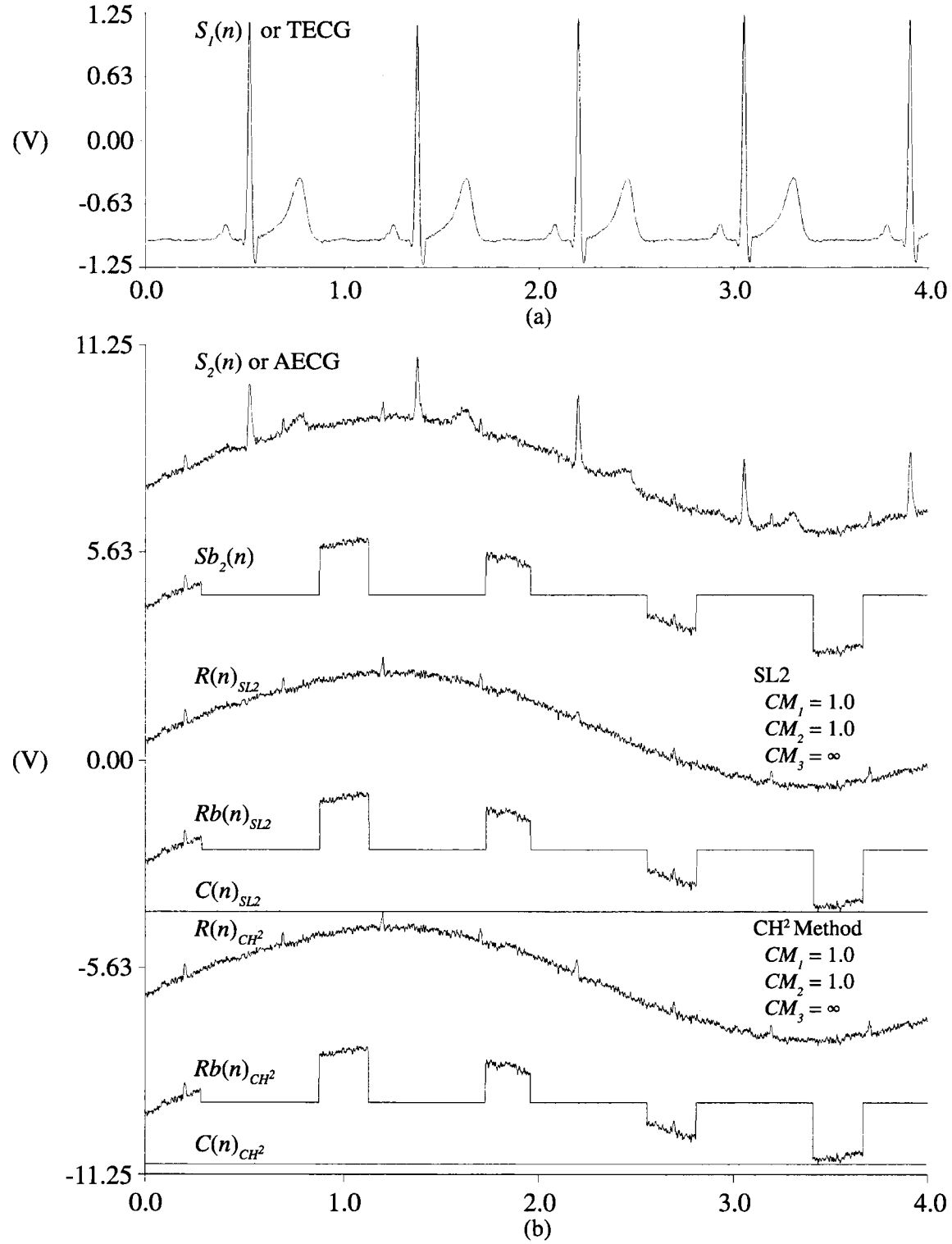

Figure 6-4. Single lead method two vs. the CH² method demonstrating test condition five (all x-axes in seconds). (a) TECG or $S_1(n)$ used only with the CH² method. (b) AECG or $S_2(n)$, AECG blanked out during the MECG complexes or $Sb_2(n)$, and resulting AECGs comparing the two methods.

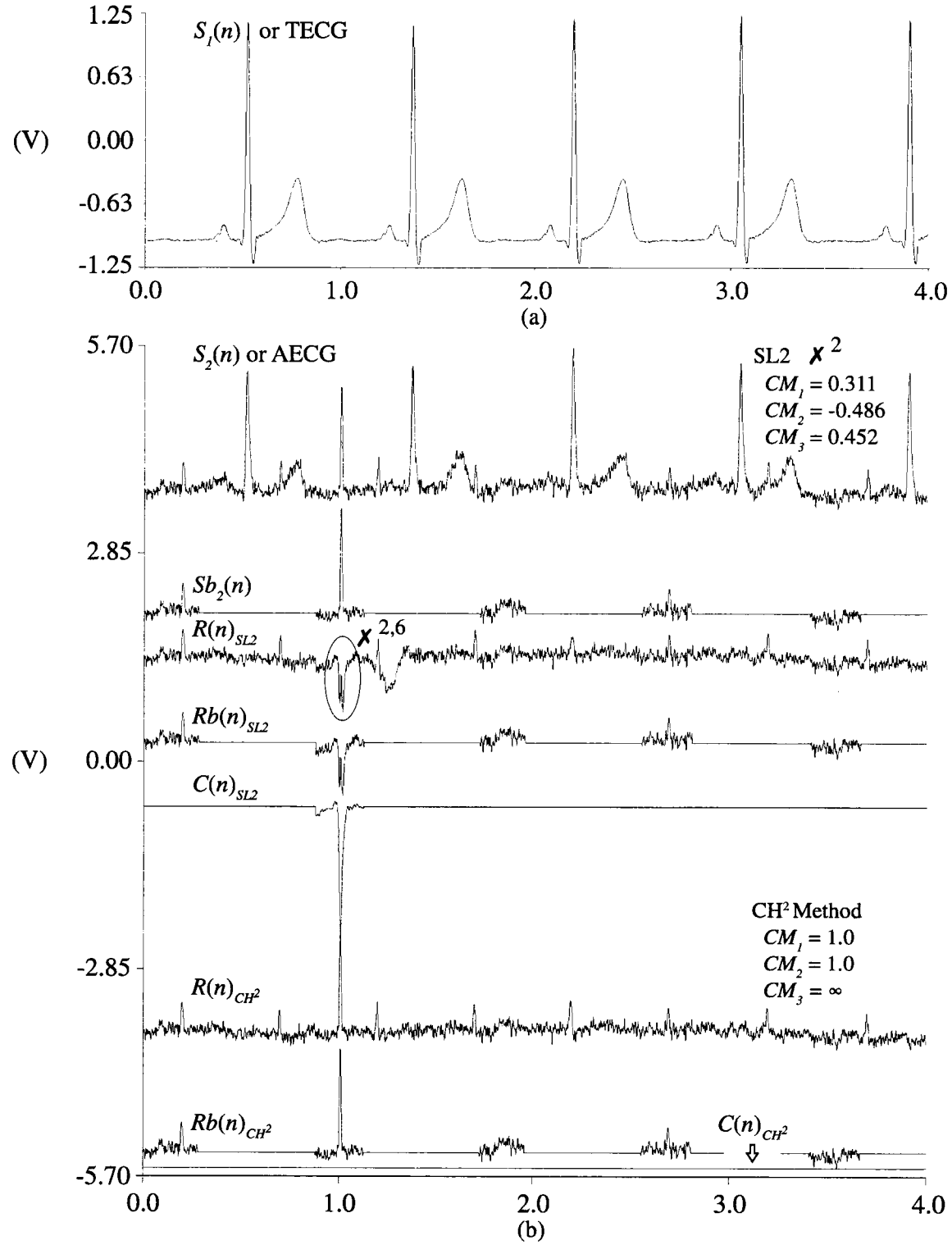

Figure 6-5. Single lead method two vs. the CH² method demonstrating test condition six (all x-axes in seconds). (a) TECG or $S_1(n)$ used only with the CH² method. (b) AECG or $S_2(n)$, AECG blanked out during the MECG complexes or $Sb_2(n)$, and resulting AECGs comparing the two methods.

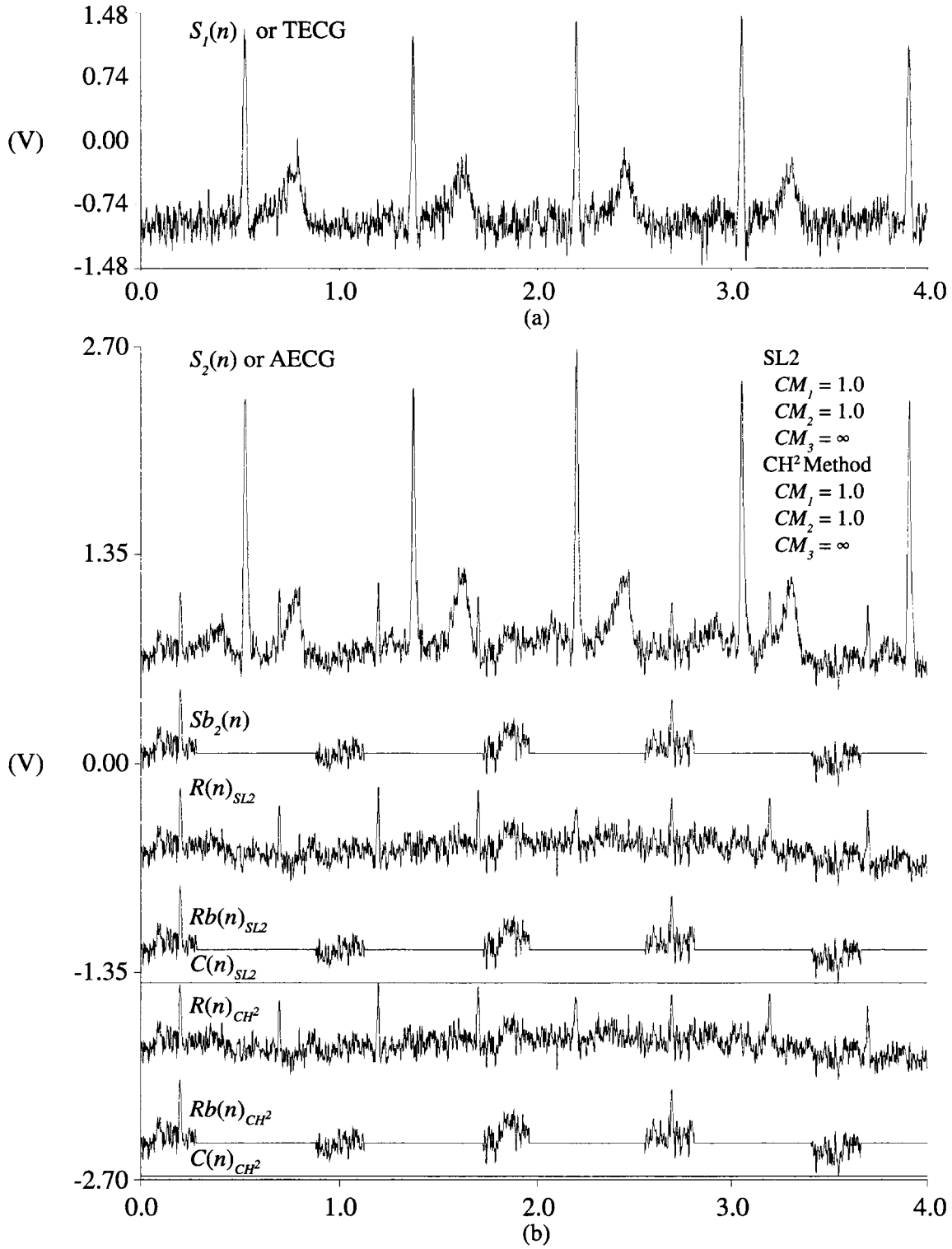

Figure 6-6. Single lead method two vs. the CH² method demonstrating test condition seven (all x-axes in seconds). (a) TECG or $S_1(n)$ used only with the CH² method. (b) AECG or $S_2(n)$, AECG blanked out during the MECG complexes or $Sb_2(n)$, and resulting AECGs comparing the two methods.

Figures 6-3 through 6-6 and Figures H-1 through H-16 are divided into five sets each containing four figures. Each set comprises all the signal information for one comparison between a prior technique and the CH^2 method. Figures 6-3 through 6-6, Figures H-1 through H-4, Figures H-5 through H-8, Figures H-9 through H-12, and Figures H-13 through H-16 are the five sets associated with SL2, SL3, SL5, TSAF, and Orth. versus the CH^2 respectively. Furthermore, each set of four figures has the same type of signal characteristics tested. Therefore, a description of Figures 6-3 through 6-6 also applies to the other set of figures that start with Figures H-1, H-5, H-9, and H-13. Figure 6-3 demonstrates test condition 4 or the success of abdominal MECG cancellation during an overlap between the FECG and MECG. All other signal characteristics are basically ideal for Figure 6-3. Figures 6-4, 6-5, and 6-5 demonstrate test conditions 5, 6, and 7 or the success of abdominal MECG cancellation with significant AECG low frequency noise, a significant AECG noise spike, and significant TECG noise respectively. Finally, the TECG and AECG of Figures 6-3 through 6-6 are exactly the same except Figures 6-4 through 6-6 each has one added non-ideal signal characteristic as noted. Therefore, Figure 6-3 can be used as a baseline or reference to determine if the test conditions analyzed passed or failed for Figures 6-4 through 6-6.

A brief explanation is presented to clarify the signals inspected to determine the grading for the seven test conditions and four clinical applications. The visual inspects for test conditions 2 through 7 and clinical applications 1 and 2 analyze the AECG $S_k(n)$ and the resulting AECG $R(n)_X$ to determine if a pass, fail, did not occur, potential, or no potential grading should be awarded (The variables of k and X have been discussed.). Test condition 1 does not inspect any ECG signals, but determines whether the algorithm considered will alter the signal bandwidth of the resulting AECG $R(n)_X$ to less than 0.05 to 100.0 Hz. Test condition 2's corruption measures of CM_1, CM_2, and CM_3 that are specified for each previously reported method and the CH^2 technique on each figure are determined from the blanked out AECG $Sb_k(n)$, the resulting AECG $Rb(n)_X$, and $C(n)_X$. These three corruption measures have been defined by (53), (54), and (55) of Chapter 5 where $Sb_k(n)$ is used for $S_{ideal}(n)$, $Rb(n)_X$ is used for $R(n)$, the variance of $Sb_k(n)$ is used for $\sigma^2_{S_{ideal}(n)}$, the variance of $C(n)_X$ is used for $\sigma^2_{N(n)}$, and the variance of $Rb(n)_X$ is used for $\sigma^2_{R(n)}$. The signals displayed in the figures for $Sb_k(n)$, $Rb(n)_X$, and $C(n)_X$ are slightly different than the signals used for the calculations. Only the signal parts and not the blanked out parts were used in the computation. The blanked parts were displayed in the figures to allow the reader to see the

differences between the analyzed signals in time. Finally, the circle(s) and ×(s) on the figures referenced by analysis I indicate the location(s) of the failing test condition(s) where the superscript number(s) denotes the problem test condition(s).

Clinical application 3's grading is determined based on the outcome of test condition 2. Therefore, the inspected signals have already been described. Clinical application 4 requires minimally two, three, or more AECGs with the MECG canceled to compute the principal fetal signal(s) or source signal(s). The source signal(s) is computed based on (32) of Chapter 2 where $\boldsymbol{S}_{K,N}$ contains several AECGs with the MECG canceled. Since only one AECG $S_k(n)$ is available for analysis I comparisons, clinical application 4's rating will be based on the success of abdominal MECG suppression and the observability of the FECG in the resulting AECG $R(n)_N$. Assuming that abdominal MECG cancellation will be similar for one AECG as for several, then clinical application 4 can be graded based on clinical application 2's grading criteria using the available AECG $S_k(n)$.

6.1.2 Single Lead Method Two Versus the CH^2 Technique

The following discusses the grading, rating, and scoring of Table 6-1. Grading for the test conditions, intrinsic characteristics, and clinical applications of the engineering aspects and clinical applicability sections will be presented first along with intrinsic characteristic ratings. Next, a discussion of the ratings for the first four test conditions and clinical applications will be presented. Then a description of the computation of the scores for SL2's and the CH^2 method's engineering aspects and clinical applicability will be performed. Finally, Appendix G also gives a detailed discussion of the grading, rating, and scoring of Table 6-1.

Since the four figures referenced by Table 6-1 are graded similarly, only the grading of Figure 6-5 will be discussed (This figure was selected because it had a failure case.). Table 6-1 presents the grades and ratings for SL2 and the CH^2 method in separate rows for each test condition, intrinsic characteristic, and clinical application. The grading of test conditions 1, 3, 5, and 7 will not be given for Figure 6-5 since Chapter 5 explains these test conditions with similar synthesized data.

Test condition 2 has a slightly different grading scheme than that used in Chapter 5. This test condition was graded a failure for SL2 because the resulting AECG $R(n)_{SL2}$ compared to the AECG's $S_2(n)$ FECG or EMG during a visual inspection of the signals reveals that the EMG is dissimilar in shape (The circle of Figure 6-5(b) indicates the discrepancy.). Furthermore, test

condition 6 failed and the three corruption measures of CM_1, CM_2, and CM_3 of test condition 2 for SL2 were less than the values required for a pass grade as specified in Appendix G ($\times^{2,6}$ of Figure 6-5(a) designates that test conditions 2 and 6 failed because of the encircled signal portion). Test condition 2 was graded pass for the CH^2 method because during a visual inspection the resulting AECG $R(n)_{CH^2}$ compared to the AECG's $S_2(n)$ FECG or EMG has negligible MECG residuals and similar shaped FECG and EMG respectively. Furthermore, test conditions 5 through 7 passed and the corruption measures CM_1, CM_2, and CM_3 were all within the pass criteria specified in Appendix G.

Test condition 4 passed for SL2 and the CH^2 technique of Figure 6-5. Test condition 4 passed because the FECG's QRS complex that overlapped the MECG's complex of $S_2(n)$ is present and similar in shape to the surrounding non-overlapping FECG's QRS complexes of $R(n)_{SL2}$ and $R(n)_{CH^2}$. Test condition 6 was graded failure for SL2 because the resulting AECG $R(n)_{SL2}$ compared to the AECG's FECG and EMG has dissimilar shaped EMG. This failure was caused by the noise spike. Finally, test condition 6 was graded pass for the CH^2 technique because the resulting AECG $R(n)_{CH^2}$ compared to the AECG's FECG or EMG has similar shaped FECG and EMG respectively.

The intrinsic characteristics of Table 6-1 deal with the design aspects of the method and do not analyze the data of Figures 6-3 through 6-6. Intrinsic characteristic 1 was graded as no requirement(s) for lead placement for SL2 because the AECG lead can be placed anywhere and abdominal MECG cancellation can still be achieved. The CH^2 method was awarded a flexible grade because the TECG lead used to cancel the abdominal MECG needs to be in a lead II position to achieve best resulting. Intrinsic characteristic 2 was graded none for SL2 because no extra leads are require to achieve abdominal MECG cancellation. The CH^2 method was graded one TECG because an TECG is required to obtain cancellation. Intrinsic characteristic 3 was graded no for SL2 and the CH^2 method because they did not require user interaction to initialize the algorithms at start up. Finally, both methods had a grade of low for computation complexity. These were awarded because the methods required less than a second to process eight seconds of data which places them within block mode real-time with a computer that has an Intel 486DX2 66 MHz microprocessor.

The grading of the four clinical applications will only analyze the data of Figure 6-5 for this example explanation. Clinical application 1 was graded potential for SL2 and the CH^2 technique

because test condition 3 passed for both methods and a visual inspection of $R(n)_{SL2}$ and $R(n)_{CH^2}$ determined that the FECG is observable. Clinical application 2 was graded potential for SL2 and the CH^2 technique because test conditions 1 and 3 passed for both techniques and a visual inspection of $R(n)_{SL2}$ and $R(n)_{CH^2}$ could discern all FECG's R waves to be averaged without question. Clinical application 3 was graded no potential for SL2 since test condition 2 failed. Clinical application 3 was graded potential for the CH^2 method because test conditions 1 and 2 passed. Finally, clinical application 4 was graded potential for SL2 and the CH^2 method because clinical application 2 had potential for both techniques.

The ratings for the first four test conditions and four clinical applications are tallied in the right hand column of Table 6-1. They are calculated based on the grades awarded for Figures 6-3 through 6-6 for each technique. An example calculation for the rating of test condition 2 for the SL2 method is given to clarify the rating computation. First, each grade of test condition 2 for SL2 is counted as one point for a pass and zero points for a fail. Since test condition 2 has three passes and one failure, 3 points are summed. Next, the 3 points are divided by four since a total of four figures were studied to determine the rating of 0.75.

The score for engineering aspects for each method of Table 6-1 is calculated using the superscript numbers of the test condition and intrinsic characteristic numbers as weights of importance. The first four test conditions are given a weight of 100 and the intrinsic characteristics a weight of 25. The superscript weights and rating values are multiplied and summed for each respective test condition and intrinsic characteristic for the method analyzed to determine the engineering aspects score. For example, SL2's ratings for the test conditions are 1, 0.75, 1, and 1 with weight factors of 100 for each rating. The intrinsic characteristic ratings for SL2 are all one with weight factors of 25. By multiplying the test condition and intrinsic characteristic ratings with their respective weight factors and summing the resulting values produces the score of 475. This value is SL2's score for engineering aspects. Clinical applicability scores are calculated by summing the four rating numbers of each method analyzed. For example, SL2 had rating values of 1, 1, 0.75, and 1 for all four clinical applications. By summing these values, a score of 3.75 results for the SL2's clinical applicability. Finally, the values for the scores for each method for the engineering aspects and clinical applicability are shown in their respective rows of Table 6-1 where the superscript abbreviations indicate the associated method.

6.2 Analysis Two

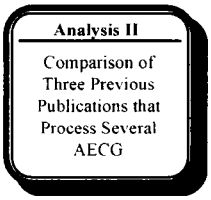

Analysis II compares three previously reported methods for abdominal MECG cancellation with the CH^2 technique. As discussed, the formerly published techniques of analysis II process several AECGs to cancel their MECG. The three methods include quadratic programming (Quad.), SVD method one (SVD1), and SVD method two (SVD2). Each of these methods has been described in Chapter 2.

Analysis II contains three tables that are used to present the analysis information (grades, ratings, and scores) for the three previously reported methods and the CH^2 technique for abdominal MECG cancellation. Appendix G contains a detailed description of the engineering aspects and clinical applicability grading, rating, and scoring schemes for these tables. Furthermore, the following section or Section 6.2.1 gives a general explanation for these tables and a description of the figures referenced by them. Finally, Section 6.2.2 contains an example explanation of the grading, rating, and scoring for quadratic programming versus the CH^2 method of Table 6-6.

6.2.1 Explanation of Tables and Respective Figures

Tables 6-6, 6-7, and 6-8 contain the analysis information for Quad., SVD1, and SVD2 versus the CH^2 method respectively. The seven test conditions and four clinical applications of Tables 6-6 through 6-8 grade data sets contained in Figures 6-7 through 6-13 and Figures I-1 through I-19. The following describes the layout of Figures 6-7 through 6-13 and Figures I-1 through I-19 along with a description of the signals inspected for the grading of Tables 6-6 through 6-8.

Figures 6-7 through 6-13 contain the results for the reimplementation and implementation of the quadratic programming and CH^2 method for abdominal MECG cancellation respectively with synthesized data. Figure 6-7 contains the six AECGs $S_{2\text{-}7}(n)$ used to demonstration test condition 4 through 6 with the Quad. and the CH^2 method. Figures 6-8 and 6-9 contain the results from demonstrating test condition 4 or the overlap between the FECG and MECG. All signals of Figure 6-8 are used by or resulting signals from the CH^2 method. Figure 6-8(a) is the TECG $S_1(n)$ used only by the CH^2 method to suppress the MECG. The TECG is also used by the CH^2 technique to demonstrate test conditions 5 and 6 of Figures 6-10 through 6-13. Figure 6-8(b) contains the resulting AECGs $R_{1\text{-}6}(n)_{CH^2}$ of the CH^2 method where only the MECG has been

Table 6-6. Quadratic programming vs. the CH^2 method for AECG MECG cancellation.

ENGINEERING ASPECTS (See Appendix G for a detailed description)			**Scores** = $350^{Quad.}$, 473^{CH^2}				
Test Conditions			Data Designation, Grading, & Rating Information				
✓ Passed × Failed - Did Not Occur			Figs. 6-8, 9	Figs. 6-10, 11	Figs. 6-12, 13		Rating
1^{100}	Bandwidth of Resulting AECGs are 0.05 to 100 Hz	Quad.	✓	✓	✓		3/3
		CH^2	✓	✓	✓		3/3
2^{100}	Signal Corruption to FECG & EMG	Quad.	×	×	×		0/6
		CH^2	✓, ⇧	✓, ⇧	✓, ⇧		6/6
3^{100}	Overall MECG Cancellation	Quad.	✓	✓	✓		3/3
		CH^2	✓	✓	✓		3/3
4^{100}	FECG & MECG Overlap	Quad.	✓	✓	✓		3/3
		CH^2	✓	✓	✓		3/3
5	Significant AECG Low Frequency Noise	Quad.	-	✓	-		
		CH^2	-	✓	-		
6	Significant AECG Noise Spike	Quad.	-	-	✓		
		CH^2	-	-	✓		
7	Significant TECG Noise	Quad.	Since quadratic programming does not use any TECG(s), this test condition is not performed.				
		CH^2					
Intrinsic Characteristics			Grading & Rating Information				
1^{25}	Flexibility of Lead Positioning	Quad.	Little Flexibility (for the six AECGs)				0
		CH^2	Flexible (TECG lead needs to be in a lead II position)				0.5
2^{25}	Number of Extra Leads Required	Quad.	Six AECGs				0
		CH^2	One TECG				0.75
3^{25}	User Interaction Required	Quad.	No				1
		CH^2	No				1
4^{25}	Computational Complexity	Quad.	Low (about 3 seconds for 8 seconds of data)				1
		CH^2	Low CH^2 (about 2 seconds for 8 seconds of data) Medium CH^2&SVD (11 seconds for 8 seconds of data)				0.66
CLINICAL APPLICABILITY (See Appendix G for a detailed description)			**Scores** = $2^{Quad.}$, 4^{CH^2}				
Clinical Applications			Data Designation, Grading, & Rating Information				
P Potential NP No Potential			Figs. 6-8, 9	Figs. 6-10, 11	Figs. 6-12, 13		Rating
1	Fetal HR Information via HR Determination Algorithm	Quad.	P	P	P		3/3
		CH^2	P	P	P		3/3
2	FECG Electrophysiological Info. via FECG Averaging	Quad.	P	P	P		3/3
		CH^2	P	P	P		3/3
3	Uterine Contraction Information via EMG	Quad.	NP	NP	NP		0/3
		CH^2	P	P	P		3/3
4	Principal Fetal Signal(s) or Source Signal(s) Obtainable	Quad.	NP	NP	NP		0/3
		CH^2	P	P	P		3/3

Table 6-7. SVD method one vs. the CH^2 method for AECG MECG cancellation.

ENGINEERING ASPECTS (See Appendix G for a detailed description)			**Scores** = 306^{SVD1}, 469^{CH^2}				
Test Conditions			Data Designation, Grading, & Rating Information				
✓ Passed ✖ Failed - Did Not Occur			Figs. I-2, 3	Figs. I-4, 5	Figs. I-6, 7	Figs. I-8, 9	Rating
1^{100}	Bandwidth of Resulting AECGs are 0.05 to 100 Hz	SVD1	✓	✓	✓	✓	4/4
		CH^2	✓	✓	✓	✓	4/4
2^{100}	Signal Corruption to FECG & EMG	SVD1	✖	✖	✖	✖	0/8
		CH^2	✓, ⇧	✓	✓, ⇧	✓, ⇧	7/8
3^{100}	Overall MECG Cancellation	SVD1	✓	✖	✓	✓	3/4
		CH^2	✓	✓	✓	✓	4/4
4^{100}	FECG & MECG Overlap	SVD1	✓	✖	✓	✓	3/4
		CH^2	✓	✓	✓	✓	4/4
5	Significant AECG Low Frequency Noise	SVD1	-	✖	-	-	
		CH^2	-	✓	-	-	
6	Significant AECG Noise Spike	SVD1	-	-	✓	-	
		CH^2	-	-	✓	-	
7	Significant TECG Noise	SVD1	-	-	-	✖	
		CH^2	-	-	-	✓	
Intrinsic Characteristics			Grading & Rating Information				
1^{25}	Flexibility of Lead Positioning	SVD1	Little Flexibility (for the three TECGs)				0
		CH^2	Flexible (TECG lead needs to be in a lead II position)				0.5
2^{25}	Number of Extra Leads Required	SVD1	Three TECGs				0.25
		CH^2	One TECG				0.75
3^{25}	User Interaction Required	SVD1	No				1
		CH^2	No				1
4^{25}	Computational Complexity	SVD1	Low (about 6 seconds for 8 seconds of data)				1
		CH^2	Low CH^2 (about a second for 8 seconds of data) Low CH^2&SVD (2 seconds for 8 seconds of data)				1
CLINICAL APPLICABILITY (See Appendix G for a detailed description)			**Scores** = 2.25^{SVD1}, 4^{CH^2}				
Clinical Applications			Data Designation, Grading, & Rating Information				
P Potential NP No Potential			Figs. I-2, 3	Figs. I-4, 5	Figs. I-6, 7	Figs. I-8, 9	Rating
1	Fetal HR Information via HR Determination Algorithm	SVD1	P	NP	P	P	3/4
		CH^2	P	P	P	P	4/4
2	FECG Electrophysiological Info. via FECG Averaging	SVD1	P	NP	P	P	3/4
		CH^2	P	P	P	P	4/4
3	Uterine Contraction Information via EMG	SVD1	NP	NP	NP	NP	0/4
		CH^2	P	P	P	P	4/4
4	Principal Fetal Signal(s) or Source Signal(s) Obtainable	SVD1	P	NP	P	P	3/4
		CH^2	P	P	P	P	4/4

Table 6-8. SVD method two vs. the CH^2 method for AECG MECG cancellation.

ENGINEERING ASPECTS (See Appendix G for a detailed description)			**Scores** = 321^{SVD2}, 465^{CH^2}				
Test Conditions			Data Designation, Grading, & Rating Information				
✓ Passed ✗ Failed - Did Not Occur			Figs. I-11-13	Figs. I-14-16	Figs. I-17-19		Rating
1^{100}	Bandwidth of Resulting AECGs are 0.05 to 100 Hz	SVD2	✓	✓	✓		3/3
		CH^2	✓	✓	✓		3/3
2^{100}	Signal Corruption to FECG & EMG	SVD2	✗	✗	✗		0/6
		CH^2	✓, ⇧	✓, ⇧	✓, ⇧		6/6
3^{100}	Overall MECG Cancellation	SVD2	✓	✓	✓		3/3
		CH^2	✓	✓	✓		3/3
4^{100}	FECG & MECG Overlap	SVD2	✓	✓	✓		3/3
		CH^2	✓	✓	✓		3/3
5	Significant AECG Low Frequency Noise	SVD2	-	✓	-		
		CH^2	-	✓	-		
6	Significant AECG Noise Spike	SVD2	-	-	✓		
		CH^2	-	-	✓		
7	Significant TECG Noise	SVD2	Since SVD method two does not use any TECG(s), this test condition is not performed.				
		CH^2					
Intrinsic Characteristics			Grading & Rating Information				
1^{25}	Flexibility of Lead Positioning	SVD2	Flexible (for all AECGs)				0.5
		CH^2	Flexible (TECG lead needs to be in a lead II position)				0.5
2^{25}	Number of Extra Leads Required	SVD2	Five AECGs (for rank = 5)				0
		CH^2	One TECG				0.75
3^{25}	User Interaction Required	SVD2	Yes (The first step of the method requires the user to select portions of the MECG complex of the AECGs.)				0
		CH^2	No				1
4^{25}	Computational Complexity	SVD2	High (about 56 seconds for 8 seconds of data)				0.33
		CH^2	Low CH^2 (about 3 seconds for 8 seconds of data) High CH^2&SVD (49 seconds for 8 seconds of data)				0.33
CLINICAL APPLICABILITY (See Appendix G for a detailed description)			**Scores** = 2^{SVD2}, 4^{CH^2}				
Clinical Applications			Data Designation, Grading, & Rating Information				
P Potential NP No Potential			Figs. I-11-13	Figs. I-14-16	Figs. I-17-19		Rating
1	Fetal HR Information via HR Determination Algorithm	SVD2	P	P	P		3/3
		CH^2	P	P	P		3/3
2	FECG Electrophysiological Info. via FECG Averaging	SVD2	P	P	P		3/3
		CH^2	P	P	P		3/3
3	Uterine Contraction Information via EMG	SVD2	NP	NP	NP		0/3
		CH^2	P	P	P		3/3
4	Principal Fetal Signal(s) or Source Signal(s) Obtainable	SVD2	NP	NP	NP		0/3
		CH^2	P	P	P		3/3

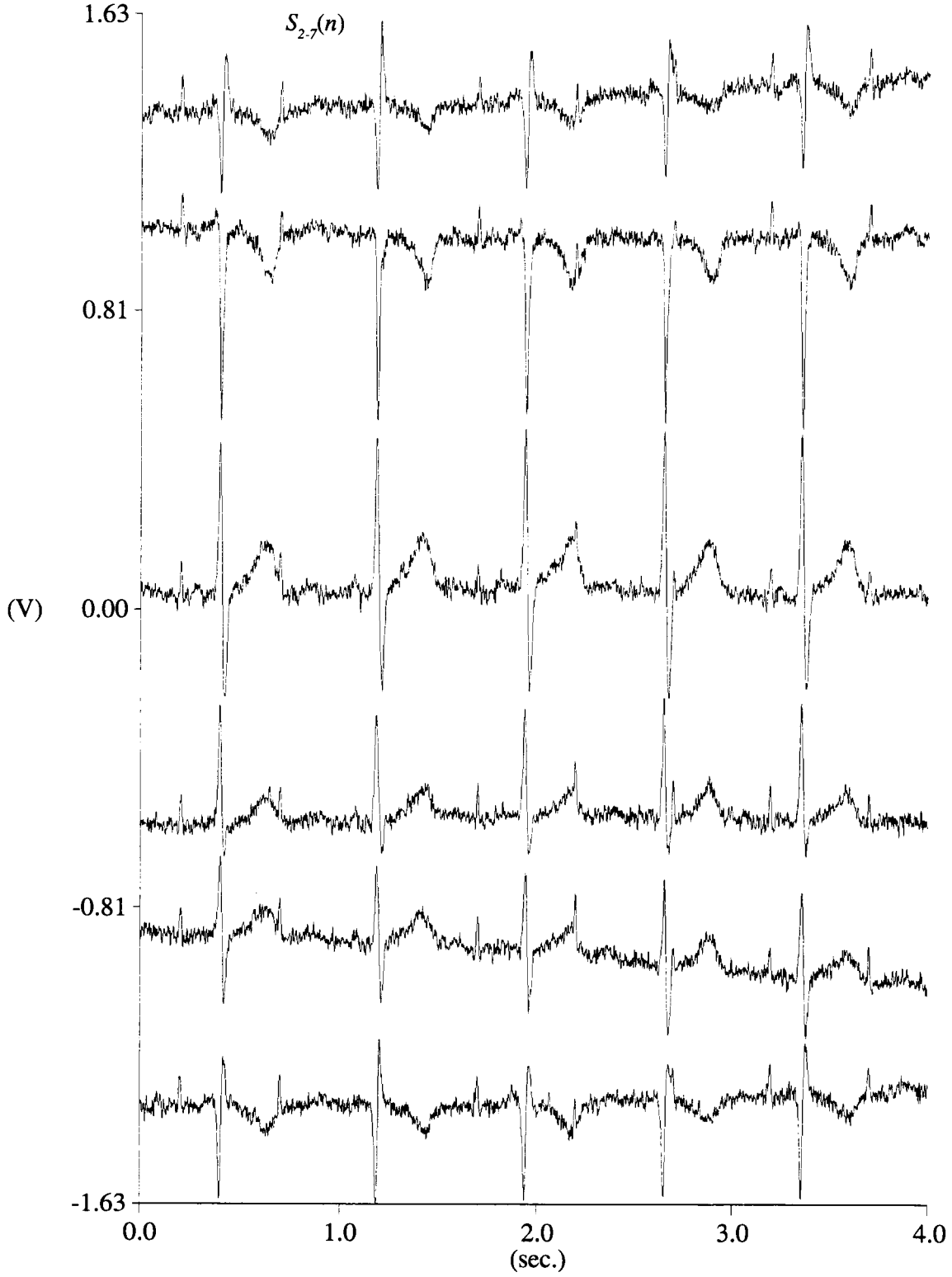

Figure 6-7. AECG signals used to compare the quadratic programming and CH^2 methods.

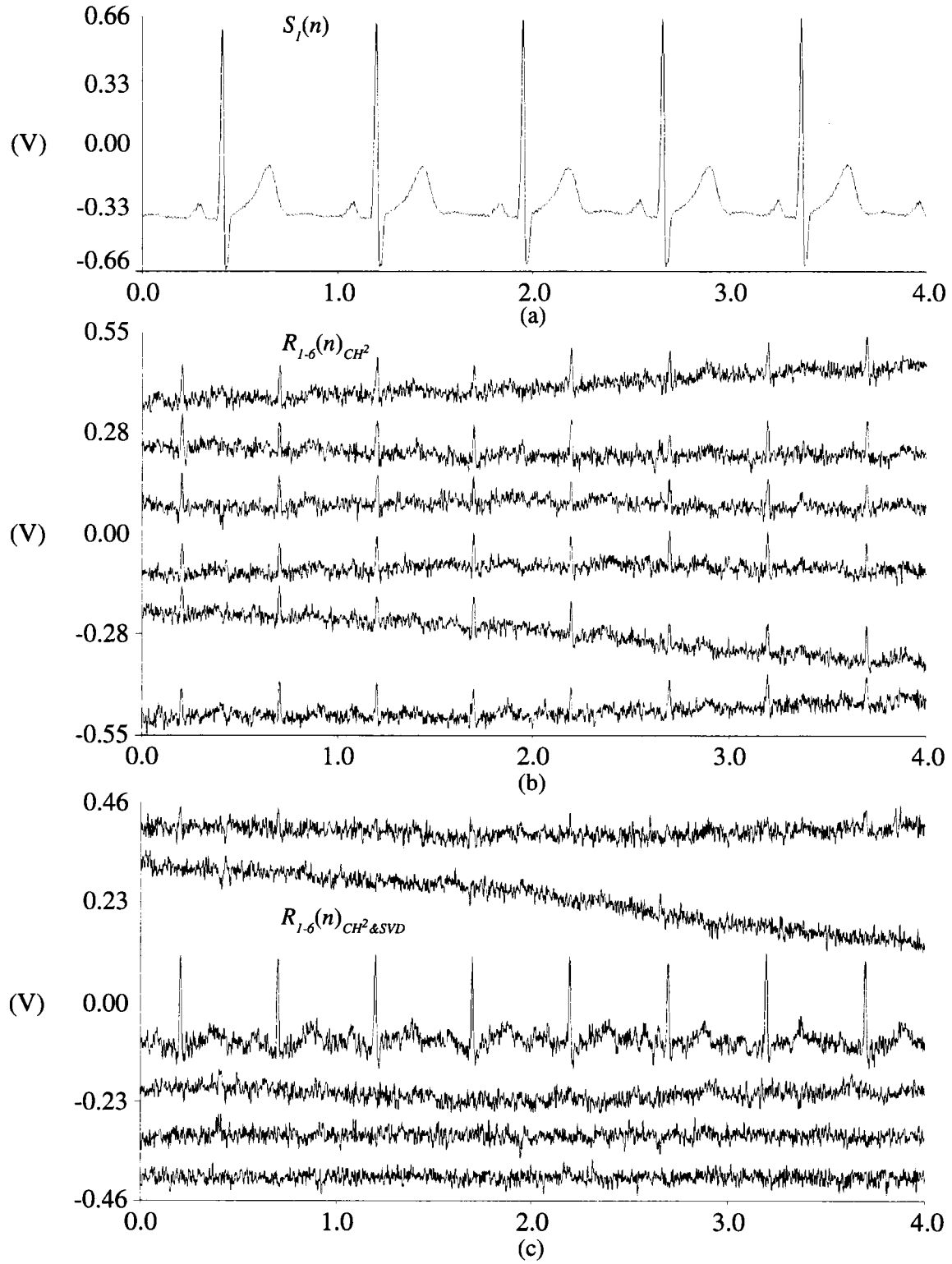

Figure 6-8. CH^2 and CH^2 & SVD results demonstrating test condition four (all x-axes in seconds). (a) TECG or $S_1(n)$ used only with the CH^2 method. (b) AECGs or $S_{2\text{-}7}(n)$ with the MECG canceled via the CH^2 method or $R_{1\text{-}6}(n)_{CH^2}$. (c) SVD of $R_{1\text{-}6}(n)_{CH^2}$ *or* $R_{1\text{-}6}(n)_{CH^2\&SVD}$.

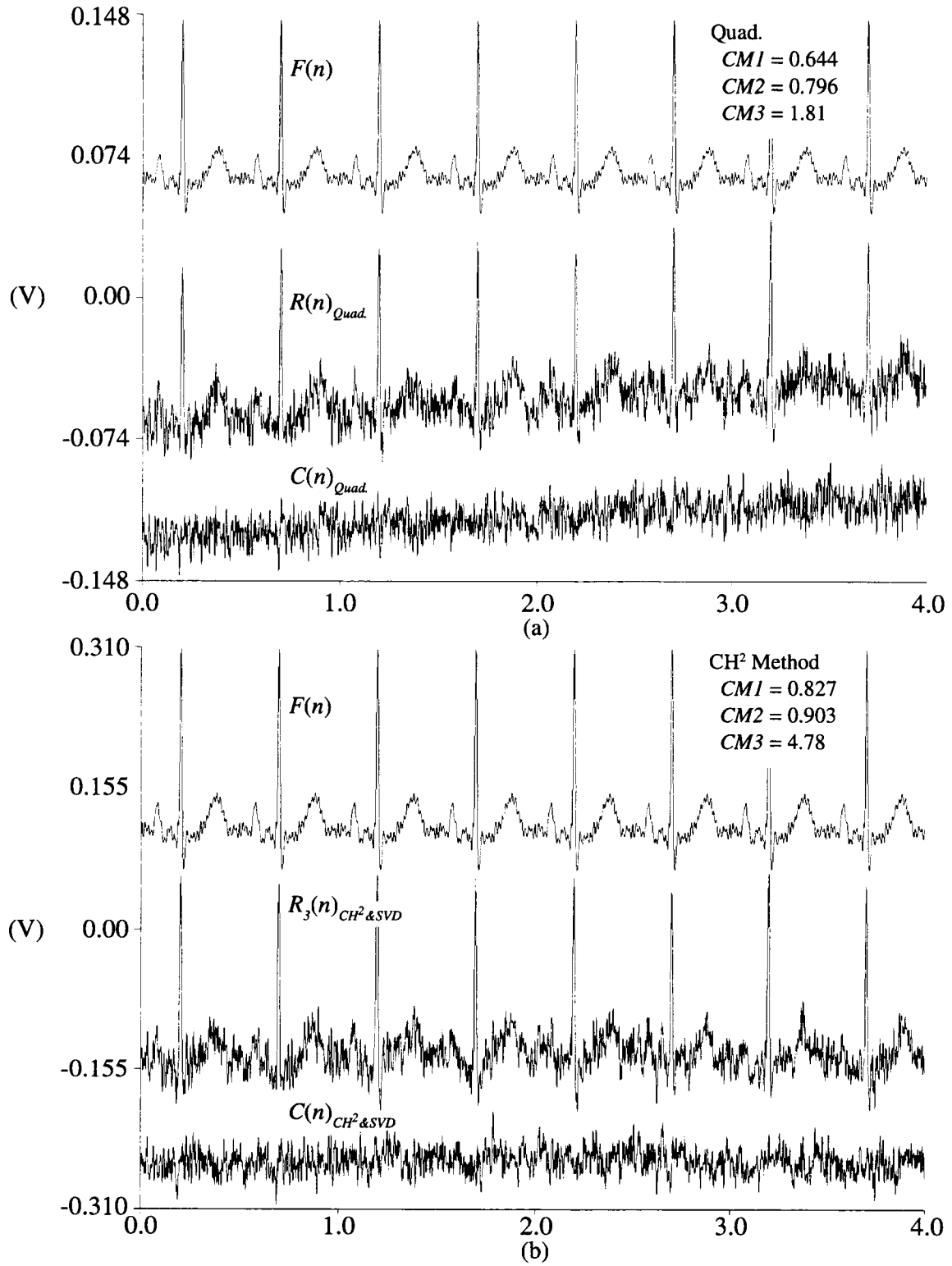

Figure 6-9. Quadratic programming vs. the CH² method demonstrating test condition four (all x-axes in seconds). (a) Ideal FECG or $F(n)$, enhanced FECG via quad. or $R(n)_{Quad.}$, and noise corrupting $R(n)_{Quad.}$ or $C(n)_{Quad.}$. (b) Ideal FECG or $F(n)$, enhanced FECG via CH² and SVD or $R_3(n)_{CH^2\&SVD}$, and noise corrupting $R_3(n)_{CH^2\&SVD}$ or $C(n)_{CH^2\&SVD}$.

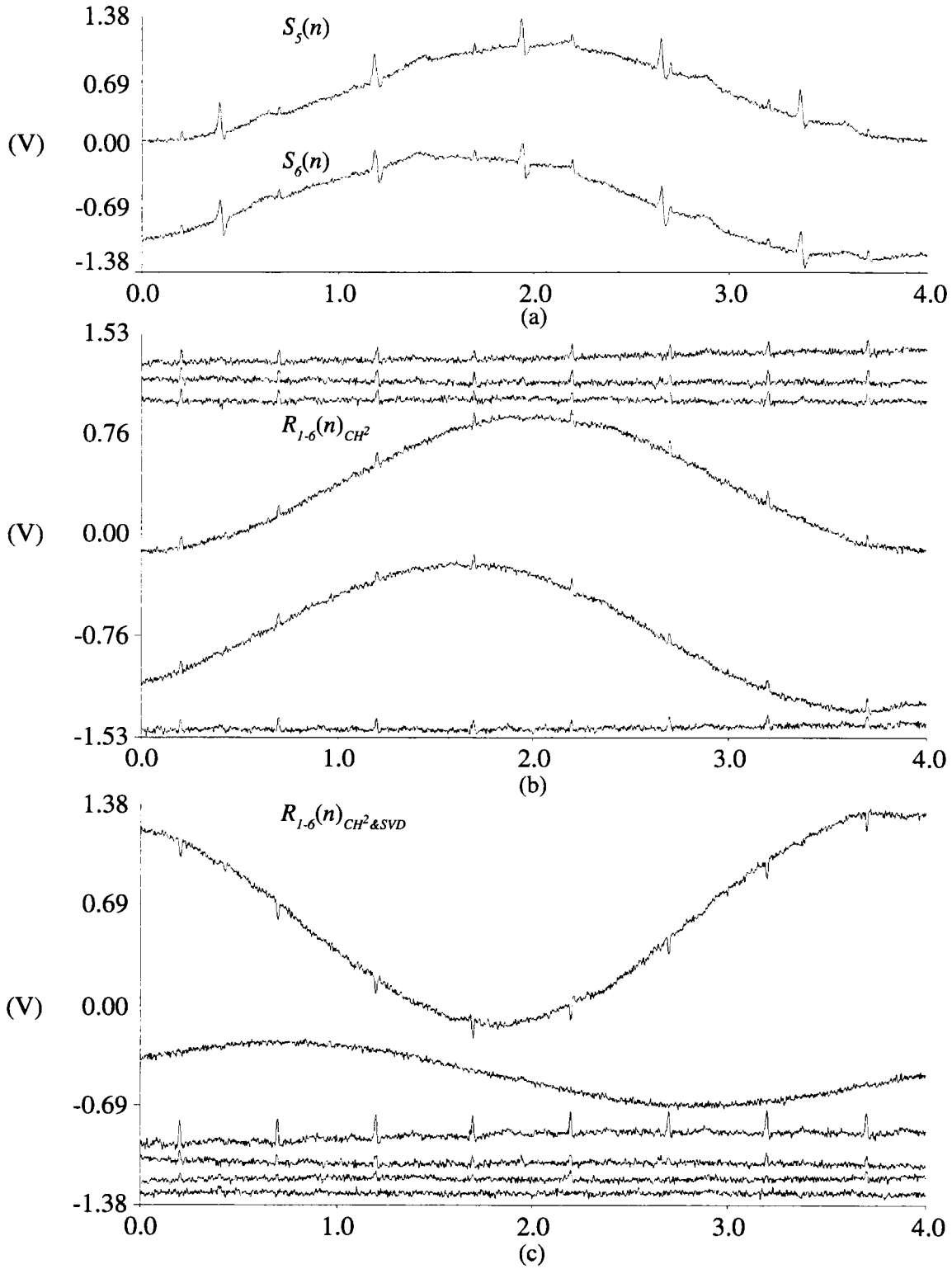

Figure 6-10. CH² and CH² & SVD results demonstrating test condition five (all x-axes in seconds). (a) AECG four and five or $S_5(n)$ and $S_6(n)$ with added low frequency noise. (b) AECGs or $S_{2\text{-}7}(n)$ with the MECG canceled via the CH² method or $R_{1\text{-}6}(n)_{CH^2}$. (c) SVD of $R_{1\text{-}6}(n)_{CH^2}$ *or* $R_{1\text{-}6}(n)_{CH^2\&SVD}$.

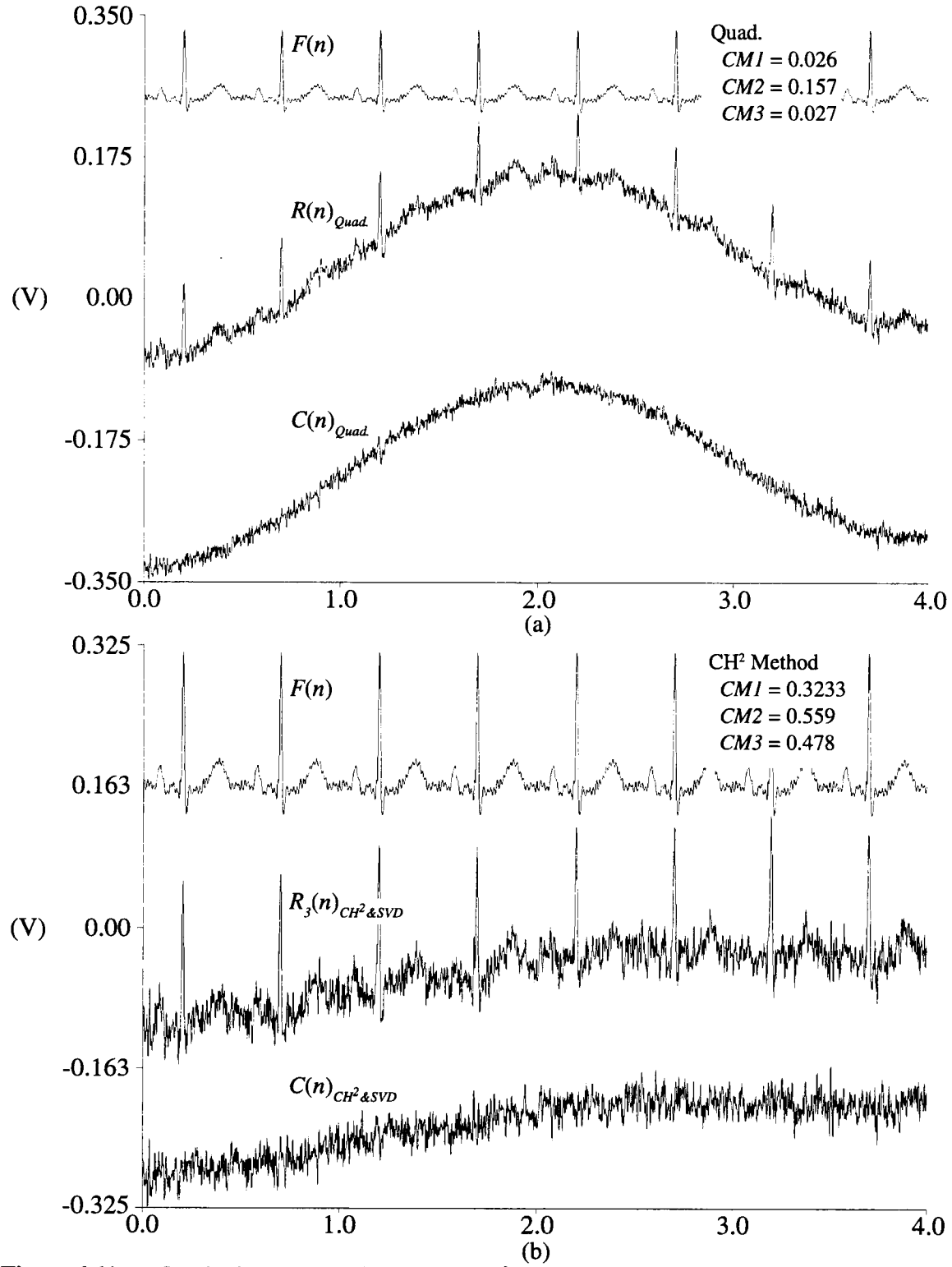

Figure 6-11. Quadratic programming vs. the CH² method demonstrating test condition five (all x-axes in seconds). (a) Ideal FECG or $F(n)$, enhanced FECG via quad. or $R(n)_{Quad.}$, and noise corrupting $R(n)_{Quad.}$ or $C(n)_{Quad.}$. (b) Ideal FECG or $F(n)$, enhanced FECG via CH² and SVD or $R_3(n)_{CH^2\&SVD}$, and noise corrupting $R_3(n)_{CH^2\&SVD}$ or $C(n)_{CH^2\&SVD}$.

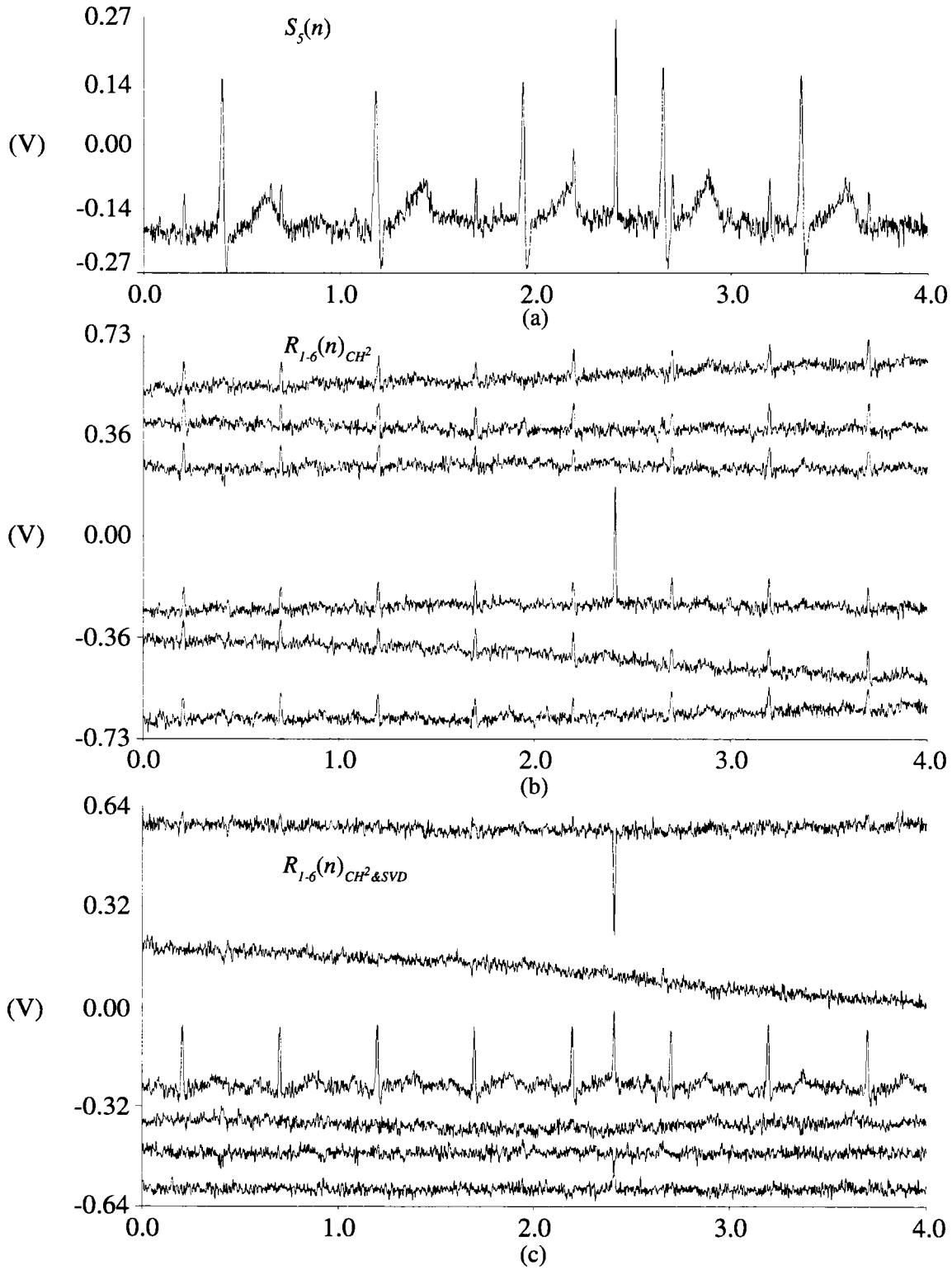

Figure 6-12. CH^2 and CH^2 & SVD results demonstrating test condition six (all x-axes in seconds). (a) AECG four or $S_5(n)$ with an added noise spike. (b) AECGs or $S_{2\text{-}7}(n)$ with the MECG canceled via the CH^2 method or $R_{1\text{-}6}(n)_{CH^2}$ (c) SVD of $R_{1\text{-}6}(n)_{CH^2}$ *or* $R_{1\text{-}6}(n)_{CH^2\&SVD}$.

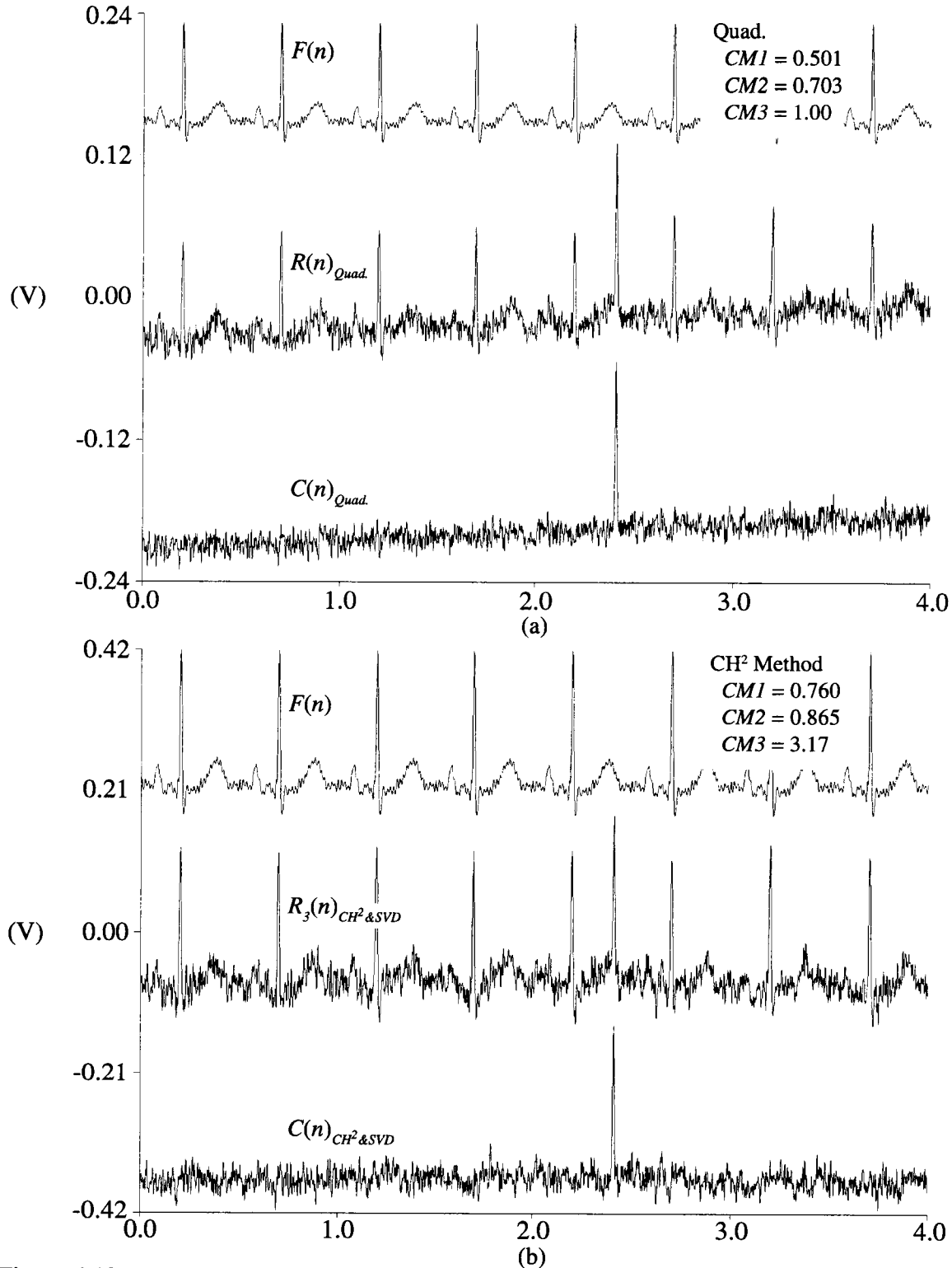

Figure 6-13. Quadratic programming vs. the CH^2 method demonstrating test condition six (all x-axes in seconds). (a) Ideal FECG or $F(n)$, enhanced FECG via quad. or $R(n)_{Quad.}$, and noise corrupting $R(n)_{Quad.}$ or $C(n)_{Quad.}$. (b) Ideal FECG or $F(n)$, enhanced FECG via CH^2 and SVD or $R_3(n)_{CH^2\&SVD}$, and noise corrupting $R_3(n)_{CH^2\&SVD}$ or $C(n)_{CH^2\&SVD}$.

canceled from the AECGs $S_{2\text{-}7}(n)$ of Figure 6-7. Figure 6-8(c) contains the resulting signals $R_{1\text{-}6}(n)_{CH^2\&SVD}$ of the SVD of the signals of Figure 6-8(b). The SVD was done by using (32) of Chapter 2 where $\boldsymbol{S}_{K,N}$ contains the resulting AECGs $R_{1\text{-}6}(n)_{CH^2}$ of Figure 6-8(b). Figure 6-9 presents the resulting signals for the Quad. and the CH^2 method. The first signal of Figure 6-9(a) is the desired FECG $F(n)$. The second signal is the resulting signal from the Quad. method and the third signal of Figure 6-9(a) is

$$C(n)_{Quad} = R(n)_{Quad.} - F(n) \tag{57}$$

or the signal corruption to $F(n)$ of $R(n)_{Quad.}$. Figure 6-9(b)'s first signal is the desired FECG $F(n)$. The second signal is the same as the third signal of Figure 6-8(c). Figure 6-9(b)'s third signal is

$$C(n)_{CH^2\&SVD} = R_3(n)_{CH^2\&SVD} - F(n) \tag{58}$$

or the signal corruption to $F(n)$ of $R_3(n)_{CH^2\&SVD}$. Figures 6-10 and 6-11 have the same format as Figures 6-8 and 6-9, but Figure 6-10(a) contains the AECGs $S_{5\text{-}6}(n)$ with added low frequency noise similar to Figure 6-2(b) to demonstrate test condition 5. Finally, Figures 6-12 and 6-13 have the same format as Figures 6-8 and 6-9, but Figure 6-12(a) contains the AECG $S_5(n)$ with an added noise spike similar to Figure 6-2(c) to demonstrate test condition 6.

The signals analyzed for Table 6-6 test conditions 1, 3, 4, 5, and 6 and clinical applications 1, 2, and 4 are $S_{2\text{-}7}(n)$, $R(n)_{Quad.}$, and $R_3(n)_{CH^2\&SVD}$ of Figures 6-7, 6-9, 6-11, and 6-13. The visual inspection of test conditions 5 and 6 that compare the AECGs' FECG shape with the resulting signal's FECG shape excluding polarity and amplitude can only be done with synthesized data. Synthesized data can only be used because one principal fetal signal (shown in Figure 6-2(a)) makes up the FECG. If clinical data was used, this visual inspection could not be done because the FECG would usually have three principal fetal signals. Test condition 2's corruption measures of CM_1, CM_2, and CM_3 that are specified for Quad. and the CH^2 technique on Figures 6-9, 6-11, and 6-13 are determined from $F(n)$, $R(n)_{Quad.}$, $C(n)_{Quad.}$, $R_3(n)_{CH^2\&SVD}$, and $C(n)_{CH^2\&SVD}$. These three corruption measures have been defined by (53), (54), and (55) of Chapter 5 where $F(n)$ is used for $S_{ideal}(n)$, $R(n)_{Quad.}$ or $R_3(n)_{CH^2\&SVD}$ is used for $R(n)$, the variance of $F(n)$ is used for

$\sigma^2_{S_{ideal}(n)}$, the variance of $C(n)_{\text{Quad.}}$ or $C(n)_{CH^2\&SVD}$ is used for $\sigma^2_{N(n)}$, and the variance of $R(n)_{Quad.}$ or $R(n)_{CH^2\&SVD}$ is used for $\sigma^2_{R(n)}$. Furthermore, test condition 2 and clinical application 3 for the CH^2 method analyzes the AECGs and resulting AECGs with only the MECG canceled or the signals of Figures 6-7, 6-8(b), 6-10(b), and 6-12(b). Separate resulting AECGs with only the MECG canceled are not available for the Quad. method. Therefore, no signal inspection can be done for test condition 2 and clinical application 3. Finally, since the resulting data sets of Figures 6-8 and 6-9, Figures 6-10 and 6-11, and Figures 6-12 and 6-13 process the same AECGs of Figure 6-7 except the last two sets of figures have an added non-ideal signal characteristic, Figures 6-8 and 6-9 can be used as baselines or references to determine if the test conditions passed or failed for Figures 6-10 through 6-11 and Figures 6-12 through 13.

Figures I-1 through I-9 contain the results for the reimplementation and implementation of SVD method one and the CH^2 method for abdominal MECG cancellation respectively with synthesized data. Figure I-1 contains the three TECG $S_{1\text{-}3}(n)$ and two AECGs $S_{4\text{-}5}(n)$ used to demonstration test condition 4 through 7 with SVD1 and the CH^2 method. Figures I-2 and I-3 contain the results from demonstrating test condition 4 or the overlap between the FECG and MECG. Figure I-2(a) contains the last two resulting signals $R_{4\text{-}5}(n)_{SVD1}$ of SVD1. Figure I-2(b) contains the resulting AECGs $R_{1\text{-}2}(n)_{CH^2}$ of the CH^2 method where only the MECG has been canceled from the AECGs $S_{4\text{-}5}(n)$ of Figure I-1. The TECG $S_1(n)$ of Figure I-1(a) was used with the CH^2 method. This TECG is also used by the CH^2 technique to demonstrate test conditions 5 through 7 of Figures I-4 through I-9. Figure I-2(c) contains the resulting signals $R_{1\text{-}2}(n)_{CH^2\&SVD}$ of the SVD of the signals of Figure I-2(b). The SVD was done by using (32) of Chapter 2 where $\boldsymbol{S}_{K,N}$ contains the resulting AECGs $R_{1\text{-}2}(n)_{CH^2}$ of Figure I-2(b). Figure I-3 presents the resulting signals for SVD1 and the CH^2 method. The first signal of Figure I-3(a) is the desired FECG $F(n)$. The second signal is the resulting signal from the SVD1 method and the third signal of Figure I-3(a) is

$$C(n)_{SVD1} = R_4(n)_{SVD1} - F(n) \tag{59}$$

or the signal corruption to $F(n)$ of $R_4(n)_{SVD1}$. Figure I-3(b)'s first signal is the desired FECG $F(n)$. The second signal is the same as the first signal of Figure I-2(c). Figure I-3(b)'s third signal is

$$C(n)_{CH^2\&SITD} = R_1(n)_{CH^2\&SITD} - F(n) \tag{60}$$

or the signal corruption to $F(n)$ of $R_1(n)_{CH^2\&SITD}$. Figures I-4 and I-5 have the same layout as Figures I-2 and I-3, but Figure I-4(a) was added to Figure I-4 and contains the AECGs $S_{5\text{-}6}(n)$ with added low frequency noise similar to Figure 6-2(b) to demonstrate test condition 5. Figures I-6 and I-7 have the same format as Figures I-2 and I-3, but Figure I-6(a) was added to Figure I-6 and contains the AECG $S_4(n)$ with an added noise spike similar to Figure 6-2(c) to demonstrate test condition 6. Finally, Figures I-8 and I-9 have the same format as Figures I-2 and I-3, but Figure I-8(a) was added to Figure I-8 and contains the TECG $S_1(n)$ with added gaussian noise with an 0.05 to 100.0 Hz bandwidth to demonstrate test condition 7.

The signals analyzed for Table 6-7 test conditions 1, 3, 4, 5, 6, and 7 and clinical applications 1, 2, and 4 are $S_{4\text{-}5}(n)$, $R_4(n)_{SVD1}$, and $R_1(n)_{CH^2\&SITD}$ of Figures I-1, I-3, I-5, I-7, and I-9. The visual inspection of test conditions 5, 6, and 7 that compare the AECGs' FECG shape with the resulting signal's FECG shape excluding polarity and amplitude can only be done with synthesized data. Synthesized data can only be used because one principal fetal signal (shown in Figure 6-2(a)) makes up the FECG. If clinical data was used, this visual inspection could not be done because the FECG would usually have three principal fetal signals. Test condition 2's corruption measures of CM_1, CM_2, and CM_3 that are specified for SVD1 and the CH^2 technique on Figures I-3, I-5, I-7, and I-9 are determined from $F(n)$, $R_4(n)_{SITD1}$, $C(n)_{SVD1}$, $R_1(n)_{CH^2\&SITD}$, and $C(n)_{CH^2\&SITD}$. These three corruption measures have been defined by (53), (54), and (55) of Chapter 5 where $F(n)$ is used for $S_{ideal}(n)$, $R_4(n)_{SITD1}$ or $R_1(n)_{CH^2\&SITD}$ is used for $R(n)$, the variance of $F(n)$ is used for $\sigma^2_{S_{ideal}(n)}$, the variance of $C(n)_{SITD1}$ or $C(n)_{CH^2\&SITD}$ is used for $\sigma^2_{N(n)}$, and the variance of $R_4(n)_{SITD1}$ or $R_1(n)_{CH^2\&SITD}$ is used for $\sigma^2_{R(n)}$. Furthermore, test condition 2 and clinical application 3 analyzes the AECGs and resulting AECGs with only the MECG canceled or the signals of Figures I-1, I-2(a-b), I-4(b-c), I-6(b-c), and I-8(b-c). Finally, since the resulting data sets of Figures I-2 and I-3, Figures I-4 and I-5, Figures I-6 and I-7, Figures I-8 and I-9 process the same AECGs of Figure I-1 except the last three sets of figures have an added non-ideal signal characteristic, Figures I-2 and I-3 can be used as baselines or references to determine if the test conditions passed or failed for Figures I-4 and I-5, Figures I-6 and I-7, and Figures I-8 and I-9.

Figures I-10 through I-19 contain the results for the reimplementation and implementation of the SVD method two and CH^2 method for abdominal MECG cancellation respectively with synthesized data. Figure I-10 contains the ten AECGs $S_{2\text{-}11}(n)$ used to demonstration test conditions 4 through 6 with the SVD2 and the CH^2 method. Figures I-11 through I-13 contain the results from demonstrating test condition 4 or the overlap between the FECG and MECG. All signals of Figure I-11 are resulting signals from SVD2. Figure I-11(a) contains the first five resulting signals $R_{1\text{-}5}(n)_{SVD2}$ of SVD2 that contain residual MECG. Figure I-11(b) contains the last five resulting AECGs $R_{6\text{-}10}(n)_{SVD2}$ of SVD2 where the MECG has been canceled. Figure I-11(c) contains the resulting signals $R`_{1\text{-}5}(n)_{SVD2}$ of the SVD of the signals of Figure I-11(b) as described by Chapter 2. All signals of Figure I-12 are used by or resulting signals from the CH^2 method. Figure I-11(a) is the TECG $S_1(n)$ used only by the CH^2 method to suppress the MECG of the AECGs of Figure I-10. This TECG is also used by the CH^2 technique to demonstrate test condition 5 and 6 of Figures I-14 through I-19. Figure I-12(b) contains the resulting AECGs $R_{1\text{-}10}(n)_{CH^2}$ of the CH^2 method where only the MECG has been canceled from the AECGs $S_{2\text{-}11}(n)$ of Figure I-10. Figure I-12(c) contains the resulting signals $R_{1\text{-}10}(n)_{CH^2\&SVD}$ of the SVD of the signals of Figure I-12(b). The SVD was done by using (32) of Chapter 2 where $\boldsymbol{S}_{K,N}$ contains the resulting AECGs $R_{1\text{-}10}(n)_{CH^2}$ of Figure I-12(b). Figure I-13 presents the resulting signals for SVD2 and the CH^2 method. The first signal of Figure I-13(a) is the desired FECG $F(n)$. The second signal is the same as the first signal of Figure I-11(c) and the third signal of Figure I-13(a) is

$$C(n)_{SVD2} = R`_1(n)_{SVD2} - F(n) \tag{61}$$

or the signal corruption to $F(n)$ of $R`_1(n)_{SVD2}$. Figure I-13(b)'s first signal is the desired FECG $F(n)$. The second signal is the same as the first signal of Figure I-12(c). Figure I-13(b)'s third signal is the same as (60) or the signal corruption to $F(n)$ of $R_1(n)_{CH^2\&SVD}$. Figures I-14 through I-16 have the same layout as Figures I-11 through I-13, but Figure I-14(a) was added to Figure I-14 and contains the AECGs $S_{9\text{-}11}(n)$ with added low frequency noise similar to Figure 6-2(b) to demonstrate test condition 5. Finally, Figures I-17 through I-19 have the same format as Figures I-11 through I-13, but Figure I-17(a) was added to Figure I-17 and contains the AECG $S_{11}(n)$ with an added noise spike similar to Figure 6-2(c) to demonstrate test condition 6.

The signals analyzed for Table 6-8 test conditions 1, 3, 4, 5, 6, and 7 and clinical applications 1, 2, and 4 are $S_{2\text{-}1I}(n)$, $R`_1(n)_{SVD2}$, and $R_{1or3}(n)_{CH^2\&SVD}$ of Figures I-10, I-13, I-16, and I-19. The visual inspection of test conditions 5, 6, and 7 that compare the AECGs' FECG with the resulting signal's FECG shape excluding polarity and amplitude can only be done with synthesized data. Synthesized data can only be used because one principal fetal signal (shown in Figure 6-2(a)) makes up the FECG. If clinical data was used, this visual inspection could not be done because the FECG would usually have three principal fetal signals. Test condition 2's corruption measures of CM_1, CM_2, and CM_3 that are specified for SVD2 and the CH^2 technique on Figures I-13, I-16, and I-19 are determined from $F(n)$, $R`_1(n)_{SVD2}$, $C(n)_{SVD2}$, $R_{1or3}(n)_{CH^2\&SVD}$, and $C(n)_{CH^2\&SVD}$. These three corruption measures have been defined by (53), (54), and (55) of Chapter 5 where $F(n)$ is used for $S_{ideal}(n)$, $R`_1(n)_{SVD2}$ or $R_{1or3}(n)_{CH^2\&SVD}$ is used for $R(n)$, the variance of $F(n)$ is used for $\sigma^2_{S_{ideal}(n)}$, the variance of $C(n)_{SVD2}$ or $C(n)_{CH^2\&SVD}$ is used for $\sigma^2_{N(n)}$, and the variance of $R`_1(n)_{SVD2}$ or $R_{1or3}(n)_{CH^2\&SVD}$ is used for $\sigma^2_{R(n)}$. Test condition 2 and clinical application 3 for the CH^2 method analyzes the AECGs and resulting AECGs with only the MECG canceled or the signals of Figures I-10, I-12(b), I-15(a), and I-18(a). Some of the AECGs with only the MECG canceled are not available for SVD2. Therefore, all the signals cannot be inspection for test condition 2 and clinical application 3. Clinical application 2 analyzes the AECGs of Figure I-10. Finally, since the resulting data sets of Figures I-11 through I-13, Figures I-14 through I-16, and Figures I-17 through I-19 process the same AECGs of Figure I-10 except the last two sets of figures have an added non-ideal signal characteristic, Figures I-11 through I-13 can be used as baselines or references to determine if the test conditions passed or failed for Figures I-14 through I-16 and Figures I-17 through I-19.

6.2.2 Quadratic Programming Versus the CH^2 Technique

The following discusses the grading, rating, and scoring of Table 6-6. Grading for the test conditions, intrinsic characteristics, and clinical applications of the engineering aspects and clinical applicability sections will be presented first along with intrinsic characteristic ratings. Next, a discussion of the ratings for the first four test conditions and clinical applications will be discussed. Then a description of the computation of the scoring for Quad.'s and the CH^2 method's engineering aspects and clinical applicability will be performed. Finally, Appendix G also gives a detailed discussion of the grading, rating, and scoring of Table 6-6.

Since the six figures referenced by Table 6-6 are graded similarly, only the grading of Figures 6-8 and 6-9 will be discussed. Table 6-6 presents the grades and ratings for Quad. and the CH^2 method in separate rows for each test condition, intrinsic characteristic, and clinical application. The grading of test conditions 1, 3, and 5 will not be given for Figures 6-8 and 6-9 since Chapter 5 explains these test conditions. However, the EMG inspection should be ignored for test condition 5.

Test condition 2 of analysis II has a different grading scheme than that used in Chapter 5 or analysis I of this chapter. This test condition was graded a failure for Quad. because the AECGs $S_{2\text{-}7}(n)$ of Figure 6-7 with only the MECG canceled are not available. Test condition 2 was graded pass for the CH^2 method because the resulting AECGs $R_{1\text{-}6}(n)_{CH^2}$ of Figure 6-8(b) compared to the AECGs' FECG or EMG have negligible MECG residuals and similar shaped FECG and EMG respectively. Finally, test condition 2 for the CH^2 method was graded the up arrow (⇧) because test condition 3 passed and its corruption measures CM_1, CM_2, and CM_3 were greater than the values for Quad.

Test condition 4 passed for Quad. and the CH^2 technique. Test condition 4 passed because the FECG's QRS complex that overlapped the MECG's complex of $S_{2\text{-}7}(n)$ is present and similar in shape excluding polarity and amplitude to the surrounding non-overlapping FECG's QRS complex of $R(n)_{Quad.}$ and $R_3(n)_{CH^2\&STD}$ of Figure 6-9. Finally, test condition 6 was graded pass for Quad. and the CH^2 technique because the resulting signal $R(n)_{Quad.}$'s and $R_3(n)_{CH^2\&STD}$'s FECG compared to the AECGs' FECG are similar in shape. Finally, since Quad. does not use any TECG(s), test condition seven was not performed.

The intrinsic characteristics of Table 6-6 deal with the design aspects of the method and do not analyze the data of Figures 6-7 through 6-13. Intrinsic characteristic 1 was graded as little flexibility because the six abdominal leads have to all be positioned so that the scaled summation of the signals produces MECG cancellation for positive scale factors. Furthermore, each AECG's FECG has to be positively correlated with the MECG. The CH^2 method was awarded a flexible grade because the TECG lead used to cancel the abdominal MECG needs to only be in a lead II position to achieve best resulting. Intrinsic characteristic 2 was graded six AECGs for Quad. because all the AECGs are required to cancel the MECG to produce the resulting signal $R(n)_{Quad.}$. The CH^2 method was graded one TECG for intrinsic characteristic 2 because an TECG is required to obtain cancellation. Intrinsic characteristics 3 was graded no for Quad. and the

CH^2 method because they did not require user interaction to initialize the algorithm at start up. Quad. had a grade of low for computational complexity because it took about 3 seconds to process 8 seconds of data. The CH^2 method in conjunction with SVD took 11 seconds to process 8 seconds of data. Therefore, it was graded medium. The timings were obtained with an Intel 486DX2 66 MHz microprocessor.

The grading of the four clinical applications will only analyze the data of Figures 6-8 and 6-9 for this example explanation. Clinical application 1 was graded potential for Quad. and the CH^2 technique because test conditions 3 and 4 passed for both methods and a visual inspection of $R(n)_{Quad.}$ and $R_3(n)_{(CH^2\&SVD)}$ determined that the FECG is observable. Clinical application 2 was graded potential for Quad. and the CH^2 technique because test conditions 1 and 3 passed for both techniques and a visual inspection of $R(n)_{Quad.}$ and $R_3(n)_{(CH^2\&SVD)}$ could discern all FECG's R waves to be averaged without question. Clinical application 3 was graded no potential for Quad. since test condition 2 failed. Clinical application 3 was graded potential for CH^2 since test conditions 1 and 2 passed. Finally, clinical application 4 was graded no potential for Quad. because no principal fetal signal(s) or source signal(s) is produce by the Quad. method. The CH^2 method passed this clinical application because $R_3(n)_{(CH^2\&SVD)}$ is a principal fetal signal or source signal.

The ratings for the first four test conditions and four clinical applications are tallied in the right hand column of Table 6-6. They are calculated based on the grades awarded for Figures 6-7 through 6-13 for each technique. An example calculation for the rating of test condition 2 for the Quad. method is given to clarify the rating computation. First, each grade including the up arrow (⇧) of test condition 2 for Quad. is counted as one point for a pass, zero points for a fail, and one point for an up arrow. Since test condition 2 for Quad. has three failures and no up arrows, 0 points are summed. Next, the 0 points are divided by the total number of data sets analyzed (three) plus the possible cases that could have been graded an up arrow (three) or six. The resulting number is the rating for test condition 2 for Quad. or zero. Since the other three rated test conditions do not have an up arrow in their grading scheme, the total points for passing grades is only divided by the number of data set studied (three) to produce the rating.

The score for engineering aspects of each method of Table 6-6 is calculated using the superscript numbers of the test condition and intrinsic characteristic numbers as weights of importance. The first four test conditions are given a weight of 100 and the intrinsic

characteristics a weight of 25. The superscript weights and rating values are multiplied and summed for each respective test condition and intrinsic characteristic to determine the engineering aspects score for the method analyzed. For example, Quad.'s ratings for the test conditions are 1, 0, 1, and 1 with weight factors of 100 for each rating. The intrinsic characteristic ratings for Quad. are 0, 0, 1, and 1 with weight factors of 25. By multiplying the test condition and intrinsic characteristic ratings with their respective weights and summing the resulting values, produces the score of 350. This value is Quad.'s score for engineering aspects. Clinical applicability scores are calculated by summing the four rating numbers of each method analyzed. For example, Quad. had rating values of 1, 1, 0, and 0 for the four clinical applications. By summing these values, a score of 2 results for Quad.'s clinical applicability. Finally, the values for the scores of each method for the engineering aspects and clinical applicability are shown in their respective rows of Table 6-6 where the superscript abbreviations indicate the associated method.

6.3 Discussion

Discussion

Effectiveness of the CH^2 Technique for AECG MECG Cancellation based on Comparison's Scores and Effectiveness Marks

This section discusses the effectiveness of the CH^2 method for abdominal MECG cancellation compared to eight previous publications. Effectiveness has been qualified by several scores for engineering aspects and clinical applicability of the former publications compared to the CH^2 method. Furthermore, engineering aspects and clinical applicability were each given a score so they could be compared separately. The scores allow the reader to determine the engineering quality and potential clinical information of a previously reported algorithm compared to the CH^2 technique. Table 6-9 presents a summary of the scores for the eight comparisons with the CH^2 algorithm where the shaded and none shaded regions indicate the eight comparisons.

Table 6-9. Summary of the scores for the eight comparisons of analysis I and II.

	Analysis I Scores										Analysis II Scores					
Method Designation	SL2	CH^2	SL3	CH^2	SL5	CH^2	TSAF	CH^2	Orth.	CH^2	Quad.	CH^2	SVD1	CH^2	SVD2	CH^2
Engineering Aspects	475	481	375	481	467	481	256	481	231	481	350	473	306	469	321	465
Clinical Applicability	3.75	4	2.75	4	4	4	1.5	4	0	4	2	4	2.25	4	2	4

To further qualify the effectiveness of the methods analyzed with one numerical value, an effectiveness mark is computed. This mark is based equally on the engineering aspects and clinical applicability scores. The computation consists of dividing the engineering aspects and clinical applicability scores by 500 and 4 respectively. Then these two resulting numbers are summed and divided by two to produce an effectiveness mark from 0 to 1. An example calculation for SL2 consists of the following. First, 475 and 3.75 are divided by 500 and 4 respectively. Then 0.95 and 0.938 are summed and divided by two to produce and effectiveness mark of 0.94. Table 6-10 contains the effectiveness marks for the eight comparisons where the shaded and none shaded regions again indicate the eight comparisons.

Table 6-10. Effectiveness marks for the eight comparisons of analysis I and II.

	Analysis I Marks										Analysis II Marks					
Method Designation	SL2	CH^2	SL3	CH^2	SL5	CH^2	TSAF	CH^2	Orth.	CH^2	Quad.	CH^2	SVD1	CH^2	SVD2	CH^2
Effectiveness Marks	0.94	0.98	0.72	0.98	0.97	0.98	0.44	0.98	0.23	0.98	0.60	0.97	0.59	0.97	0.57	0.97

Ascertaining that the CH^2 method for abdominal MECG cancellation had the highest scores and effectiveness marks for all eight comparisons is trivial from an inspection of Tables 6-9 and 6-10. The following discusses the major reasons for these results.

Single lead method two had lower scores and effectiveness mark compared to the CH^2 method because of failure of test condition 6. Furthermore, single lead method three also had lower scores and effectiveness mark because of failure of test condition 6 along with test condition 4. The following explains test condition 6's failures for SL2 and SL3. Since these methods detect the abdominal MECG's R waves for MECG averaging and subtraction via peak detection, a significant AECG noise spike to easily be mistaken for an MECG's R wave. If a noise spike is detected as an R wave, the spike is averaged into the MECG average creating an inaccurate estimate of the MECG complex. This estimate is then subtracted from each detected MECG complex including the noise spike. The resulting AECG has noticeable signal corruption at the time location of the noise spike. Signal corruption caused test conditions 2 and 6 to fail and clinical application 3 to be awarded no potential for Figures 6-5 and H-3. The failure of test condition 4 for SL3 can be attributed to the use of scale factors during abdominal MECG cancellation as the following explains. First, a large amount of correlation exists between the FECG's and MECG's QRS complexes during overlap. Since the scale factors are found from a correlation based operation, the FECG's overlapping QRS complex is canceled during

attenuation. Furthermore, with an FECG complex missing because of a faulty abdominal MECG cancellation algorithm, HR information derived from the resulting AECG will be misleading. Clinical application 1 therefore was graded no potential for Figures H-1 through H-4.

Single lead method five had scores and effectiveness mark close or tied with the CH^2 method's values. Intrinsic characteristic 3's rating of zero is the main reason for the lower score and effectiveness mark. User interaction at start up of SL5 is a disadvantage because the algorithm's success becomes dependent on the characteristics of the FECG-free near pure abdominal MECG complex that the user selects. The user may also have to inspect several MECG complexes before the desired complex is found which could produce a large delay at start up. This delay may be permissible if only one AECG lead position is analyzed. However, if several different AECG lead positions are experimented with to find an FECG with an acceptable SNR, the SL5 would have to be restarted for each new position created many undesired delays.

The time-sequenced adaptive filter approach for abdominal MECG cancellation had few positive results which are reflected in its scores and effectiveness mark. TSAF's engineering problems range from large signal corruption to an inability to accurately process non-ideal signals to an undesired grade for computational complexity. The poor results can be directly attributed to the design architecture of the algorithm.

Orthogonal basis had lower scores and effectiveness mark compared to the CH^2 method because of intrinsic characteristic 1 and test condition 7 as the following explains. Intrinsic characteristic 1 caused test conditions 2 and 3 to fail for Figures H-13 through H-16. The failures are from the fact that positioning the TECGs in the appropriate positions (these positions very from patient to patient) is extremely critical to achieve full abdominal MECG suppression. The TECGs of Figures H-13 through H-16 were moved slightly from the locations that full MECG cancellation could be obtained to demonstrate the little flexibility this method has for lead positioning. The result was devastating as seen in the scores and effectiveness mark. If the lead positioning had not been slightly adjusted, Orth.'s scores and effectiveness mark would have been greater than the reported values (projected engineering aspect score of 381, clinical applicability score of 3, and effectiveness mark of 0.76). However, the values would still have been below the CH^2 method's values because significant TECG noise (test condition 7) would still have been graded a failure for Figure H-16.

The three methods of analysis II had scores and effectiveness marks lower than the CH^2 method for similar reasons. These lower scores and effectiveness marks have to do with the fact

that Quad., SVD1, and SVD2 achieve abdominal MECG cancellation and FECG SNR enhancement basically simultaneously (SVD2 is not totally simultaneous, but this method will still have the same type of restrictions as Quad. and SVD1.). From simultaneous cancellation, there are some or no resulting AECGs with only the MECG suppressed. Therefore, test condition 2 was graded failure for Quad., SVD1, and SVD2 and clinical application 3 was graded no potential. Furthermore, simultaneous cancellation limits the degree of freedom or the search space for improving the FECG's SNR. This loss was capitalized by the CH^2 method in conjunction with SVD of the resulting AECGs with only the abdominal MECG attenuated. The result was an FECG that had corruption measures CM_1, CM_2, and CM_3 of greater values than those of Quad., SVD1, and SVD2 for all the data except Figures I-4 and I-5. However, since test condition 3 failed for Figures I-4 and I-5 of SVD1, the resulting signals $R_1(n)_{CH^2\&SVD}$ of the CH^2 method is much more desired than $R_4(n)_{SVD1}$ of Figure I-5. Finally, Quad. and SVD2 achieve abdominal MECG cancellation and FECG SNR enhancement without producing orthogonal fetal signals. No principal fetal signal(s) or source signal(s) could be obtained with these methods and clinical application 4 was graded no potential for Quad. and SVD2.



CONCLUSION

Dissertation Goal IV

Conclude from Dissertation Goals II & III If the CH^2 FECG System's Method for AECG MECG Cancellation is Effective

Non-invasive FECG enhancement embodies abdominal MECG cancellation and FECG SNR enhancement. The success of both is crucial for obtaining a clinically useful non-invasive FECG. As discussed in Section 1.2, the focus of this dissertation is to develop a technique for abdominal MECG cancellation and to ascertain its effectiveness. **Therefore, the effectiveness conclusions of dissertation goal four pertain to the CH^2 FECG system's method for abdominal MECG cancellation and not FECG SNR enhancement!** However, P and T wave filtering of the FECG average is introduced as an FECG SNR enhancement algorithm in Section 3.2.3 and implemented with synthesized and clinical data in Sections 5.1 and 5.2 respectively. Only the effectiveness of abdominal MECG cancellation was analyzed to keep the length of the dissertation reasonable.

Abdominal MECG cancellation was investigated in depth and the CH^2 method introduced because most of the previously reported methods (for abdominal MECG suppression) have been good academic studies, but have been ineffective (except single lead method five). The ineffectiveness is evident in the quantitative effectiveness marks of Table 6-10. Finally, the conclusions from Sections 7.1 and 7.2 indicate that the CH^2 technique for abdominal MECG cancellation is effective. Thus, the algorithm would be a reliable method to combine with an FECG SNR enhancement technique to obtain a non-invasive FECG.

7.1 Effectiveness with Synthesized and Clinical Data

The CH^2 FECG system's method for abdominal MECG cancellation generally proved to be effective with synthesized and clinical data of Chapter 5 as seen in Table 5-7. This table shows

that nine of twelve test conditions had percentage successes of 92% or greater for clinical data (The success of synthesized data is implied in the clinical data results since it was initially used to verify the effectiveness or accuracy of the DSP. See Sections 5.1 and 5.3.). However, improvements can still be made for a modulated MECG of the AECG (test condition 9) as indicated by its low percentage successes. Furthermore, test conditions 2's, 3's, and 4's percentage successes of Table 5-7 were below 100% mostly from test condition 9's failures. One possible solution for the resulting MECG residual(s) from test condition 9 is to reduce it during FECG SNR enhancement. FECG SNR Enhancement could be achieved through FECG averaging and P and T wave filtering, or the SVD of the resulting AECGs from the CH^2 technique (assuming several AECGs are available) as was done in analysis II of Chapter 6. Finally, the CH^2 method's effectiveness for abdominal MECG cancellation is further reinforced from the experimentally expected value of 12 V/V for the abdominal MECG suppression ratio.

The percentage potentials for the first two clinical applications of Table 5-8 were partially calculated based on a visual inspection for the presence or non-presence of the FECG in the AECG or resulting AECG. Since effectiveness determination is for the CH^2 method for abdominal MECG suppression and not for the visual detection of the FECG, the percentages for these two clinical applications cannot be considered (Clinical applications 1 and 2 were included to give the reader percentages for the clinical data that had a visually detectable FECG.). However, clinical application 3's percentage potentials can be used and were 88% or greater for the clinical data. Again, the major reason the percentages of clinical application 3 were not closer to 100% is from the difficulty the CH^2 method has with a modulated MECG of the AECG.

7.2 Effectiveness Compared to Eight Previous Publications

The CH^2 FECG system's method for abdominal MECG cancellation generally proved to be effective compared to eight previous publications as seen in Table 6-10. This table shows the CH^2 technique had the highest effectiveness marks (Clinical applications 2 and 3 can be used in the effectiveness analysis of Chapter 6 because synthesized data was created with a visually detectable FECG.).

The CH^2 technique had higher effectiveness marks for seven of the eight comparisons of Chapter 6. For single lead method five, the marks were similar (0.97 for SL5 and 0.98 for the CH^2 method). Since the marks were basically equal, a more focused analysis between the two

techniques would be required to determine which is most effective. To differentiate the marks, the following analysis criteria could be added to the existing analysis:

- A modulated MECG of the AECG
- Stability of single lead method five from user interaction at start up
- Computational complexity for a large number of AECGs (more than 10)
- Analyze further the stability of correlation detection of the abdominal MECG compared to triggering from the TECG.

Single lead method three utilizes scale factors for each abdominal MECG complex to improve the abdominal MECG suppression ratio (See Section 2.1.1 for a description of single lead method three.). Scale factors have also been suggested to improve MECG suppression during a modulated MECG of the AECG (test condition 9). However, there is a trade-off. The scale factors cause some of the FECG's complexes to be canceled during overlap between the FECG's and MECG's QRS complexes (See Table 6-2 test condition 4.). If the overlapping FECG complex is canceled during abdominal MECG cancellation, clinical application 1 may be compromised. Therefore, the attending physician could be mislead regarding the fetus' HR which is unacceptable. Thus, scale factors are an unsatisfactory solution for test condition 9.

The multiple lead methods (TSAF, Orth., Quad., SVD1, and SVD2) had significantly lower effectiveness marks of Table 6-10 compared to the CH^2 method. Since the CH^2 method is based on abdominal MECG averaging and subtraction and the multiple lead techniques are based on combining several ECG signals, Table 6-10's marks indicate that abdominal MECG averaging and subtraction can be more effective as opposed to combining several ECG signals for abdominal MECG cancellation. **This conclusion only applies to abdominal MECG cancellation and not FECG SNR enhancement.**

The CH^2 method was more effective compared to the multiple lead methods of analysis II of Chapter 6 as indicated by Table 6-10. To further reinforce this conclusion, the three previous publications of analysis II of Chapter 6 had corruption measures (CM_1, CM_2, and CM_3) less than the CH^2 technique in conjunction with SVD as explained in the following paragraph.

Abdominal MECG cancellation and FECG SNR enhancement are obtained with the quadratic programming and SVD method one simultaneously. Therefore, FECG SNR enhancement is going to be limited to the search space that achieves abdominal MECG

cancellation. SVD method two does not achieve abdominal MECG cancellation and FECG SNR enhancement simultaneously. However, FECG information is lost during abdominal MECG cancellation. FECG information is lost because SVD method two finds a solution space where the MECG is canceled (null space of the MECG) for some of the acquired AECGs. Usually ten or more AECGs are used to find the null space, but four or five of the resulting AECGs will not be in the null space and contain an MECG residual. Only five or six of the resulting AECGs will have the MECG suppressed. These resulting AECGs are then used in FECG SNR enhancement. Since all FECG information from the 10 AECGs is unlikely to be projected to the four or five resulting AECGs during MECG cancellation, FECG information is lost and FECG SNR enhancement becomes restricted for SVD method two. The CH^2 method in conjunction with SVD avoids restraints from abdominal MECG cancellation. By suppressing the abdominal MECG in each AECG first and then calculating the SVD of the resulting AECGs, FECG SNR enhancement is no longer restricted. Therefore, FECG SNR enhancement via the CH^2 technique combined with SVD produced an FECG signal with better corruption measures compared to Quad., SVD1, and SVD2. Finally, from the above discussion for quadratic programming and SVD method one, another conclusion can be made. Abdominal MECG cancellation and then FECG SNR enhancement sequentially will most likely produce a more favorable results as compared to doing both operations simultaneously.

7.3 Future Research

Future research will include developing an approach for acquiring AECG signals with a favorable FECG's SNR (visually detectable FECG) along with FECG SNR enhancement. Other ongoing research includes applying the CH^2 method for MECG cancellation to signals obtained via an intrauterine catheter electrode that is placed invasively inside the uterus, but is non-invasive to the fetus. This electrode can be used immediately before delivery to give physicians an alternate and possibly a safer means of obtaining an FECG as compared to the scalp electrode (invasive to the mother and fetus).

A portable and battery powered system was built as shown in Figure 7-1 to reduce space and transport difficulties required by the CH^2 FECG system. This system contains an analog front-end to amplify the invasive (intrauterine or scalp electrode) or non-invasive AECG and TECG. The outputs of the analog electronics are digitized (ADC card plugs into the laptop's PCMCIA slot) and the signals are processed by the laptop.

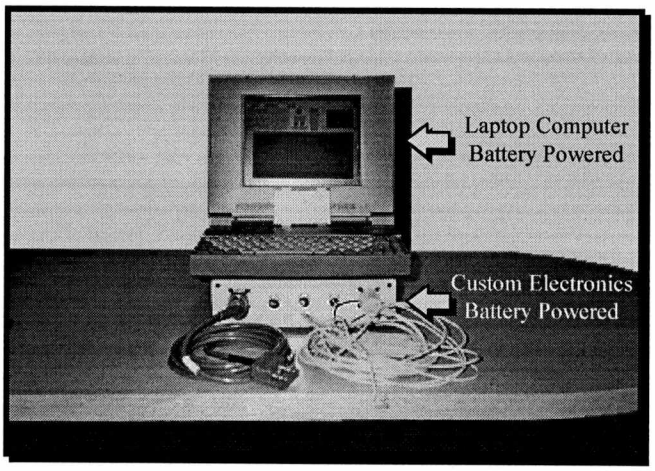

Figure 7-1. A photo of the invasive intrauterine catheter FECG monitoring system.

REFERENCES

REFERENCES

[1] Deans, A. C. and Steer, P. J., "The use of the fetal electrocardiogram in labour," *Brit. J. Obst. & Gynaec.*, vol. 101, pp. 9-17, 1994.

[2] Abboud, S. and Sadeh, D. "Power spectrum analysis of fetal heart rate variability using the abdominal maternal electrocardiogram," *J. Biomed. Eng.*, vol. 12, pp. 161-164, 1990.

[3] Ferrazzi, E, Pardi, G., Setti, P. L., Rodolfi, M., Civardi, S., and Cerutti, S., "Power spectral analysis of the heart rate of the human fetus at 26 and 36 weeks of gestation," *Clin. Phys. Physiol. Meas.*, vol. 10, suppl. B, pp. 57-60, 1989.

[4] Greene, K. R., "The ECG waveform," *Bailliere's Clin. Obst. & Gyn.*, vol. 1, no. 1, pp. 131-155, 1987.

[5] Jenkins, H. M. L., Symonds, E. M., Kirk, D. L., and Smith, P. R., "Can fetal electrocardiography improve the prediction of intrapartum fetal acidosis?," *Brit. J. Obst. Gynaec.*, vol. 93, pp. 6-12, 1986.

[6] Karin, J., Hirsch, M., Sagiv, C., and Akselrod, S., "Fetal ANS activity by spectral analysis of HR variations," *Proceedings of Computers in Cardiology*, pp. 479-482, 1992.

[7] Kendall, B., Farell, D. M., Kane, H. A., and van Ostrand, J. R., "Detection of fetal distress by the abnormal fetal radioelectrocardiogram," *Am. J. Obst. & Gynec.*, vol. 90, no. 3, pp. 340-344, 1964.

[8] Lilja, H., Greene, K. R., Karlsson, K., and Rosen, K. G., "ST waveform changes of the fetal electrocardiogram during labour-A clinical study," *Brit. J. Obst. Gynaec.*, vol. 92, pp. 611-617, 1985.

[9] Nageotte, M. P., Freeman, R. K., Freeman, A. G., and Dorchester, W., "Short-term variability assessment from abdominal electrocardiogram during the antepartum period," *Am. J. Obst. Gynec.*, vol. 145, no. 5, pp. 566-569, 1983.

[10] Pardi, G., Ferrazzi, E., Cetin, I., Rampello, S., Baselli, G., Cerutti, S., and Civardi, S., "The clinical relevance of the abdominal fetal electrocardiogram," *J. Perinat. Med.*, vol. 14, pp. 371-377, 1986.

[11] Rosen, K. G., "Alterations in the fetal electrocardiogram as a sign of fetal asphxia-experimental data with a clinical implementation," *J. Perinat. Med.*, vol. 14, pp. 355-363, 1986.

[12] Nagel, J. H., "Progresses in fetal monitoring by improved data acquisition," *IEEE Eng. Med. & Biol. Mag.*, vol. 3, pp. 9-13, 1984.

[13] Bergveld, P., Kölling, A. J., and Peuscher, J. H. J., "Real-time fetal ECG recording," *IEEE Trans. Biomed. Eng.*, vol. 33, no. 5., pp. 505-509, 1986.

[14] Callaerts, D., DeMoor, B., Vandewalle, J., Sansen,W., Vantrappen, J., and Janssens, J., "Comparison of SVD methods to extract the foetal electrocardiogram from cutaneous electrode signals," *Med. & Biol. Eng. & Comput.*, vol. 28, pp. 217-224, 1990.

[15] Vanderschoot, J., Callaerts, D., Sansen, W., Vandewalle, J., Vantrappen, G., and Janssens, J., "Two methods for optimal MECG elimination and FECG detection from skin electrode signals," *IEEE Trans. on Biomed. Eng*, vol. 34, no. 3, pp. 233-243, 1987.

[16] Whitfield, C. R., "A source of diagnostic error in fetal electrocardiography," *Am. J. Obst. Gynec.*, vol. 95, no. 5, pp. 669-675, 1966.

[17] Adam, D. and Shavit, D., "Complete foetal ECG morphology recording by synchronized adaptive filtration," *Med. & Biol. Eng. & Comput.*, vol. 28, pp. 287-292, 1990.

[18] Kennedy, E., *Operational Amplifier Circuits Theory and Applications.* Holt, Rinehart, and Winston, Inc., New York, 1987, ch. 4, pp. 116-156.

[19] Carter, M. C., Gunn, P., and Beard, R. W., "Fetal heart rate monitoring using the abdominal fetal electrocardiogram," *Br. J. Obstet. Gynaecol.*, vol. 87, pp. 396-401, 1980.

[20] Oldenburg, J. T. and Macklin, M., "Changes in the conduction of the fetal electrocardiogram to the maternal abdominal surface during gestation," *Am. J. Obst. Gynec.*, vol. 129, no. 4, pp. 425-433, 1977.

[21] Saini,V. D. and Maulik, D., "Computerized detection of low-level fetal signals in the maternal abdominal electrocardiogram," *Comput. Biol. Med.*, vol. 15, no. 2, pp. 81-93, 1985.

[22] Oostendorp, T. F. and van Oosterom, A., "Electrical properties of tissues involved in the conduction of foetal ECG," *Med. & Biol. Eng. & Comput.*, vol. 27, pp. 322-324, 1989.

[23] Oostendorp, T. F., van Oosterom, A., and, Jongsma, H. W., "The fetal ECG throughtout the second half of gestation," *Clin. Phys. Physiol. Meas.*, vol. 10, no. 2, pp 147-160, 1989.

[24] Oostendorp, T. F., van Oosterom, A., and Jongsma, H. W., "The effect of changes in the conductive medium on the fetal ECG throughout gestation," *Clin. Phys. Physiol. Meas.*, vol. 10, pp. 11-20, 1989.

[25] Oostendorp, T. F., van Oosterom, A., Jongsma, H. W., and van Dongen, P. W. J., "The potential distribution generated by the fetal heart at the maternal abdomen," *J. Perinat. Med.*, vol. 14, pp. 435-444, 1986.

[26] van Oosterom, A., "Lead systems for the abdominal fetal electrocardiogram," *Clin. Phys. Physiol. Meas.*, vol. 10, pp. 21-26, 1989.

[27] Jenkins, H. M. L., "Technical progress in fetal electrocardiograph-A Review," *J. Perinat. Med.*, vol. 14, pp. 365-370, 1986.

[28] Goodlin, R. C., "History of fetal monitoring," *Am. J. Obst. & Gynec.*, vol. 133, no. 3, pp. 323-352, 1979.

[29] Cameron, M. D., "Fetal electrocardiography: A survey of the literature," *Develop. Med. Child Neurol.*, vol. 9, pp 329-337, 1967.

[30] Shenker, L., "Fetal electrocardiography," *Obst.l and Gynec.l Survey*, vol. 21, pp. 367-388, 1966.

[31] Caughey, A. F., "Electronic detection of fetal life," *Obst. and Gynec.*," vol. 17, no. 3, pp. 382-391, 1961.

[32] Bernstine, R. L. and Borkowski, W. J., "Prenatal fetal electrocardiography," *Am. J. Obst. & Gynec.*, vol. 70, no. 3, pp. 631-638, 1955.

[33] Schuler, G., "Low-noise, interference-resistance amplifier suitable for biological signals," *Science*, vol. 154, no. 2, pp. 1191-1192, 1966.

[34] Buxton, T. M., Hsu, I., and Barter, R. H., "Fetal electrocardiography a study of 254 patients using a preamplifier and a standard electrocardiograph, *JAMA*, vol. 185, no. 6, pp. 441-444, 1963.

[35] Hon, E. H., "Instrumentation of fetal heart rate and fetal electrocardiography II. A vaginal electrode," *Am. J. Obst. & Gynec.*, vol. 86, no. 6, pp. 772-784, 1963.

[36] Hon, E. H., "Instrumentation of fetal heart rate and fetal electrocardiography," *Obst. & Gyn.*, vol. 30, no. 2, pp. 281-286, 1967.

[37] Organ, L. W., "Scalp lead fetal electrocardiography," *Canad. Med. Ass. J.*, vol. 98, pp. 199-204, 1968.

[38] Berard, M. J., Katz, L., and Uner, E., "Fetal cardiotachomerty," Am. J. *Obst. & Gynec.*, vol. 100, no. 4, pp. 472-482, 1968.

[39] La Croix, G. E., "Fetal electrocardiography in labor: A new scalp electrode," *Michigan Medicine*, pp. 976-979, 1968.

[40] Paul, R. H. and Hon, E. H., "Endoscopic examination of fetal scalp and fetal electrocardiography value of lateral position," *Obstet. & Gynecol.*, vol. 35, no. 1, pp. 111-113, 1970.

[41] Eisenberg De Smoler, P. and Karchmer, S., "Four leads in fetal electrocardiography," *Am. J. Obstet. Gynecol.*, vol. 112, no. 2, pp. 239-245, 1972.

[42] Paul, R. H. and Hon, E. H., "Clinical fetal monitoring IV. Experience with a spiral electrode," *Obstet. & Gynecol.*, vol. 41, no. 5, pp. 777-780, 1973.

[43] Westgate, J., Keith, R. D. F., Curnow, J. S. H., Ifeachor, E. C., and Greene, K. R., "Suitability of fetal scalp electrodes for monitoring the fetal electrocardiogram during labour," *Clin. Phys. Physiol. Meas.*, vol. 11, no. 4., pp. 297-306, 1990.

[44] Sachs, B. P., Abitbol, M. M., Cho, G., and Acker, D., "New multipronged fetal scalp electrode: A preliminary report," *Obstet. & Gynecol.*, vol 128, no. 3, 1985.

[45] Hon, E. H. and Hess, O. W., "Instrumentation of fetal electrocardiography," *Science*, vol. 125, pp. 553-554, 1957.

[46] Hon, E. H. and Lee, S. T., "Noise reduction in fetal electrocardiography II. Averaging techniques," *Am. J. Obst. & Gynec.*, vol. 87, no. 8, pp. 1086-1096, 1963.

[47] Hon, E. H., "Noise reduction in fetal electrocardiography," *Medical Arts and Sciences*, Fourth Quarter, pp. 120-123, 1961.

[48] Favret, A. G. and Caputo, A. F., "Evaluation of autocorrelation techniques for detection of the fetal electrocardiogram," *IEEE Trans. Biomed. Eng.*, vol. 13, no. 1, pp. 37-43, 1966.

[49] Goddard, B. A., Newell, J. A., Edwards, R. L., and Farr, R. F., "A clinical foetal electrocardiograph," *Med. & Biol. Eng.*, vol. 4, pp. 159-167, 1966.

[50] Widrow, B., Glover, J. R., McCool, J. M., Kaunitz, J., Williams, C. S., Hearn, R. H., Zeidler, J. R., Dong, E., and Goodlin, R. C., "Adaptive noise cancelling: Principles and applications," *Proc. IEEE*, vol. 63, no. 12, pp. 1692-1716, 1975.

[51] Longini, R. L., Reichert, T. A., Yu, J. M. C., and Crowley, J. S., "Near-orthogonal basis functions: A real time fetal ECG technique," *IEEE Trans. Biomed. Eng.*, vol. 24, no. 1, pp. 39-43, 1977.

[52] Bergveld, P. and Meijer, J. H. W., "A new technique for the suppression of the MECG," *IEEE Trans. Biomed. Eng.*, vol. 28, no. 4, pp. 348-354, 1981.

[53] Ferrara, E. R. and Widrow, B., "Fetal electrocardiogram enhancement by time-sequenced adaptive filtering," *IEEE Trans. Biomed. Eng.*, vol 29, no. 6, pp. 458-460, 1982.

[54] Randall N. J., Steer, P. J., and Sutherland, I. A., "Detection of the fetal ECG during labour by an intrauterine probe," *J. Biomed. Eng.*, vol. 10, pp. 159-164, 1988.

[55] Strong, T. H., Paul, R. H., Park, G. D., Cheng, Y., Lewis, D. E., McCart, D. F., Mueller, E. A., "The intrauterine probe electrode," *Am. J. Obstet. Gynecol.*, vol. 164, pp.1233-1234, 1991.

[56] Riggs, T., Isenstein, B., and Thomas, C., "Spectral analysis of the normal ECG in children and adults," *J. Electrocardiol.*, vol. 12, no. 4, pp. 377, 1979.

[57] Hon, E. H. and Hess, O. W., "The clinical value of fetal electrocardiography," *Am. J. Obst. & Gynec.*, vol. 79, no. 5, pp. 1012-1023, 1960.

[58] Caughey, A. F. and Krohn, L. H., "Variation in the fetal electrocardiogram with period of gestation," *Am. J. Obst. Gynec.*, vol. 87, no. 4, pp. 525-528, 1963.

[59] Teteris, N. J., "Variation in the fetal electrocardiogram with period of gestation," *Am. J. Obst. Gynec.*, vol. 88, no. 7, pp. 982-983, 1964.

[60] Plonsey, R., *Bioelectric Phenomena*. McGraw-Hill, New York , 1969.

[61] van Oosterom, A., "Spatial filtering of the fetal electrocardiogram," *J. Perinat. Med.*, vol. 14, pp. 411-419, 1986.

[62] Wheeler, T., Murrills, A., and Shelley,T., "Measuring of the fetal heart rate during pregnancy by a new electrocardiographic technique," *Brit. J. Obst. & Gynaec.*, vol. 85, pp. 12-17, 1978.

[63] Favret, A. G. and Marchetti, A., "Fetal electrocardiographic wave forms from abdominal-wall recording," *Obst. & Gynec.*, vol. 27, no. 3, pp. 355-362, 1966.

[64] Favret, A. G., "Computer matched filter location of fetal R-waves," *Med. & Biol. Eng.*, vol. 6, pp. 467-475, 1968.

[65] Cerutti, S., Baselli, G., Civardi, S., Ferrazzi, E., Marconi, A. M., Pagani, M., and Pardi, G., "Variability analysis of fetal heart rate signals as obtained from abdominal electrocardiographic recordings," *J. Perinat. Med.*, vol. 14, pp. 445-452, 1986.

[66] Karin, J., Hirsch, M., and Akselrod, S., "An estimate of fetal autonomic state by spectral analysis of fetal heart rate fluctuations," *Pediatric Research*, vol. 34, no. 2, pp. 134-138, 1993.

[67] Akselrod, S., Karin, J., and Hirsch, M., "Computerized detection of fetal ECG from maternal abdominal signal," *Proceedings of Computers in Cardiology*, pp. 261-264, 1987.

[68] Woolfson, M. S., Peasgood, W., Sahota, D. S., and Crowe, J. A., "Signal processing of the fetal electrocardiogram," *J. Electrocardiol.*, vol. 23, pp. 51-57, 1990.

[69] Abboud, S. and Beker, A., "An improved algorithm in fetal electrocardiography," *J. Electrocardiol.*, vol. 22, pp. 238-242, 1989.

[70] Abboud, S., Barkai, G., Mashiach, S., and Sadeh, D., "Quantification of the fetal electrocardiogram using averaging technique," *Comput. Biol. Med.*, vol. 20, no. 3, pp. 147-155, 1990.

[71] Abboud, S., Alaluf, A., Einav, S., and Sadeh, D., "Real-time abdominal fetal ECG recording using a hardware correlator," *Comput. Biol. Med.*, vol. 22, no. 5, pp. 325-335, 1992.

[72] Kendall, B., Amoss, D. C., Sun, H. H., Hahn, A. W., and Farrell, D. M., "The noise-free electrocardiogram recorded from the maternal abdomen," *Am. J. Obst. & Gynec.*, vol. 97, no. 8, pp. 1129-1134, 1967.

[73] Offner, F. and Moisand, B., "A coincidence technique for fetal electrocardiography," *Am. J. Ost. Gynec.*, vol. 95, no. 5, pp. 676-680, 1966.

[74] Sureau, C. and Trocellier, R., "Etude de quelques problems techniques en electrocardiographie foetale," *Med. Electron Biol. Eng.*, vol. 1, pp. 181-188, 1963.

[75] Walden, W. D. and Birnbaum, S. J., "Fetal electrocardiology with cancellation of maternal complexes," *Am. J. Obst. & Gynec.*, vol. 94, no. 4, pp. 596-598, 1966.

[76] Horner, S. L., *Genetic Algorithms and Non-invasive FECG Enhancement*. M.S. Thesis, University of Tennessee, Knoxville, Tennessee, December 1991.

[77] Horner, S. L., Holls, W. M., and Crilly, P. B., "Non-invasive fetal electrocardiograph enhancement," *Proceedings of Computers in Cardiology*, pp. 163-166, 1992.

[78] Widrow, B. and Stearns, S., *Adaptive Signal Processing*. Prentice-Hall, Englewood Cliffs, New Jersery, 1985, ch. 12, pp. 334-337.

[79] Iyer, V. K., Ploysongsang, Y., and Ramamoorthy, P. A., "Adaptive filtering in biological signal processing," *Critical Reviews in Biomedical Engineering*, vol. 17, no. 6, pp. 531-584, 1990.

[80] Mazzeo, J. R., "Non-invasive fetal electrocardiography," *Medical Progress through Technology*, vol. 20, pp. 75-79, 1994.

[81] Thaler, I., Shavit, D., and Adam, D., "Correlating fetal doppler cardiography and maternal abdominal electrocardiography," *Fetal and Neonatal Physiological Measurement III*, pp. 193-199, 1989.

[82] Ferrara, E. R. and Widrow, B., "The time-sequenced adaptive filter," *IEEE Trans. Acoustics, Speech, and Signal Processing*, vol. 29, no. 3, pp. 679-683, 1981.

[83] Matthews, M. B., *The Time-Sequenced Adaptive Filter: An Application to Electrocardiogram Signal Estimation*. M.S. Thesis, University of Washington, Seattle, Washington, December 1985.

[84] Ferrara, E. R., *The Time-sequenced Adaptive Filter*. Ph.D. Dissertation, Stanford University, Stanford, California, December 1977.

[85] Pan, J. and Tompkins, W. J., "A real-time QRS detection algorithm," *IEEE Trans. Biomed. Eng.*, vol. 32, no. 3, pp. 230-236, 1985.

[86] Ferrara, E. R. and Widrow, B., "Multichannel adaptive filtering for signal enhancement," *IEEE Transactions on Acoustics, Speech, and Signal Processing*, vol. 29, no. 3, pp. 766-770, 1981.

[87] Reichert, T. A., Longini, R. L., Crowley, J. S., and Yu, J. M., "A non-invasive extraction of the fetal electrocardiogram," *Computers & Biomed. Research*, vol. 10, pp. 1-7, 1977.

[88] Frank, T. H., Blaumanis, O. R., Chen, S. H., Petrie, R. H., Gibbs, R. K., Wells, R. L., and Johnson, T. R. B., "Noninvasive fetal ECG mode fetal heart monitoring by adaptive digital filering," *J. Perinat. Med.*, vol. 20, pp. 93-100, 1992.

[89] Frank, T. H., Blaumanis, O. R., Gibbs, R. K., and Wells, R. K., "Adaptive filtering in ECG monitoring of the fetal heart rate," *J. Electrocardiol.*, pp. 108-113, 1987.

[90] den Exter, T. H., van Eykern, L.A., de Kreek, J., Mulder, E. J. H., Peuscher, J. H. J., and Visser, G. H. A., "Simultaneous recording of fetal ECG and uterine activity by transcutaneous abdominal electrodes; A new way for non-invasive cadiotocography?," *Fetal and Neonatal Physiological Measurement III*, pp. 185-191, 1989.

[91] Kunzi, H. P., Krelle, W., Oettli, W., and Levin, F., *Nonlinear Programming*. Blaisdell Publishing Company, Waltham, Massachusetts, 1966, ch. 5, pp. 78-84.

[92] Meijer, W. J. H. and Bergveld, P., "The simulation of the abdominal MECG," *IEEE Trans. Biomed. Eng.*, vol. 28, no. 4, pp. 354-357, 1981.

[93] Callaerts, D., Sansen, W., and Vandewalle, J., "Real-time fetal ECG extraction," *Proceedings of the IEEE Engineering Medicine and Biology Conference*, vol. 12, no. 3, pp. 1056-1057, 1990.

[94] Callaerts, D., Sansen, W., Vandewalle, J., Vantrappen, G., and Janssens, J., "Description of a real-time system to extract the fetal electrocardiogram," *Clin. Phys. Physiol. Meas.*, vol. 10, suppl. B, pp. 7-10, 1989.

[95] Callaerts, D., Vandershoot, J., Vandewalle, J., Sansen, W., Vantrappen, G., and Janssens, J., "An adaptive on-line method for the extraction of the complete fetal electrocardiogram from cutaneous multilead recordings," *J. Perinat. Med.*, vol. 14, pp. 421-433, 1986.

[96] van Oosterom, A. and Alsters, J., "Removing the maternal component in the fetal ECG using singular value decomposition," *Proceedings of the 10th International Congress on Electrocardiology*, pp. 171-176, 1983.

[97] Vanderschoot, J., Vantrappen, G., Janssens, J., Vandewalle, J., and Sansen, W., "A reliable method for fetal ECG extraction from abdominal recordings," *Proceedings of Sixth International Conference on Analysis and Optimization of Systems*, pp. 249-254, 1984.

[98] Vanderschoot, J., Vandewalle, J., Janssens, J., Sansen, W., and Vantrappen, G., "Extraction of weak bioelectrical signals by means of singular value decomposition," *JL Lions: Analysis and Optimization of Systems Lectures Notes in Control and Information Sciences*, vol. 63, pp. 434-448, 1984.

[99] Vanderschoot, J., Vandewalle, J., Janssens, J., Sansen, W., and Vantrappen, G., "An application of sigular value decomposition to the extraction of weak bioelectrical signals," *Revue HF XII*, pp. 253-258, 1983.

[100] Forsythe, G. E., Malcolm, M.A., and Moler, C. B., *Computer Methods for Mathematical Computations*. Prentice-Hall, New York, 1977, ch. 9, pp. 192-239.

[101] Wilkinson, J. H. and Reinsch, C., *Linear Algebra*. Springer-Verlag, New York, 1971, pp. 134-151.

[102] Schuler, G., Puddicombe, P., and Park, G., "Fetal ECG improvement due to selective signal addition," *Am. J. Obst. & Gynec.*, vol. 101, no. 8, pp. 1120-1123, 1968.

[103] Hon, E. H. and Lee, S. T., "Averaging techniques in fetal electrocardiography," *Med. Electron. Biol. Eng.*, vol. 2, pp. 71-76, 1964.

[104] Oldenburg, J. T. and Macklin, M., "Processing the abdominal fetal ECG," *IEEE Trans. Biomed. Eng.*, vol. 24, no. 6, pp. 501-507, 1977.

[105] Phoenix, R. G., Crowe, J. A., Gibson, N. M., Peasgood, W., Woolfson, M. S., and Faulkner, T. R., "The application of finite impulse response filters to the detection of fetal electrocardiogram signals," *Medical Progress through Technology*, vol. 19, pp. 89-103, 1993.

[106] Rhyne, V. T., "A digital system for enhancing the fetal electrocardiogram," *IEEE Trans. Biomed. Eng.*, vol. 16, no. 1, pp. 80-86, 1969.

[107] Rhyne, V. T., "Digital signal enhancement of the fetal electrocardiogram," *Am. J. Obst. & Gynec.*, vol. 102, no. 4, pp. 549-555, 1968.

[108] Tal, Y. and Akselrod, S., "A new method for fetal ECG detection," *Computers & Biomedical Research*, vol. 24, pp. 296-306, 1991.

[109] van Bemmel, J. H., Peeters, L., and Hengeveld, S. J., "Influence of the maternal ECG on the adbominal fetal ECG complex," *Am. J. Obst. & Gynec.*, vol. 102, no. 4, pp. 556-562, 1968.

[110] Webster, J.G., *Medical Instrumentation Application and Design*. Boston, Mass: Houghton Mifflin, 1978, ch.5, pp. 236-241.

[111] Cicinelli, E., Bortone, A., Carbonara, I., Incampo, G., Bochicchio, M., Ventura, G., Montanaro, S., and Aloisio, G., "Improved equipment for abdominal fetal electrocardiogram recording: description and clinical evaluation," *International Journal of Bio-Medical Computing*," vol. 35, pp. 193-205, 1994.

[112] Horner, S. L., Holls, W. M., and Crilly, P. B., "A Robust real-time algorithm for enhancing a non-invasive fetal electrocardiogram," *Digital Signal Processing: A Review Journal*, vol. 5, no. 3, pp. 184-194, 1995.

[113] Horner, S. L., Holls, W. M., and Crilly, P. B., "A non-invasive and invasive fetal electrocardiogram real-time monitoring system," *Proceedings of Computers in Cardiology*, pp. 417-420, 1994.

[114] Horner, S. L., Holls, W. M., and Crilly, P. B., "A real-time system for monitoring a non-invasive and invasive FECG," *Proceedings of the International Conference on Signal Processing Applications and Technology*, pp. 204-209, 1994.

[115] Burbank, D.P. and Webster, J.G., "Reducing skin potential motion artifact by skin abrasion," *Med. & Biol. & Comput.*, vol. 16, pp. 31-38, 1978.

[116] Burns, R., "Study of skin impedance," *Electronics*, pp. 190-196, 1950.

[117] Gatzke, R. D., *Biomedical Electrode Technology: Theory and Practice*. Academic Press, New York, 1974, pp. 99-116.

[118] Geddes, L.A. and Baker, L.E., *Principles of Applied Biomedical Instrumentation*. John Wiley & Sons, New York, 1989, ch 9, pp. 370-372.

[119] Tam, H.W. and Webster, J.G., "Minimizing electrode motion artifact by skin abrasion," *IEEE Trans. Biomed. Eng.*, vol. 24, no. 2, 1977.

[120] Gray, P., and Meyer, G., *Analysis and Design of Analog Integrated Circuits*. Wiley, New York, 1993, ch. 11, pp. 715-784.

[121] Motchenbacher, C. and Fitchen, F., *Low-Noise Electronic Design*. Wiley, New York, 1973, ch7. ch. 12, ch. 14, pp. 119-137, pp. 217-259, pp. 273-305.

[122] Leeming, M. N., Ray, C., and Howland, W. S., "Low-Voltage Direct-Current Burns," *JAMA*, vol. 214, no. 9, pp. 1681-1684, 1970.

[123] Sedra, A., and Smith, K. *Microelectronic Circuits*. Holt, Rinehart, and Winston, Inc., New York, 1987, ch. 6, ch. 8-9, pp. 261-328, pp. 398-547.

[124] Leach, W. M., "Fundamentals of Low-noise Analog Circuit Design," Proceedings of the IEEE, vol. 82, no. 10, pp. 1514-1538, 1994.

APPENDICES



ECG WAVEFORM DESCRIPTION

An ECG is the summation of all the action potentials of the cardiac muscle measured at the skin surface. One heart beat corresponds to an ECG complex. Figure A-1 presents an example of an ECG complex where the waveform consists of an P wave, QRS complex, and T wave. Each part of the ECG complex originates from different parts of the heart labeled in Figure A-2. The P wave is associated with atrial depolarization which starts at the sinoatrial node (SA) and propagates through the right and then left atriums. Atrial depolarization is demonstrated with the shaded area in Figure A-3(a) where the arrows indicate the depolarization direction from the SA node. Finally, Figure A-3(b) indicates through shading the depolarization of right and left atriums.

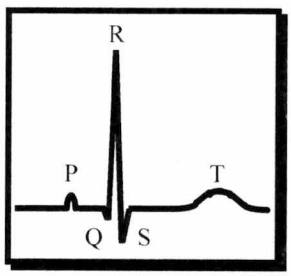

Figure A-1. An example ECG complex for one heart beat.

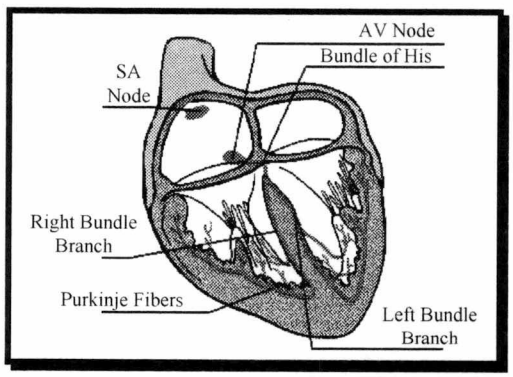

Figure A-2. The parts of the heart that are associated with the ECG complex.

The time between the P wave deflection and the start of the Q wave of the QRS complex is from the atrialventricular (AV) node. This node takes a long time for the action potentials to depolarize the area from the cells having small diameters. The delay allows extra blood to be pumped from the atriums into the ventricles before they contract. Next, the action potentials then



(a) (b)

Figure A-3. Propagation of action potentials through the right and left atriums that result in the P wave of the ECG complex. (a) Depolarization of the right atrium originating from the SA node. (b) Depolarization of both atriums that results in the P wave.

move down the bundle of His and split into the right and left bundle branches. At the end of each bundle, the action potentials distribute further through the Purkinje fibers of the right and left ventricles which causes the ventricles to depolarize. Depolarization starts at the bottom of the ventricles as indicated in Figure A-4(b) with the small shaded regions around the Purkinje fibers. Then depolarization spreads through the rest of the ventricles as shown in Figure A-4(b) with shading. The QRS complex is produced from the depolarization of the two ventricles. Finally, the T wave is from the ventricles repolarizing. Atrial repolarization occurs after the P wave deflection, but is not visible in the ECG waveform since the signal is small in amplitude.



(a) (b)

Figure A-4. Propagation of action potentials between the atriums and ventricles that result in the QRS complex of the ECG waveform. (a) Depolarization of the ventricles starting at the Purkinje fibers. (b) Depolarization of both ventricles that results in the QRS complex.

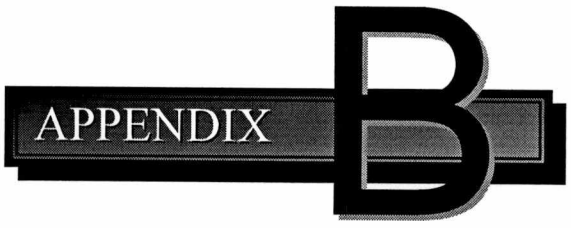

PATENT, HUMAN STUDIES COMMITTEE APPROVALS, AND PATIENT SIGNATURE FORM

US005372139A

United States Patent [19]

Holls et al.

[11] Patent Number: 5,372,139

[45] Date of Patent: Dec. 13, 1994

[54] **METHOD FOR SUPPRESSING A MATERNAL ELECTROCARDIOGRAM SIGNAL FROM A FETAL ELECTROCARDIOGRAM SIGNAL OBTAINED WITH INVASIVE AND NON-INVASIVE TECHNIQUES USING AN ALMOST PURE MATERNAL ELECTROCARDIOGRAM SIGNAL AS A TRIGGER**

[75] Inventors: **William M. Holls**, Knox; **Steven L. Horner**, Davidson, both of Tenn.

[73] Assignee: **Paul Benjamin Crilly**, Knoxville, Tenn.

[21] Appl. No.: **96,669**

[22] Filed: **Jul. 26, 1993**

Related U.S. Application Data

[63] Continuation-in-part of Ser. No. 719,377, Jun. 24, 1991, abandoned.

[51] Int. Cl.[5] **A61B 5/02**

[52] U.S. Cl. **128/698**; 128/708

[58] Field of Search 128/696, 698, 708, 700, 128/701

[56] **References Cited**

U.S. PATENT DOCUMENTS

4,456,959	6/1984	Hirano et al.	364/417
4,519,396	5/1985	Epstein et al.	128/698
4,569,356	2/1986	Kyoznka	128/698
4,573,479	3/1986	Tuccillo	128/698
4,781,200	11/1988	Baker	128/670
4,945,917	8/1990	Akselrod et al.	128/696
4,951,680	8/1990	Kirk et al.	128/698
4,961,428	10/1990	Nikias et al.	128/699
4,974,598	12/1990	John	128/696

OTHER PUBLICATIONS

Widrow, Glover, et al, "Adaptive Noise Canceling: Principals and Applications", *Proc. of the IEEE*, vol. 63, No. 12, Dec. 1975, pp. 1692–1716.

D. Adam and D. Shavit, "Complete Fetal ECG Morphology Recording by Synchronized Adaptive Filtration", *Med. & Biol. Eng. & Comput.*, vol. 28, pp. 287–292, Jul. 1990.

E. R. Ferrara and B. Widrow, "Fetal Electrocardiogram Enhancement by Time Sequences Adaptive Filtering," *IEEE Trans. Biomed. Eng.*, vol. BME-29, No. 6, pp. 458–460, Jun. 1982.

R. L. Longini, T. A. Reichert, J. M. C. Yu, and J. S. Cromley, "Near Orthogonal Basis Function: A Real Time Fetal ECG Technique", *IEEE Trans. on Biomedical Eng.*, vol. BME-24, No. 1, pp. 39–43, Jan. 1977.

(List continued on next page.)

Primary Examiner—William E. Kamm
Assistant Examiner—Scott M. Getzow
Attorney, Agent, or Firm—Pitts and Brittian

[57] **ABSTRACT**

A method (**10**) for suppressing the maternal electrocardiograph (MECG) signal from a composite abdominal ECG including an MECG signal, an fetal ECG (FECG) signal and noise to obtain a substantially MECG-free FECG trace. The method (**10**) of the present invention includes the placement of a plurality of electrodes (**26**) about the periphery of the mother to detect a substantially pure MECG (**12**) and a composite MECG+FECG signal (**14**). A scalp electrode (**32A**), which is invasive to the fetus (**72**), and an intrauterine catheter electrode (**32B**), which is non-invasive to the fetus (**72**), may be alternately used to detect the signal (**14**), both electrodes (**32A,32B**) being invasive to the mother. A preprocessor (**34**) converts the signals (**12,14**) obtained by the individual electrodes (**26,32A,32B**) attached to, or invasive to, the mother (**70**) into appropriate electrical or digital signals for MECG suppression, and selectively performs a filtering operation to remove noise and other distortions. The MECG suppression is achieved by using a substantially pure MECG trace (**12**) as a trigger signal to calculate an MECG complex template (**18**) which is subtracted from the composite signal (**14**) using the MECG trace (**12**) to align the MECG complex template (**18**) with each MECG complex (**16**) in the composite signal (**14**).

18 Claims, 5 Drawing Sheets

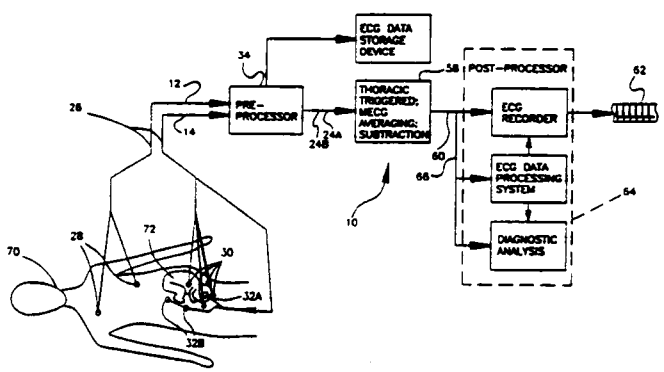

THE UNIVERSITY OF TENNESSEE
MEDICAL CENTER AT KNOXVILLE

• University Memorial Hospital
• Graduate School of Medicine

Office of Institutional Review Board
1924 Alcoa Highway
Knoxville 37920-6999
(615) 544-9781

January 15, 1993

William Holls, M.D.
Department of OB/GYN
The University of Tennessee Medical Center
at Knoxville
1924 Alcoa Highway
Knoxville, Tennessee 37920

RE: IRB Protocol #0335 - **"Prenatal EKG Determination"**

Dear Dr. Holls:

Thank you for submitting the modified version of the above referenced protocol, "Prenatal EKG Determination."

This constitutes full approval of your proposal. Any alterations in the protocol must be promptly reported to the Institutional Review Board. In addition, annual reapproval is required, and it is the responsibility of the investigator to initiate said request for approval.

You have individual responsibility for reporting to the Board in the event of adverse occurrences.

Sincerely,

Joseph E. Fuhr, Ph.D., Chairman
Institutional Review Board

JEF:tll

THE UNIVERSITY OF TENNESSEE
KNOXVILLE

Research Administration
Compliances
Grants & Contracts
Research Advancement
404 Andy Holt Tower
Knoxville, Tennessee 37996-0140
(615) 974-3466
FAX (615) 974-2805

04/23/93

CRP # 4079 B

Title: "Prenatal EKG Determination"

Holls, Dr. William
OB/GYN
1924 Alcoa Hwy.
1924 Alcoa Hwy.

Crilly, Dr. Paul Benjamin
Electrical Engineering
314 Ferris Hall
Campus

Your project listed above was reviewed. It qualified for expedited review and has been approved.

This approval is for a period ending one year from the date of this letter. Please make timely submission of renewal or prompt notification of project termination (see item #3 below).

Responsibilities of the investigator during the conduct of this project include the following:

1. To obtain prior approval from the Committee before instituting any changes in the project.

2. To retain signed consent forms from subjects for at least three years following completion of the project.

3. To submit a Form D to renew approval, to report changes in the project or to report termination at 12-month or less intervals.

The Committee wishes you every success in your research endeavor.

Sincerely,

Edith M. Szathmary
Coordinator of Compliances

cc: Dr. Joseph Googe
406 Ferris Hall

PERMISSION TO MEASURE ABDOMINAL FETAL ECG

Just as in the adult the fetal electrocardiogram (ECG) can be a measure of health. The strength of the ECG is low so it can be difficult to pick up. This is an attempt to improve the ability to measure the fetal ECG. I the undersigned here by acknowledge my permission to undergo measurement of abdominal ECG. This will entail utilizing a skin cleansing agent to clean a number of areas of the skin on my abdomen and place conventional EKG electrodes. Though a conventional skin cleansing agent will be used, there may possibly be some irritation at the surface of the skin and with the placement of the EKG electrodes. This is not anyway any different than with placement anywhere else on my body. The device for measuring the fetal EKG consist of a conventional EKG monitor with all the appropriate safeguards present for a commercial machine. Incorporated in this system is a small battery-powered device to amplify the signal from the electrodes placed on my abdomen. This poses no danger to me or my fetus as the maximum voltage is that of a flash light. Both the amplifier and the EKG equipment passed hospital review for electrical safety.

The actual measurement will entail placing EKG electrodes on my chest and abdomen to measure the electrical activity of my heart and measure the electrode activity of the fetus on my abdomen. The duration of the study will be approximately 30 minutes. Should I have any questions concerning the study, the principal investigator, Dr. William Holls, will be available for questions. I can withdraw from this study at any time. Participation or non-participation in this study does not effect any other medical care I may receive and the results will not be used for my care.

I understand that I am not waiving any legal rights or releasing the hospital or its agents from liability for negligence. I understand that in the event of physical injury resulting from the research procedures, the University of Tennessee does not have funds budgeted for compensation either for lost wages or for medical treatment. Therefore, the University does not provide reimbursement for such injuries.

I have read and understand these statements. I give my permission to be part of this study. I also give my permission for the doctor who is doing this study to look at and to use the information from my chart. I will not be identified by name in any aspect of this study's publication.

If you have questions or want to know what is learned from the study, you may contact Dr. Holls.

Dr. William M. Holls, III
Phone (615) 544-9300
Address: The University of Tennessee Medical Center
Department of Obstetrics and Gynecology
1924 Alcoa Highway, Box U-27
Knoxville, TN 337996-2700

_____
Patient/date

_____
Witness/date



ONE BLOCK CLINICAL DATA

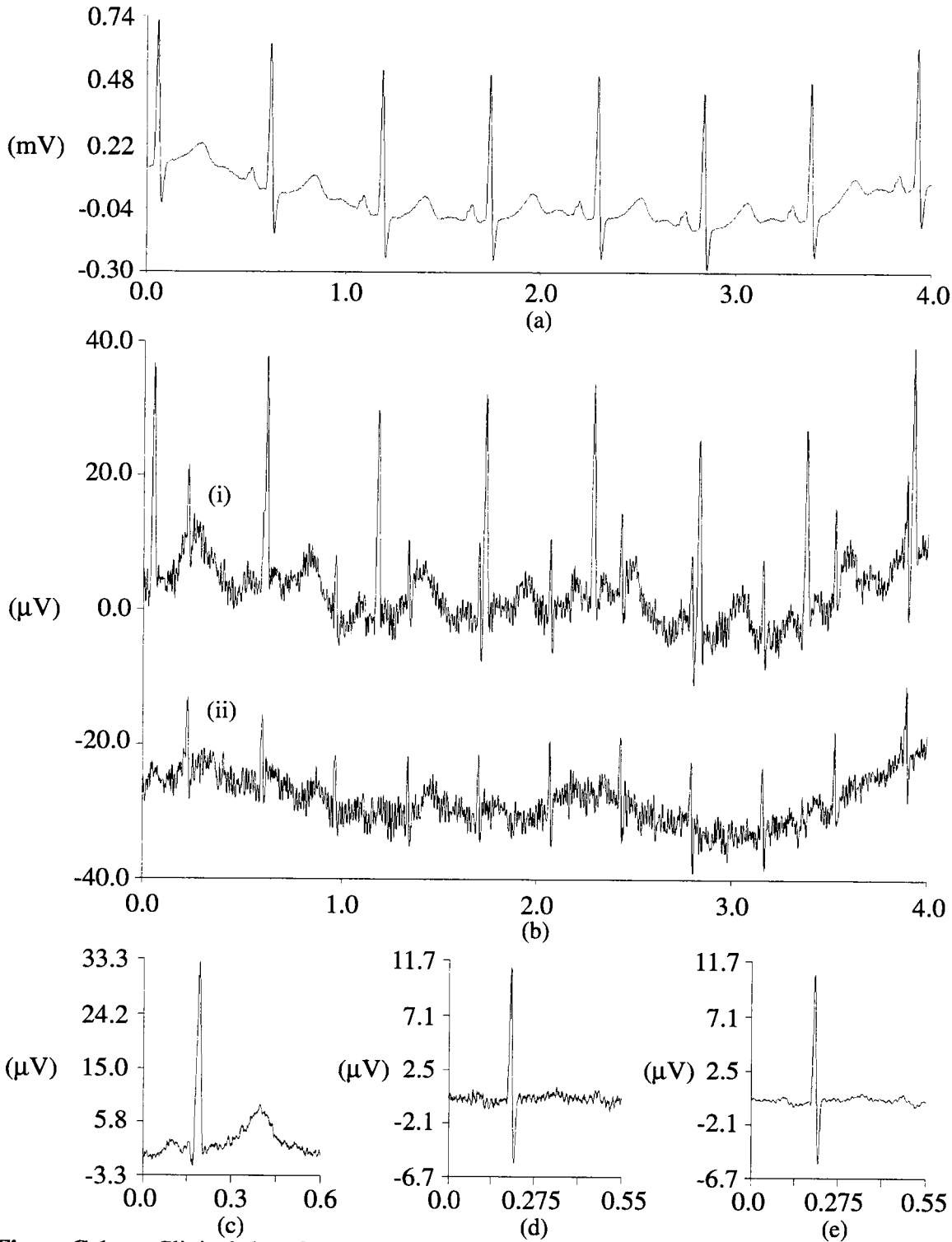

Figure C-1. Clinical data from patient 3 at 23 weeks of gestation (all x-axes in seconds). (a) TECG. (b)(i) AECG. (b)(ii) AECG with the MECG canceled. (c) Abdominal MECG average (28 complexes averaged). (d) FECG average (40 complexes averaged). (e) Filtered FECG average (P wave - f_{cutoff} = 25.0 Hz and T wave - f_{cutoff} = 25.0 Hz).

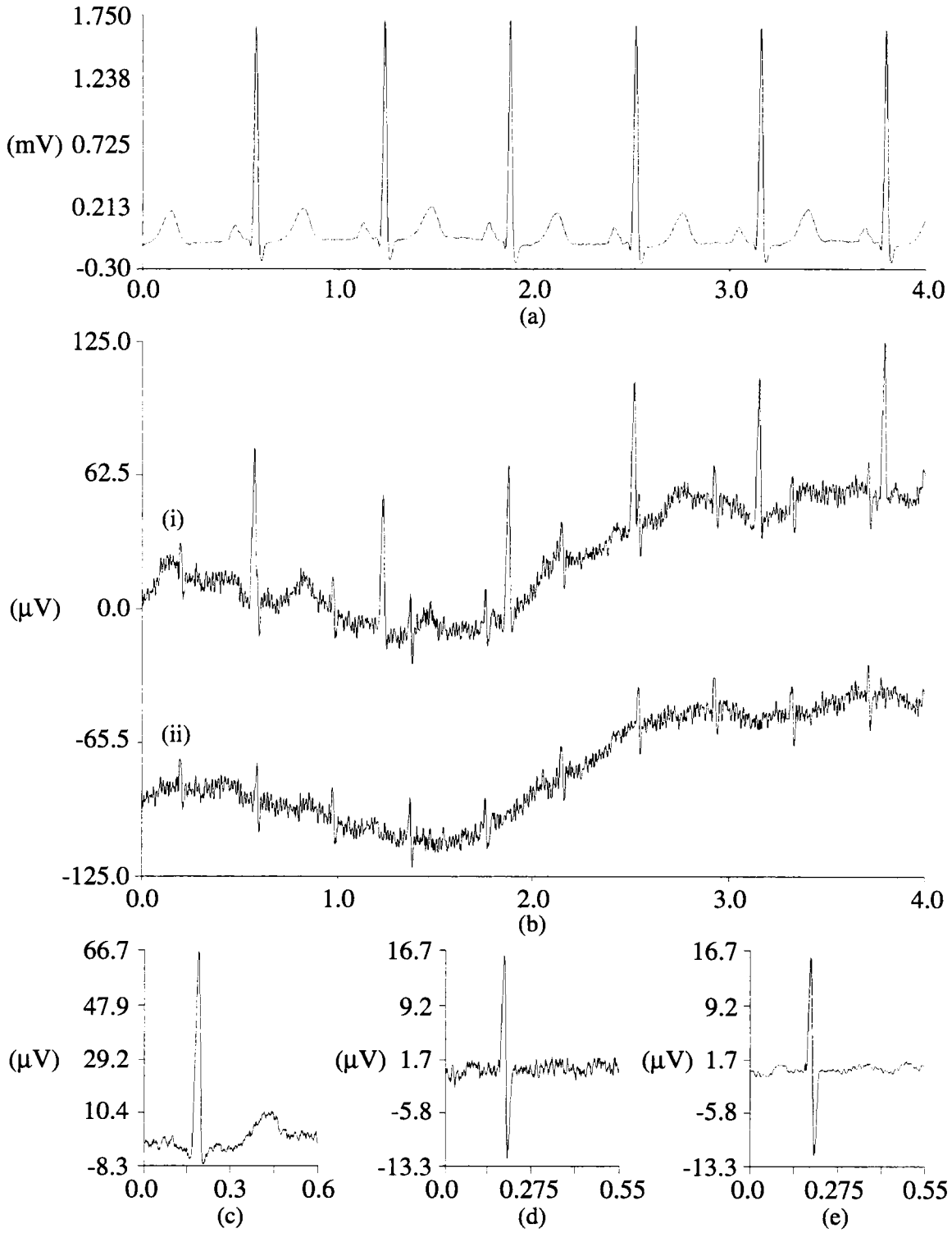

Figure C-2. Clinical data from patient 3 at 24 weeks of gestation (all x-axes in seconds). (a) TECG. (b)(i) AECG. (b)(ii) AECG with the MECG canceled. (c) Abdominal MECG average (21 complexes averaged). (d) FECG average (33 complexes averaged). (e) Filtered FECG average (P wave - f_{cutoff} = 20.0 Hz and T wave - f_{cutoff} = 20.0 Hz).

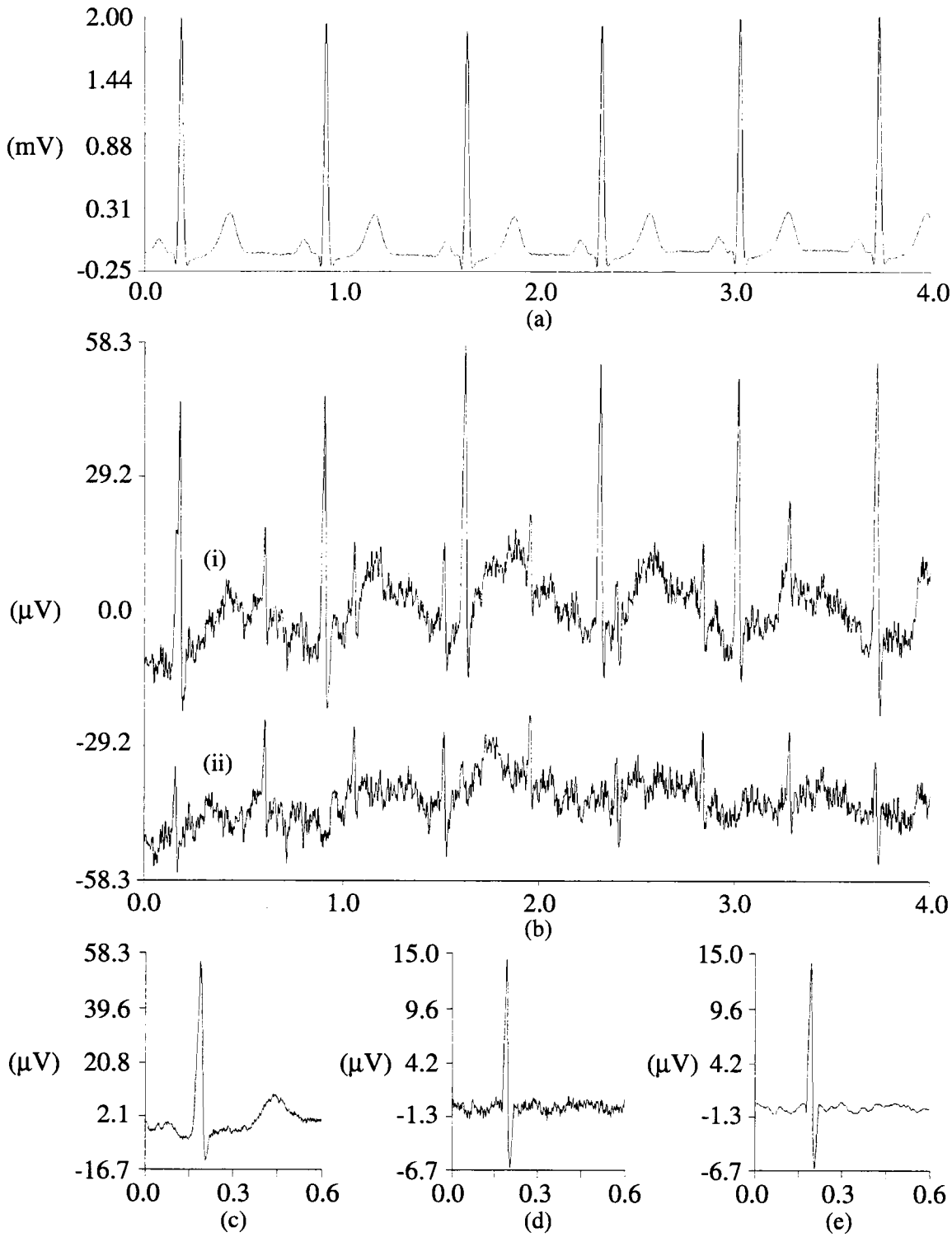

Figure C-3. Clinical data from patient 3 at 25 weeks of gestation (all x-axes in seconds). (a) TECG. (b)(i) AECG. (b)(ii) AECG with the MECG canceled. (c) Abdominal MECG average (28 complexes averaged). (d) FECG average (40 complexes averaged). (e) Filtered FECG average (P wave - f_{cutoff} = 30.0 Hz and T wave - f_{cutoff} = 30.0 Hz).

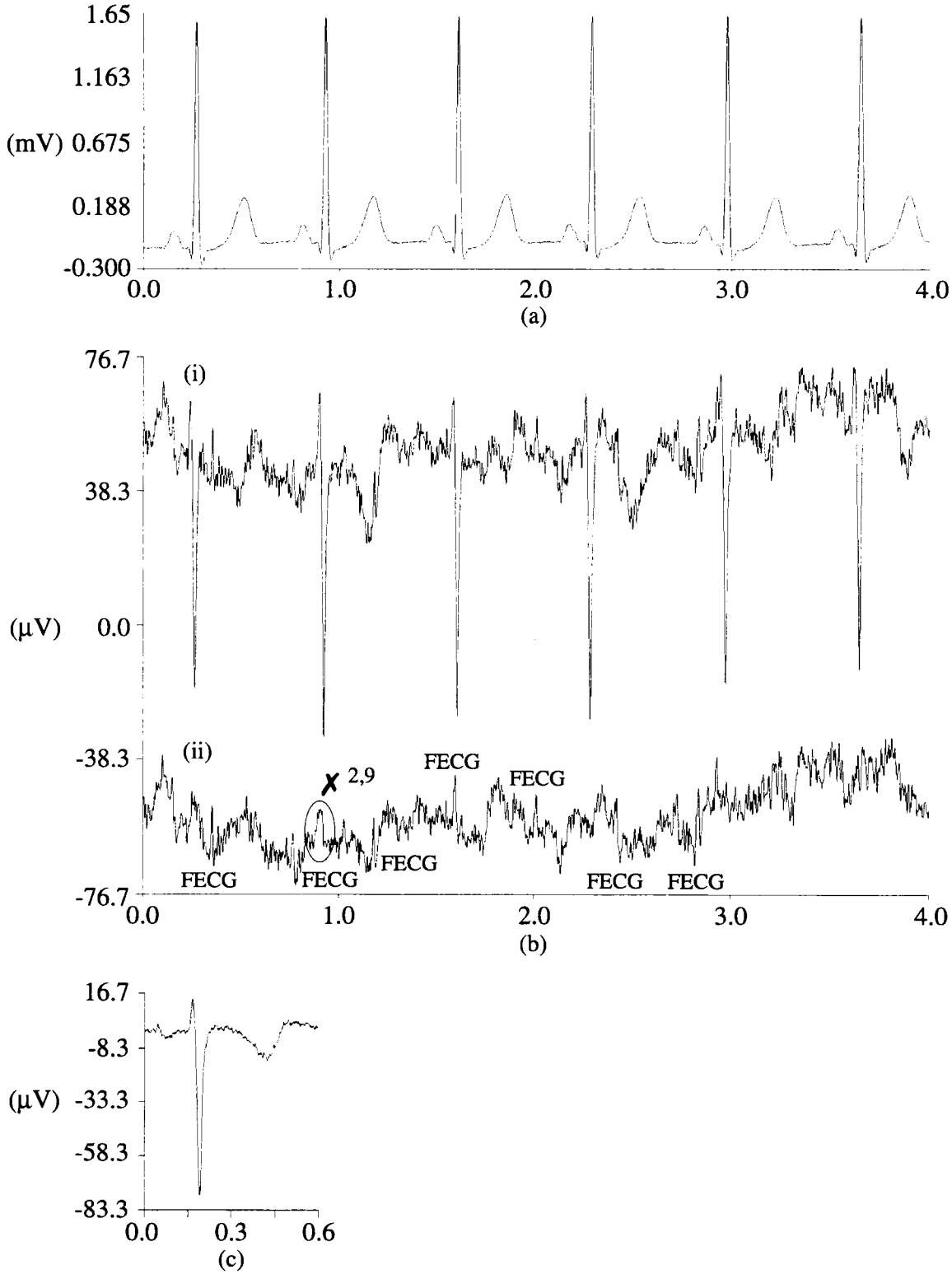

Figure C-4. Clinical data from patient 3 at 26 weeks of gestation (all x-axes in seconds). (a) TECG. (b)(i) AECG. (b)(ii) AECG with the MECG canceled. (c) Abdominal MECG average (26 complexes averaged).

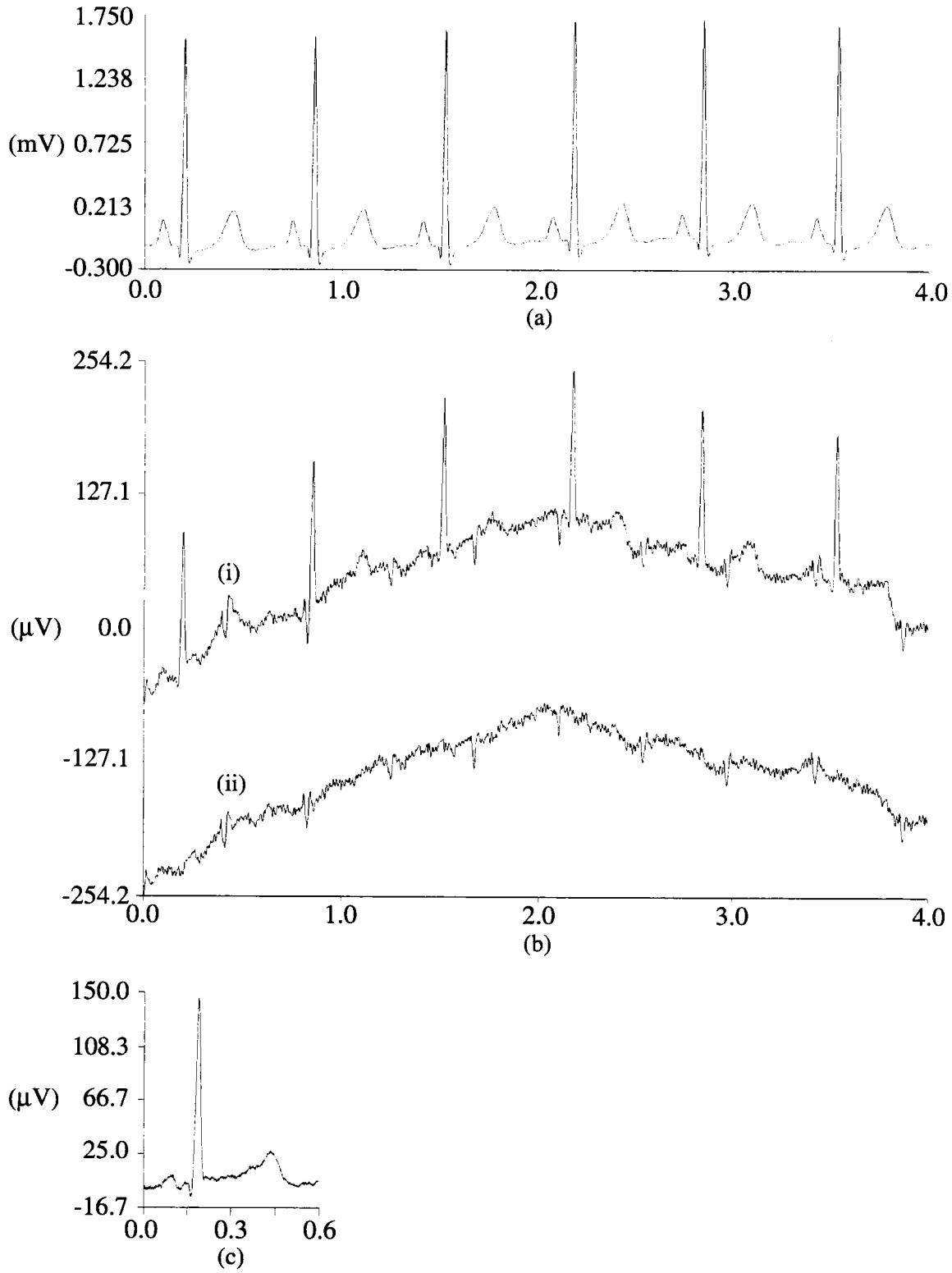

Figure C-5. Clinical data from patient 3 at 31 weeks of gestation (all x-axes in seconds). (a) TECG. (b)(i) AECG. (b)(ii) AECG with the MECG canceled. (c) Abdominal MECG average (21 complexes averaged).

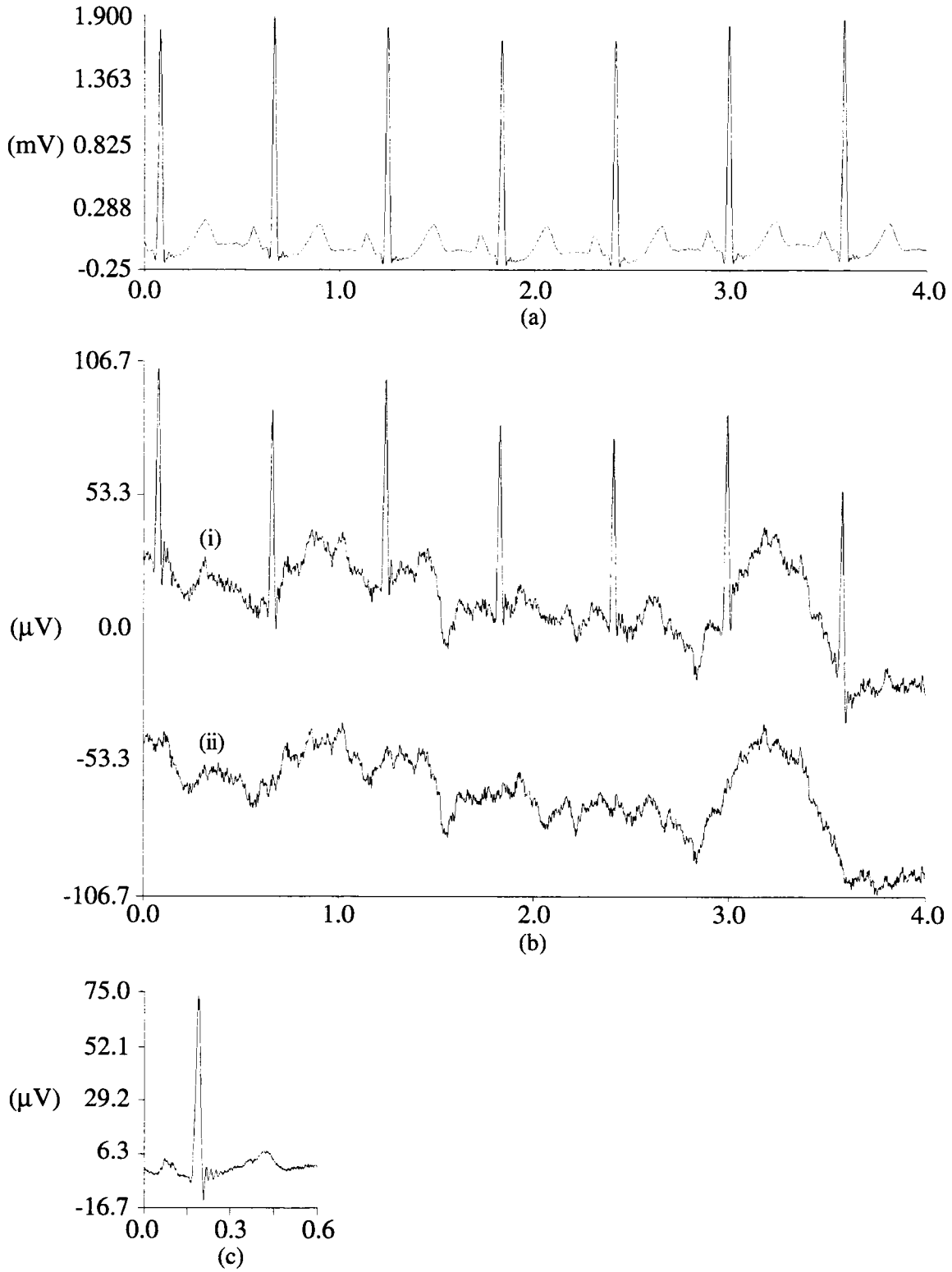

Figure C-6. Clinical data from patient 3 at 33 weeks of gestation (all x-axes in seconds). (a) TECG. (b)(i) AECG. (b)(ii) AECG with the MECG canceled. (c) Abdominal MECG average (25 complexes averaged).

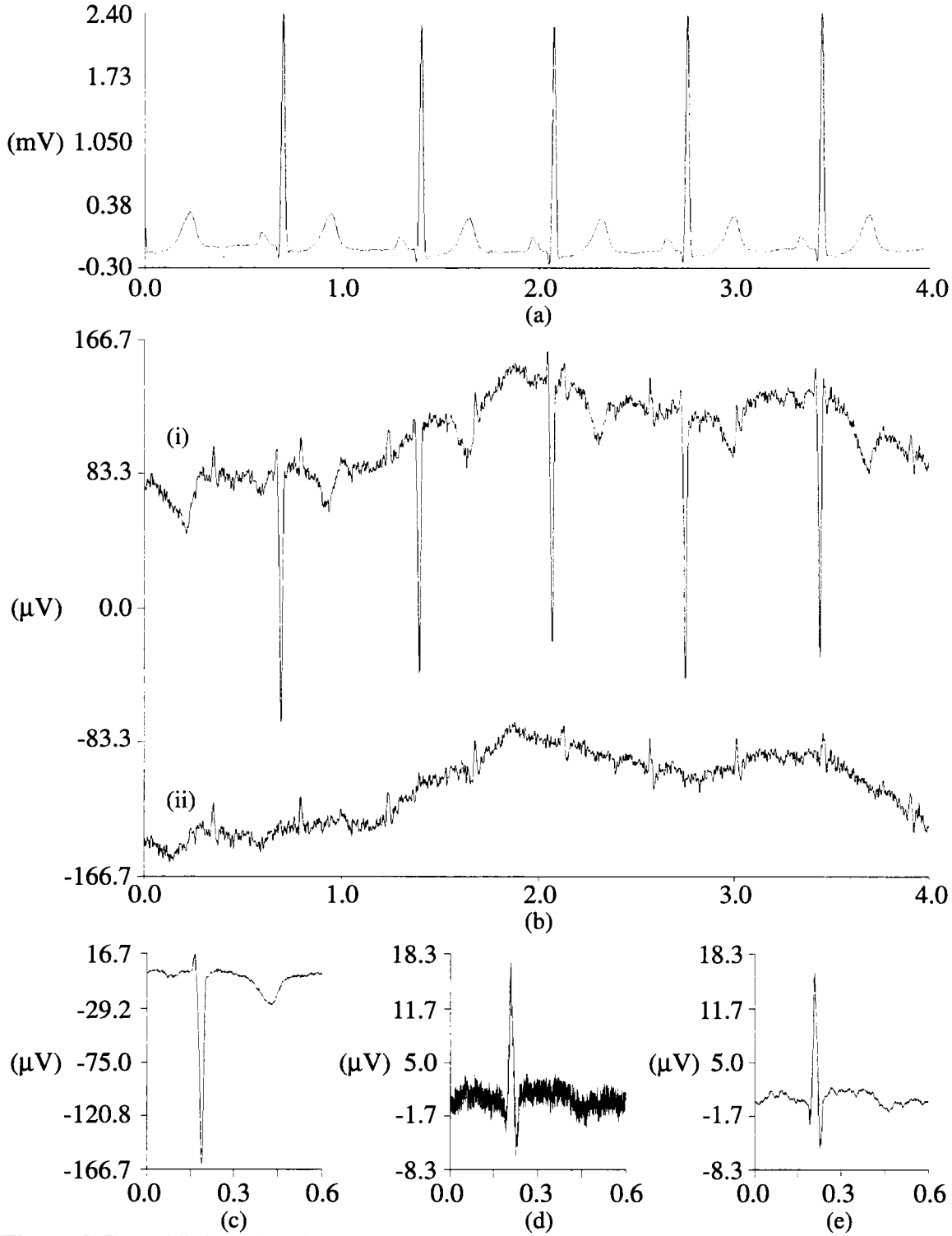

Figure C-7. Clinical data from patient 3 at 35 weeks of gestation (all x-axes in seconds). (a) TECG. (b)(i) AECG. (b)(ii) AECG with the MECG canceled. (c) Abdominal MECG average (30 complexes averaged). (d) FECG average (42 complexes averaged). (e) Filtered FECG average (P wave - f_{cutoff} = 30.0 Hz and T wave - f_{cutoff} = 30.0 Hz).

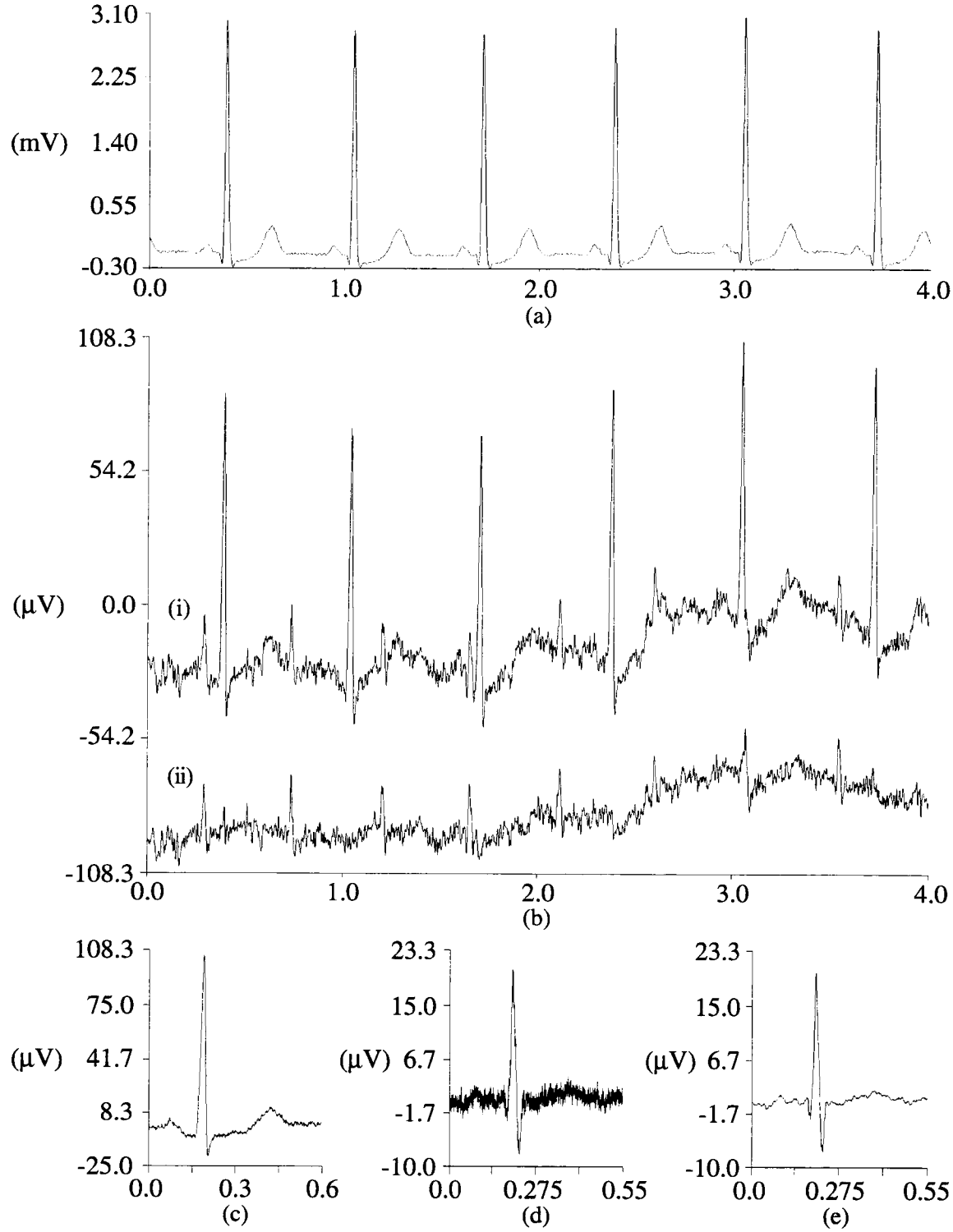

Figure C-8. Clinical data from patient 3 at 36 weeks of gestation (all x-axes in seconds). (a) TECG. (b)(i) AECG. (b)(ii) AECG with the MECG canceled. (c) Abdominal MECG average (30 complexes averaged). (d) FECG average (42 complexes averaged). (e) Filtered FECG average (P wave - f_{cutoff} = 25.0 Hz and T wave - f_{cutoff} = 25.0 Hz).

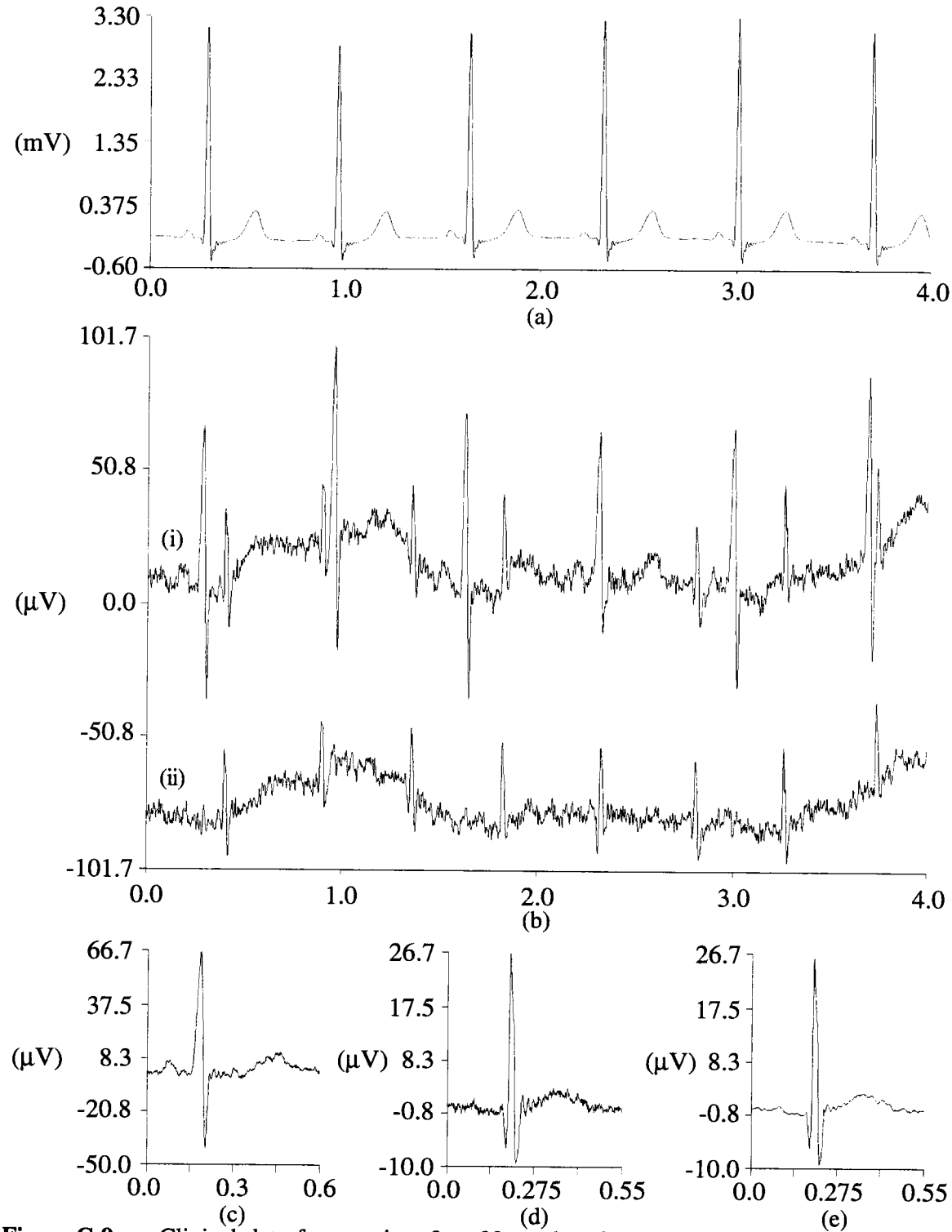

Figure C-9. Clinical data from patient 3 at 38 weeks of gestation (all x-axes in seconds). (a) TECG. (b)(i) AECG. (b)(ii) AECG with the MECG canceled. (c) Abdominal MECG average (24 complexes averaged). (d) FECG average (33 complexes averaged). (e) Filtered FECG average (P wave - f_{cutoff} = 35.0 Hz and T wave - f_{cutoff} = 35.0 Hz).

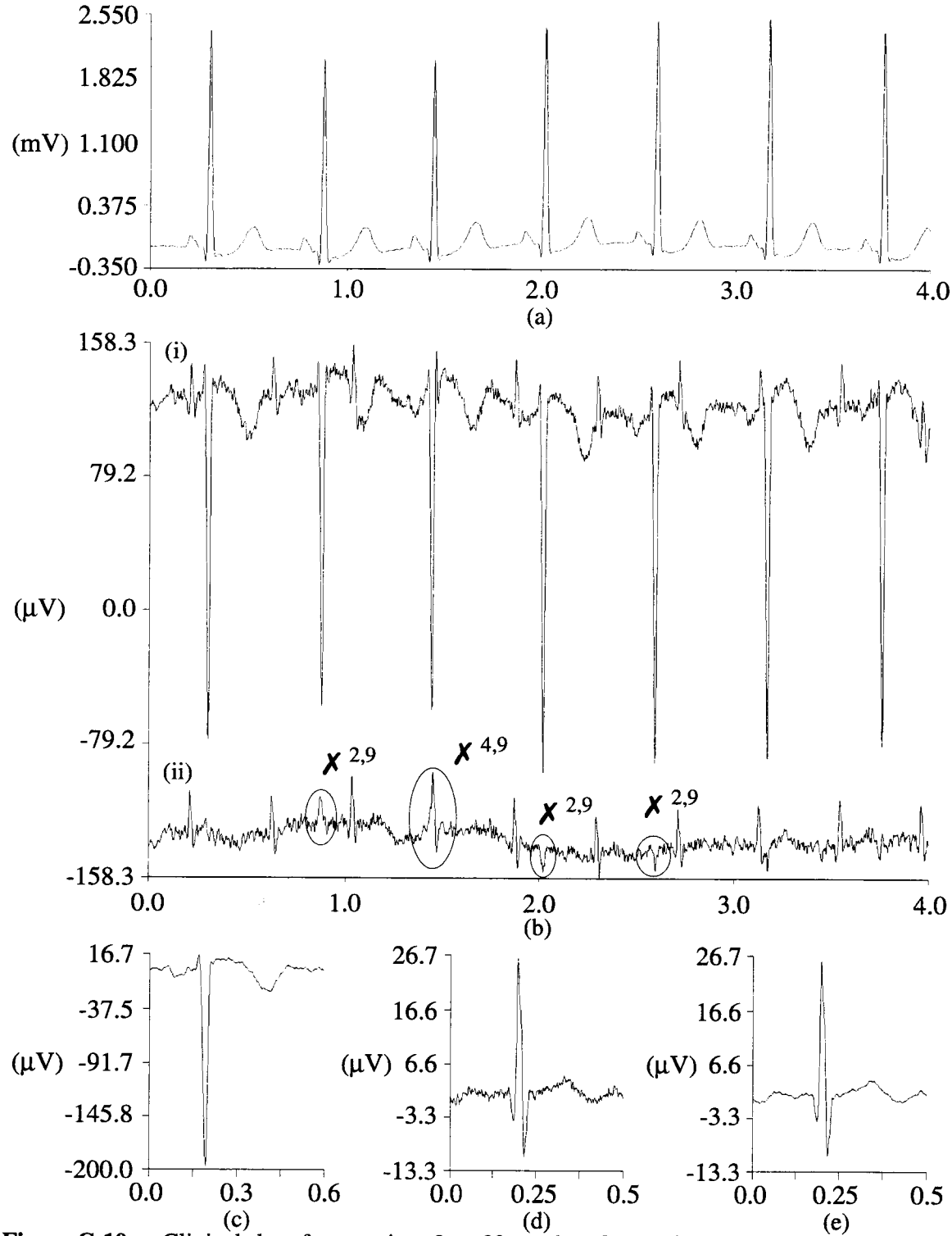

Figure C-10. Clinical data from patient 3 at 39 weeks of gestation (all x-axes in seconds). (a) TECG. (b)(i) AECG. (b)(ii) AECG with the MECG canceled. (c) Abdominal MECG average (27 complexes averaged). (d) FECG average (38 complexes averaged). (e) Filtered FECG average (P wave - f_{cutoff} = 35.0 Hz and T wave - f_{cutoff} = 35.0 Hz).

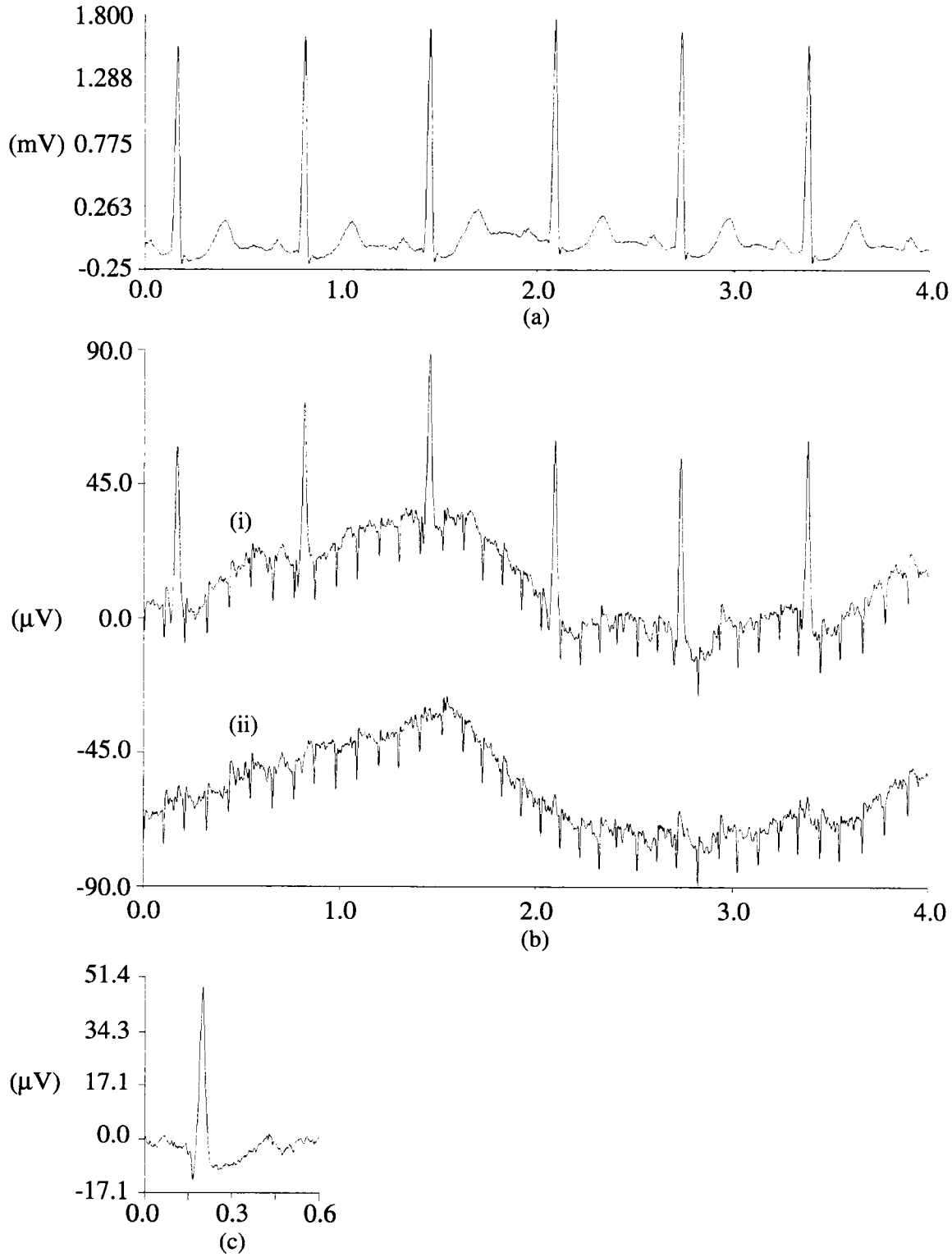

Figure C-11. Clinical data from patient 16 at 36 weeks of gestation (all x-axes in seconds). (a) TECG. (b)(i) AECG. (b)(ii) AECG with the MECG canceled (The high rate periodic spikes are not R waves of the FECG, but EMG). (c) Abdominal MECG average (23 complexes averaged).

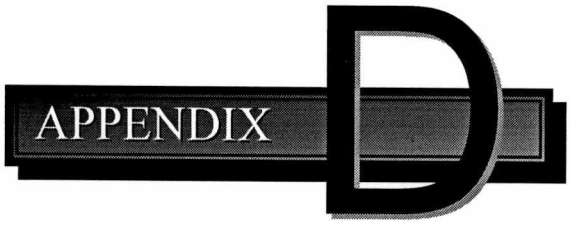

CONTINUOUS CLINICAL DATA

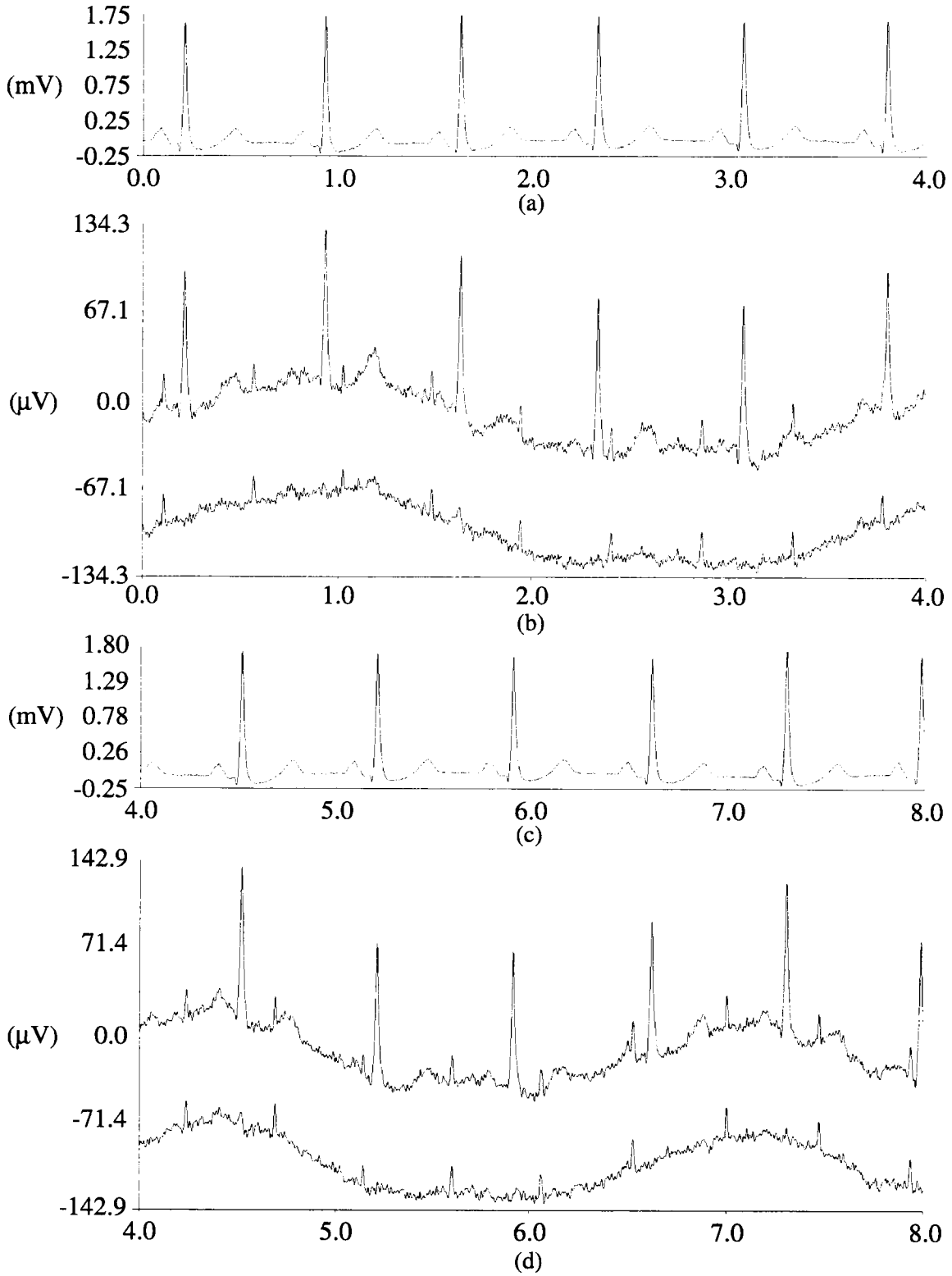

Figure D-1. A demonstration of continuous AECG MECG cancellation from 0.0 to 8.0 seconds (all x-axes in seconds). (a) TECG. (b) AECG and AECG with the MECG canceled. (c and d) Same as (a) and (b), but 4.0 seconds latter.

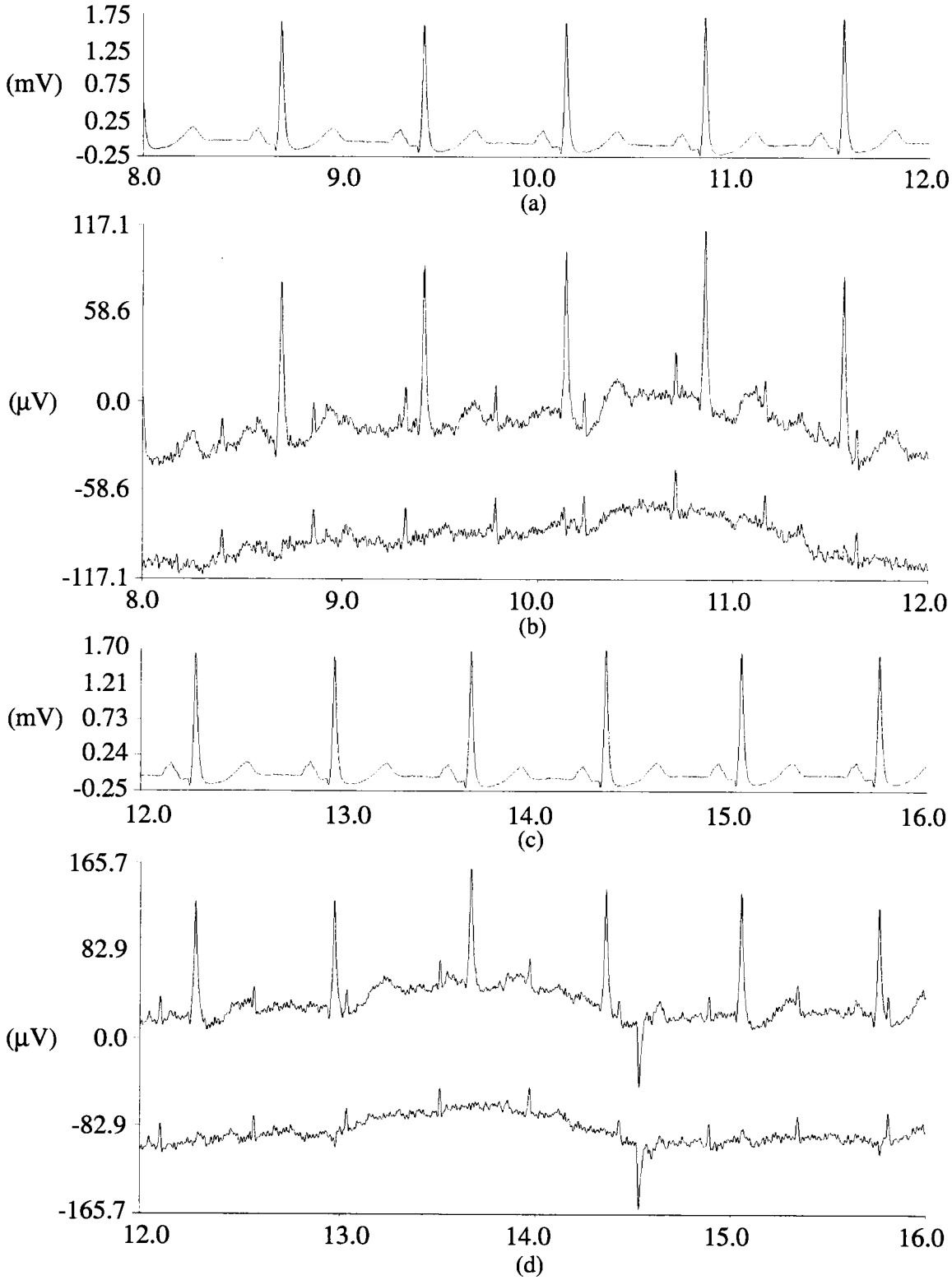

Figure D-2. A demonstration of continuous AECG MECG cancellation from 8.0 to 16.0 seconds (all x-axes in seconds). (a) TECG. (b) AECG and AECG with the MECG canceled. (c and d) Same as (a) and (b), but 4.0 seconds latter.

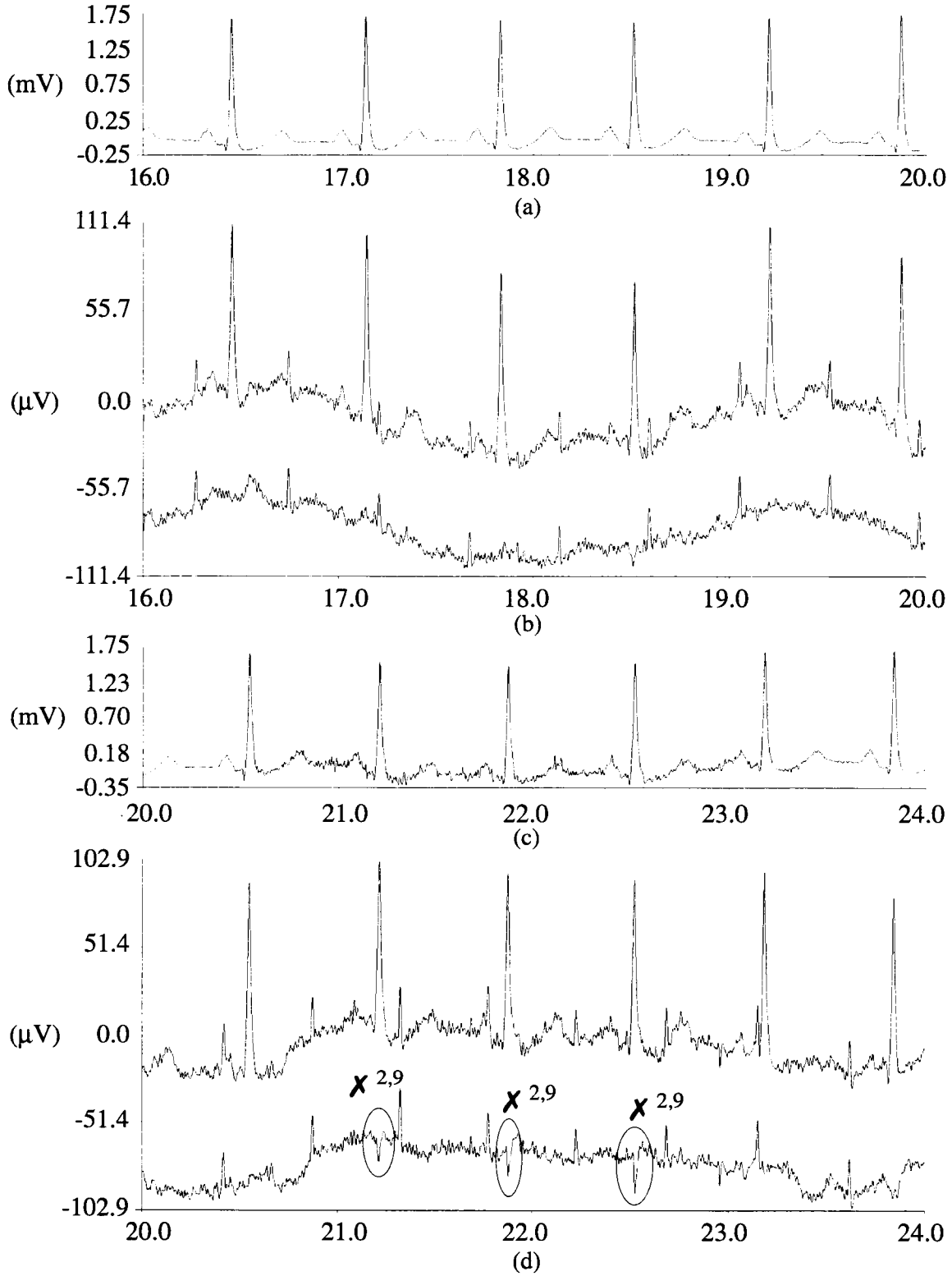

Figure D-3. A demonstration of continuous AECG MECG cancellation from 16.0 to 24.0 seconds (all x-axes in seconds). (a) TECG. (b) AECG and AECG with the MECG canceled. (c and d) Same as (a) and (b), but 4.0 seconds latter.

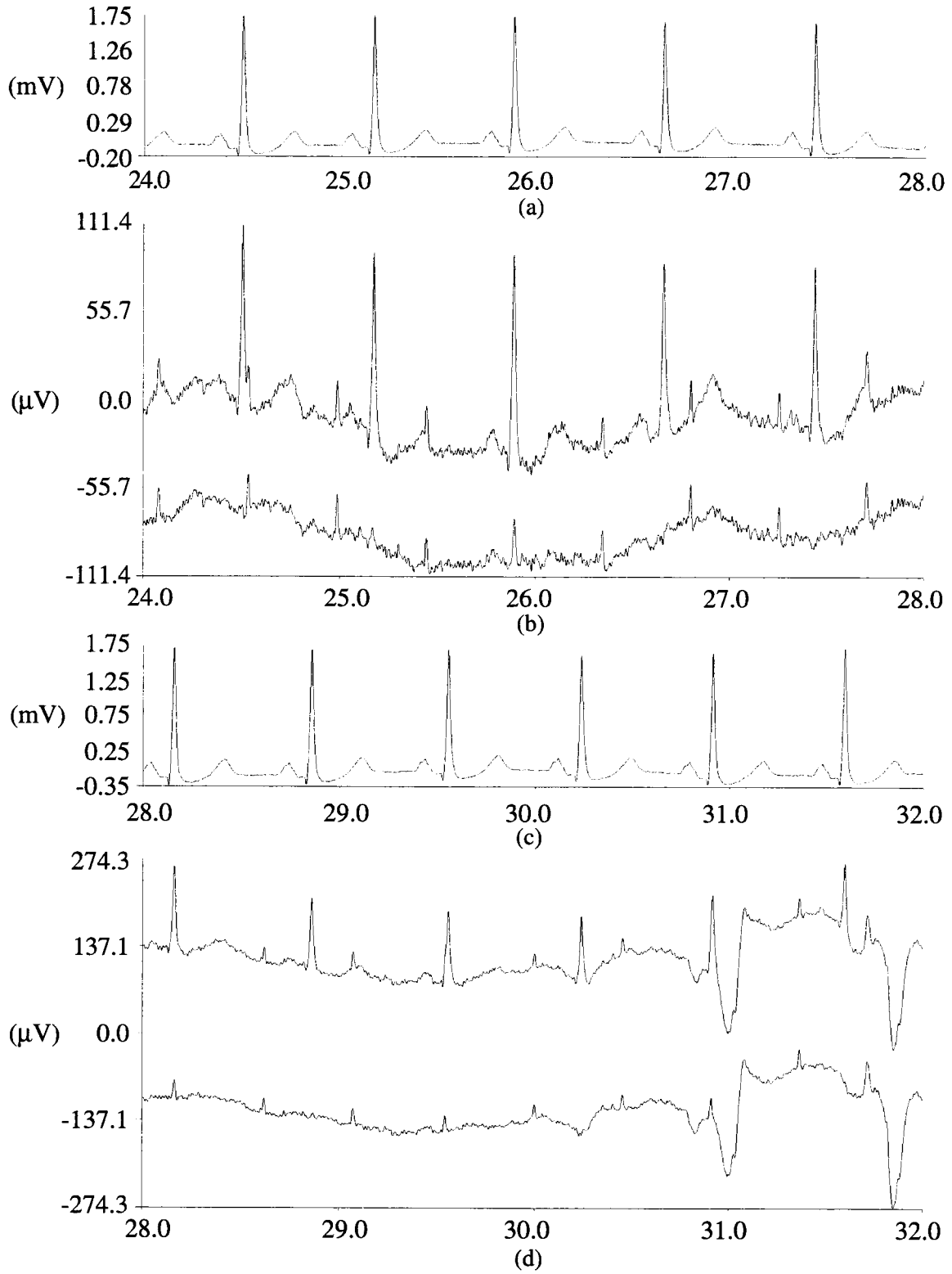

Figure D-4. A demonstration of continuous AECG MECG cancellation from 24.0 to 32.0 seconds (all x-axes in seconds). (a) TECG. (b) AECG and AECG with the MECG canceled. (c and d) Same as (a) and (b), but 4.0 seconds latter.

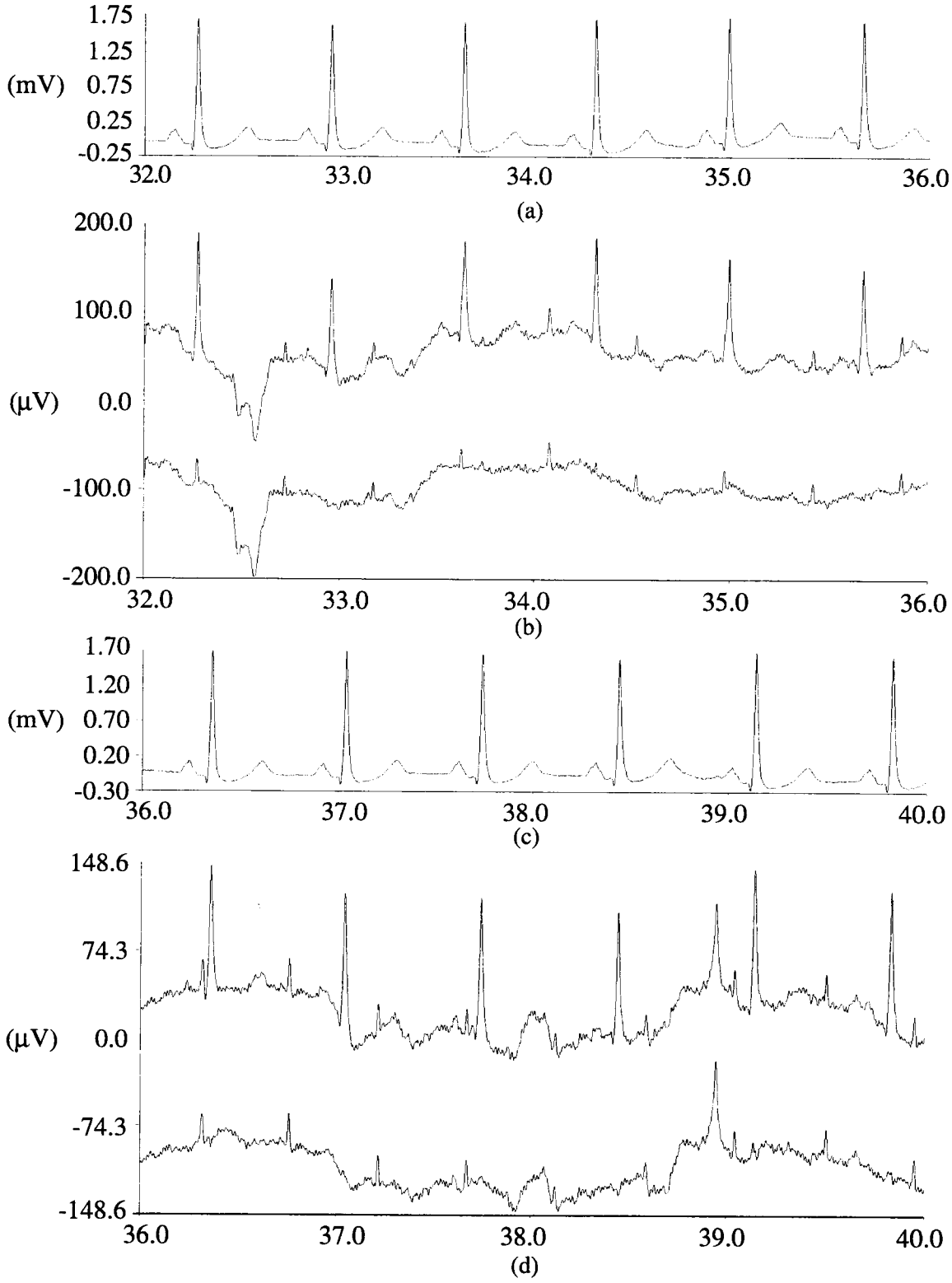

Figure D-5. A demonstration of continuous AECG MECG cancellation from 32.0 to 40.0 seconds (all x-axes in seconds). (a) TECG. (b) AECG and AECG with the MECG canceled. (c and d) Same as (a) and (b), but 4.0 seconds latter.

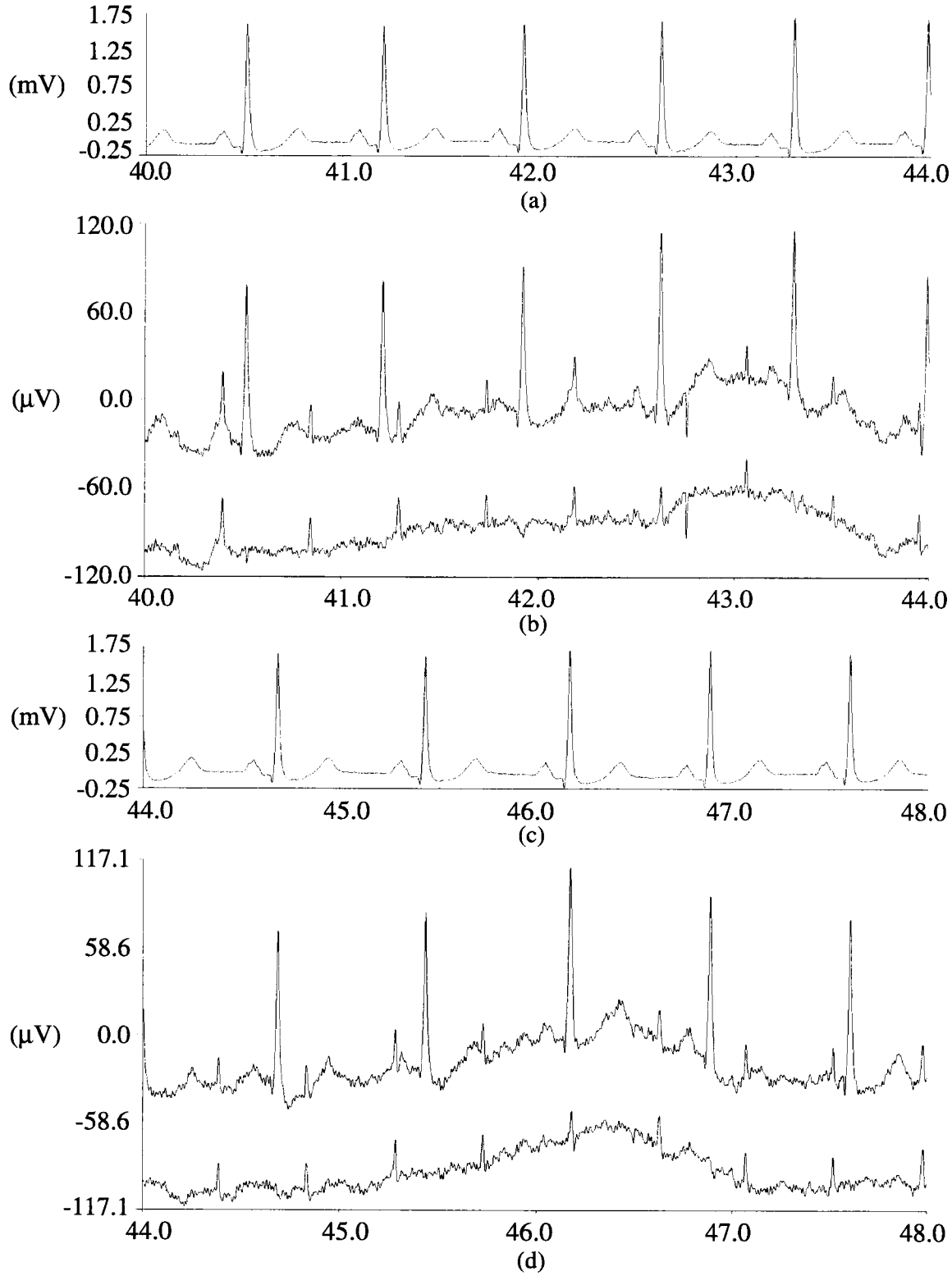

Figure D-6. A demonstration of continuous AECG MECG cancellation from 40.0 to 48.0 seconds (all x-axes in seconds). (a) TECG. (b) AECG and AECG with the MECG canceled. (c and d) Same as (a) and (b), but 4.0 seconds latter.

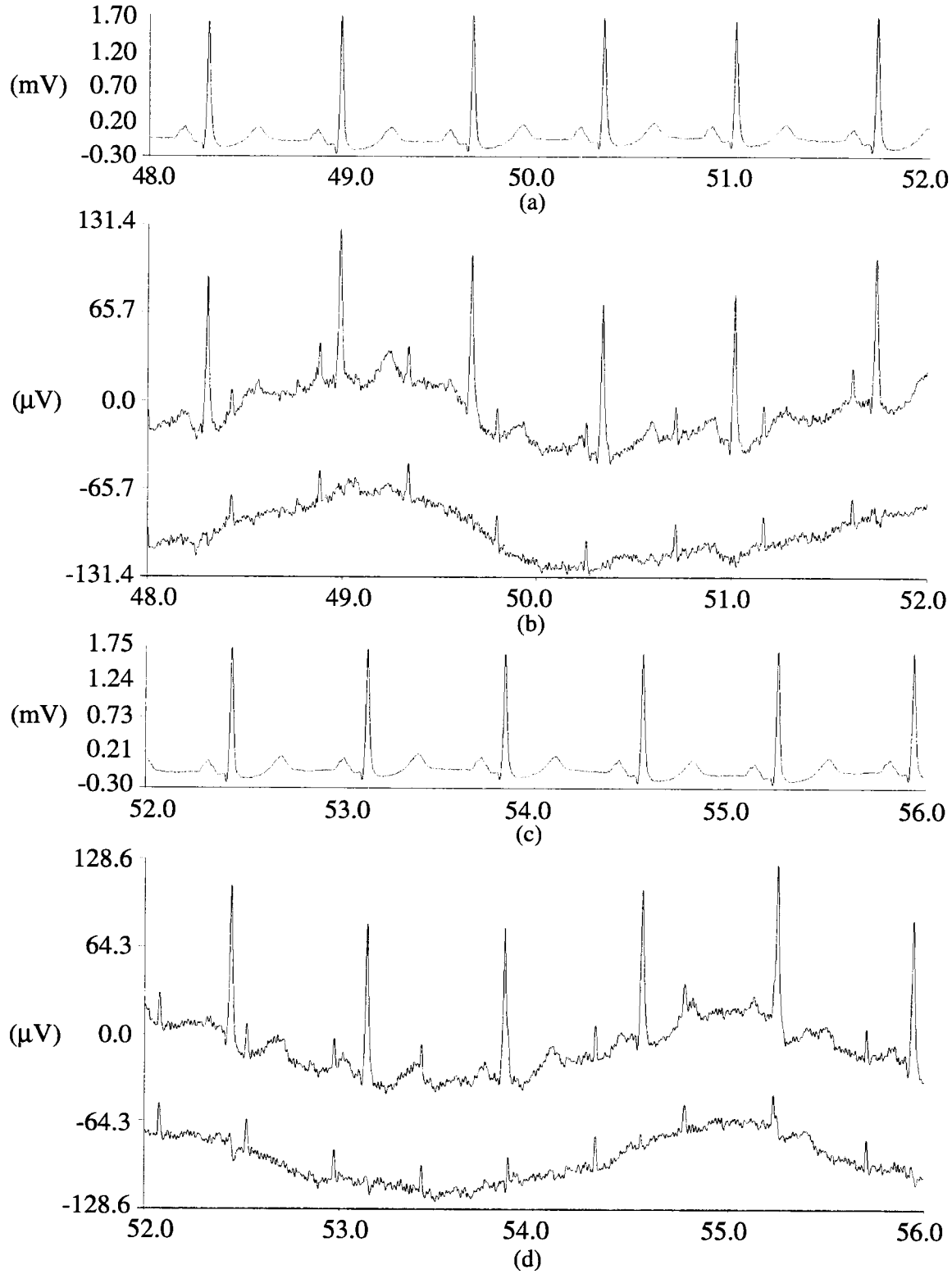

Figure D-7. A demonstration of continuous AECG MECG cancellation from 48.0 to 56.0 seconds (all x-axes in seconds). (a) TECG. (b) AECG and AECG with the MECG canceled. (c and d) Same as (a) and (b), but 4.0 seconds latter.

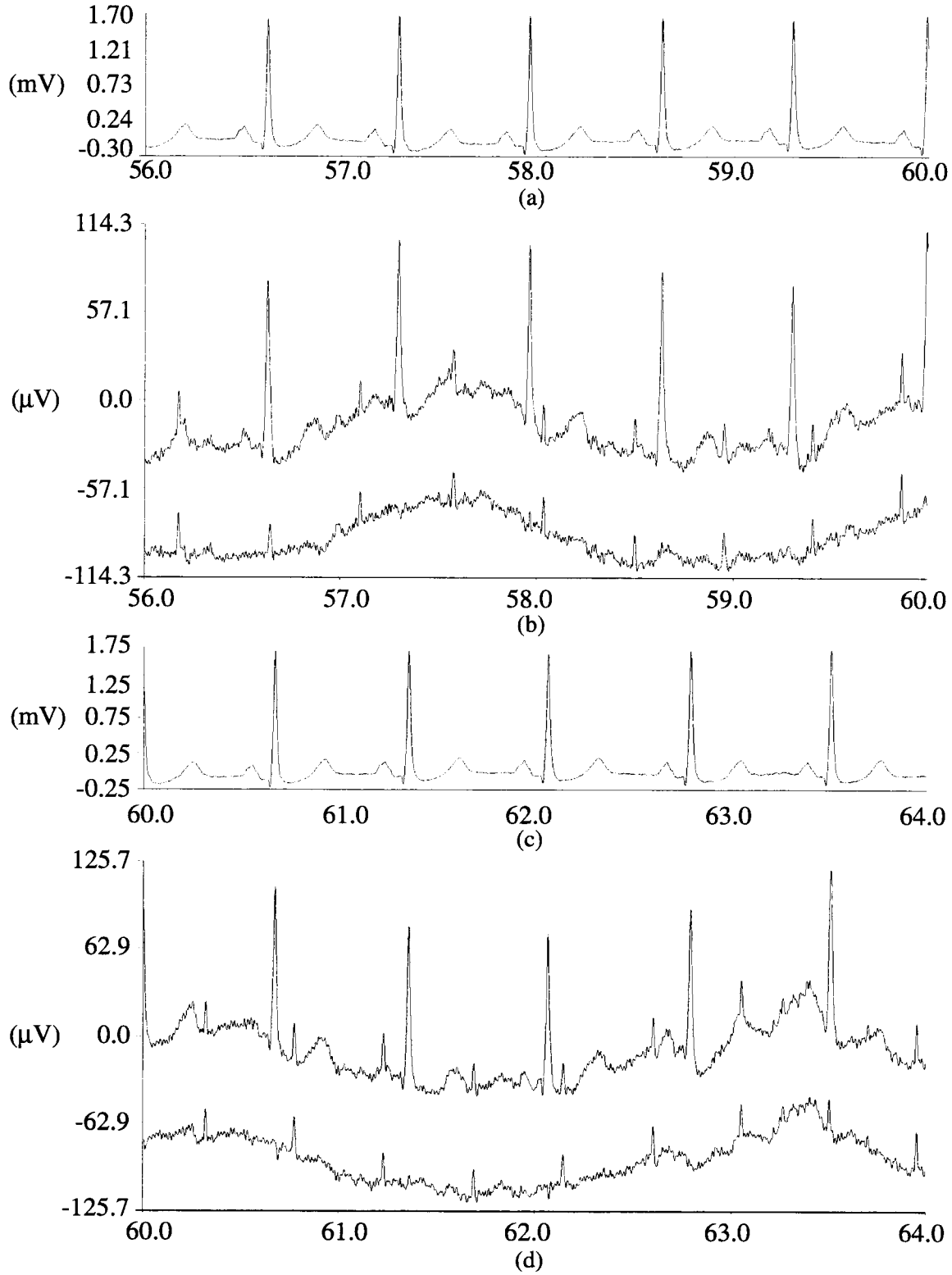

Figure D-8. A demonstration of continuous AECG MECG cancellation from 56.0 to 64.0 seconds (all x-axes in seconds). (a) TECG. (b) AECG and AECG with the MECG canceled. (c and d) Same as (a) and (b), but 4.0 seconds latter.

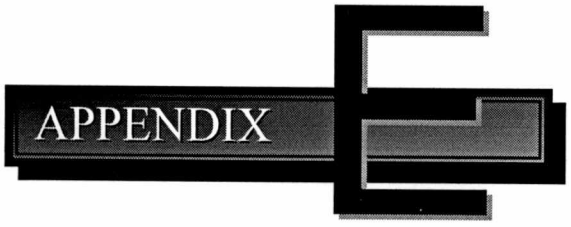

DISSERTATION GOAL II INFORMATION

Table E-1. Description of test conditions 1-5 for dissertation goal II.

ENGINEERING ASPECTS			
Test conditions 2 through 5 consist of a visual inspection that compare the original and resulting AECG to determine if AECG MECG cancellation was successful (A visual inspection is not done for test condition 1).			
Test Conditions		Grading Description	✓ Passed ✖ Failed - Did Not Occur
1	Bandwidth of Resulting AECG is 0.05 to 100 Hz	✓	The resulting AECG is 0.05 to 100.0 Hz.
		✖	The resulting AECG is not 0.05 to 100.0 Hz.
		-	Does not apply.
		Comments	By definition, the CH^2 method for AECG MECG cancellation does not alter the signal bandwidth (See Chapter 3 for method description.). All clinical data passed this test.
2	Signal Corruption to FECG & EMG	✓	The resulting AECG compared to the AECG's FECG or EMG has negligible MECG residuals and similar shaped FECG and EMG respectively.
		✖	The resulting AECG compared to the AECG's FECG or EMG has noticeable MECG residual(s) and/or dissimilar shaped FECG and EMG respectively.
		-	Does not apply.
		Comments	This test will usually be reported a failure when any of the test conditions 5 through 12 fail. Figs. 5-3 and 5-4 are examples of data that pass and fail respectively.
3	Overall MECG Cancellation	✓	The majority of the MECG complexes result in negligible residuals in the resulting AECG compared to the AECG's FECG and EMG.
		✖	The majority of the MECG complexes result in noticeable residuals in the resulting AECG compared to the AECG's FECG and EMG.
		-	Does not apply.
		Comments	Figs. 5-3 and 5-4 are examples of data that pass and fail respectively.
4	FECG & MECG Overlap	✓	The FECG's QRS complex that overlapped an MECG's QRS complex of the AECG is present and similar in shape to the surrounding non-overlapping FECG's QRS complexes in the resulting AECG.
		✖	The FECG's QRS complex that overlapped an MECG's QRS complex of the AECG is missing or significantly dissimilar in shape to the surrounding non-overlapping FECG's QRS complexes in the resulting AECG.
		-	The MECG and FECG did not overlap in the original AECG.
		Comments	Figs. 5-13 and C-10 are examples of data that pass and fail respectively.
5	Significant AECG Low Frequency Noise	✓	In the event of significant AECG low frequency noise, the resulting AECG compared to the AECG's FECG or EMG has negligible MECG residuals and similar shaped FECG and EMG respectively.
		✖*	In the event of significant AECG low frequency noise, the resulting AECG compared to the AECG's FECG or EMG has noticeable MECG residual(s) and/or dissimilar shaped FECG and EMG respectively.
		-	Significant low frequency noise did not occur.
		Comments	Significant AECG low frequency noise is usually less than 2.0 Hz with a signal amplitude greater than half the abdominal MECG complex peak-to-peak value. Test conditions 6 through 12 should be considered before failure is awarded. All clinical data passed this test.
*Before this test condition is graded failure, the test conditions specified under comments should be considered. If they did not occur, then this test condition is likely to be causing the problem and failure should be awarded. If some or all occurred, make an educated guess to determine which test conditions (including the one under consideration) are most likely causing the signal corruption and grade these as failure. Then pass the rest.			

Table E-2. Description of test conditions 6-9 for dissertation goal II.

ENGINEERING ASPECTS			
Test conditions 6 through 9 consist of a visual inspection that compare the original and resulting AECG to determine if AECG MECG cancellation was successful.			
Test Conditions		Grading Description	✓ Passed ✗ Failed - Did Not Occur
6	Significant AECG Noise Spike	✓	In the event of a significant AECG noise spike, the resulting AECG compared to the AECG's FECG and EMG has similar shaped FECG and EMG respectively.
		✗*	In the event of a significant AECG noise spike, the resulting AECG compared to the AECG's FECG and EMG has dissimilar shaped FECG and EMG respectively.
		-	A significant noise spike did not occur.
		Comments	The amplitude of a significant noise spike is greater than one third the amplitude of the MECG complex and/or three times the peak value of the background noise. Test conditions 5, 7, 8, 11, and 12 should be considered before failure is awarded. All clinical data passed this test.
7	Significant TECG Noise	✓	In the event of significant TECG noise, the resulting AECG compared to the AECG's FECG or EMG has negligible MECG residuals and similar shaped FECG and EMG respectively.
		✗*	In the event of significant TECG noise, the resulting AECG compared to the AECG's FECG or EMG has noticeable MECG residual(s) and/or dissimilar shaped FECG and EMG respectively.
		-	Significant TECG noise did not occur.
		Comments	Figs. 5-3(a) and 5-4(a) contain insignificant and significant TECG noise respectively. Test conditions 5, 6, and 8 through 12 should be considered before failure is awarded. Figs. 5-3 and 5-4 are examples of data that pass and fail respectively.
8	AECG Noise	✓	The resulting AECG compared to the AECG's FECG or EMG has similar shaped FECG and EMG respectively.
		✗*	The resulting AECG compared to the AECG's FECG or EMG has dissimilar shaped FECG and EMG respectively.
		-	Does not apply.
		Comments	Test conditions 5, 6, 7, 11, and 12 should be considered before failure is awarded. All clinical data passed this test. A failure could occur if not enough MECG complexes were averaged. The AECG noise would be noticeable in the MECG average and would be introduced in the resulting AECG as added noise during the subtraction of the MECG average.
9	Modulated MECG of the AECG	✓	In the event of a modulated MECG of the AECG, the resulting AECG compared to the AECG's FECG or EMG has negligible MECG residuals.
		✗*	In the event of a modulated MECG of the AECG, the resulting AECG compared to the AECG's FECG or EMG has noticeable MECG residual(s).
		-	The AECG MECG is not modulated.
		Comments	Test conditions 5, 7, 10, and 12 should be considered before failure is awarded. Figs. 5-13 and C-10 are examples of data that pass and fail respectively.
*Before this test condition is graded failure, the test conditions specified under comments should be considered. If they did not occur, then this test condition is likely to be causing the problem and failure should be awarded. If some or all occurred, make an educated guess to determine which test conditions (including the one under consideration) are most likely causing the signal corruption and grade these as failure. Then pass the rest.			

Table E-3. Description of test conditions 10-12 for dissertation goal II.

ENGINEERING ASPECTS			
Test conditions 10 through 12 consist of a visual inspection that compare the original and resulting AECG to determine if AECG MECG cancellation was successful.			
Test Conditions		Grading Description	✓ Passed ✗ Failed - Did Not Occur
10	Modulated MECG of the TECG	✓	In the event of a modulated MECG of the TECG, the resulting AECG compared to the AECG's FECG or EMG has negligible MECG residuals.
		✗*	In the event of a modulated MECG of the TECG, the resulting AECG compared to the AECG's FECG or EMG has noticeable MECG residual(s).
		-	The TECG MECG is not modulated.
		Comments	Test conditions 5, 7, 9, and 12 should be considered before failure is awarded. All clinical data passed this test.
11	Periodic EMG Impulses	✓	The resulting AECG's periodic EMG impulses are similar in shape to the AECG's and the resulting AECG's periodic EMG impulses that were overlapped with the AECG's MECG complex(es) are similar to the surrounding impulses. Furthermore, no noise is introduced from the impulses into the resulting AECG through MECG averaging and subtraction.
		✗*	The resulting AECG's EMG impulses are distorted compared to the AECG's and/or MECG averaging and subtraction introduced noise to the resulting AECG.
		-	The periodic EMG impulses did not occur.
		Comments	The periodic EMG impulses can easily be identified because they look like the FECG, but at a rate that is much higher than even a high rate FECG. Test conditions 5, 6, 7, 8, and 12 should be considered before failure is awarded. All clinical data passed this test.
12	Unexpected Ventricle Contraction	✓	In the event of an unexpected ventricle contraction, the resulting AECG compared to the AECG's FECG or EMG has negligible MECG residuals and similar shaped FECG and EMG respectively.
		✗*	In the event of an unexpected ventricle contraction, the resulting AECG compared to the AECG's FECG or EMG has noticeable MECG residual(s) and/or dissimilar shaped FECG and EMG respectively.
		-	An unexpected ventricle contraction did not occur.
		Comments	Test conditions 5 through 11 should be considered before failure is awarded. Figure 5-15 demonstrates a failure case of test condition 12 from a residual T wave. Furthermore, this test can fail the added noise inspection from to few MECG complexes being averaged. With the MECG R waves close together from the extra ECG complex, a significant amount of complexes should be averaged to reduce the interference from the R waves in the average. If this is not done, the MECG average will have a large R wave and two smaller R waves depending on the number of complexes averaged. When the MECG average is subtracted, added noise from the two smaller R waves is introduced into the resulting AECG.
*Before this test condition is graded failure, the test conditions specified under comments should be considered. If they did not occur, then this test condition is likely to be causing the problem and failure should be awarded. If some or all occurred, make an educated guess to determine which test conditions (including the one under consideration) are most likely causing the signal corruption and grade these as failure. Then pass the rest.			

Table E-4. Description of clinical applications 1-3 dissertation goal II.

CLINICAL APPLICABILITY			
The grades for clinical application 1 through 3 indicate that clinical information is not limited or limited by the success of AECG MECG cancellation or observability of the FECG.			
Clinical Applications		Grading Description	P Potential NP No Potential
1	Fetal HR Information via HR Determination Algorithm	P	A visual inspection of the resulting AECG determines that the FECG is observable and test conditions 3 and 4 passed.
		NP	A visual inspection of the resulting AECG determines that the FECG is not observable, or observable and test conditions 3 and/or 4 failed.
		Comments	For an HR determination algorithm to consistently detect each FECG's R wave to calculate the instantaneous HR, the R waves should be noticeable during a visual inspection of the resulting AECG. Furthermore, the majority of the AECG MECG complexes result in negligible residuals in the resulting AECG compared to the original's FECG and EMG.
2	FECG Electrophysiological Information via FECG Averaging	P	Test conditions 1 and 3 passed and FECG averaging has potential to produce an FECG average with a favorable SNR.
		NP	Test conditions 1 and/or 3 failed and/or FECG averaging has little potential to produce an FECG average with a favorable SNR.
		Comments	For FECG averaging to have potential to produce an average with a favorable SNR, a visual inspection of the AECG(s) can discern all FECG's R waves to be averaged (except the ones overlapping the MECG and a noise spike(s)) without question. Furthermore, the grades of this clinical application indicate that conditions will most likely exist or not exist for FECG averaging to produce an FECG complex that electrophysiological information can be read or not read respectively.
3	Uterine Contract Information via EMG	P	If test conditions 1 and 2 passed, then there is potential to obtain uterine contract information provided uterine contraction information is present in the EMG.
		NP	If test conditions 1 and/or 2 failed, then most likely there is no potential to obtain accurate uterine contract information.
		Comments	For EMG information to be used for uterine contraction determination, the EMG of the resulting AECG has to be unfiltered and undistorted compared to the AECG. Therefore, potential or no potential uterine contract information is determined based on the pass or fail status of test conditions 1 and 2 respectively. **Finally, the rating of potential or no potential is an indicator that the EMG is undistorted or distorted and should not be interpreted as an indicator for uterine contract information being present or not present!**

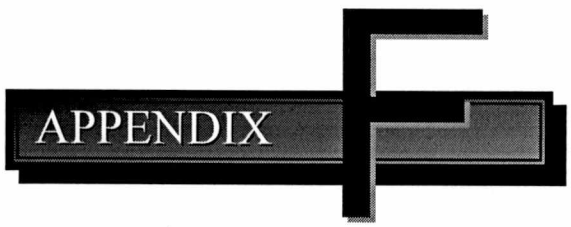

DISSERTATION GOAL II RESULTS

Table F-1. MECG suppression ratios for patients 1 through 3 of the objective analysis.

Patient Number	MECG Suppression Ratios (Ordered sequentially by row)											
Patient 1	18	18	17	13	9	20	18	18	18	9	9	18
36 Weeks	18	9	12	18	15	9	12	10	10	20	12	10
Mean = 15	20	18	12	10	10	18	18	10	18	12	18	12
Stand. Dev. = 4	18	18	15	18	15	12	10	18	15	10	18	20
	10	18	12	15	18	12	18	12	18	18	16	10
Patient 2	33	9	14	14	15	10	26	20	18	33	13	10
36 Weeks	20	25	10	8	16	16	16	16	25	16	16	8
Mean = 15	10	25	16	12	8	25	16	15	10	16	8	8
Stand. Dev. = 7	6	8	8	8	14	25	20	6	15	8	10	20
	20	15	33	16	8	8	6	9	13	16	16	16
Patient 3	6	11	11	11	11	11	16	9	10	10	8	8
23 Weeks	7	9	9	6	23	9	14	9	9	10	12	11
Mean = 10	10	12	11	8	8	10	10	10	10	12	14	11
Stand. Dev. = 3	9	9	14	9	11	7	9	22	16	11	9	10
	9	12	10	11	12	9	9	9	9	7	7	10
Patient 3	9	8	10	8	8	10	10	10	11	7	7	6
24 Weeks	7	10	8	9	9	9	10	12	13	9	8	9
Mean = 8	10	6	6	7	9	8	8	6	9	6	7	8
Stand. Dev. = 2	6	6	6	6	8	8	7	10	9	11	10	11
	12	6	8	7	8	9	8	6	8	6	7	9
Patient 3	9	7	7	11	6	9	9	12	6	10	8	7
25 Weeks	8	4	7	9	5	9	8	6	4	7	6	6
Mean = 8	4	7	8	5	9	5	8	10	8	8	8	7
Stand. Dev. = 3	10	12	6	15	10	10	4	7	6	8	10	7
	6	6	10	4	7	7	11	10	10	17	5	12
Patient 3	7	8	9	6	8	12	8	8	7	6	6	9
26 Weeks	9	6	6	8	15	10	9	9	7	7	9	12
Mean = 9	20	14	7	12	7	10	6	6	14	10	12	15
Stand. Dev. = 3	9	15	8	16	8	6	8	7	6	8	8	7
	9	7	7	8	6	7	8	10	7	8	9	9
Patient 3	6	12	12	10	8	8	9	8	18	23	10	11
31 Weeks	6	14	14	15	11	19	16	8	13	14	15	17
Mean = 13	13	14	10	7	10	12	11	8	10	6	9	11
Stand. Dev. = 4	9	14	12	20	18	12	12	12	10	12	15	12
	18	18	12	21	11	21	11	21	11	18	12	12
Patient 3	12	12	13	13	10	24	12	18	12	12	12	10
33 Weeks	14	12	11	18	12	12	12	12	13	12	10	12
Mean = 12	10	12	12	7	10	12	11	10	9	12	13	11
Stand. Dev. = 3	10	10	10	12	10	10	12	12	12	13	24	20
	9	15	12	12	10	11	11	9	6	12	12	10
Patient 3	13	15	11	5	7	9	8	13	15	7	8	8
34 Weeks	9	11	10	12	12	11	12	5	8	12	11	9
Mean = 10	13	12	8	8	7	11	7	7	5	9	8	11
Stand. Dev. = 3	7	6	9	12	10	10	7	18	10	6	13	10
	11	12	15	9	8	10	10	7	13	8	8	7

Table F-2. MECG suppression ratios for patients 3 through 9 of the objective analysis.

Patient Number	MECG Suppression Ratios (Ordered sequentially by row)											
Patient 3	18	7	13	11	15	18	10	15	17	14	24	18
35 Weeks	7	15	19	15	28	11	16	7	20	8	16	13
Mean = 14	18	13	8	14	11	13	9	22	16	15	24	15
Stand. Dev. = 5	11	13	16	14	11	11	9	10	14	8	17	17
	13	13	15	13	12	9	10	20	12	11	15	30
Patient 3	11	9	13	6	13	11	12	12	14	9	17	8
36 Weeks	9	14	10	8	11	9	8	11	12	10	9	9
Mean = 10	6	8	10	10	11	6	5	14	15	8	6	12
Stand. Dev. = 3	11	11	13	7	12	23	9	8	7	8	9	17
	13	11	13	6	10	9	9	6	9	9	10	6
Patient 3	11	12	13	22	14	22	15	13	12	13	12	18
38 Weeks	14	13	18	14	13	6	14	4	8	7	13	14
Mean = 12	14	7	7	8	13	9	13	10	11	13	7	11
Stand. Dev. = 3	13	13	13	9	10	13	8	8	10	13	14	9
	13	14	7	13	13	14	12	13	14	8	12	13
Patient 3	7	9	10	13	11	13	10	9	11	11	9	20
39 Weeks	10	12	14	12	11	14	8	10	13	6	15	5
Mean = 13	8	8	18	20	10	19	18	13	8	19	13	20
Stand. Dev. = 5	26	11	11	17	9	26	18	22	12	13	11	7
	9	6	14	6	12	12	15	6	11	12	17	20
Patient 4	9	9	9	9	18	11	12	27	18	12	26	18
21 Weeks	10	9	9	23	18	10	15	27	12	10	12	18
Mean = 15	9	18	11	18	23	18	9	9	9	15	13	15
Stand. Dev. = 6	16	28	13	13	26	15	11	15	10	15	20	10
	15	27	27	22	15	11	12	17	15	11	12	11
Patient 5	10	10	17	8	20	17	16	20	16	24	16	10
36 Weeks	21	24	29	15	9	14	27	22	20	15	9	10
Mean = 17	9	10	17	24	21	17	14	17	21	17	14	15
Stand. Dev. = 7	12	12	13	22	20	15	29	15	9	11	20	15
	35	12	28	28	13	7	40	25	14	17	23	14
Patient 7	14	47	19	20	8	9	8	35	44	9	35	33
39 Weeks	18	20	6	25	7	19	25	13	20	21	25	25
Mean = 19	6	14	15	25	20	26	7	14	28	25	8	9
Stand. Dev. = 10	13	10	13	14	15	10	11	15	16	15	7	30
	10	23	35	30	40	8	26	27	12	7	12	10
Patient 8	23	12	9	20	40	20	18	6	23	46	30	46
36 Weeks	13	20	23	23	35	23	22	20	21	31	20	11
Mean = 19	12	23	20	21	30	12	22	21	12	13	10	15
Stand. Dev. = 9	22	18	15	16	8	43	12	18	11	12	8	12
	18	23	12	10	10	10	9	12	23	12	13	15
Patient 9	17	15	13	12	15	9	15	19	8	20	15	11
27 Weeks	12	15	18	15	11	12	12	12	15	11	13	14
Mean = 13	9	14	17	15	7	9	18	9	12	10	13	18
Stand. Dev. = 3	12	9	10	15	14	11	15	11	12	10	12	15
	14	10	10	10	12	15	20	20	12	12	10	10

Table F-3. MECG suppression ratios for patients 10 through 16 of the objective analysis.

Patient Number	MECG Suppression Ratios (Ordered sequentially by row)											
Patient 10	25	25	11	25	16	15	15	14	7	6	7	14
37 Weeks	16	15	25	6	6	9	10	14	16	11	12	16
Mean = 13	16	6	13	27	13	12	14	16	9	7	9	7
Stand. Dev. = 6	9	13	9	13	25	13	11	20	13	12	12	9
	9	13	7	7	14	30	14	11	11	6	6	6
Patient 11	5	8	9	9	5	4	5	4	7	9	8	7
38 Weeks	6	13	11	5	10	8	8	11	6	4	5	9
Mean = 7	8	7	6	5	10	6	8	7	8	6	6	5
Stand. Dev. = 2	7	7	7	6	6	6	5	5	6	7	6	5
	5	5	4	7	5	8	6	7	7	5	7	10
Patient 12	18	11	8	11	5	4	4	4	12	11	6	5
34 Weeks	15	9	12	5	9	12	8	14	9	9	21	19
Mean = 10	10	5	11	16	26	7	6	6	17	7	4	10
Stand. Dev. = 5	8	10	5	4	4	4	10	10	6	5	15	8
	11	5	9	14	7	17	10	10	22	19	12	6
Patient 13	8	13	11	50	9	10	8	11	9	6	7	16
39 Weeks	6	8	7	7	13	8	8	11	7	6	8	14
Mean = 10	8	12	9	8	8	20	16	6	9	14	7	9
Stand. Dev. = 6	8	17	7	9	9	8	10	10	7	12	8	13
	11	12	11	10	7	7	9	9	9	9	10	6
Patient 15	20	11	4	11	16	12	18	13	10	14	10	7
41 Weeks	11	4	12	4	10	5	16	8	9	13	10	10
Mean = 10	9	8	12	5	15	5	6	14	13	8	10	14
Stand. Dev. = 4	11	13	10	13	6	10	9	11	7	7	4	16
	5	8	13	9	12	14	8	7	9	7	9	5
Patient 16	13	14	14	26	50	9	13	9	11	13	13	13
26 Weeks	16	8	20	16	22	16	17	11	17	12	10	30
Mean = 14	30	22	16	15	16	13	6	17	10	10	11	12
Stand. Dev. = 8	10	22	5	5	6	17	17	33	15	7	5	17
	6	11	11	7	4	4	6	7	7	20	13	13
Patient 16 36 Weeks	The abdominal MECG suppression ratios were not calculated for this data set because the periodic EMG spikes significantly corrupted the calculation.											



DISSERTATION GOAL III INFORMATION

Table G-1. Description of test conditions 1-5 for dissertation goal III.

ENGINEERING ASPECTS			
Test conditions 2 through 5 consist of a visual inspection that compare the original and resulting AECGs to determine if AECG MECG cancellation was successful (A visual inspection is not done for test condition 1).			
Test Conditions		Grading Description	✓ Passed ✖ Failed - Did Not Occur
1	Bandwidth of Resulting AECG(s) is 0.05 to 100 Hz	✓	See Appendix E. Table E-1. test condition 1.
		✖	See Appendix E. Table E-1. test condition 1.
		-	Does not apply.
		Comments†	The bandwidth of the AECG processed by the previously reported methods and the CH^2 method was not reduced. Therefore. all methods passed this test condition.
2	Signal Corruption to FECG & EMG	✓	Analysis I - See Appendix E. Table E-1. test condition 2: and CM_1 & $CM_2 \geq 0.95$: and $CM_3 \geq 19.0$. Analysis II - All AECGs with only their MECGs canceled are available. Furthermore. these resulting AECGs compared to the AECGs' FECG or EMG have negligible MECG residuals and similar shaped FECG and EMG respectively.
		✖	Analysis I - See Appendix E. Table E-1. test condition 2: and CM_1 & $CM_2 < 0.95$: and $CM_3 < 19.0$. Analysis II - Some or all AECGs with only the MECG canceled are not available. If they are available. then these resulting AECGs compared to the AECGs' FECG or EMG have noticeable MECG residual(s) and/or dissimilar shaped FECG and EMG respectively.
		⇧	Analysis I - Does not apply. Analysis II - Indicates which method has greater values for CM_1. CM_2. and CM_3 provided test condition 3 has passed.
		-	Does not apply.
		Comments†	This test will usually be reported a failure when any of the test conditions 5 through 7 fail.
3	Overall MECG Cancellation	✓	See Appendix E. Table E-1. and test condition 3.
		✖	See Appendix E. Table E-1. and test condition 3.
		-	Does not apply.
		Comments†	None
4	FECG & MECG Overlap	✓	See Appendix E. Table E-1. and test condition 4.
		✖	See Appendix E. Table E-1. and test condition 4.
		-	See Appendix E. Table E-1. and test condition 4.
		Comments†	None
5	Significant AECG Low Frequency Noise	✓	See Appendix E. Table E-1. and test condition 5‡.
		✖*	See Appendix E. Table E-1. and test condition 5‡.
		-	See Appendix E. Table E-1. and test condition 5.
		Comments†	Significant AECG low frequency noise is usually less than 2.0 Hz with a signal amplitude greater than half the abdominal MECG complex peak-to-peak value. Test conditions 6 and 7 should be considered before failure is awarded.
†Ignore the comments of Appendix E. Table E-1. ‡For Analysis II. disregard EMG inspection.			
*Before this test condition is graded failure. the test conditions specified under comments should be considered. If they did not occur. then this test condition is likely to be causing the problem and failure should be awarded. If some or all occurred. make an educated guess to determine which test conditions (including the one under consideration) are most likely causing the signal corruption and grade these as failure. Then pass the rest.			

Table G-2. Description of test conditions 6-7 and intrinsic characteristics 1-4 for dissertation goal III.

ENGINEERING ASPECTS			
Test conditions 6 and 7 consist of a visual inspection that compare the original and resulting AECGs to determine if AECG MECG cancellation was successful.			
Test Conditions		Grading Description	✓ Passed ✖ Failed - Did Not Occur
6	Significant AECG Noise Spike	✓	See Appendix E, Table E-2, and test condition 6‡.
		✖*	See Appendix E, Table E-2, and test condition 6‡.
		-	See Appendix E, Table E-2, and test condition 6.
		Comments†	The amplitude of a significant noise spike is greater than one third the amplitude of the MECG complex and/or three times the peak value of the background noise. Test conditions 5 and 7 should be considered before failure is awarded.
7	Significant TECG Noise	✓	See Appendix E, Table E-2, and test condition 7‡.
		✖*	See Appendix E, Table E-2, and test condition 7‡.
		-	See Appendix E, Table E-2, and test condition 7.
		Comments†	Figs. 6-1(a) and 6-4(a) contain insignificant and significant TECG noise respectively. Test conditions 5 and 6 should be considered before failure is awarded.
Intrinsic Characteristics		Grading and Rating Description	
1	Flexibility of Lead Positioning	**No requirement(s) for lead placement** (rating = 1) - No restriction(s) is placed on lead positioning to obtain AECG MECG cancellation.	
		Flexible (rating = 0.5) - The TECG lead necessary for AECG MECG cancellation has to be in a lead II position or leads can be anywhere on the abdominal cavity.	
		Little Flexibility (rating = 0) - The ECG leads have to be positioned for a set of scale factors or filter coefficients to exist so that a linear combination of the ECG signals or subtraction of the filtered TECG signals from the AECG obtains AECG MECG cancellation.	
2	Number of Extra Leads Required	**None** (rating = 1) - No extra lead(s) is required to produce AECG MECG cancellation.	
		Number and type of ECG(s) (For each extra lead or ECG signal required for AECG MECG cancellation, 0.25 is subtracted from the initial rating of 1.) - The two types of ECGs are TECG and AECG.	
3	User Interaction Required	**No** (rating = 1.0) - No user interaction is required to initialize the algorithm.	
		Yes (rating = 0.0) - The user has to initialize the program at start up for the algorithm to operate correctly (e.g. some methods require the user to select a near pure AECG MECG complex FECG free at the start of the algorithm).	
4	Computational Complexity	**Low** (rating = 1) - 8 seconds of data takes less than 8 seconds to process**.	
		Medium (rating = 0.66) - 8 seconds of data takes 8 to 32 seconds to process**.	
		High (rating = 0.33) - 8 seconds of data takes 32 to 64 seconds to process**.	
		Very High (rating = 0) - 8 seconds of data takes more than 64 sec. to process**.	

†Ignore the comments of Appendix E, Table E-2. ‡For Analysis II, disregard EMG inspection.

*Before this test condition is graded failure, the test conditions specified under comments should be considered. If they did not occur, then this test condition is likely to be causing the problem and failure should be awarded. If some or all occurred, make an educated guess to determine which test conditions (including the one under consideration) are most likely causing the signal corruption and grade these as failure. Then pass the rest.

**These grades are relative to an Intel 486DX2 66 MHz microprocessor.

Table G-3. Description of clinical applications 1-3 for dissertation goal III.

CLINICAL APPLICABILITY			
The grades for clinical application 1 through 4 indicate that clinical information is not limited or limited by the success of AECG MECG cancellation or observability of the FECG.			
Clinical Applications		Grading Description	P Potential NP No Potential
1	Fetal HR Information via HR Determination Algorithm	P	See Appendix E. Table E-4. clinical application 1.
		NP	See Appendix E. Table E-4. clinical application 1.
		Comments	See Appendix E. Table E-4. clinical application 1.
2	FECG Electrophysiological Information via FECG Averaging	P	See Appendix E. Table E-4. clinical application 2.
		NP	See Appendix E. Table E-4. clinical application 2.
		Comments	See Appendix E. Table E-4. clinical application 2.
3	Uterine Contract Information via EMG	P	Test conditions 1 and 2 passed for the considered analysis (Analysis I or Analysis II).
		NP	Test conditions 1 and 2 failed for the considered analysis (Analysis I or Analysis II).
		Comments	For EMG information to be used for uterine contraction determination. the EMG of the resulting AECG(s) has to be unfiltered and undistorted compared to the AECG(s). Therefore. potential uterine contract information is determined based on the pass or fail status of test conditions 1 and 2.
4	Principal Fetal Signal(s) or Source Signal(s) Obtainable	P	Analysis I - Clinical application two had potential. Analysis II - The resulting AECG(s) is a source signal(s) for the FECG and test conditions 1 and 3 passed for this signal(s).
		NP	Analysis I - Clinical application two had no potential. Analysis II - The resulting AECG(s) is not a source signal(s) for the FECG. If the resulting AECG is a source signal(s). no potential will still be award if test conditions 1 and/or 3 fail.
		Comments	Analysis I - See Chapter 6 section 1 for further description. Analysis II - The resulting signal(s) considered include the final signal(s) resulting from the previously reported methods and the signals resulting from the SVD of the AECGs with the MECG canceled via the CH^2 method.

Grading and Rating Descriptions

Grading for the test conditions, intrinsic characteristics, and clinical applications has been described in Tables G-1 through G-3. Table G-2 also includes ratings for the intrinsic characteristics. Ratings for the test conditions and clinical applications are tallied in the right hand column of Tables 6-1 through 6-8. They are calculated based on the grades awarded for the figures specified by each table. A pass or potential grading is worth one point and failure or no potential grading is worth zero points. By summing the point values for the grades of the method analyzed for each test condition or clinical application and dividing the summed values by the total number of figures studied, produces the ratings for each method studied. Finally, analysis II's rating calculation for test condition 2 is slightly different than analysis I. All the points are summed for the pass and fail grades as with analysis I. However, if an up arrow (⇧) appears, then the arrow is worth one point and also summed with the pass or fail points. Then the summed value is divided by total number of figures analyzed plus the possible occurrences of the up arrow.

Scoring Description

For each of the eight tables, the scores for the previous publication and CH^2 method engineering aspects and clinical applicability are calculated from their respective ratings. The score for engineering aspects for each method is calculated using the superscript numbers of the test condition and intrinsic characteristic numbers as weights of importance. The first four test conditions are given a weight of 100 and the intrinsic characteristics a weight of 25. These weights were used because the test conditions or the accuracy of obtaining AECG MECG suppression is more important than the ease in which the method is operated or implemented. Only the first four test conditions are rated because the other three are figured into test conditions 2's grading. The superscript weights and rating values are multiplied and summed for each respective test condition and intrinsic characteristic for the method analyzed to determine the engineering aspects score. Clinical applicability scores are calculated by summing the four rating numbers of each method analyzed. The values for the scores for each method for the engineering aspects and clinical applicability are shown in their respective rows of the eight tables where the superscript abbreviations indicate the associated method.

Justification of Intrinsic Characteristics' Grades and Ratings

The grades for each intrinsic characteristic of Table G-2 were chosen to describe the most to least desired characteristics of the eight previous publications and the CH^2 method. The rating associated with each grade ranges from 1 to 0 where 1 and 0 indicate the most and least desired characteristics respectively. If the reader disagrees with the following justifications for the intrinsic characteristics' grades and ratings, they are encourage to devise a new system and recalculate the scores and effectiveness marks for the eight comparisons of Chapter 6.

Three different grades were used to describe intrinsic characteristic 1 (flexibility of lead positioning) since the eight former publications and the CH^2 method had no requirements, flexible requirements, or little flexibility for lead placement to achieve abdominal MECG cancellation. The **no requirement(s) for lead placement** grade is the desired characteristic; therefore, it was awarded a 1 rating. **Little flexibility** grade is the least desired characteristic. Accordingly, it was given a 0 rating. Finally, the **flexible** grade was given a rating of 0.5 to evenly divide the possible ratings from 1 to 0.

Intrinsic characteristic 2 consists of a grading and rating system for the number of extra leads required for abdominal MECG cancellation. Two grades were used to describe intrinsic characteristic 2 since the previous publications and the CH^2 method required no extra leads or extra leads. The **none** grade is the desired because no extra leads are required to achieve abdominal MECG cancellation; therefore, it was awarded a 1 rating. The rating for the **number and type of ECG(s)** grade is based on the number of extra leads required. Since three of the five former publications that required extra leads used three leads, a rating deduction value was chosen to reflect each additional lead up to three uniformly in the rating. Therefore, 0.25 was deducted from the ideal rating of 1 for each extra lead required. The two methods that required more than three leads were given a rating of 0. If the deduction value was set to reflect more than three extra leads uniformly, the ratings for the methods that require one or three leads would not have represented the seriousness of requiring extra leads to achieve abdominal MECG cancellation.

Two different grades describe intrinsic characteristic 3 (user interaction required) since the previous publications and CH^2 method required no user interaction and user interaction to initialize the algorithm for abdominal MECG cancellation. The **no** grade is the desired characteristic because no user interaction is required. Accordingly, it was awarded a 1 rating. The **yes** grade is the least desired characteristic; therefore, it was given a 0 rating.

Four different grades were used to describe intrinsic characteristic 4 (computational complexity). The first grade or **low** was defined to reflect whether the abdominal MECG cancellation method could be implemented in block mode real-time. Since all processing times were for 8 seconds of data, the **low** grade was defined as 0 to 8 seconds of processing time (all processing times are relative to an Intel 486DX2 66 MHz microprocessor using LabVIEW DSP software). Real-time implementation is the most desired mode of implementation; therefore, the **low** grade is awarded a rating of 1. The final three grades or **medium**, **high**, **very high** were defined based on the five worst computation times for all methods analyzed. These five values were 11, 30, 49, 56 and 168 seconds. The five worst times were used so intrinsic characteristic 4's grading and rating would reflect all computation times. **Medium** grade was defined from 8 to 32 seconds of processing time to include the 5th and 4th worst computation times of 11 and 30 seconds. The grade of **high** was defined from 32 to 64 seconds of processing time to include the 3rd and 2nd worst computation times of 49 and 56 seconds. Finally, the grade **very high** was defined as more than 64 seconds of processing time to include worst case computational time of 168 seconds. The ratings for the three grades were divided uniformly from 1 to 0. **Very high** grade was the least desired and it was given a rating of 0. **Medium** and **high** grades were awarded ratings between 1 and 0 of 0.66 and 0.33 respectively.

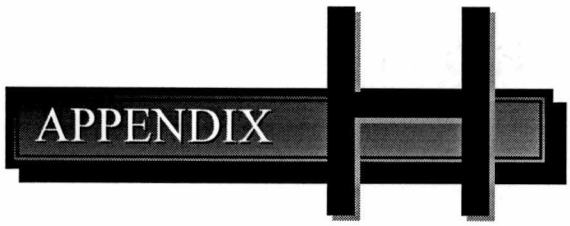

DISSERTATION GOAL III ANALYSIS I DATA

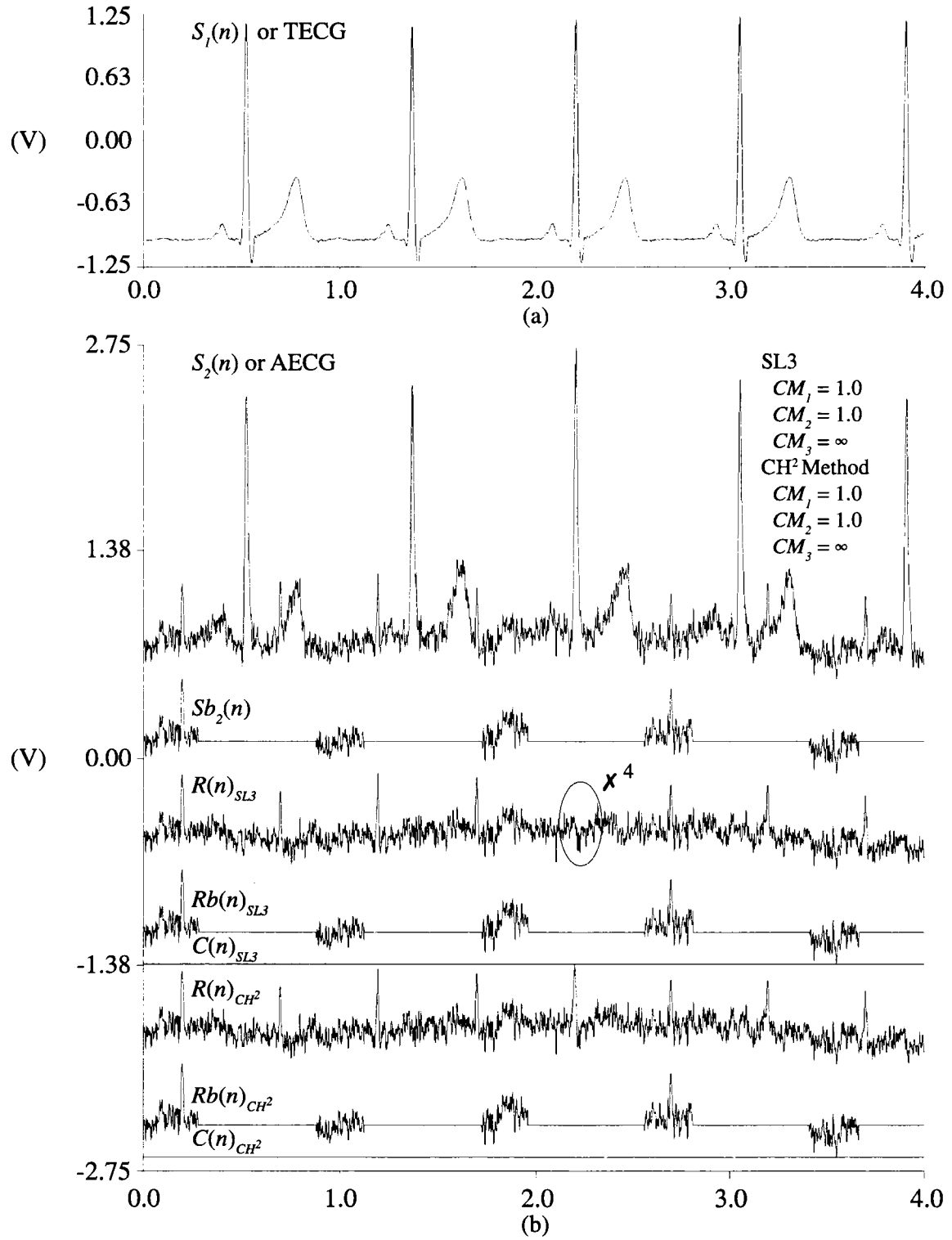

Figure H-1. Single lead method three vs. the CH^2 method demonstrating test condition four (all x-axes in seconds). (a) TECG or $S_1(n)$ used only with the CH^2 method. (b) AECG or $S_2(n)$, AECG blanked out during the MECG complexes or $Sb_2(n)$, and resulting AECGs comparing the two methods.

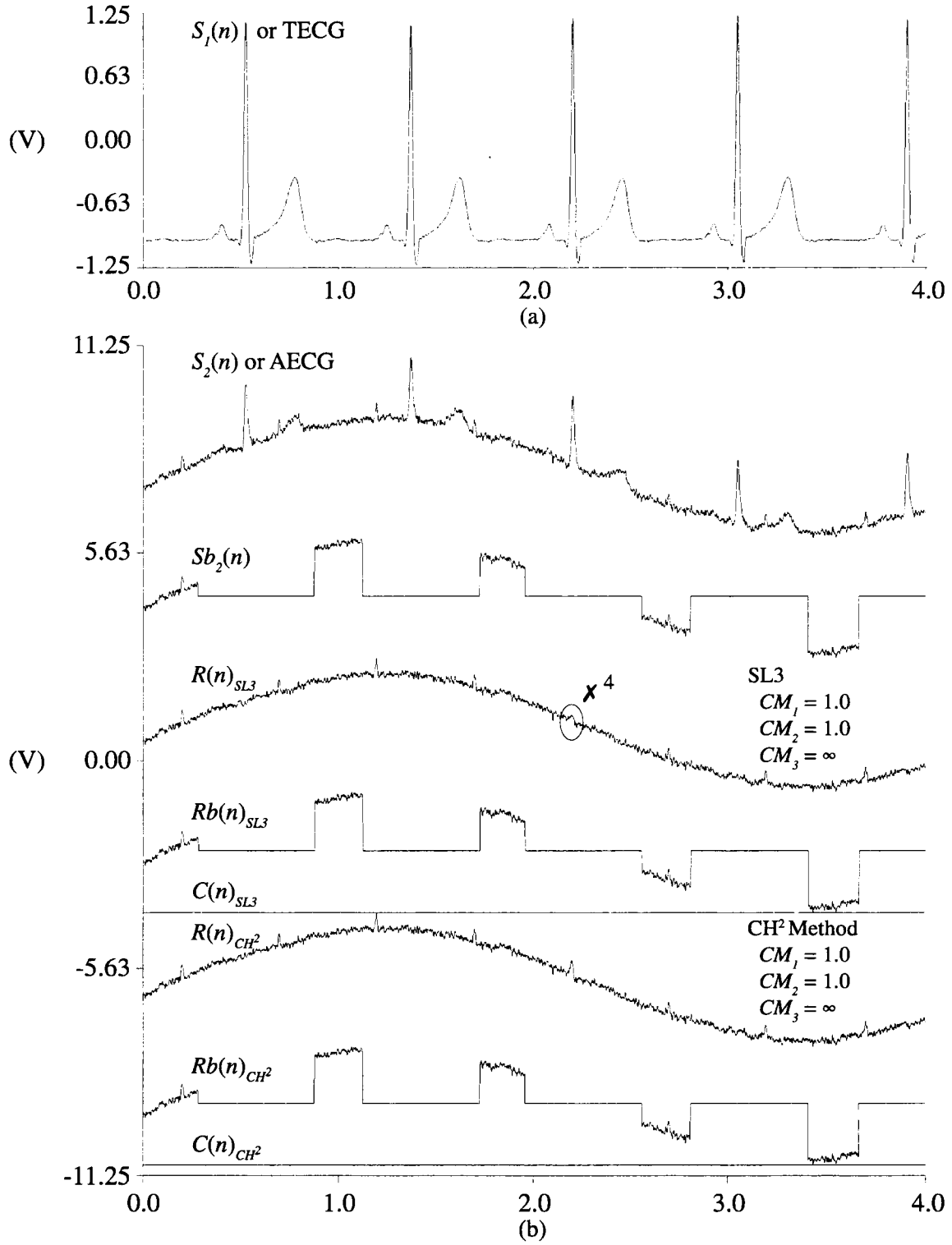

Figure H-2. Single lead method three vs. the CH² method demonstrating test condition five (all x-axes in seconds). (a) TECG or $S_1(n)$ used only with the CH² method. (b) AECG or $S_2(n)$, AECG blanked out during the MECG complexes or $Sb_2(n)$, and resulting AECGs comparing the two methods.

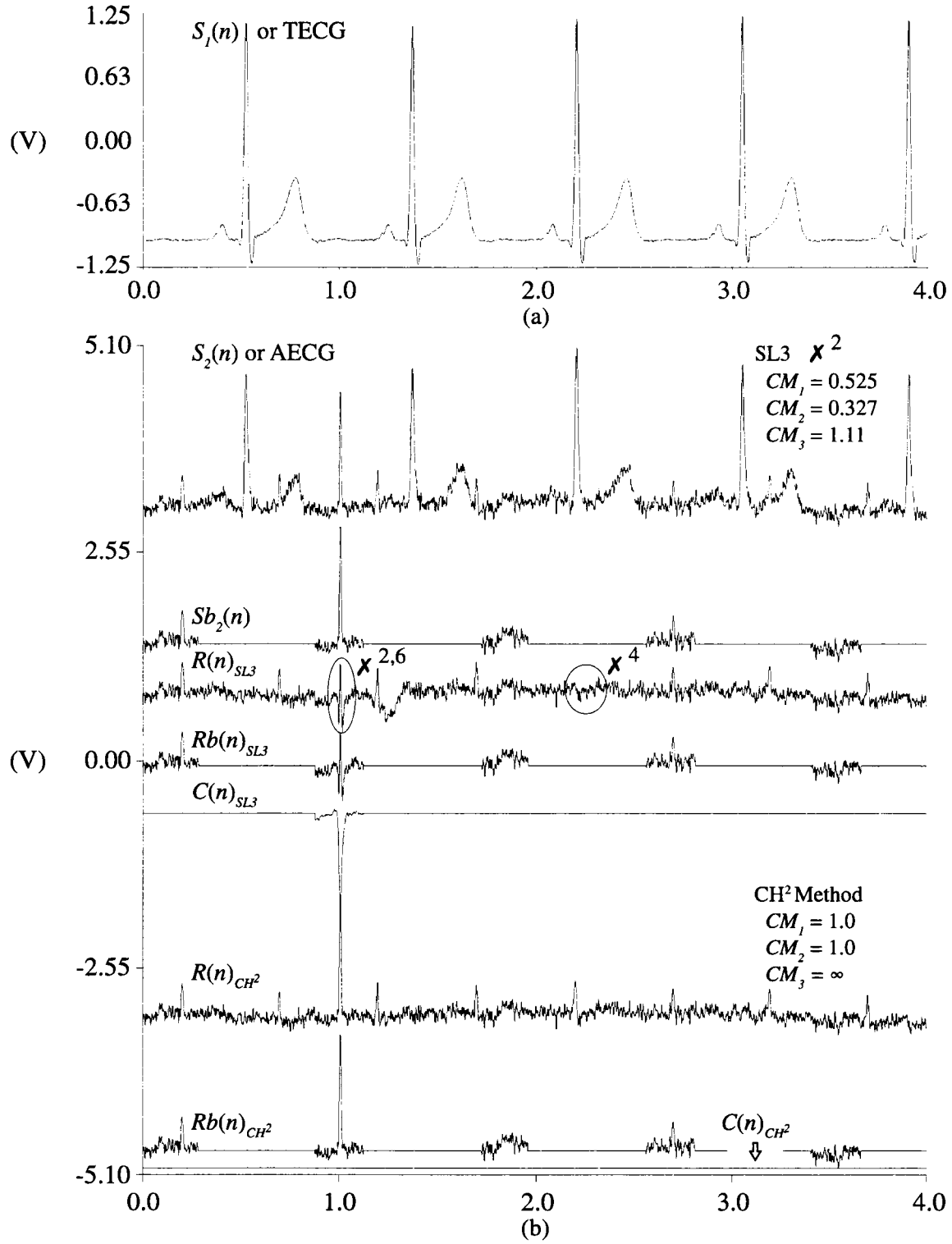

Figure H-3. Single lead method three vs. the CH² method demonstrating test condition six (all x-axes in seconds). (a) TECG or $S_1(n)$ used only with the CH² method. (b) AECG or $S_2(n)$, AECG blanked out during the MECG complexes or $Sb_2(n)$, and resulting AECGs comparing the two methods.

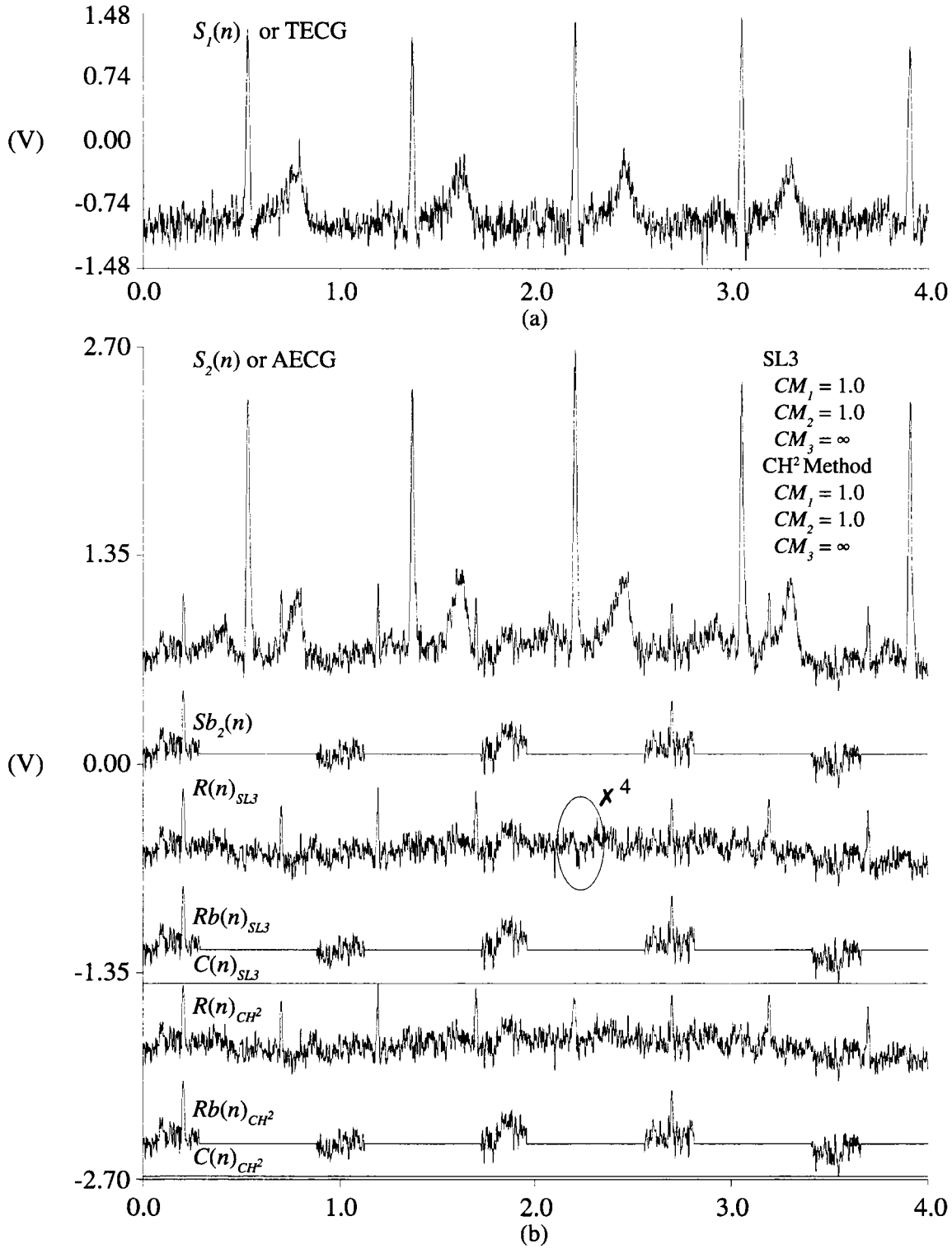

Figure H-4. Single lead method three vs. the CH² method demonstrating test condition seven (all x-axes in seconds). (a) TECG or $S_1(n)$ used only with the CH² method. (b) AECG or $S_2(n)$, AECG blanked out during the MECG complexes or $Sb_2(n)$, and resulting AECGs comparing the two methods.

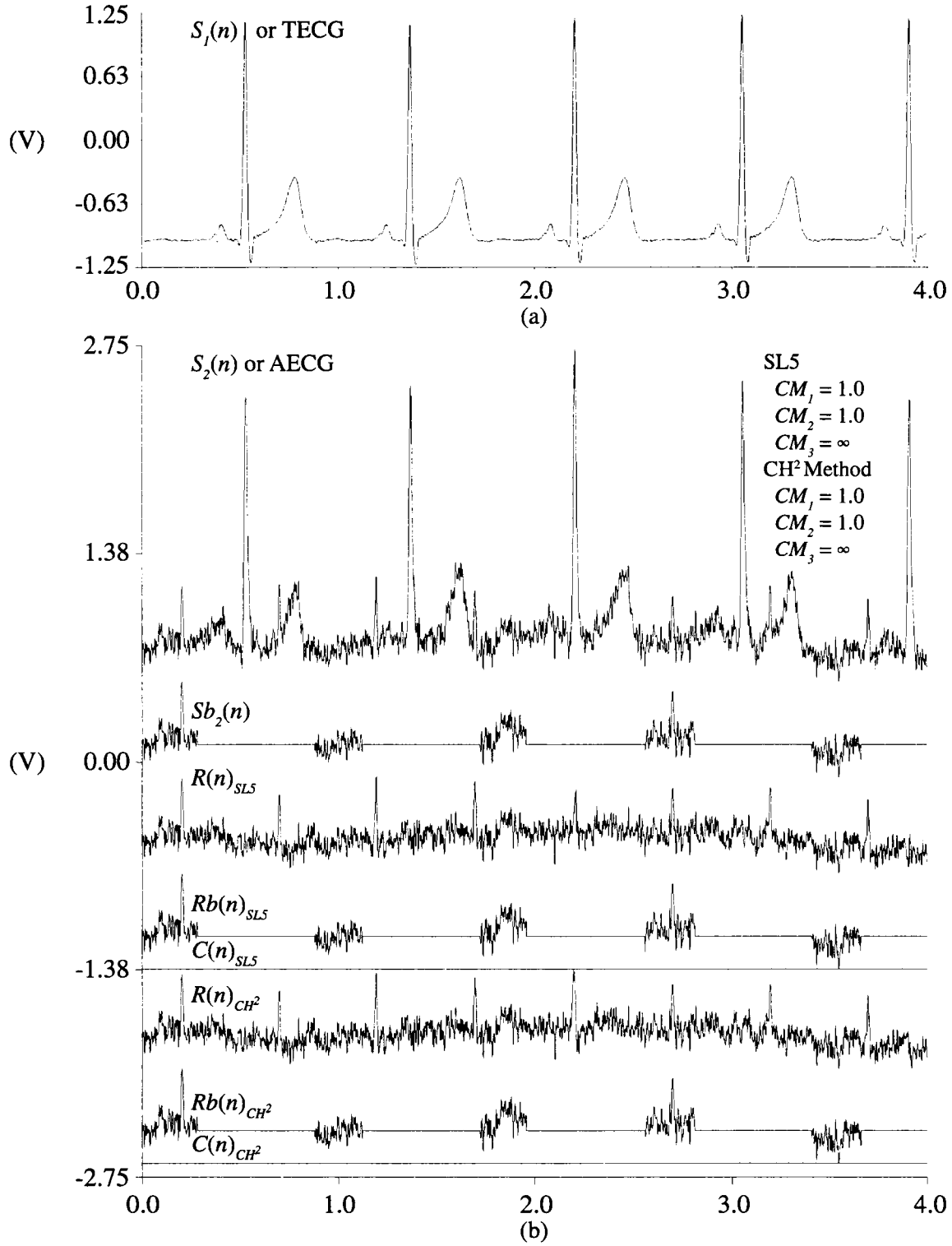

Figure H-5. Single lead method five vs. the CH² method demonstrating test condition four (all x-axes in seconds). (a) TECG or $S_1(n)$ used only with the CH² method. (b) AECG or $S_2(n)$, AECG blanked out during the MECG complexes or $Sb_2(n)$, and resulting AECGs comparing the two methods.

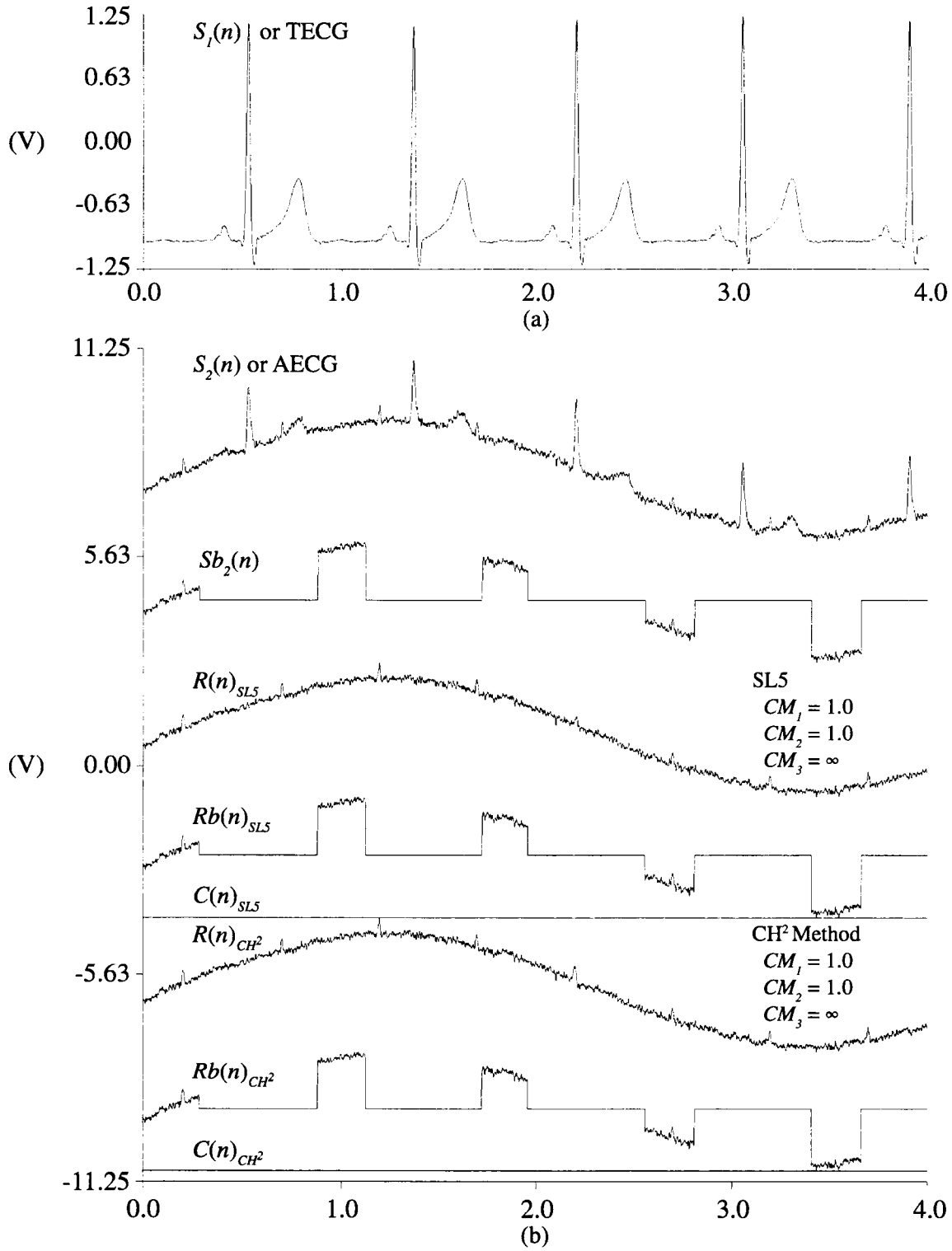

Figure H-6. Single lead method five vs. the CH² method demonstrating test condition five (all x-axes in seconds). (a) TECG or $S_1(n)$ used only with the CH² method. (b) AECG or $S_2(n)$, AECG blanked out during the MECG complexes or $Sb_2(n)$, and resulting AECGs comparing the two methods.

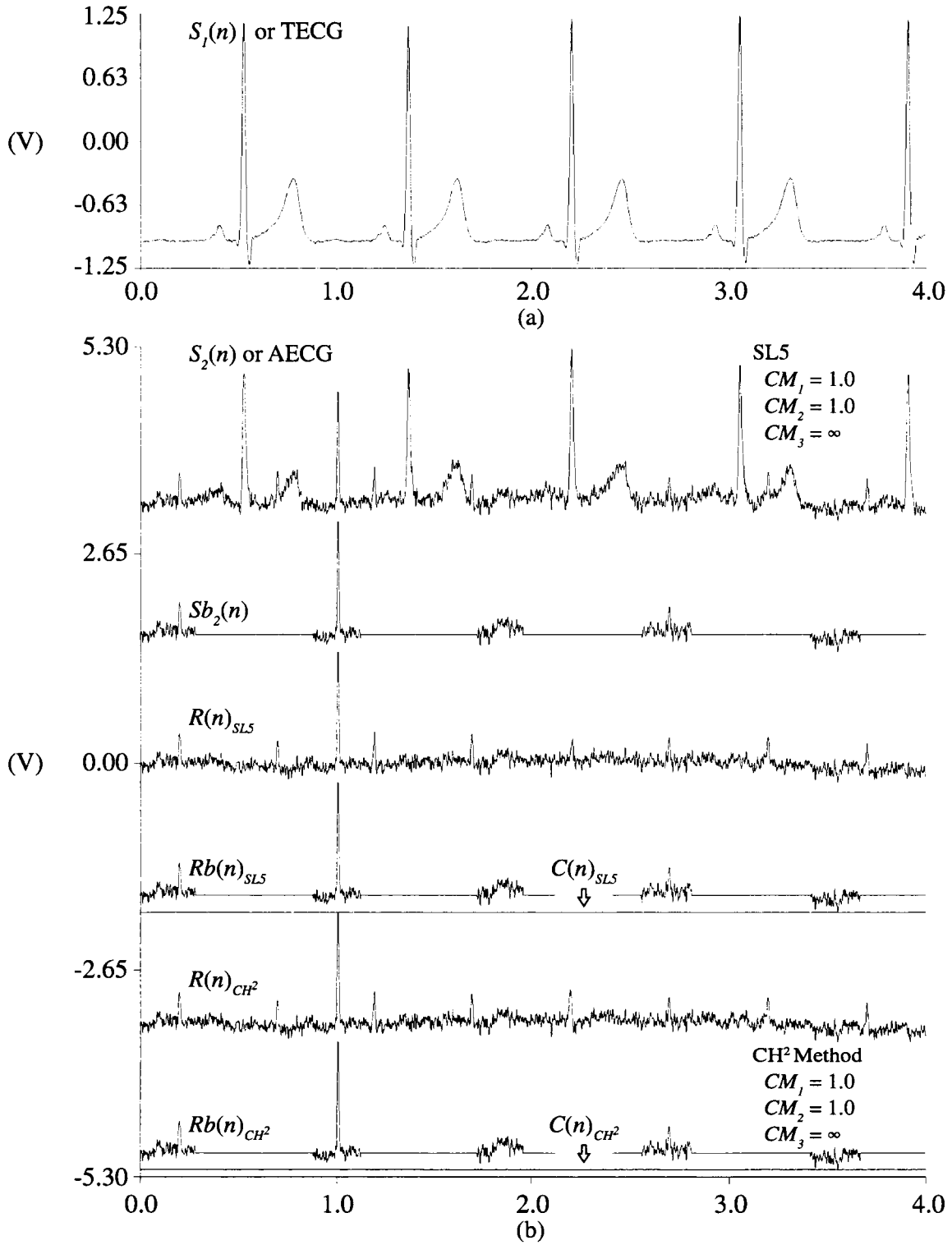

Figure H-7. Single lead method five vs. the CH^2 method demonstrating test condition six (all x-axes in seconds). (a) TECG or $S_1(n)$ used only with the CH^2 method. (b) AECG or $S_2(n)$, AECG blanked out during the MECG complexes or $Sb_2(n)$, and resulting AECGs comparing the two methods.

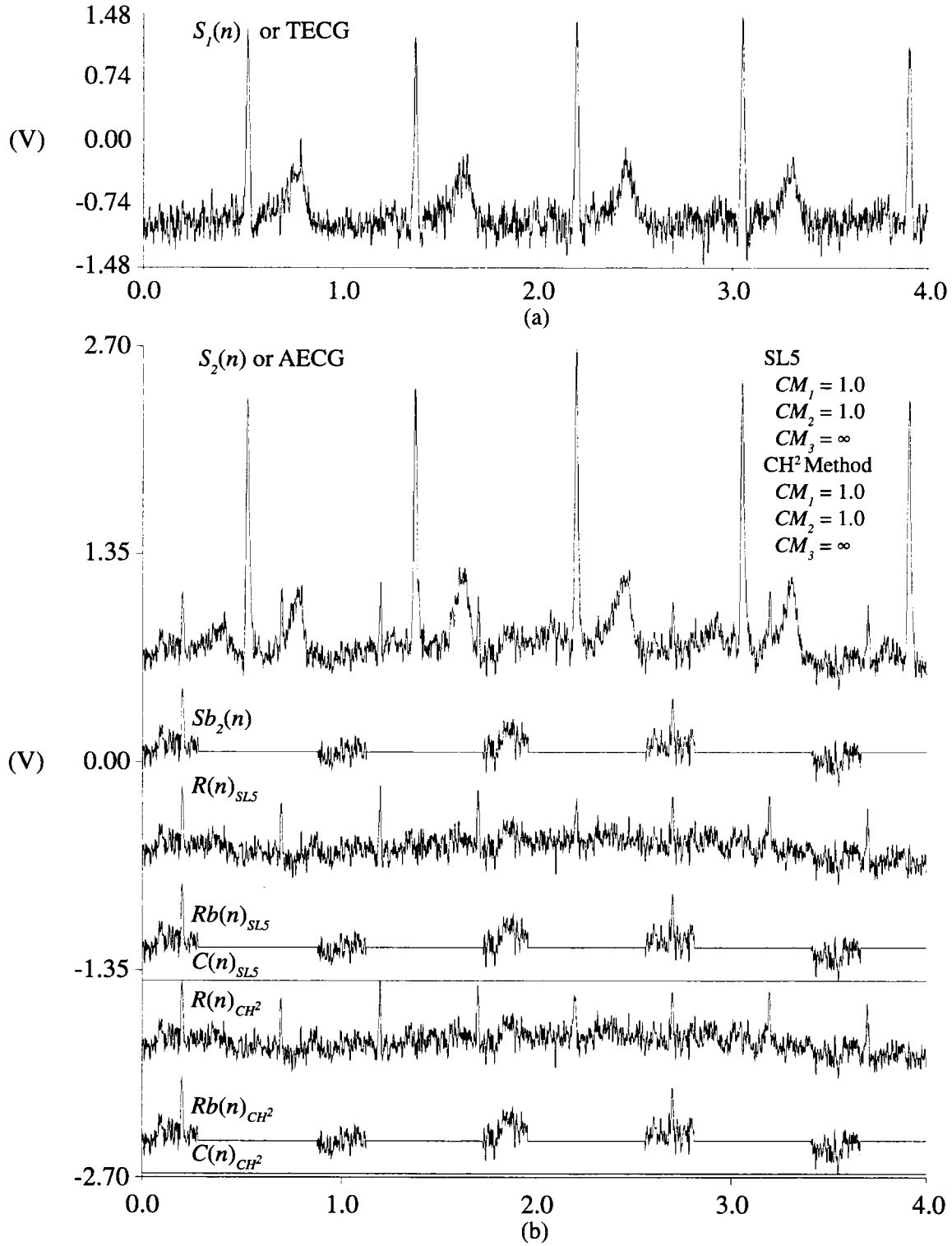

Figure H-8. Single lead method five vs. the CH² method demonstrating test condition seven (all x-axes in seconds). (a) TECG or $S_1(n)$ used only with the CH² method. (b) AECG or $S_2(n)$, AECG blanked out during the MECG complexes or $Sb_2(n)$, and resulting AECGs comparing the two methods.

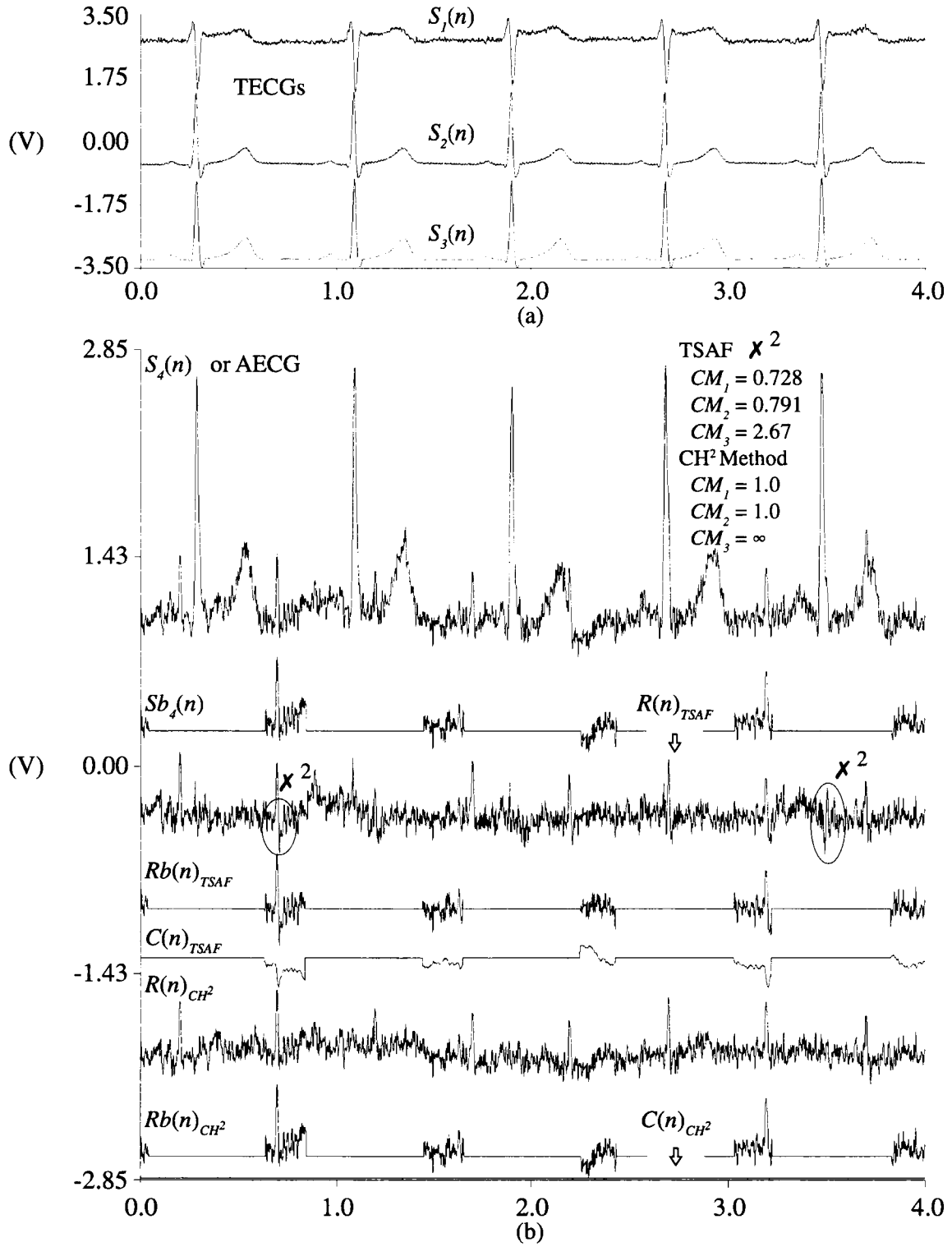

Figure H-9. Time-sequenced adaptive filter vs. the CH² method demonstrating test condition four (all x-axes in seconds). (a) TECGs where $S_3(n)$ is the trigger signal for the CH² method. (b) AECG or $S_4(n)$, AECG blanked out during the MECG complexes or $Sb_4(n)$, and resulting AECGs comparing the two methods.

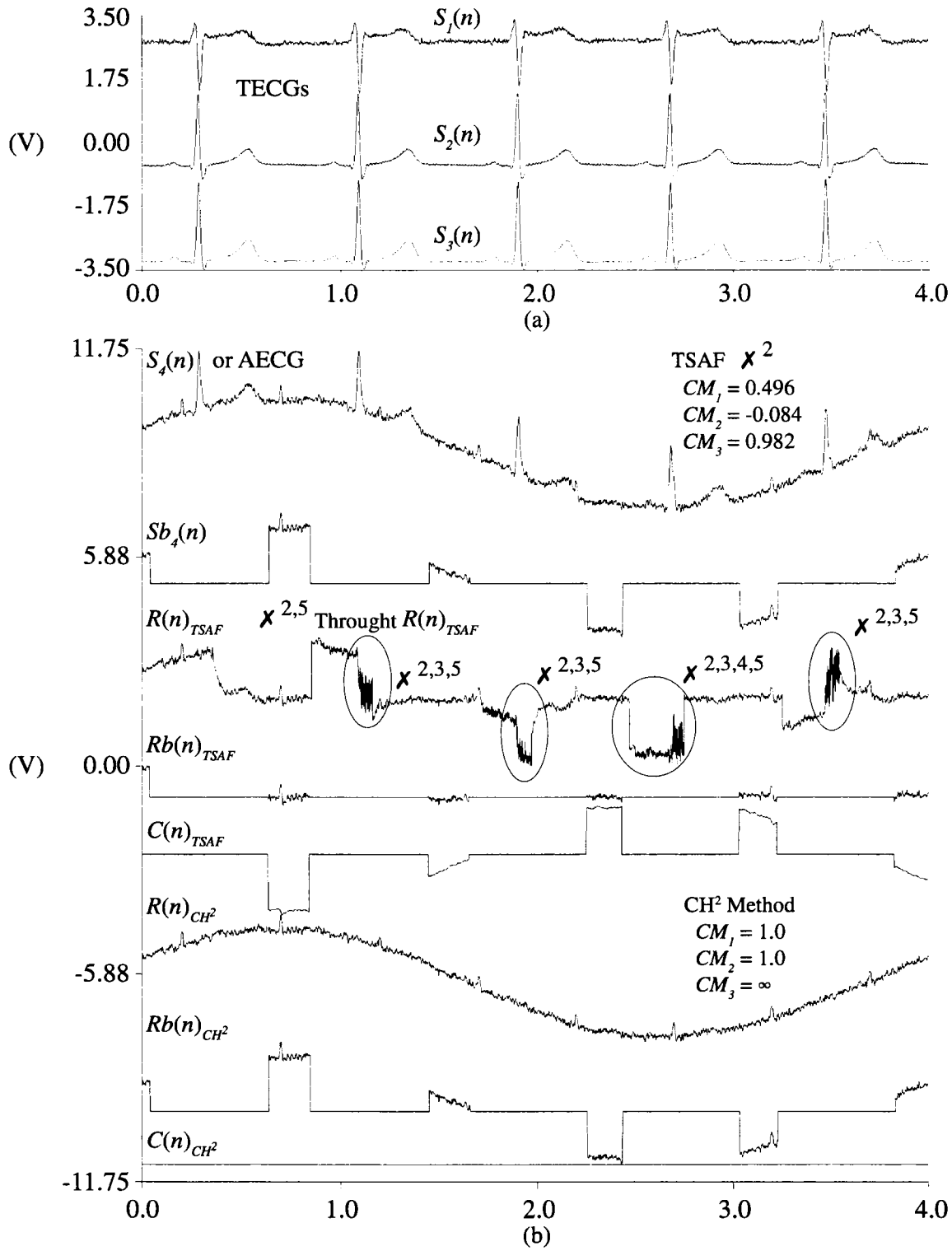

Figure H-10. Time-sequenced adaptive filter vs. the CH² method demonstrating test condition five (all x-axes in seconds). (a) TECGs where $S_3(n)$ is the trigger signal for the CH² method. (b) AECG or $S_4(n)$, AECG blanked out during the MECG complexes or $Sb_4(n)$, and resulting AECGs comparing the two methods.

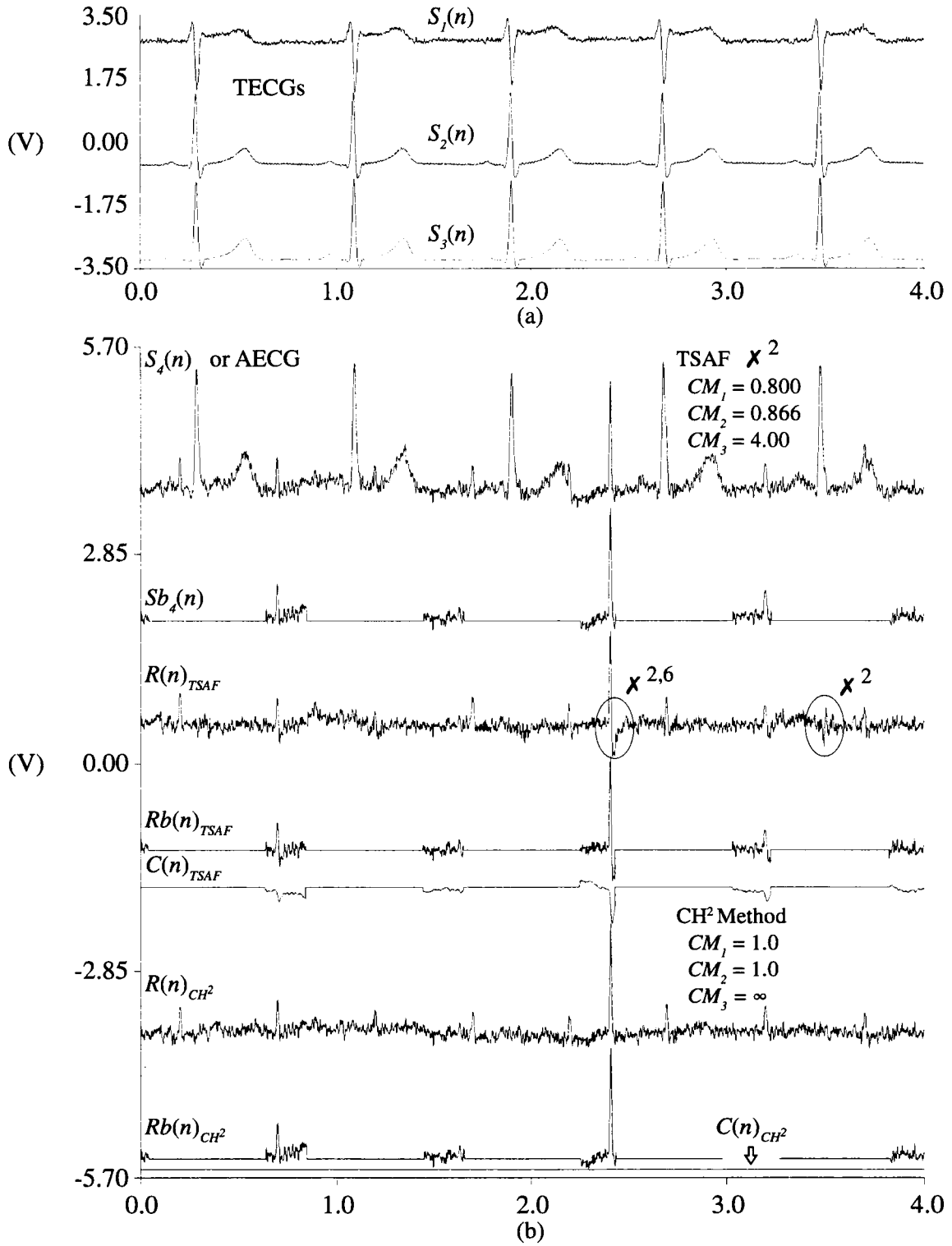

Figure H-11. Time-sequenced adaptive filter vs. the CH² method demonstrating test condition six (all x-axes in seconds). (a) TECGs where $S_3(n)$ is the trigger signal for the CH² method. (b) AECG or $S_4(n)$, AECG blanked out during the MECG complexes or $Sb_4(n)$, and resulting AECGs comparing the two methods.

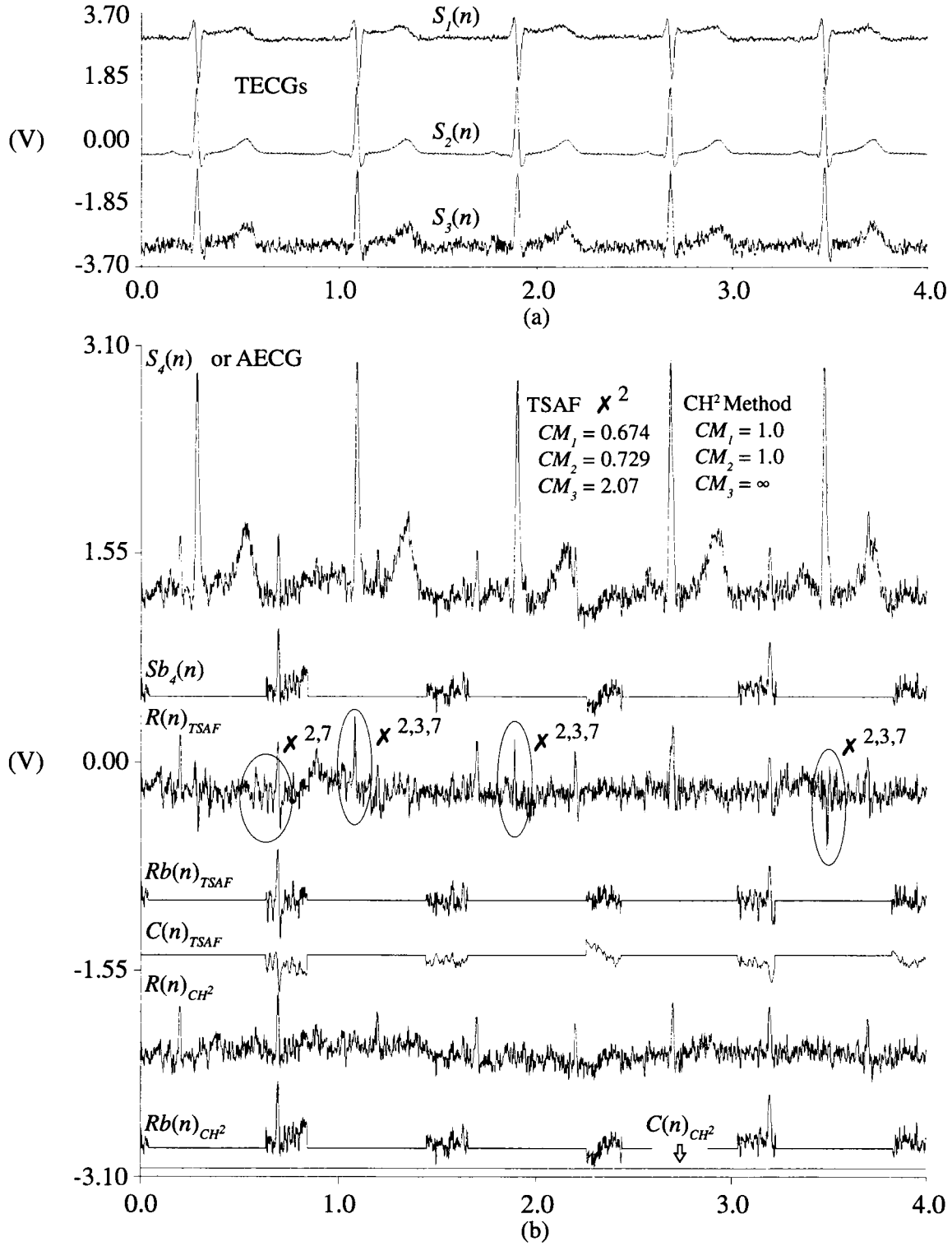

Figure H-12. Time-sequenced adaptive filter vs. the CH² method demonstrating test condition seven (all x-axes in seconds). (a) TECGs where $S_3(n)$ is the trigger signal for the CH² method. (b) AECG or $S_4(n)$, AECG blanked out during the MECG complexes or $Sb_4(n)$, and resulting AECGs comparing the two methods.

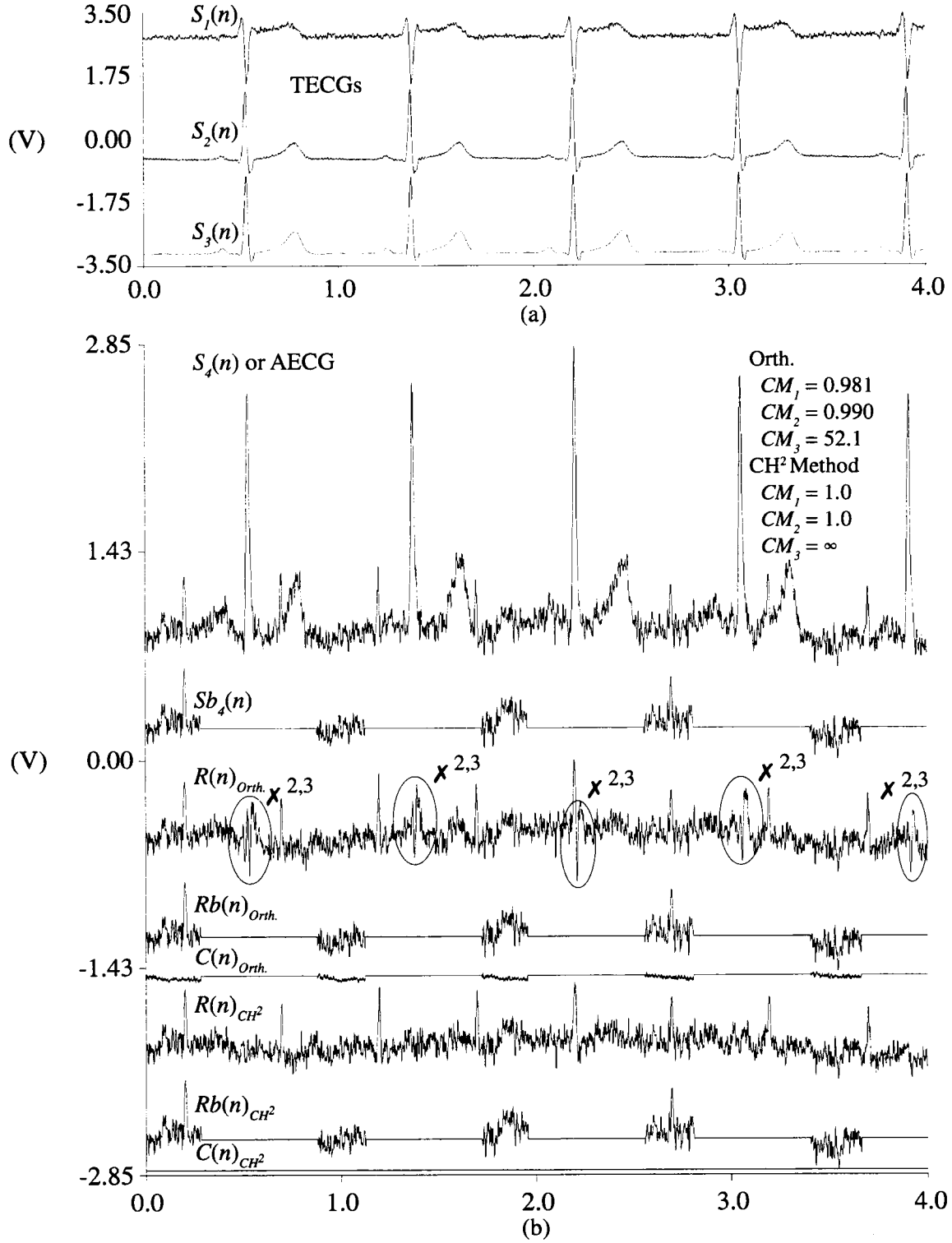

Figure H-13. Orthogonal basis vs. the CH² method demonstrating test condition four (all x-axes in seconds). (a) TECGs where $S_3(n)$ is the trigger signal for the CH² method. (b) AECG or $S_4(n)$, AECG blanked out during the MECG complexes or $Sb_4(n)$, and resulting AECGs comparing the two methods.

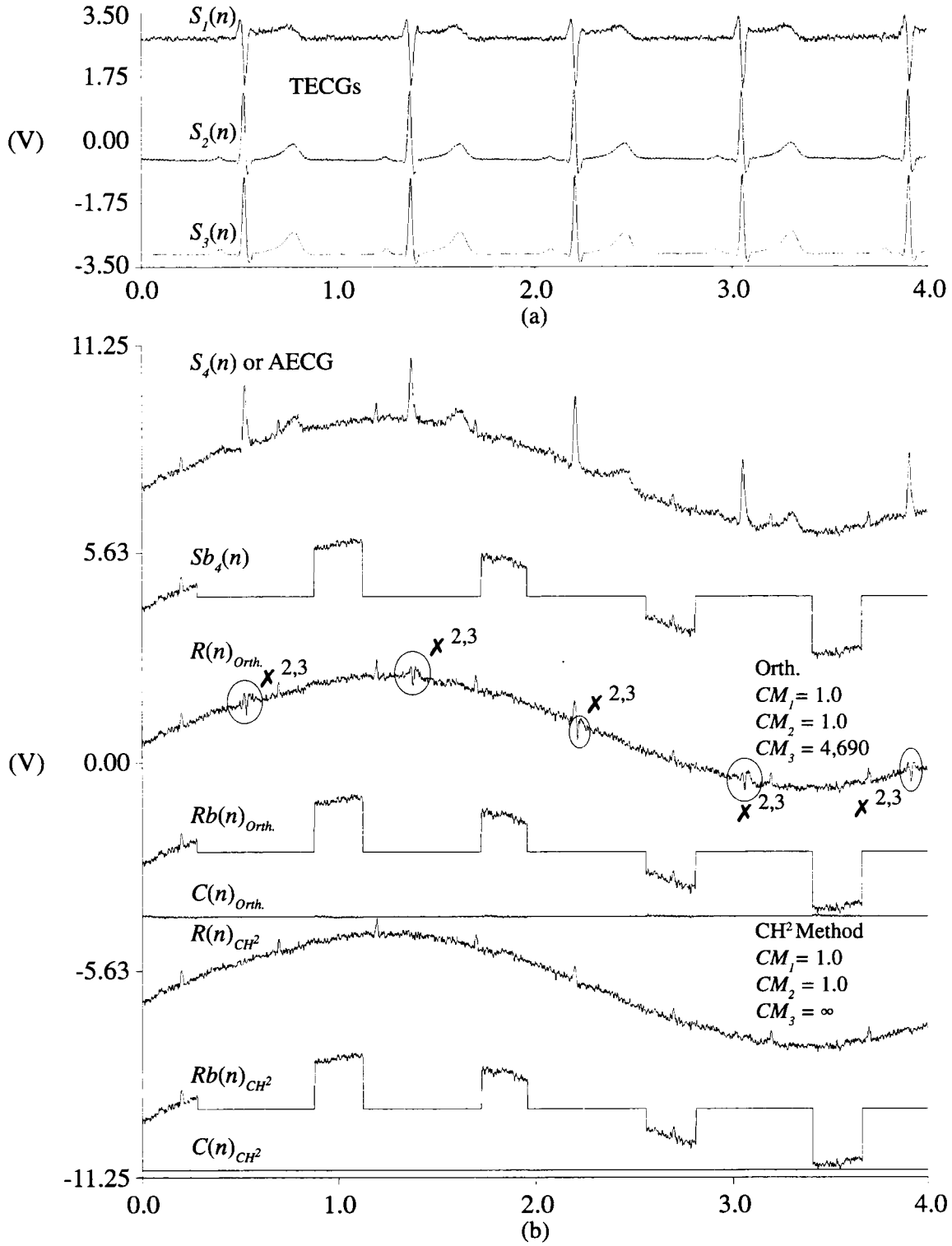

Figure H-14. Orthogonal basis vs. the CH^2 method demonstrating test condition five (all x-axes in seconds). (a) TECGs where $S_3(n)$ is the trigger signal for the CH^2 method. (b) AECG or $S_4(n)$, AECG blanked out during the MECG complexes or $Sb_4(n)$, and resulting AECGs comparing the two methods.

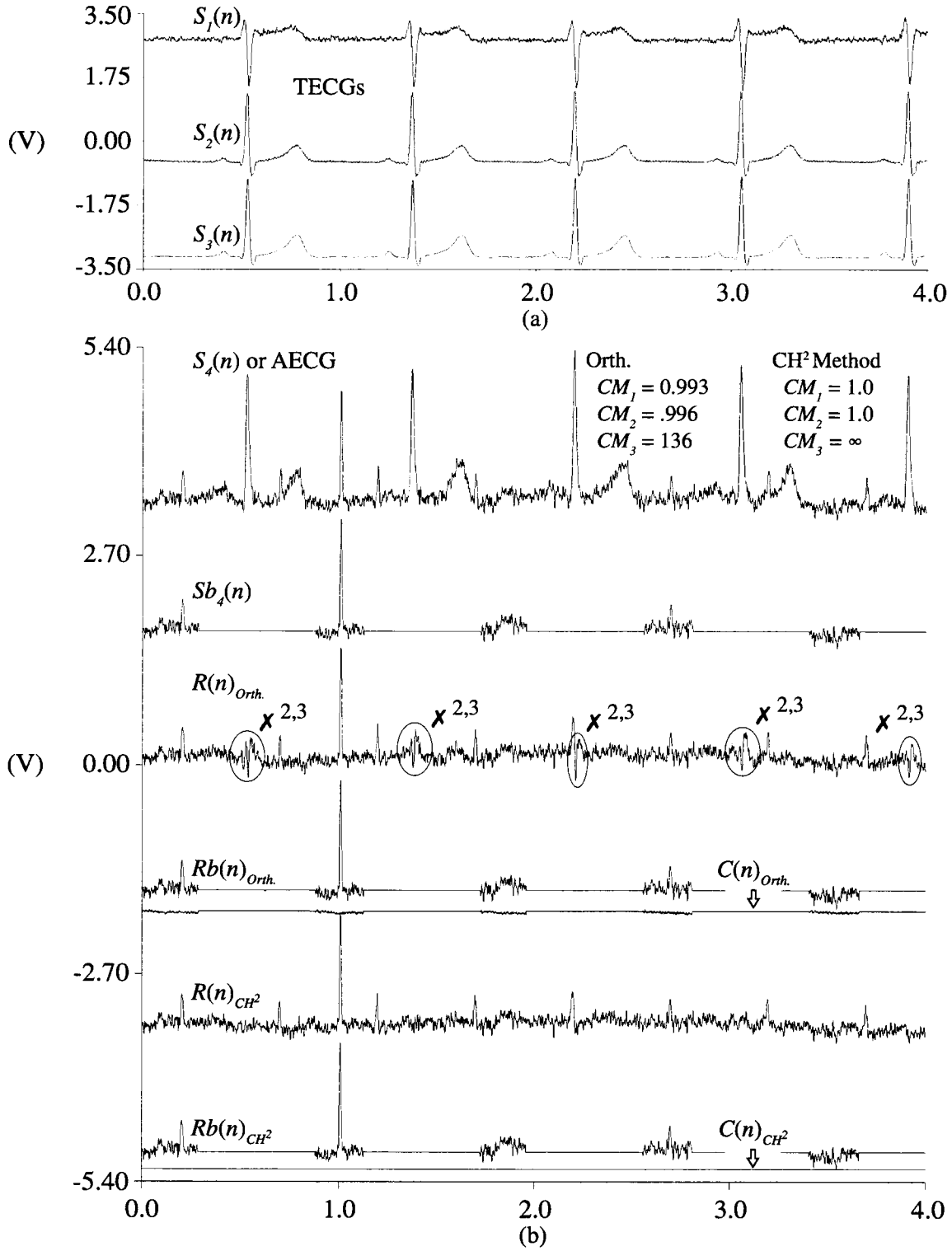

Figure H-15. Orthogonal basis vs. the CH² method demonstrating test condition six (all x-axes in seconds). (a) TECGs where $S_3(n)$ is the trigger signal for the CH² method. (b) AECG or $S_4(n)$, AECG blanked out during the MECG complexes or $Sb_4(n)$, and resulting AECGs comparing the two methods.

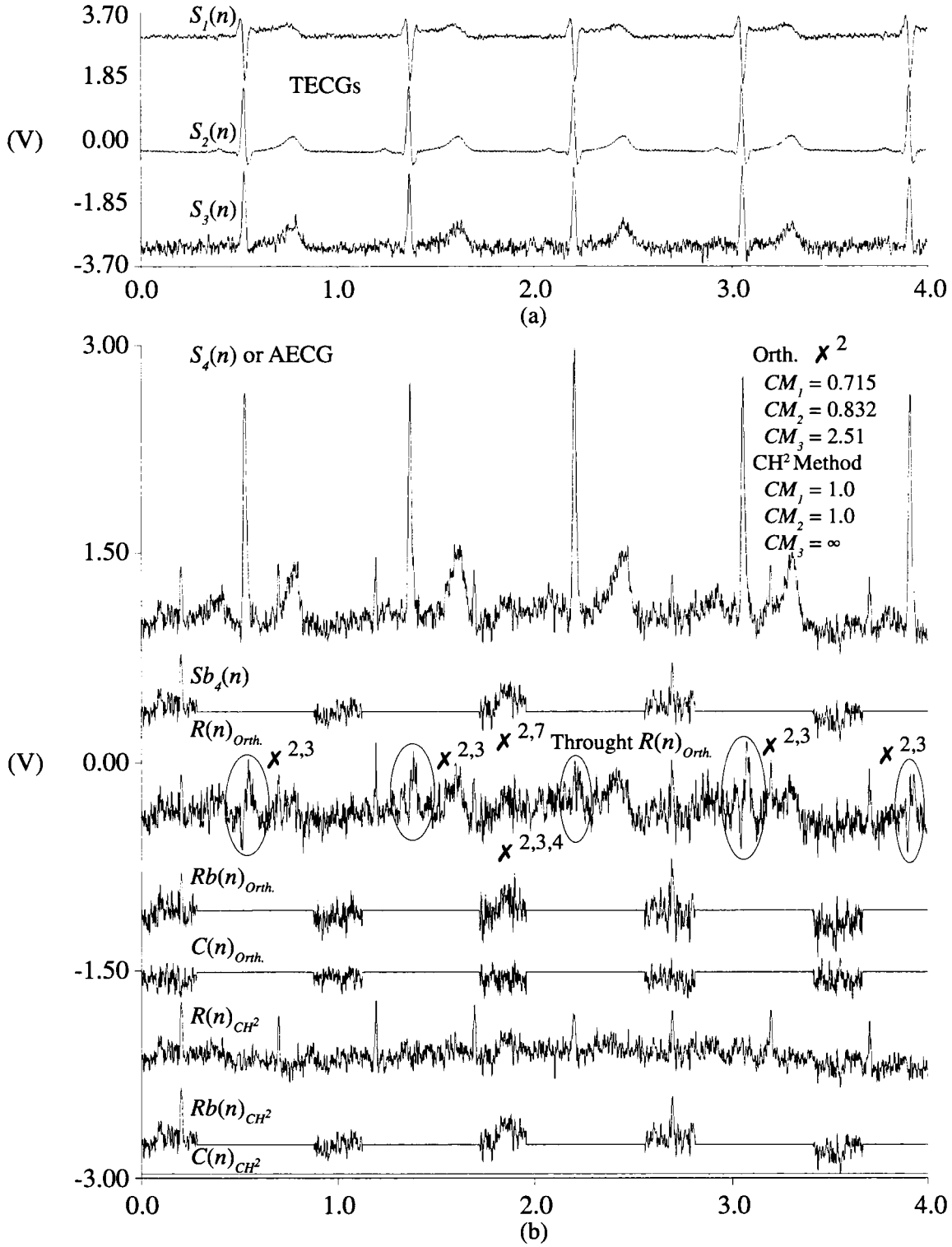

Figure H-16. Orthogonal basis vs. the CH² method demonstrating test condition seven (all x-axes in seconds). (a) TECGs where $S_3(n)$ is the trigger signal for the CH² method. (b) AECG or $S_4(n)$, AECG blanked out during the MECG complexes or $Sb_4(n)$, and resulting AECGs comparing the two methods.

APPENDIX

DISSERTATION GOAL III ANALYSIS II DATA

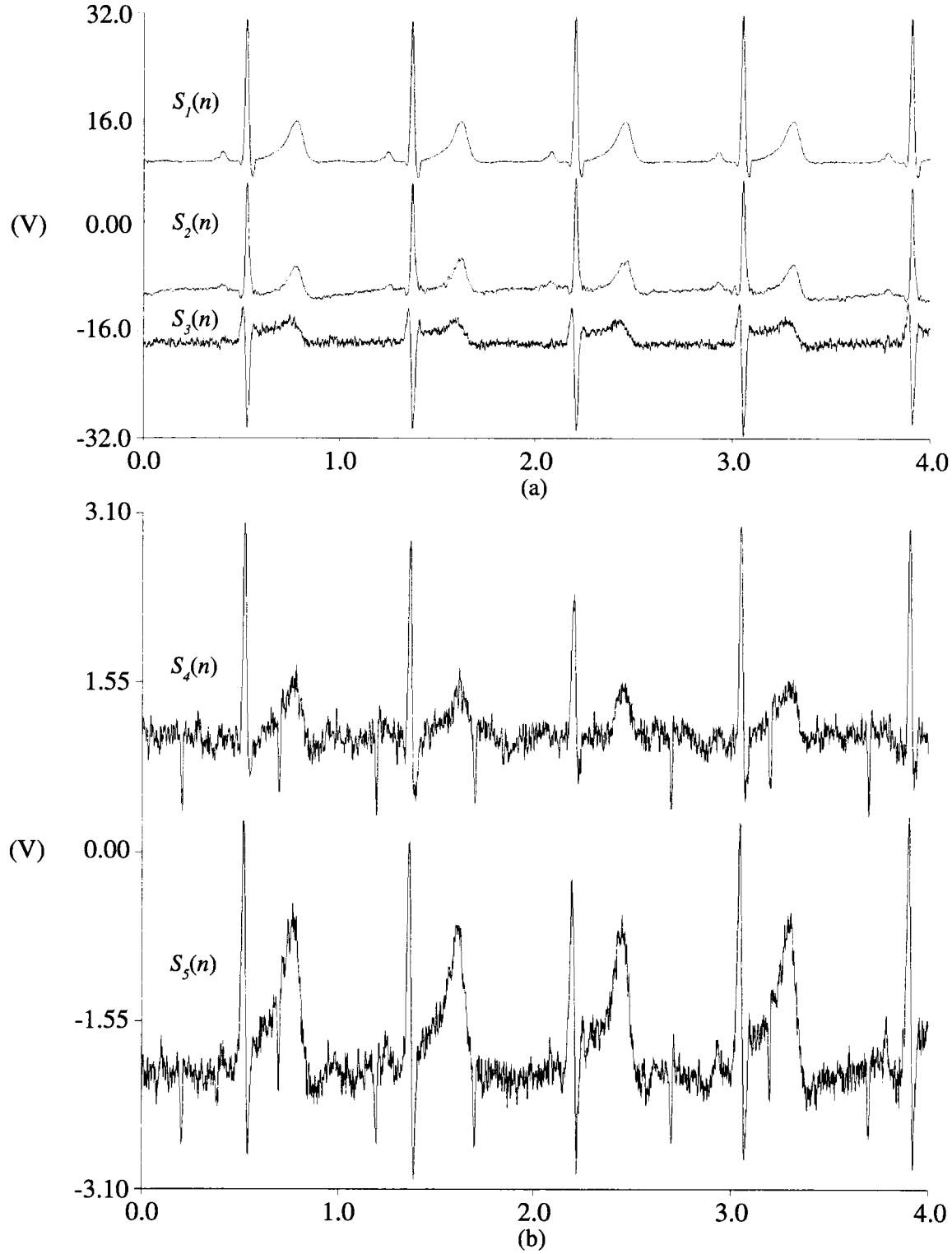

Figure I-1. ECG signals used to compare SVD method one and the CH² method (all x-axes in seconds). (a) Three TECG signals or $S_{1\text{-}3}(n)$. (b) Two AECG signals or $S_{4\text{-}5}(n)$.

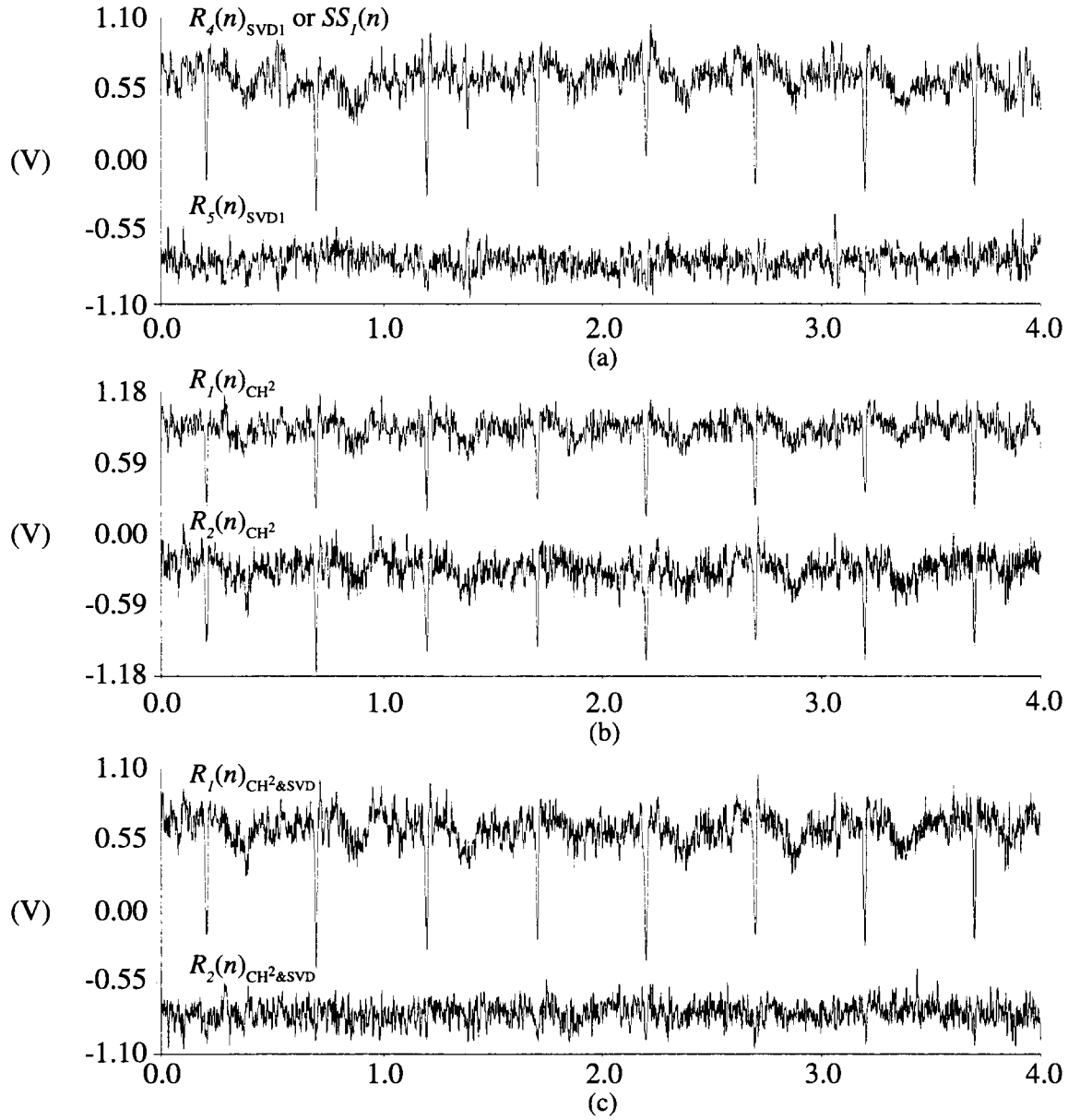

Figure I-2. SVD method one, CH^2, and CH^2 & SVD results demonstrating test condition four (all x-axes in seconds). (a) Resulting AECGs of SVD method one. (b) Resulting AECGs of the CH^2 method. (c) Resulting signals of CH^2 & SVD.

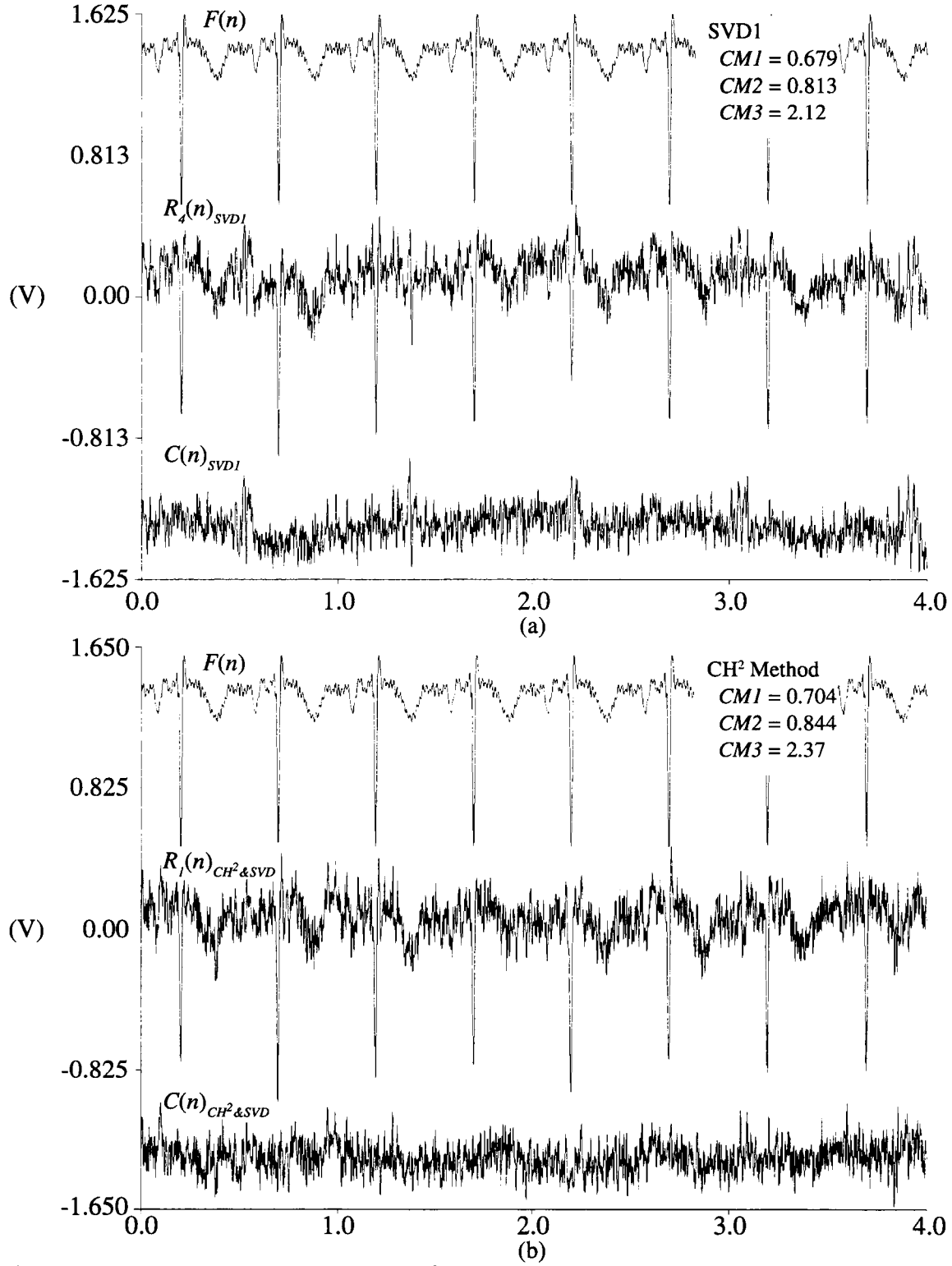

Figure I-3. SVD method one vs. the CH² method demonstrating test condition four (all x-axes in seconds). (a) Ideal FECG or $F(n)$, enhanced FECG via SVD1 or $R_4(n)_{SVD1}$, and noise corrupting $R_4(n)_{SVD1}$ or $C(n)_{SVD1}$. (b) Ideal FECG or $F(n)$, enhanced FECG via CH² & SVD or $R_1(n)_{CH^2\&SVD}$, and noise corrupting $R_1(n)_{CH^2\&SVD}$ or $C(n)_{CH^2\&SVD}$.

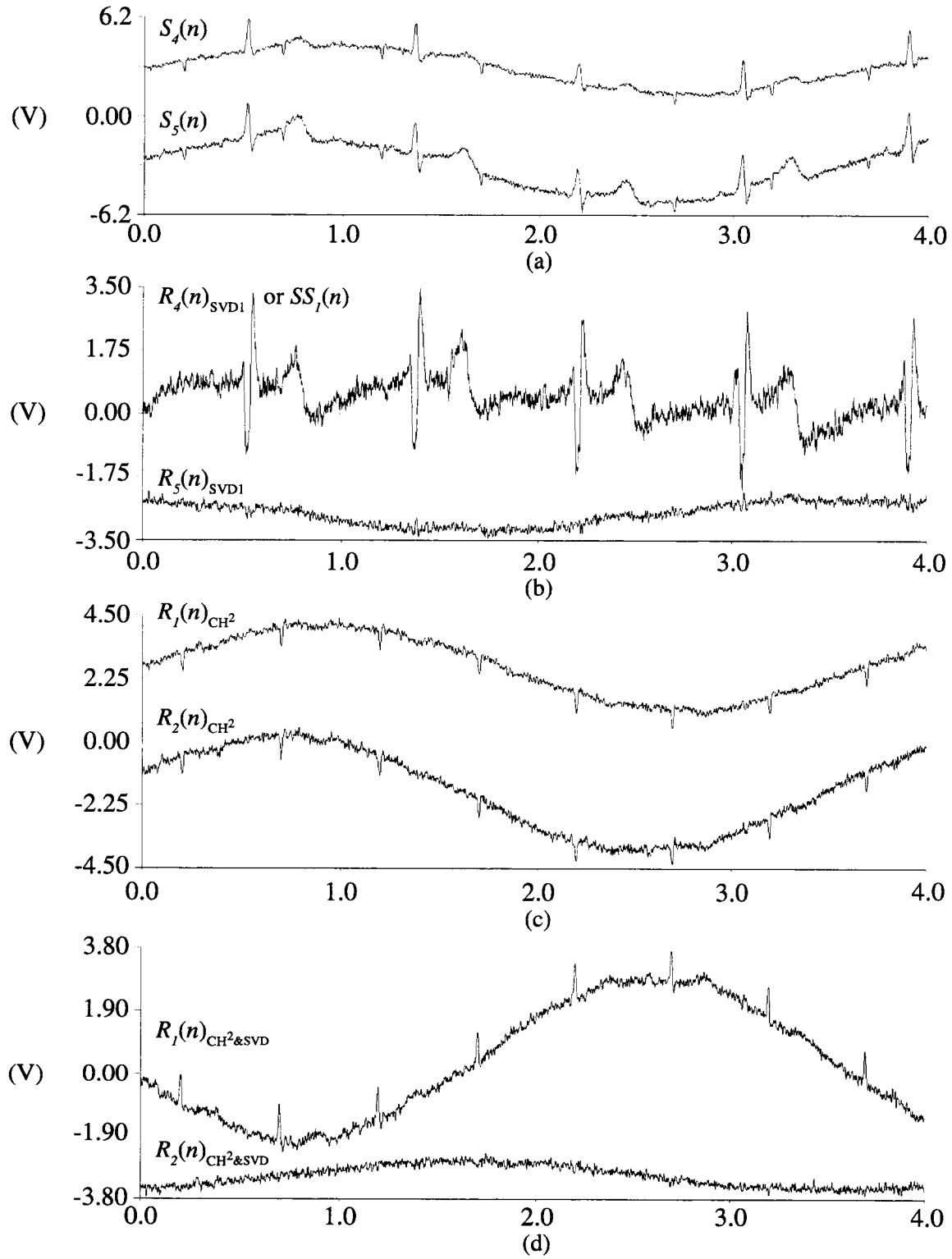

Figure I-4. SVD method one, CH^2, and CH^2 & SVD results demonstrating test condition five (all x-axes in seconds). (a) AECGs $S_{4\text{-}5}(n)$ with added low frequency noise. (b) Resulting AECGs of SVD method one. (c) Resulting AECGs of the CH^2 method. (d) Resulting signals of CH^2 & SVD.

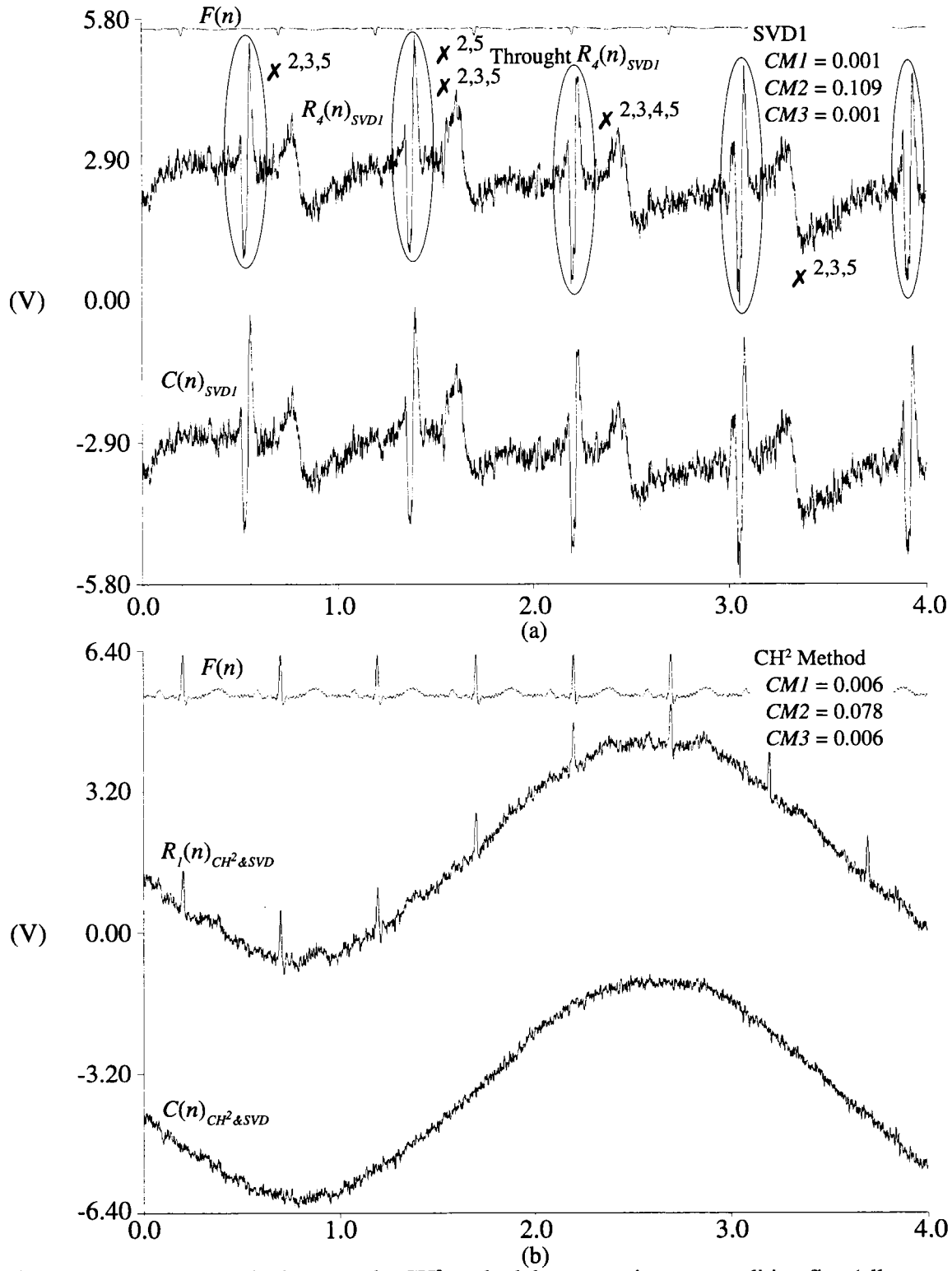

Figure I-5. SVD method one vs. the CH² method demonstrating test condition five (all x-axes in seconds). (a) Ideal FECG or $F(n)$, enhanced FECG via SVD1 or $R_4(n)_{SVD1}$, and noise corrupting $R_4(n)_{SVD1}$ or $C(n)_{SVD1}$. (b) Ideal FECG or $F(n)$, enhanced FECG via CH² & SVD or $R_1(n)_{CH^2\&SVD}$, and noise corrupting $R_1(n)_{CH^2\&SVD}$ or $C(n)_{CH^2\&SVD}$.

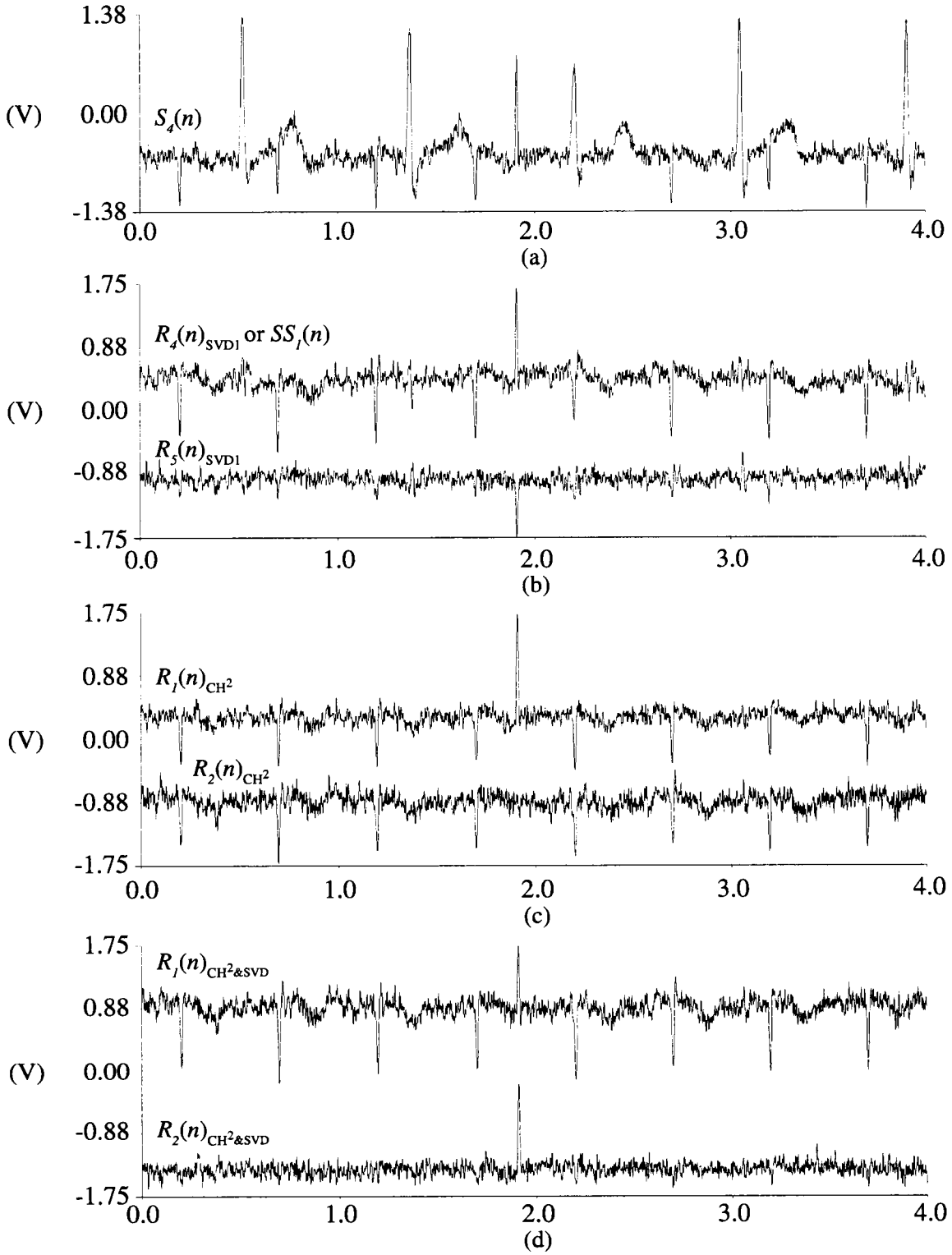

Figure I-6. SVD method one, CH^2, and CH^2 & SVD results demonstrating test condition six (all x-axes in seconds). (a) AECG $S_4(n)$ with an added noise spike. (b) Resulting AECGs of SVD method one. (c) Resulting AECGs of the CH^2 method. (d) Resulting signals of CH^2 & SVD.

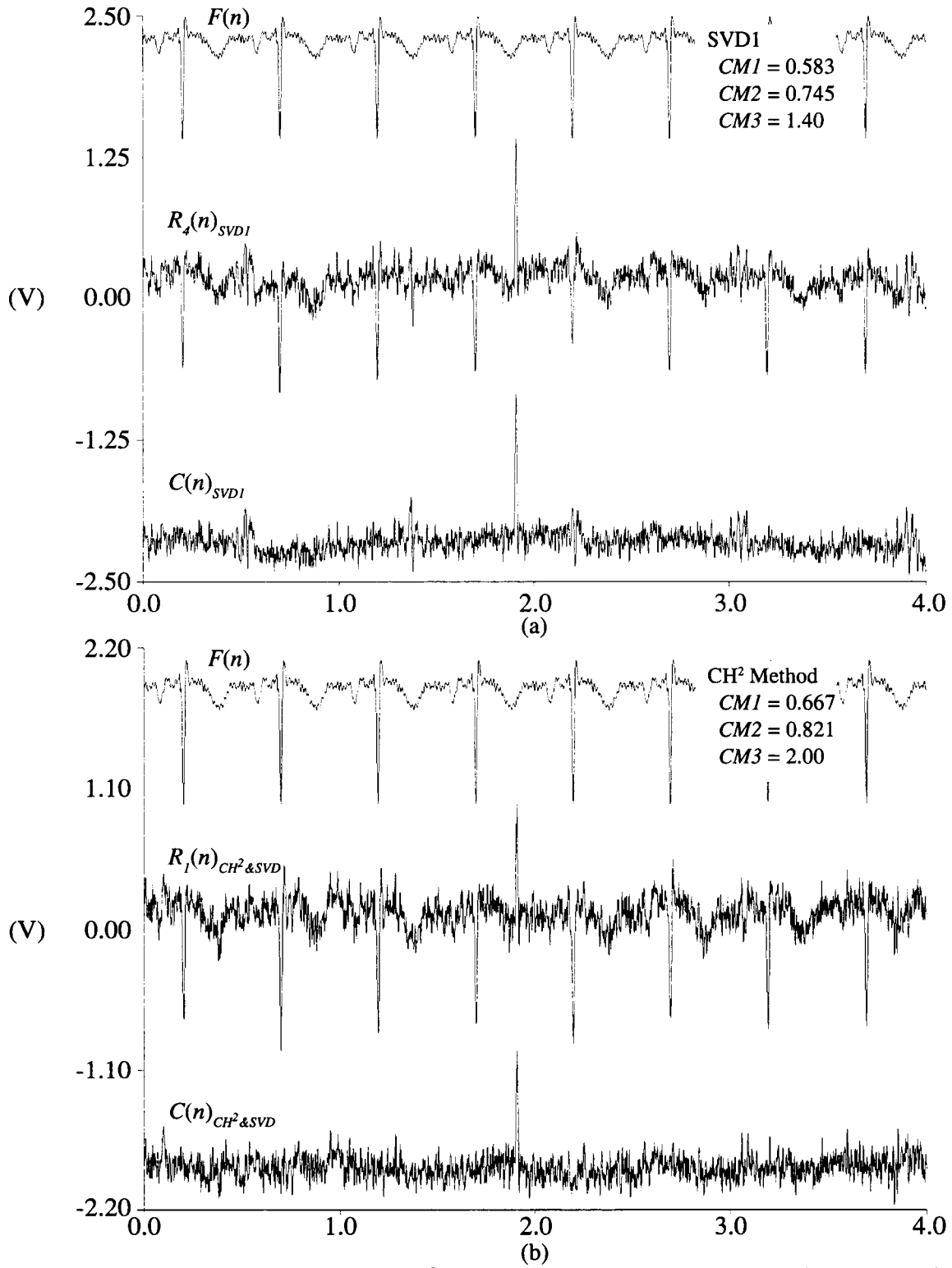

Figure I-7. SVD method one vs. the CH² method demonstrating test condition six (all x-axes in seconds). (a) Ideal FECG or $F(n)$, enhanced FECG via SVD1 or $R_4(n)_{SVD1}$, and noise corrupting $R_4(n)_{SVD1}$ or $C(n)_{SVD1}$. (b) Ideal FECG or $F(n)$, enhanced FECG via CH² & SVD or $R_1(n)_{CH^2\&SVD}$, and noise corrupting $R_1(n)_{CH^2\&SVD}$ or $C(n)_{CH^2\&SVD}$.

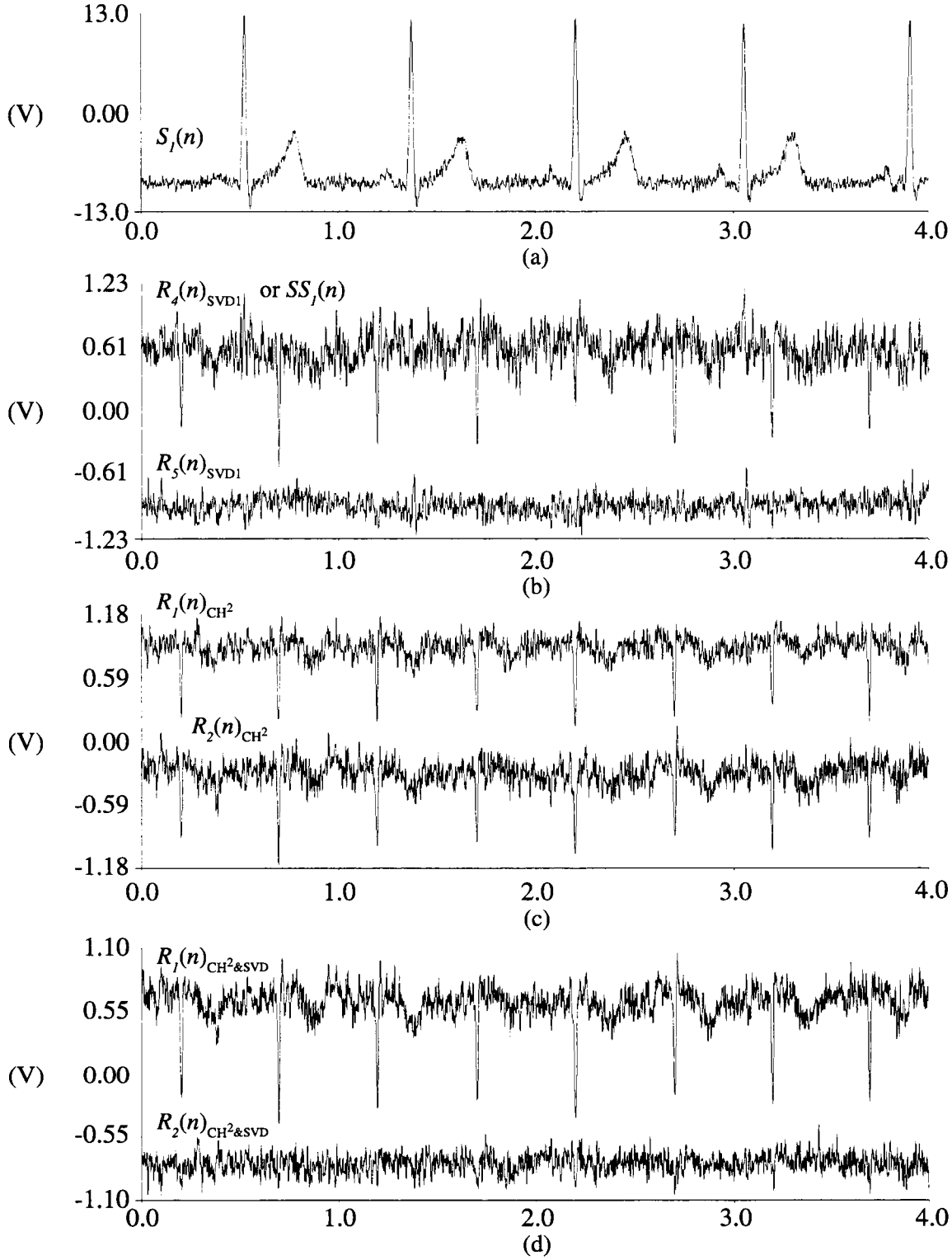

Figure I-8. SVD method one, CH^2, and CH^2 & SVD results demonstrating test condition seven (all x-axes in seconds). (a) TECG $S_1(n)$ with added noise. (b) Resulting AECGs of SVD method one. (c) Resulting AECGs of the CH^2 method. (d) Resulting signals of CH^2 & SVD.

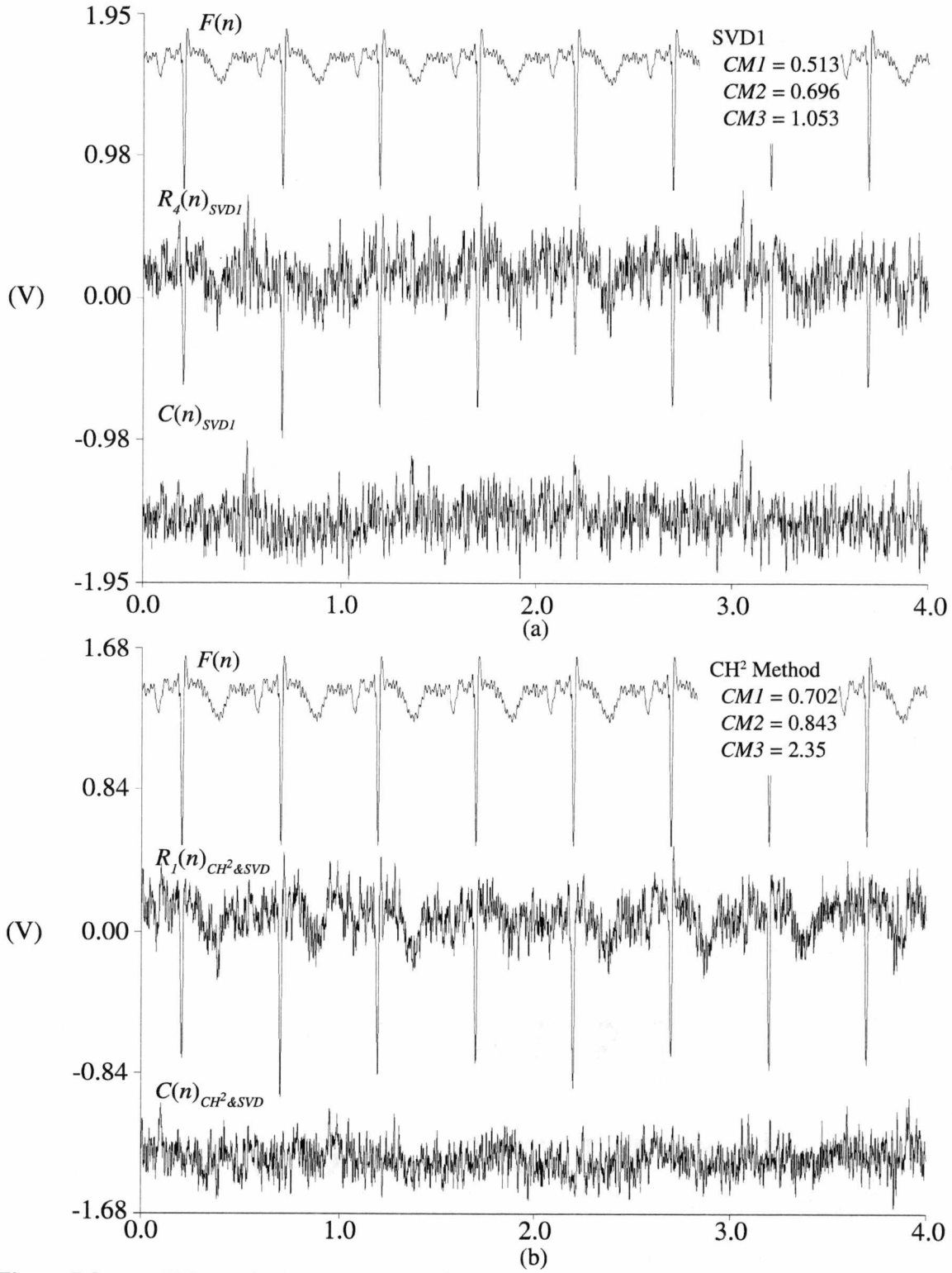

Figure I-9. SVD method one vs. the CH² method demonstrating test condition seven (all x-axes in seconds). (a) Ideal FECG or $F(n)$, enhanced FECG via SVD1 or $R_4(n)_{SVD1}$, and noise corrupting $R_4(n)_{SVD1}$ or $C(n)_{SVD1}$. (b) Ideal FECG or $F(n)$, enhanced FECG via CH² & SVD or $R_1(n)_{CH^2\&SVD}$, and noise corrupting $R_1(n)_{CH^2\&SVD}$ or $C(n)_{CH^2\&SVD}$.

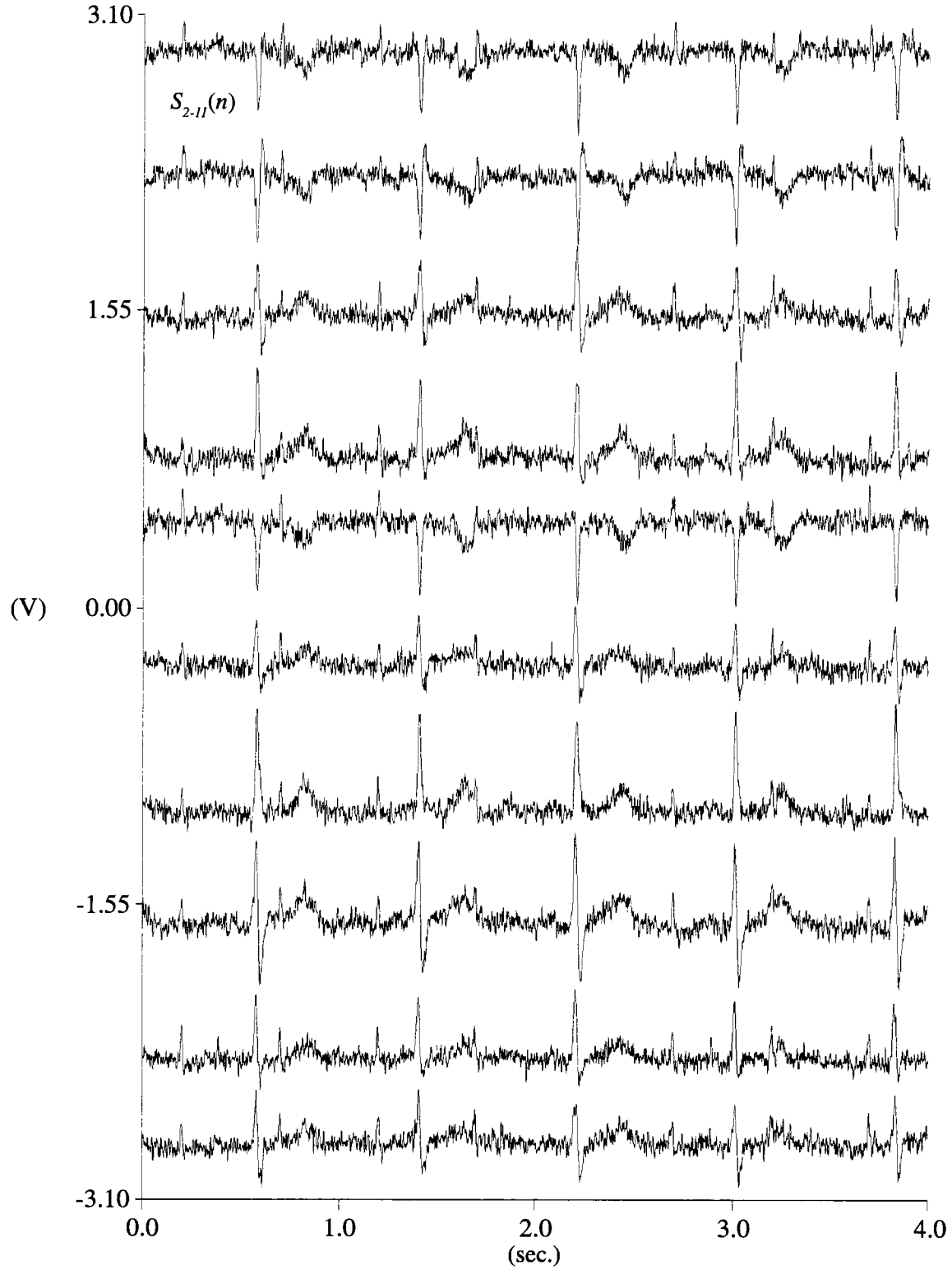

Figure I-10. AECG signals $S_{2\text{-}II}(n)$ used to compare SVD method two and the CH^2 method.

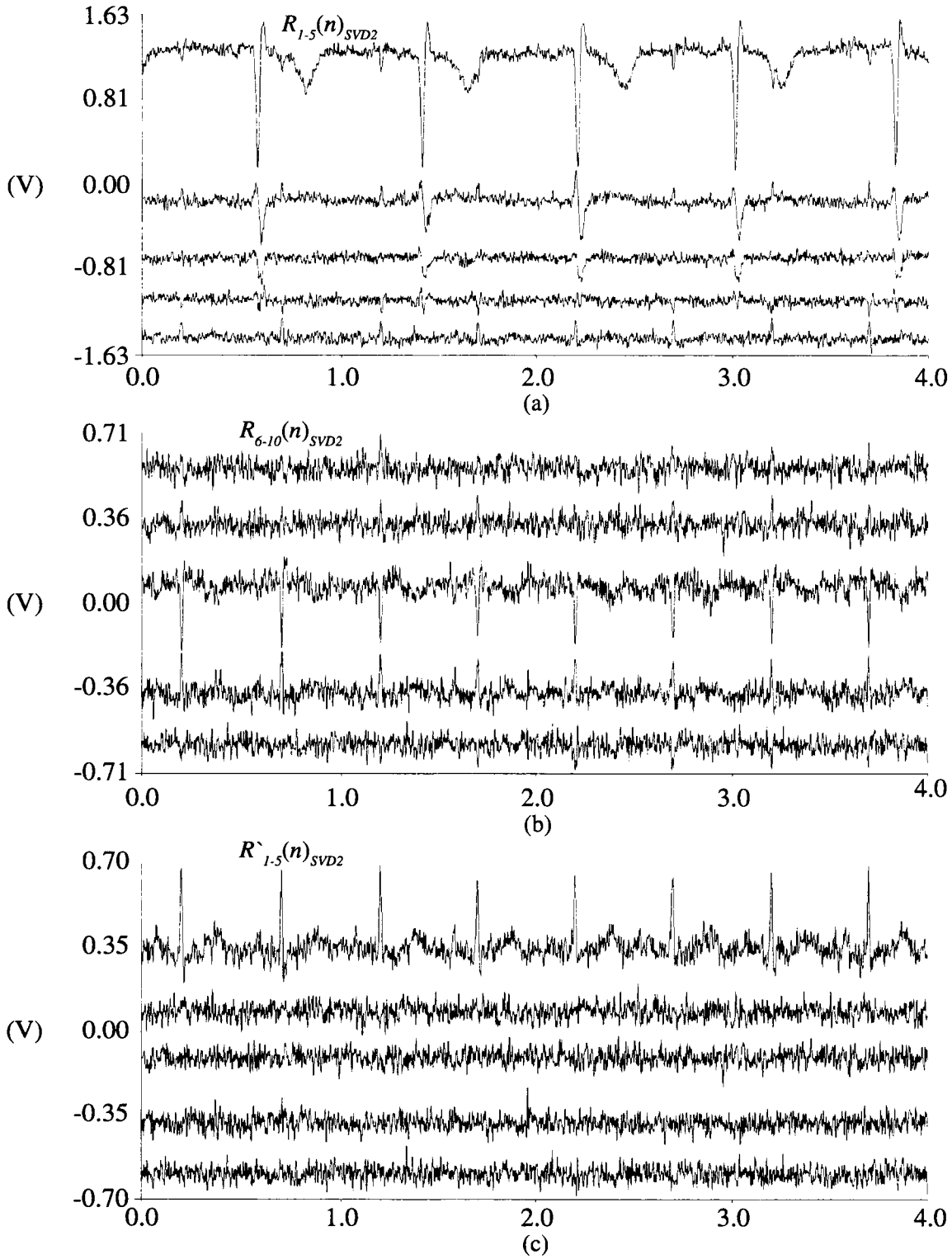

Figure I-11. SVD method two results demonstrating test condition four (all x-axes in seconds). (a) Resulting ECGs $R_{1\text{-}5}(n)_{SVD2}$ of SVD method two. (b) Resulting ECGs $R_{6\text{-}10}(n)_{SVD2}$ of SVD method two. (c) Resulting ECGs of SVD method two or $R`_{1\text{-}5}(n)_{SVD2}$.

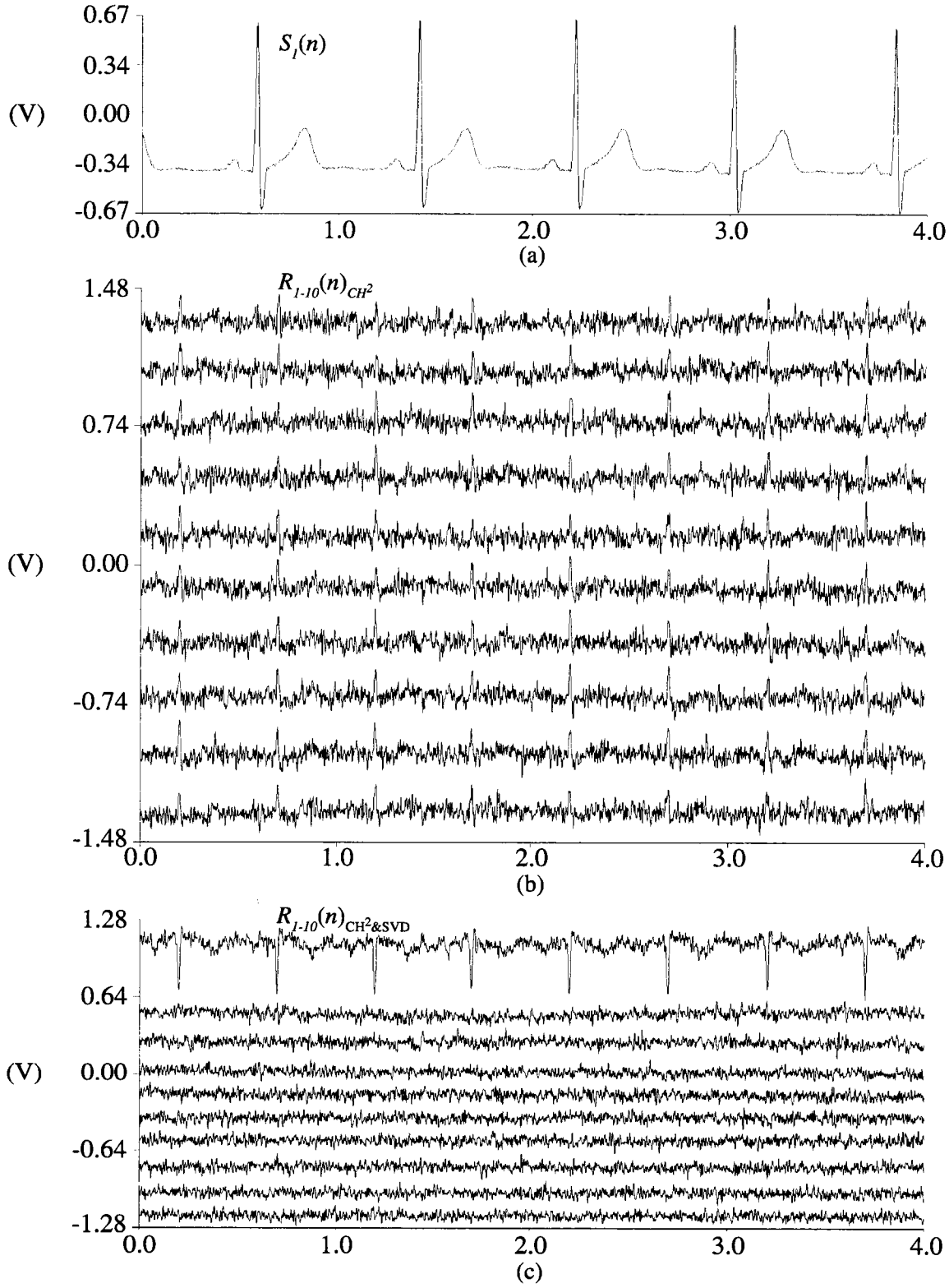

Figure I-12. Results of the CH² method demonstrating test condition four (all x-axes in seconds). (a) TECG $S_1(n)$ used only with the CH² method. (b) Resulting AECGs of the CH² method or $R_{1\text{-}10}(n)_{CH^2}$. (c) Resulting signals of CH² & SVD or $R_{1\text{-}10}(n)_{CH^2\&SVD}$.

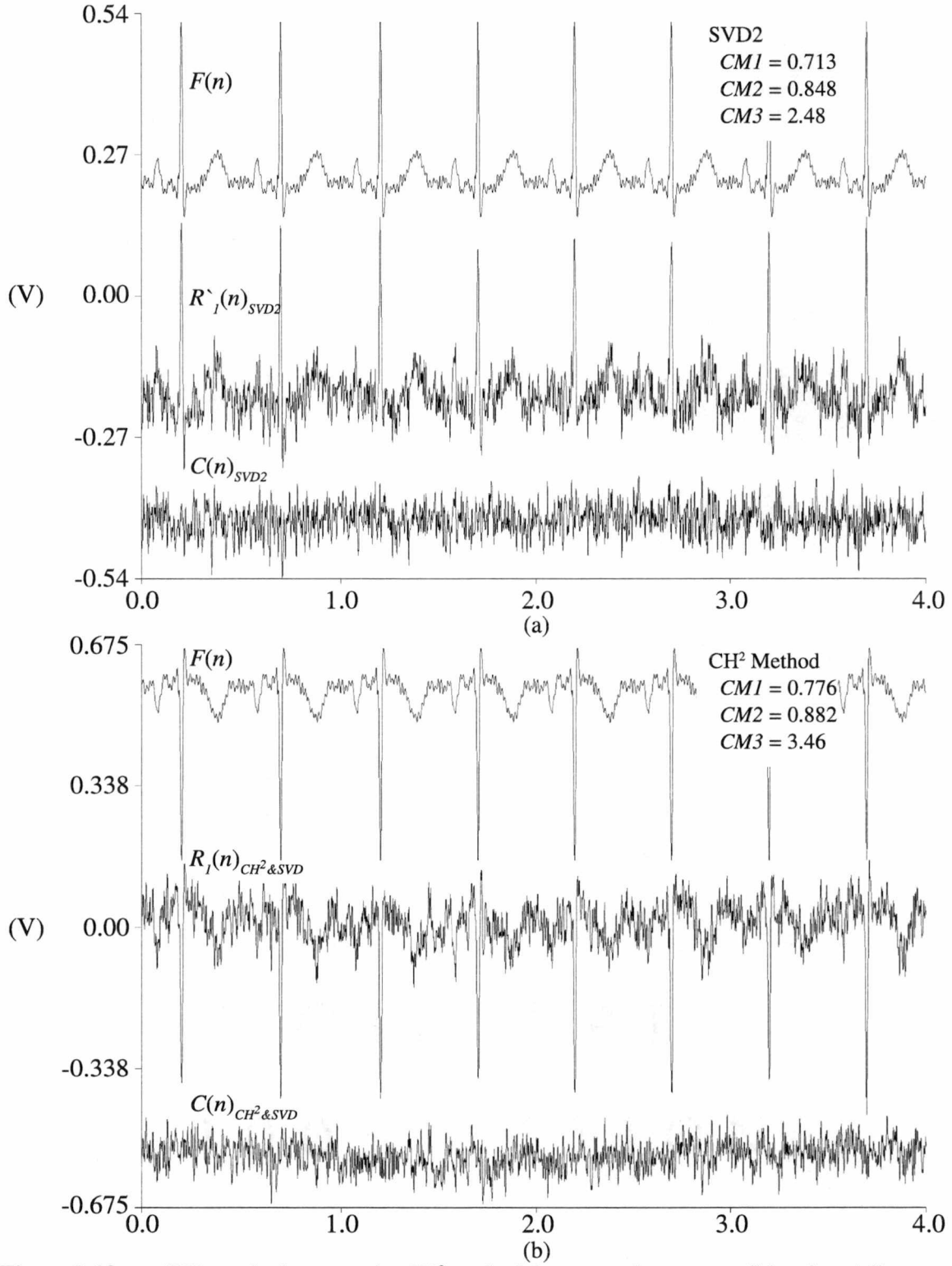

Figure I-13. SVD method two vs. the CH² method demonstrating test condition four (all x-axes in seconds). (a) Ideal FECG or $F(n)$, enhanced FECG via SVD2 or $R`_1(n)_{SVD2}$, and noise corrupting $R`_1(n)_{SVD2}$ or $C(n)_{SVD2}$. (b) Ideal FECG or $F(n)$, enhanced FECG via CH² & SVD or $R_1(n)_{CH^2\&SVD}$, and noise corrupting $R_1(n)_{CH^2\&SVD}$ or $C(n)_{CH^2\&SVD}$.

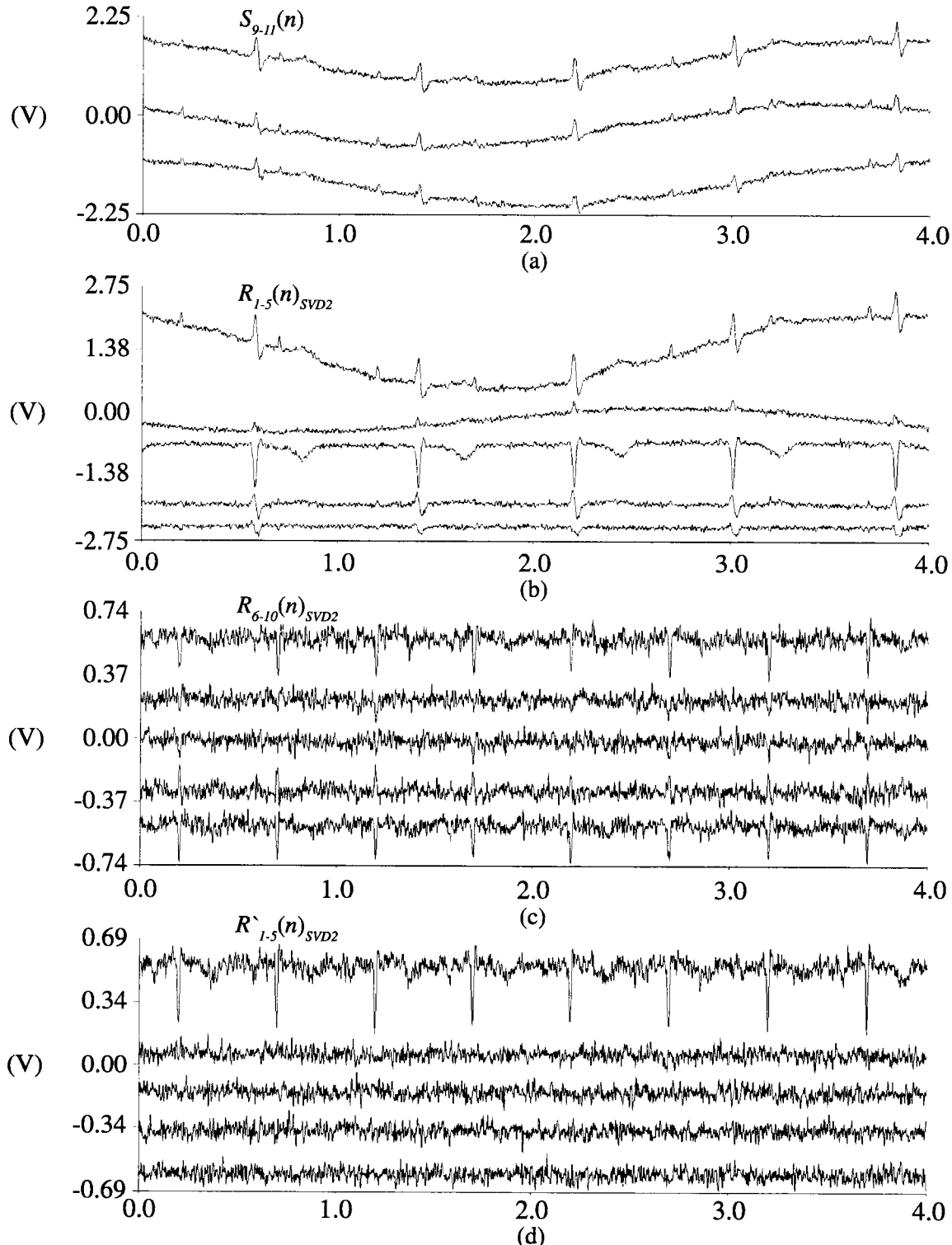

Figure I-14. SVD method two results demonstrating test condition five (all x-axes in seconds). (a) AECGs $S_{9\text{-}11}(n)$ with added low frequency noise. (b) Resulting ECGs $R_{1\text{-}5}(n)_{SVD2}$ of SVD method two. (c) Resulting ECG's $R_{6\text{-}10}(n)_{SVD2}$ of SVD method two. (d) Resulting ECGs of SVD method two or $R`_{1\text{-}5}(n)_{SVD2}$.

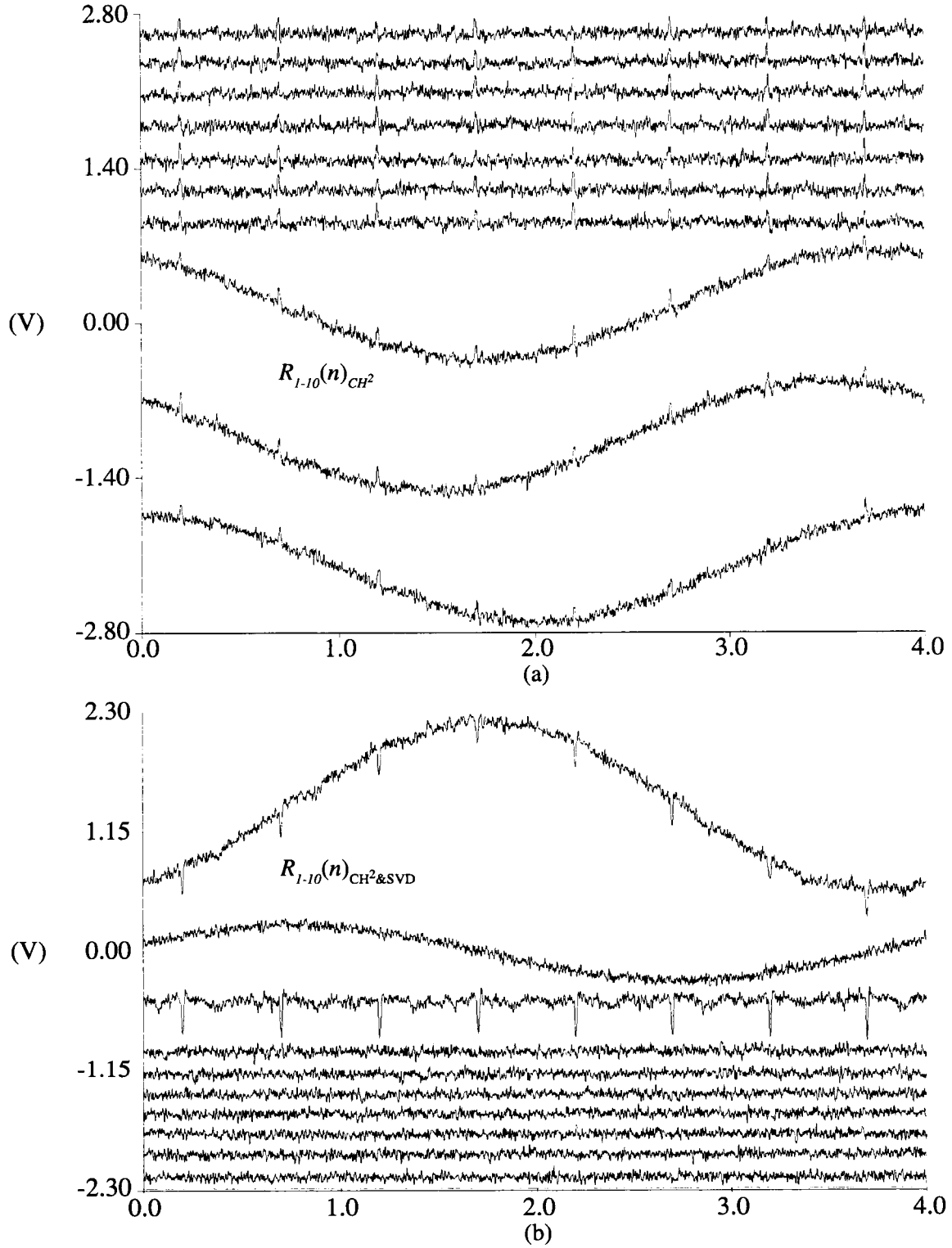

Figure I-15. Results of the CH² method demonstrating test condition five (all x-axes in seconds). (a) Resulting AECGs of the CH² method or $R_{1\text{-}10}(n)_{CH^2}$. (b) Resulting signals of CH² & SVD or $R_{1\text{-}10}(n)_{CH^2\&SVD}$.

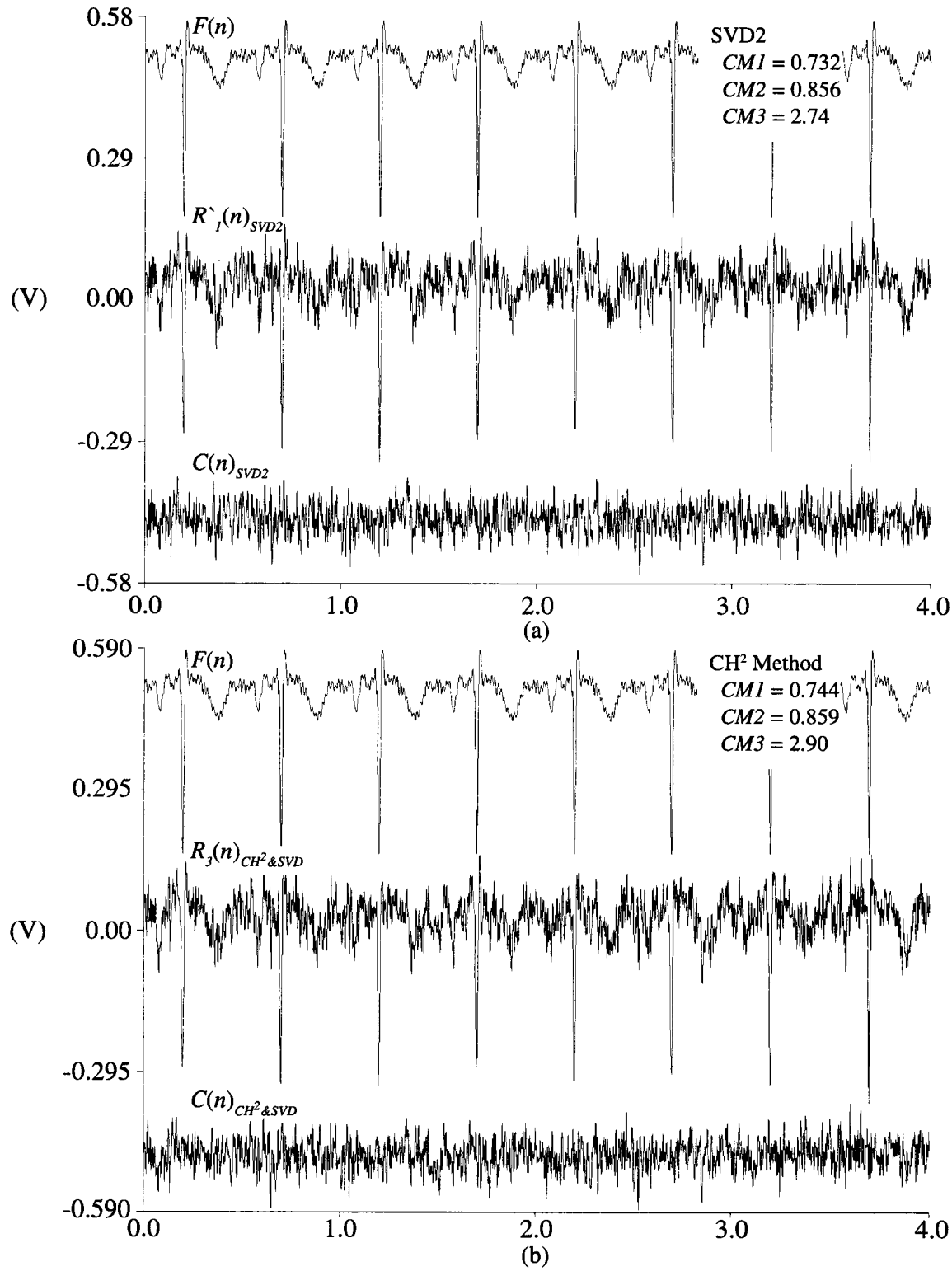

Figure I-16. SVD method two vs. the CH² method demonstrating test condition five (all x-axes in seconds). (a) Ideal FECG or $F(n)$, enhanced FECG via SVD2 or $R`_1(n)_{SVD2}$, and noise corrupting $R`_1(n)_{SVD2}$ or $C(n)_{SVD2}$. (b) Ideal FECG or $F(n)$, enhanced FECG via CH² & SVD or $R_3(n)_{CH^2\&SVD}$, and noise corrupting $R_3(n)_{CH^2\&SVD}$ or $C(n)_{CH^2\&SVD}$.

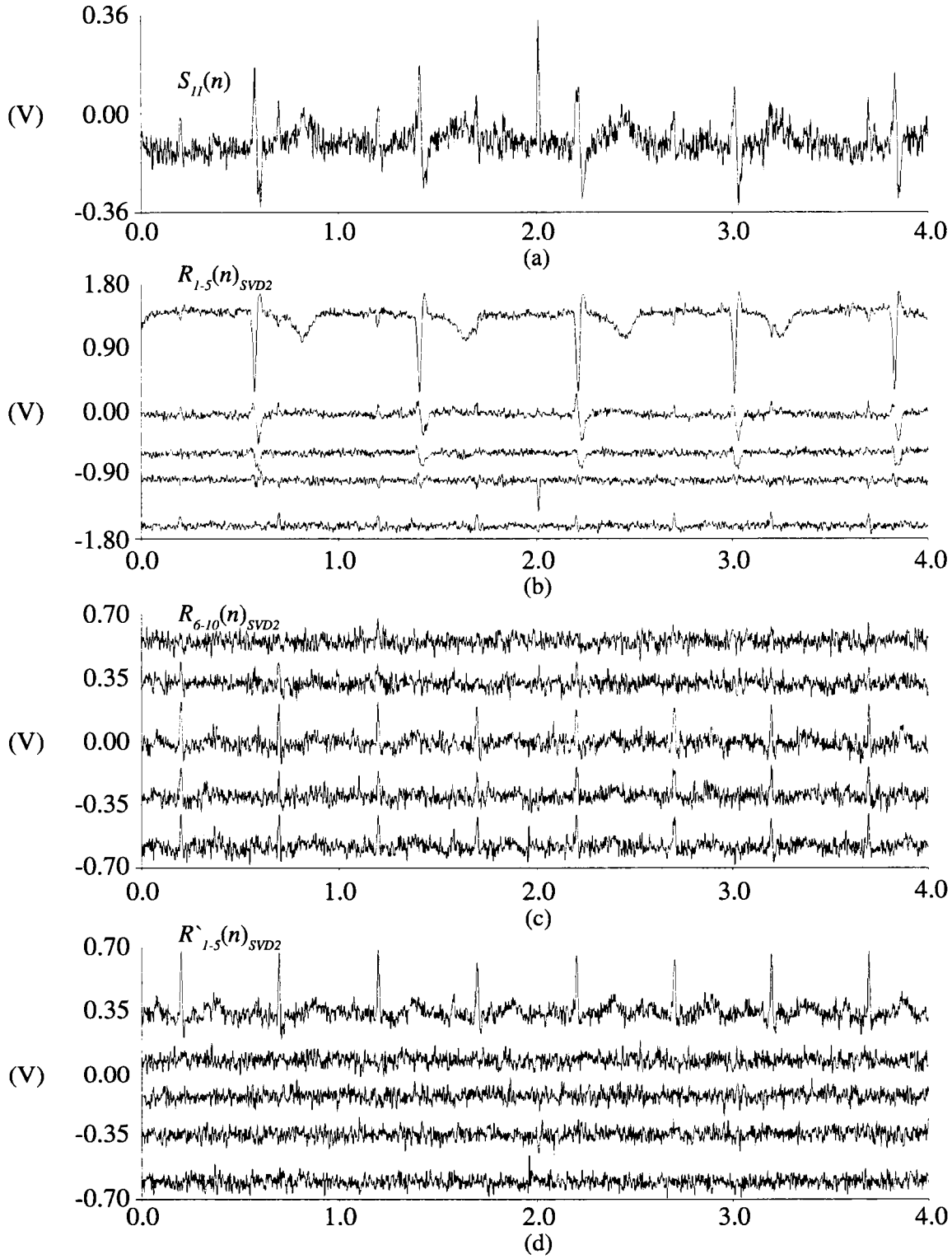

Figure I-17. SVD method two results demonstrating test condition six (all x-axes in seconds). (a) AECG $S_{11}(n)$ with an added noise spike. (b) Resulting ECGs $R_{1\text{-}5}(n)_{SVD2}$ of SVD method two. (c) Resulting ECGs $R_{6\text{-}10}(n)_{SVD2}$ of SVD method two. (d) Resulting ECGs of SVD method two or $R`_{1\text{-}5}(n)_{SVD2}$.

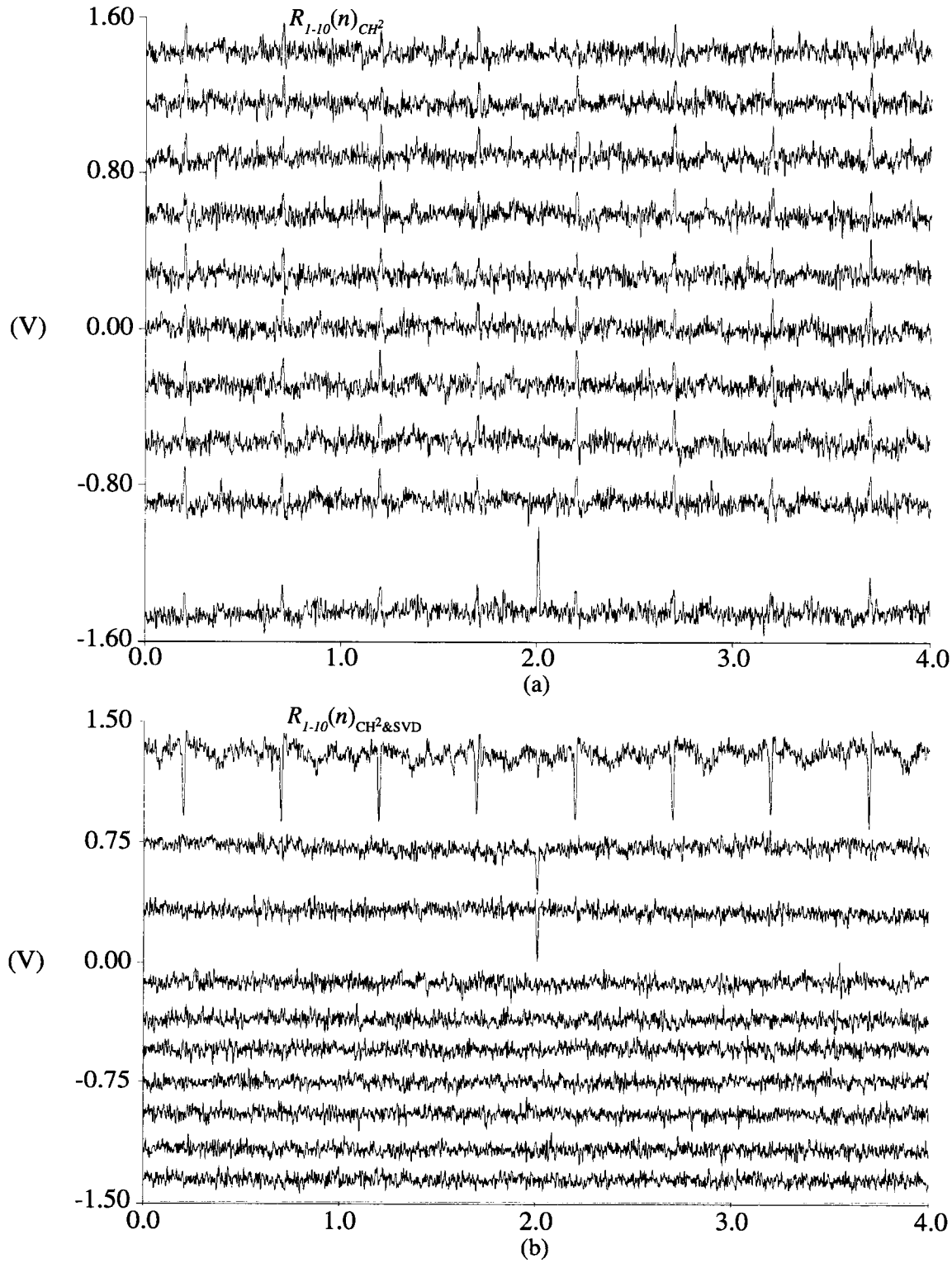

Figure I-18. Results of the CH² method demonstrating test condition six (all x-axes in seconds). (a) Resulting AECGs of the CH² method or $R_{1\text{-}10}(n)_{CH^2}$. (b) Resulting signals of CH² & SVD or $R_{1\text{-}10}(n)_{CH^2\&SVD}$.

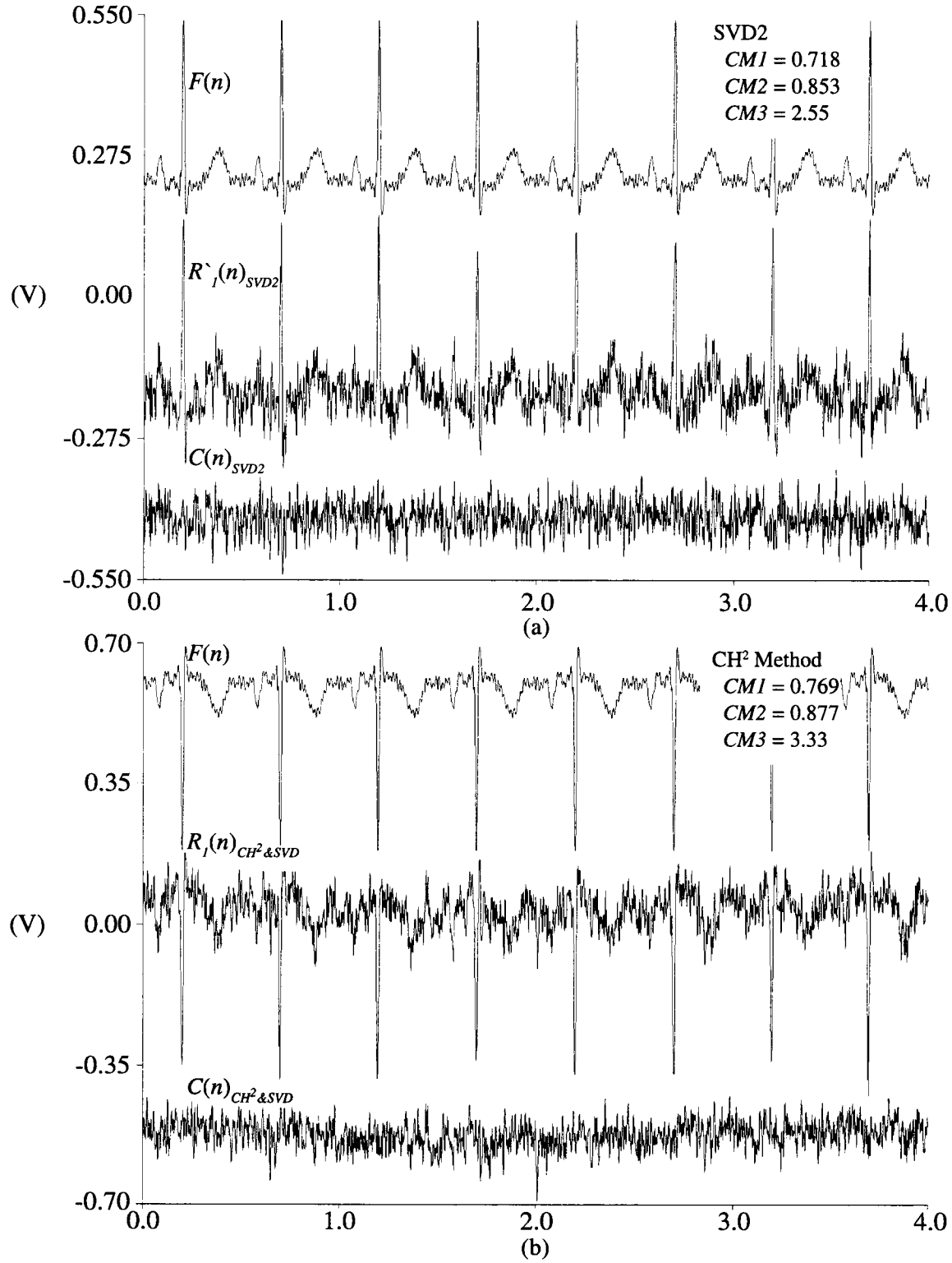

Figure I-19. SVD method two vs. the CH² method demonstrating test condition six (all x-axes in seconds). (a) Ideal FECG or $F(n)$, enhanced FECG via SVD2 or $R`_1(n)_{SVD2}$, and noise corrupting $R`_1(n)_{SVD2}$ or $C(n)_{SVD2}$. (b) Ideal FECG or $F(n)$, enhanced FECG via CH² & SVD or $R_1(n)_{CH^2\&SVD}$, and noise corrupting $R_1(n)_{CH^2\&SVD}$ or $C(n)_{CH^2\&SVD}$.

VITA

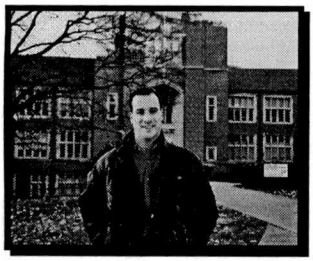

Steven Lee Horner was born in Grand Rapids, Michigan on November 22, 1967. He attended David Lipscomb College, Indiana University in Bloomington, and completed his undergraduate education at the University of Tennessee Knoxville with a Bachelor of Science in Electrical Engineering in August 1990. The author graduated as the top graduate of the College of Engineering. In December 1991, the author graduated from the University of Tennessee Knoxville with a Master of Science in Electrical Engineering and in January 1992 work was initiated towards a Ph.D. in Electrical Engineering.

The author has been a research assistant in the Department of Obstetrics and Gynecology at the University of Tennessee Medical Center Knoxville for the last five years. His research interests include digital and analog signal processing with application to biopotential signals particularly non-invasive and invasive fetal electrocardiograms and custom very large scale integrated circuits (VLSI) for biomedical digital signal processing applications. He has co-authored a journal article and several conference papers along with being a co-inventor for a patent. The author is a member of Phi Kappa Phi, Golden Key, Tau Beta Pi, Eta Kappa Nu, Gamma Beta Phi, and The Institute of Electrical and Electronics Engineers.